Lipid nanoparticles for membrane protein target drug discovery

Aneel Akram

Doctor of Philosophy

Aston University

September 2022

Lipid nanoparticles for membrane protein target drug discovery

Aneel Akram

Doctor of Philosophy

September 2022

Thesis Summary

Membrane proteins are essential in a plethora of physiological processes and perturbation of their function often leads to disease. As such, membrane proteins are the target for over 50% of pharmaceuticals. Their location within the lipid bilayer has meant that the study of their structure and function still lags behind that of easier to isolate, soluble proteins; this has hindered progress in drug design and development. The application of styrene maleic acid (SMA) polymers to isolate proteins directly from cell membranes, forming SMA lipid particles (SMALPs) where the proteins retain their lipid bilayer environment makes them potentially more suitable for structural and functional studies and could be used for drug development purposes. The aim of this project was to develop polymer-lipid particle approaches for biophysical assays such as surface plasmon resonance (SPR) or microscale thermophoresis (MST) suitable for medium to high throughput screening. To achieve this aim, two model proteins were used, Atm1 and LeuT. Atm1 is an ATP Binding Cassette (ABC) transporter and LeuT is a prokaryotic homologue of neurotransmitter transporters of the neurotransmitter: sodium symporter (NSS) family.

Recombinant Atm1 and LeuT were expressed in *E. coli* cells, extracted, and purified using several different polymers and stability and function investigated. Immobilisation studies for SPR were undertaken, which found that amine-coupling an anti-his antibody to the sensor chip and then binding the his-tagged SMALP-LeuT to that antibody was the most effective method for immobilisation. However, the level of immobilisation was too low to detect small molecule binding. Initial studies with MST showed SMALP-LeuT could be successfully labelled with a fluorophore at the his tag. Detection of leucine binding was highly variable and poorly reproducible. However, binding of the drug desipramine to SMALP-LeuT could be successfully measured and a dose-response curve obtained.

Chemical modification of the SMA polymer was tested, to potentially enable immobilisation or labelling of the polymer rather than the protein. Sulfhydryl groups were added to SMA forming SMA-SH, and the modified polymer was able to solubilise and purify proteins. Future work would look at labelling with biotin for immobilisation. Molecular biology approaches to add a SNAP-tag to the Atm1 protein was also started. The SNAP-tag enables site specific labelling with a range of different probes. Finally, two series of novel SMA polymer variants were tested to see if they offered any improvement over SMA2000. The first series were partially esterified SMA polymers, and the second series were benzylamine modified SMA polymers. Whilst all of the novel polymers were able to solubilise and purify membrane proteins, they did not offer an improvement over SMA2000, and were even more sensitive to divalent cations.

This thesis is dedicated to my family, especially my mother, I could not have made it through my PhD journey without her unwavering support and encouragement.

Acknowledgement

I would like to take this opportunity to express my gratitude to Dr Alice Rothnie and Dr Alan Goddard. I am extremely thankful and indebted to them for sharing their expertise, and sincere and valuable guidance throughout my PhD.

I would also like to thank Dr Scott Pollack, Dr Philip Addis and Dr Aaron Horsey at Sygnature Discovery for their continued support. I am also grateful to Prof. Bert Klumperman from Stellenbosch University for providing me with novel Benzylamine polymers.

Contents

Abbreviations

ABC transporter – ATP Binding Cassette transporter

AcrB – AcrAB TolC multidrug efflux pump

AQP0 - Aquaporin-0

BSA – bovine serum albumin

CHAPSO - (3-(3-Cholamidopropyl)dimethylammonio)-2-hydroxy-1-propanesulfonate)

DAG – diacylglycerol

DDM - n-dodecyl-β-d-maltoside

DIBMA - Diisobutylene/maleic acid

DM - n-decyl-β-D-maltopyranoside

DTT - dithiothreitol

E. coli – Escherichia coli

EDC - (1-Ethyl-3-[3-dimethylaminopropyl]carbodiimide hydrochloride)

GPCR – G protein-coupled receptor

HEGA-11 - Undecanoyl-N-Hydroxyethylglucamide

IPTG - Isopropyl β-D-1-thiogalactopyranoside

LB - Lysogeny broth

LDAO - Lauryldimethylamine Oxide

LeuT – leucine transporter

LSB - Laemmli sample buffer

MSP – membrane scaffold protein

NHS- N-hydroxysuccinimide

Ni-NTA – Nickel Resin

NSS - neurotransmitter: sodium symporter

OD - optical density

OG – octyl β-D glucoside

PagP - Lipid A palmitoyltransferase PagP

PBS - Phosphate buffered saline

RGS - Regulator of G-protein signalling

SA – streptavidin

SDS-PAGE - sodium dodecyl sulphate polyacrylamide gel electrophoresis

SMA – polystyrene-co-maleic acid

SMAd-A - styrene maleimide – amine

SMA-EA - styrene maleic anhydride – ethanol amine

SMA-ED - styrene maleic acid – ethylene diamine

SMALP – SMA lipid particle

SMA-QA - styrene maleimide quaternary ammonium

SMI - styrene maleic imide

Sulfo-NHS - (N-hydroxysulfosuccinimide)

TCEP - Tris Carboxy Ethyl Phosphene

zSMA – zwitterionic styrene maleic acid

List of Figures

Chapter 7

List of Tables

1. Introduction

1.1 The importance of membrane proteins

Membrane proteins are found embedded in the lipid bilayer of cells and are essential for life as they are involved in maintaining various cellular functions in all organisms (von Heijne, 2007). They have diverse cellular roles including signal transduction, cell adhesion and endocytosis (Bagag *et al*., 2013), as well as ATP synthesis, oxidative phosphorylation, transport of metabolites and proton pumping (Denisov and Sligar, 2017). This range of functions means there is great variation in their size, structure, and composition (Denisov and Sligar, 2017).

Membrane proteins can act as mediators of material and information, between cells and the environment and are responsible for mediating responses to cells and hormones, such as immune system cells and growth hormones (Maynard *et al*., 2009). Membrane proteins are essential for the biosynthesis of compounds such as lipids and steroid hormones and are vital for the breakdown of internal metabolites and xenobiotics (Denisov and Sligar, 2017). They can form supra-molecular complexes composed of proteins, lipids, and nucleic acids and such complexes are typically involved in processes such as generation of motility and intercompartmental communication (Denisov and Sligar, 2017).

It is estimated that almost 30% of the proteins found in eukaryotic cells are membrane proteins (Wallin and Heijne, 2008) and Fagerberg *et al* have proposed that one third of the human genes code for membrane proteins (Fagerberg *et al*., 2010).

Membrane proteins also play a major role in the central nervous system. For example, for the nervous system to effectively function, neuron cells must be able to communicate with adjacent cells including other neurons (Pereda, 2014). The communication between neuron cells in the central nervous system is reliant upon the transmission of nerve impulses through chemical synapses. Neuronal synapses are intricate structures in which various proteins and extracellular matrix components are involved (Kornberg and Roy, 2014). In a typical chemical synapse, the arrival of action potential at the presynaptic terminal triggers the release of neurotransmitters which then subsequently go onto bind and activate receptors on the postsynaptic cells (Ruediger and Bolz, 2007). The binding of released neurotransmitters on the post synaptic cells can cause excitation or inhibition (Ruediger and Bolz, 2007). Therefore, the intracellular communication between neurons in the central nervous system necessitates control of duration and intensity of neurotransmitter action (Masson *et al*., 2019). The effects of neurotransmitters can be moderated by regulating synaptic transmissions and synaptic transmissions are regulated by enzymatic breakdown of neurotransmitters or by uptake of neurotransmitters by specific, high-affinity integral membrane transporters situated on the presynaptic terminals (Masson *et al*., 2019).

In humans, membrane proteins have been linked to several diseases. For example, mutations in the cystic fibrosis transmembrane conductance regulator proteins are known to cause cystic fibrosis (Clunes and Boucher, 2007) and mutations in the vasopressin receptor proteins have been shown to cause X-linked nephrogenic diabetes insipidus (Bichet, 2008). Verkman *et al*., 2008 have revealed that defects in aquaporin AQP0 proteins can cause congenital cataract (Verkman, Ruiz-Ederra and Levin, 2008). Studies have also implicated transient receptor potential channels in cancer, hypertension and kidney disorders (Prevarskaya, Zhang and Barritt, 2007; Firth, Remillard and Yuan, 2007; Hsu, Hoenderop and Bindels, 2007; Warschawski *et al*., 2011)

Membrane proteins are also complicit in infectious diseases, as they can act as receptors for viruses and can also cause antibiotic resistance, and because of this are often the target of many pharmacological drugs (Overington, Al-Lazikani, and Hopkins, 2006).

Prior studies have indicated that up to 60% of the drugs on the market target membrane proteins. Membrane proteins such as G protein-coupled receptors (GPCRs) and ion channels are often specifically targeted in drug design as they are involved in signal transduction and are responsible for initiating signal cascades (Terstappen and Reggiani, 2001; Davey, 2004; Wallin and Heijne, 2008) ,.

Membrane proteins are therefore invaluable diagnostic and therapeutic targets, and this assertion is supported by Yin and Flynn who have proposed that the majority of therapeutics available target membrane proteins (Yin and Flynn, 2016). Membrane proteins have tremendous potential in assisting in the characterisation of new biological markers and the identification of new targets for therapeutics (Bagag *et al*., 2013).

1.2 The challenges in studying membrane proteins

Despite the evident importance of membrane proteins, the development of high-resolution protein structures and the study of protein mode of action is lagging. The study of membrane protein structure and function is difficult due to the surface of membrane proteins being split into spatially separate regions, which have different physicochemical properties. Membrane proteins are often hydrophobic and in native conditions are found embedded in lipid bilayers, where the hydrophobic surface of the protein is shielded away from the aqueous phase (Dörr *et al*., 2015).

Biological membranes are lipid bilayers composed of amphipathic lipid molecules which have a polar/hydrophilic headgroup and non-polar/hydrophobic chains. Lipid bilayers are composed of various lipid groups and individual lipid molecules can diffuse within individual monolayers. The three main classes of membrane lipids are glycolipids , cholesterol, and phospholipids. Phospholipids are the most common lipid group present within lipid bilayers, and they have a polar head group and two hydrophobic hydrocarbon tails. The hydrophobic tails can vary in length and are typically composed of fatty acids (Wilson and Hunt 2002).

The composition of outer and inner monolayers of lipid bilayers are different and this reflects the individual role of monolayers in the lipid bilayer. The mixture and composition of lipid bilayers can vary from cell to cell and from organism to organism (Devaux and Morris, 2004). The lipid composition of biological membranes is important because the specific lipid head groups can be required by certain enzymes to function or to form docking sites for proteins. Additionally, protein signalling cascades can also exhibit their effect by activating phospholipases which cleave phospholipids and subsequently generate lipid fragments which can function as signalling molecules within the cell (Wilson and Hunt 2002).

Both the polar lipid head groups and the hydrophobic tails are necessary for membrane protein fold and stability (Jamshad *et al*., 2011). Currently there is a limited understanding of membrane protein structure and folding in comparison to water soluble proteins (Dörr *et al*., 2015). It has been proposed that only 2% of the proteins listed in the protein data base are membrane proteins (White, 2016).

Membrane proteins from eukaryotes are often glycosylated, which is an important mechanism of secondary protein processing (Arey, 2012). Protein glycosylation permits the control of important biological pathways which are vital for regulating various cellular activities such as cell adhesion, protein trafficking and even host pathogen interactions (Hang, 2010). Protein glycosylation also plays a vital role in determining protein structure, function, and stability, and it is also proposed to impact the three-dimensional configuration of proteins (Arey, 2012). However, glycosylation confers heterogeneity to protein samples and can be challenging for structural studies.

Membrane proteins can be divided into 2 main categories, peripheral proteins, and integral proteins. Peripheral and integral proteins interact with the membranes in different ways. Peripheral membrane proteins can bind transiently to the cell membrane surface and are able to exist in membrane bound and in soluble forms (Tubiana *et al.,* 2022). Peripheral membrane proteins are typically bound to the membrane through indirect interactions with integral proteins, by interactions with lipid polar head groups, or by lipid anchors (Lodish *et al*., 2000). In contrast integral membrane proteins have segments embedded into the phospholipid bilayer. Amino acids with hydrophobic side chains interact with fatty acyl groups in the lipid bilayer (Lodish *et al*., 2000).

Integral membrane proteins can be further subclassified into proteins which only insert into one half of the lipid bilayer, and those which traverse the entire lipid bilayer. Proteins may traverse the bilayer just once, or multiple times, with the transmembrane regions joined by intracellular and extracellular loops. The majority of transmembrane regions of proteins are alpha-helical in structure, however beta-barrels formed of multiple beta sheets are also found, predominantly in the outer membrane of bacteria (Lodish *et al*., 2000).

A typical example of integral membrane proteins are G protein-coupled receptors (GPCRs). GPCRs are found in the plasma membrane of eukaryotic cells and are classified as transmembrane proteins as they have seven α-helices embedded in the cell plasma membrane (Latorraca *et al*., 2016). GPCRs

are one of the main classes of cell surface receptors and are responsible for mediating cellular responses to external stimuli and are capable of inducing physiological effects in response to extracellular signals (Yang *et al*., 2021). GPCRs are also the largest family of proteins encoded in the human genome (Weis and Kobilka, 2018). GPCRs bind to G proteins, which are an example of a peripheral membrane protein. G proteins are heterotrimers composed of three different subunits , alpha subunit, beta subunit, and gamma subunit. Each of the subunits are encoded for by a different family of related genes The alpha subunits are responsible for catalysing GTPase activity and the beta, and gamma subunits are responsible for blocking the alpha subunits from interacting with the effectors (Schulman *et al*., 2013). The alpha subunits of G proteins can bind GTP or GDP, however GPCRs remains inactive when alpha subunits are bound to GDP. In the absence of extracellular signals, the alpha subunits are typically bound to GDP and the beta and gamma subunits (Weis and Kobilka, 2018). Ligand binding to extracellular surface of GPCRs induces conformational changes to occur within the receptors which subsequently lead to the G proteins activating and the GDP bound to alpha subunit being replaced by GTP (Weis and Kobilka, 2018). The binding of GTP to alpha subunits of G proteins subsequently leads to the G protein subunits unbinding from GPCRs and separating into two parts, A GTP bound alpha subunit and a beta gamma subunit dimer , both parts remain anchored within the plasma membrane however they can diffuse laterally and can interact with other proteins (Weis and Kobilka, 2018).

The separated alpha subunits and beta and gamma subunits of G protein can relay signals to a wide variety of downstream effectors such as protein tyrosine kinases, phospholipases ,adenylyl cyclase isoforms and ion channels (Dupré *et al*., 2009). The GTP bound G proteins remain active until the GTP is hydrolysed back to into GDP and the subunits then reassociate with the beta gamma subunits to form an inactive heterotrimer, which subsequently binds to the GPCR again.

Findings from earlier investigations have suggested an intricate relationship between membrane proteins and the lipid bilayer. The lipid composition of cell membranes can influence membrane protein function directly or indirectly. The lipid composition of a membrane dictates its physical properties, including thickness, fluidity, and lateral pressure (Cantor, 1997). These physical factors can greatly influence the structure, function, and localisation of membrane proteins. Changes to the lipid bilayer configuration or drugs binding to the lipids can have dire effects on the embedded membrane proteins (Lundbaek, Koeppe and Andersen, 2010). Lateral pressure can affect the conformational transitions of membrane protein and therefore changes in lateral pressure can also induce large shifts in the conformational distributions of membrane proteins (Cantor, 1997). In addition to these general factors, some membrane proteins are known to interact with specific lipids. Lipid bilayers are not simply involved in preserving membrane protein structure, lipid bilayers actively interact with membrane proteins and affect their function (Andersen and Koeppe, 2007; Marsh, 2008; Phillips *et al.,* 2009). For example, specific lipids can be required for membrane orientated processes like blood coagulation cascades, which are enabled via exposure to anionic surfaces and phospholipids such as cardiolipins which can

have regulatory roles in the functions of some transporters (Morrissey *et al.,* 2008; Denisov and Sligar, 2017).

1.3 Membrane protein solubilisation

To study the structure and many features of function in *in vitro* experiments, membrane protein first needs to be extracted from the lipid bilayer, and then purified whilst maintaining structure and function. Some of the properties of membrane proteins can be elucidated using non-bilayer mimetics such as detergents and amphipols to solubilise and purify membrane proteins however many aspects of membrane protein structure and function depend on association with lipids and therefore require a lipid environment (Denisov and Sligar, 2017). An ideal solubilisation method should therefore maintain a protein's native environment, provide stability for the solubilised protein, not interfere with purification, and enable the study of membrane protein structure and function (Dörr *et al*., 2015).

Traditionally during the solubilisation stages of a typical membrane protein study, detergents have been utilised to extract membrane proteins from the lipid bilayer into micelles (Garavito and Ferguson-Miller, 2001). Detergents have a hydrophilic head group and usually a single hydrophobic tail. The hydrophobic tails bind to the hydrophobic regions of the transmembrane protein and shield it from the aqueous solution. A variety of detergents exist such as DM (n-decyl-β-D-maltopyranoside), DDM (n-dodecyl-β-d-maltoside) and OG (n-octyl beta-D-glucopyranoside) which can all be utilized to extract membrane proteins (Seddon, Curnow, and Booth, 2004; Privé, 2007; Moraes *et al*., 2014).

However, there are several inherent disadvantages with detergent usage, for example when working with proteins with unknown properties an extensive screening process is required to identify a suitable detergent, which can be time consuming and challenging (Privé, 2007; Arachea *et al.,* 2012). Detergent usage can also affect the structure and composition of extracted membrane proteins as it promotes different intramolecular interactions in comparison to native membrane bilayer conditions (Stangl *et al*., 2012). For example, the bacteriorhodopsin protein was previously crystallized as a monomer in a bicellar environment (Faham and Bowie, 2002) and as a trimer in lipid cubic phase crystallization (Pebay-Peyroula *et al*., 1997; Stangl *et al*., 2012). Studies have established that protein structure, fold, and function are impacted by the lipid environment in biological membranes (Laganowsky *et al*., 2014). However, detergent usage strips membrane proteins of their native lipid environment leading to loss of native interactions and ultimately protein instability (Rasmussen *et al*., 2007; Duquesne, Prima and Sturgis, 2016).

Protein stability is essential for protein structure and protein function studies (Deller *et al*., 2016). For structural studies multiple copies of the exact same structure are needed, and if the protein is unstable, it will cause variation in the structures, and subsequently loss of protein function. Membrane proteins in micelles can inactivate or aggregate when exposed to aqueous environments, this is likely due to the

difference in lateral pressure and water permeability of micelles and lipid bilayers, as previous studies have highlighted the importance of pressure in maintaining membrane protein structure (Charalambous et al., 2008; Miller et al., 2009).Detergents are also unable to completely mimic the lipid bilayer as they exhibit different physiochemical properties (Bordag and Keller, 2010; Zhou and Cross, 2013) and can interfere with protein function (Quick *et al*., 2012) and physiological conformation (Zhou and Cross, 2013). Native membranes are composed of a variety of components and even a minor change in composition can alter the physical properties of the membrane, and in turn affect membrane proteins (Charalambous et al., 2008; Debnath *et al.,* 2010).

Due to the challenges associated with using detergents for solubilisation, several alternative approaches to extracting membrane proteins have been explored and developed. This includes the application of amphipols, protein stabilized lipid nanodiscs and polymer solubilised lipid nanoparticles, (Schmidt and Sturgis, 2018).

Amphipols are amphipathic polymers which function by adsorbing onto the surface of membrane proteins (Popot, 2010). Amphipols keep membrane proteins stable and functional, as shown by studies on Bacteriorhodopsin from *Halobacterium salinarum* and cytochrome b6f complex from *Chlamydomonas reinhardtii,* which have shown the protein to be in its native state and highly stable (Bazzacco *et al*., 2012). Amphipols can be used to produce proteins with higher stability in comparison to detergents and an additional benefit of amphipol application is the presence of functional groups on the amphipol side chains which permit chemical modifications and labelling of fluorophores (Dörr *et al*., 2015). Potential disadvantages of amphipol application include size heterogeneity and the presence of a high charge (Tribet *et al.,* 1996). Also, most amphipols are not effective at solubilising proteins directly from membranes, and require an initial detergent solubilisation step before being exchanged into amphipols. A wide variety of amphipols are available however some of them are sensitive to pH changes and the presence of divalent cations, both of which could cause the solubilised protein to aggregate or precipitate out of solution (Zoonens and Popot, 2014).

Protein stabilised lipid nanodiscs are composed of discoidal fragments of a non-native lipid bilayer which are stabilized by encircling amphipathic scaffold proteins (Schuler *et al.,* 2014; Denisov and Sligar, 2016), often referred to as MSP (membrane scaffold protein) nanodiscs. The application of MSP nanodiscs methodology is effective as it facilitates the provision of a native-like membrane environment with desired lipid composition for the extracted proteins . An additional benefit of MSP nanodiscs is that they are relatively small in size and have good size homogeneity and can be utilised in nuclear magnetic resonance studies (Günsel and Hagn, 2021). Proteins reconstituted in MSP nanodiscs are generally stable and maintain functionality, and the nanodiscs methodology can be utilised to study peripheral and integral membrane proteins (Günsel and Hagn, 2021). However, a major limitation of MSP nanodiscs are that they require an initial detergent solubilisation and subsequent reconstitution into the disc. Optimisation of this process is needed for each different protein and this can be time consuming.

It also requires the production of the MSP itself in addition to the target protein. In addition to extensive sample preparation processes, for solution nuclear magnetic resonance studies ultrahigh-field nuclear magnetic resonance magnets and cryogenic probes can be required (Günsel and Hagn, 2021). The presence of the MSP can also interfere in various downstream applications such as CD spectroscopy.

Polymer solubilised lipid nanoparticles are composed of small discs of the lipid bilayer which contain membrane proteins alongside native lipids encircled by a belt of amphipathic polymer (Knowles *et al*., 2009). Styrene Maleic Acid (SMA) copolymers have primarily been used in the pharmaceutical and plastics industries and only in the last 10 years have started being employed in membrane protein research due to their amphipathic properties (Knowles *et al*., 2009; Jamshad *et al*., 2011).

SMA polymers have a different mode of action to traditional non-bilayer mimetics (Figure 1.1), the styrene present in SMA polymers is hydrophobic and the maleic acid is hydrophilic, these alternating moieties of SMA polymer enable SMA molecules to insert into biological membranes and form ring like structures which encircle lipid membranes with the styrene moieties intercalated between lipid acyl chains (Prabudiansyah *et al*., 2015). Thus, SMA is able to directly extract membrane proteins from biological membranes whilst maintaining their lipid bilayer environment and the nanoparticles formed are referred to as styrene maleic acid lipid particles (SMALPs). SMALPs preserve bilayer environment and are stable (Orwick *et al*., 2012; Gulati *et al*., 2014; Jamshad *et al*., 2015a; Dörr *et al*., 2016).

Studies on a variety of membrane proteins have shown that SMA polymers have great general applicability regardless of the expression hosts and can be used to isolate various membrane proteins from a range of organisms (Dörr *et al*., 2014). For example, prior studies on several eukaryotic proteins of the ABC transporter family (Gulati *et al*., 2014) as well as the bacterial enzyme PagP, the secondary transporter AcrB and the GPCR Adenosine2a receptor have shown that SMA polymer can be used to successfully extract numerous membrane proteins into SMALPs (SMA lipid particles), which retain the native lipid environment of the membrane protein and preserve function (Knowles *et al*., 2009; Jamshad *et al*., 2011; Postis *et al*., 2015).

However other studies have shown that the application of SMA polymers for GPCRs solubilisation from mammalian cells can lead to low yield (Tedesco *et al*., 2021), whilst studies on rhodopsin have shown that the amount of SMA polymer employed in ratio to protein membranes can affect the activity of the solubilised protein (Szundi *et al*., 2021). Using low SMA/rhodopsin molar ratios can lead to production of rhodopsin SMALPs which are suitable for photokinetic studies. In contrast the application of high SMA/protein molar ratios can produce slow photokinetics and the solubilised rhodopsin can fail to reach active state (Szundi *et al.,* 2021).
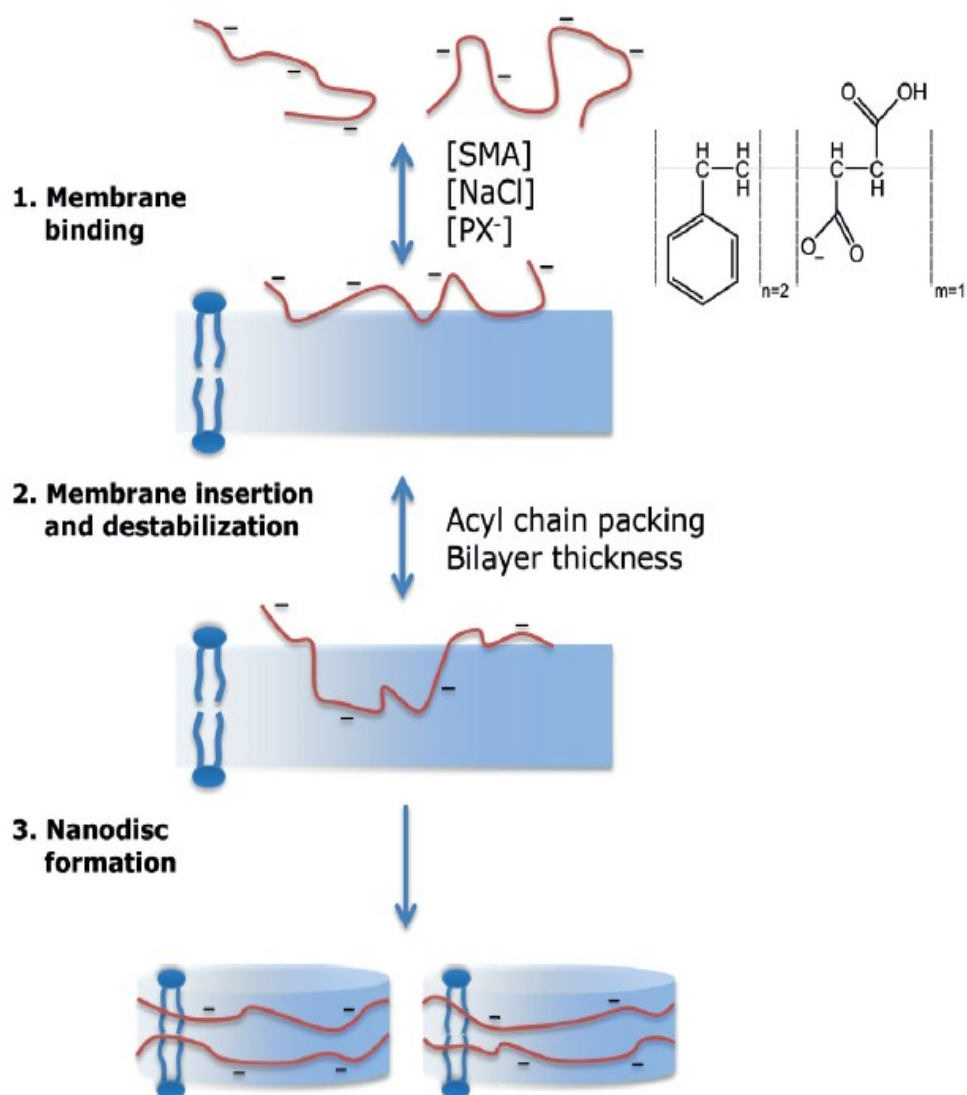
Figure 1.1 SMA copolymer Mode of Action. *1) The binding of SMA copolymers to lipid rich membrane is driven by hydrophobic and electrostatic interactions and is affected by salt concentrations (NaCl) and the number of anionic lipids (PX) present. 2) SMA copolymer insertion into hydrophobic core of membrane driven by acyl-chain packing. 3) SMA copolymers insertion leads to membrane destabilization and formation of nanodiscs. Reprinted from Biophysical Journal , 108,Stefan Scheidelaar,Martijn C. Koorengevel,Juan Dominguez Pardo,Johannes D. Meeldijk,Eefjan Breukink,J. Antoinette Killian, Molecular Model for the Solubilization of Membranes into Nanodisks by Styrene Maleic Acid Copolymers , 279-290, 2015 , with permission from Elsevier.*

Swainsbury *et al.*, 2017 showed that SMA copolymers with a 2:1 or 3:1 ratio of styrene:maleic acid can be employed to successfully solubilise *Rhodobacter sphaeroides* reaction centres with comparable solubilisation effectiveness to detergents. They have also showed that short chain variants of styrene maleic acid polymer which are smaller than 30 kDa in average molecular weight were the most effective at solubilising *Rhodobacter sphaeroides* reaction centres from photosynthetic membranes (Swainsbury *et al.,* 2017). However, they also revealed a substantial limitation/drawback of the SMA polymer application in that the effectiveness of the SMA polymers decreased as the size of target protein/protein

complex increased . For example the small chain variants of SMA could successfully solubilise *Rhodobacter sphaeroides* reaction centres which are normally monomeric , however when those monomers were artificially tethered into dimeric, trimeric and tetrameric multimers, the solubilisation efficiency gradually decreased. The SMA polymers also poorly solubilised reaction centre-light harvesting 1 complexes from photosynthetic membranes. It was hypothesized this was partially due to the photosynthetic membranes being densely packed and highly ordered (Swainsbury *et al*., 2017).

Investigations on mitochondrial membranes have shown that SMA copolymers can effectively solubilise and extract protein complexes (Long *et al*., 2013), whilst studies on bacterial proteins have shown that SMA polymer can be used to solubilise and extract proteins involved in diverse processes such as cell division and photosynthesis (Paulin *et al*., 2014; Swainsbury *et al*., 2014).

SMA polymers mode of action has been shown to be able to trap a diverse range of lipids with variable lengths of acyl chains and head groups (Scheidelaar *et al*., 2015; Prabudiansyah *et al*., 2015), and this is important because it's known that lipids can modulate membrane protein structure and function Laganowsky *et al*., 2014; Yeagle, 2014).

The application of SMA polymers is also compatible with established purification techniques such as affinity chromatography and gel filtration (Prabudiansyah *et al*., 2015) and this is very important for protein yield and purity. SMALPs have a variety of useful characteristic's which makes them ideal for membrane protein studies, for example SMALPS are soluble and therefore can be utilized in solution-based techniques to characterize membrane protein and structure (Pollock *et al*, 2018). SMALPs are also relatively small with a diameter between 10 - 12 nm (Knowles *et al.,* 2009; Orwick *et al.,* 2012). This enables downstream analysis by methods such as X-ray crystallography (Broecker, Eger and Ernst, 2017), as well as optical techniques such as circular dichroism (Knowles *et al.,* 2009; Dörr *et al*., 2014; Gulati *et al*., 2014), and fluorescence spectroscopy (Dörr *et al.,* 2014; Gulati *et al*., 2014). Furthermore, SMALPs also enable biophysical characterization of membrane proteins as the soluble domains of proteins in SMALPs are accessible to the aqueous environment, therefore solutes can be studied in a native like environment (Dörr *et al.,* 2015). Based on this principle, several studies using radioactive ligands (Gulati *et al.,* 2014; Jamshad *et al*., 2015a) and fluorescence quenching (Gulati *et al*., 2014) have established that small molecules can bind to proteins in SMALPs. SMALPs can also be used in protein activity studies (Prabudiansyah *et al*., 2015) and general results have suggested that SMALPs have comparable or better activity than protein extracted via detergents (Dörr *et al*., 2015).

However, there are some limitations with SMA utilization, for example the high order of lipids in SMALPs can increase the overall rigidity of the lipid environment and hinder conformational transitions ultimately resulting in interference with protein function (Dörr *et al*., 2015). SMALPS are also sensitive to low pH and divalent cations (Morrison *et al*, 2016; Hawkins *et al* 2021).

SMA polymers have amphipathic properties due to having styrene units which are hydrophobic and maleic acid units which are hydrophilic due to the presence of carboxyl/carboxylate groups. The overall

hydrophobicity of SMA polymers however is not only affected by the ratio of styrene and maleic acid units but also the pH of the environment (Dörr *et al.*, 2015). In a low pH environment, the SMA polymers are generally not charged, at neutral pH levels the maleic acid units of the polymer carry a single negative charge and in a high pH environment both carboxyl groups of the maleic acid carry a negative charge (Dörr *et al.*, 2015). The pH levels of the environment can affect SMA polymer conformation and therefore polymer solubilisation. At neutral or high pH levels, electrostatic repulsions are present between carboxylate groups and these electrostatic repulsions are able to dominate the hydrophobic effect. In neutral or high pH environments SMA polymers are able to form a random coil conformation which is able to dissolve in aqueous solutions (Dörr *et al.*, 2015). However, in low pH environments the SMA polymers undergo complete protonation, which promotes the hydrophobicity of the co-polymers as the charge repulsion is lost and the presence of the hydrophobic effect leads to polymers adopting a globular conformation and ultimately precipitating out as aggregates (Dörr *et al.*, 2015).

Similarly, studies have shown that concentrations higher than 5mM of Mg^{2+} can cause SMALPs and encompassed proteins to precipitate out of solution (Morrison *et al.*, 2016). This can be particularly problematic for proteins that need ions such as Mg^{2+} or Ca^{2+} to function. SMA is known to carry high negative charge densities and the presence of such densities is thought to cause positively charged divalent cations to bind to SMALPS. At low concentration, this type of binding is tolerated however as divalent cations concentrations increase, an increasing burden is placed upon the SMALP structure. Alternatively, it is also possible that the divalent cations directly bind to lipids within is the SMALP structure at increasing concentrations and this eventually leads to SMALP instability and ultimately proteins precipitating out of solution. For example, it's been shown that divalent cations such as Mg^{2+} or Ca^{2+} can bind to a phosphatidylserine monolayer coated air/water interface and cause an increase in surface tension by bridge binding. Bridge binding results from divalent cation binding to two adjacent lipids instead of one (Ohshima & Ohki, 1984).

1.4 LeuT

In the present study, one of the proteins of interest is the leucine transporter (LeuT). LeuT is a prokaryotic homologue of neurotransmitter transporters of the neurotransmitter: sodium symporter (NSS) family (Shi *et al.*, 2008). The NSS family of proteins are present in both eukaryotes and prokaryotes (Kantcheva *et al.*, 2013). In humans NSS's are referred to as solute carrier 6 family (Hediger *et al.*, 2004).

NSS's are essential for life as they help regulate neurotransmission in the nervous system and are responsible for terminating synaptic transmissions by recycling neurotransmitters (Rudnick, 1997). In humans NSS's are located on the plasma membrane of nerve terminals and are responsible for uptaking neurotransmitters from the synapse into the presynaptic neurons (Reith, 2002; Torres, Gainetdinov and Caron, 2003). This uptake of neurotransmitters returns synaptic neurotransmitter

concentrations to a basal level and permits the replenishment of neurotransmitter stores in the lumen of presynaptic vesicles (Yamashita et al., 2005).

NSS's play a vital role in the central nervous system and are the primary mechanism by which the termination of monoaminergic neurotransmission is achieved and therefore are necessary for maintaining monoamine homeostasis in the central nervous system (Coyle and Snyder, 1969;Iversen, 1971; Giros *et al*., 1996; Hoffman *et al*., 1998; Jones *et al*., 1998).

NSS are secondary active transporters and function by exploiting pre-existing ion gradients across the plasma membranes (Shi *et al*., 2008; Malinauskaite *et al*., 2014). NSS's can uptake a range of neurotransmitters against their concentration gradients by utilising the electrochemical gradient of sodium ions between the outside and inside of cell membranes to provide thermodynamic energy to transport neurotransmitters from low extracellular concentrations to high intracellular concentrations using the cotransport mechanism (Torres, Gainetdinov and Caron, 2003; Kantcheva *et al*., 2013). NSS's can bind and transport several biogenic amines such as serotonin, dopamine, and norepinephrine as well as osmolytes such as betaine and creatine. NSS's can also transport amino acids like glycine, proline, and γ-aminobutyric acid (Sonders, Quick and Javitch, 2005).

NSS are of particular importance as they have been implicated in the pathophysiology and treatment of several neuropsychiatric disorders such as schizophrenia, autism, depression, epilepsy, and attention deficit hyperactivity disorder (Gether *et al.,* 2006; Singh, 2008). NSS's are also the targets of antidepressant including amitriptyline, amoxepine and desipramine (Iversen, 2009) as well as recreational psychostimulants such as amphetamines, cocaine, and ecstasy (Amara and Sonders, 1998; Gether *et al*., 2006).

In mammals NSS's uptake mechanisms are Na^+ and Cl^--dependent however in bacteria the uptake is Cl^- independent and stimulated by generation of a reverse proton gradient through a proton-antiport mechanism (Kantcheva *et al.,* 2013). LeuT is an amino acid transporter from *Aquifex aeolicus* . *Aquifex aeolicus* is an hyperthermophilic and obligate chemolithoautotrophy bacterium. It is Gram-negative, rod-shaped, flagellated, and non-spore-forming. *Aquifex aeolicus* bacteria grows best at 85 °C however it can still grow at even higher temperatures such as 95 °C*. Aquifex aeolicus* does not require any organic molecules to flourish and instead it is efficient in utilising molecular oxygen, molecular hydrogen, and inorganic sulphur compounds, and thrive in the absence of light (Guiral and Giudici-Orticoni, 2020).

LeuT can transport several hydrophobic amino acids such as leucine, glycine, and alanine as well as aromatic amino acids like tyrosine and phenylalanine in exchange for sodium (Singh *et al.,* 2008). Amino acids are the building block of proteins and therefore essential for growth and repair (Erlendsson *et al.,* 2017). Not all cells can synthesise the full range of amino acids and therefore require amino acid transporters for uptake of amino acids from the extracellular environment (Erlendsson *et al.,* 2017).

LeuT structure is comprised of a twelve-helix bundle, with the transmembrane segments being connected via short extracellular and intracellular loops (Shaikh and Tajkhorshid, 2010; Merkle *et al*., 2018). The first 5 transmembrane segments have similar structural repeats to transmembrane segments 6 – 10 however have inverted symmetry due to the first 5 segments being inverted in the membrane plane (Yamashita *et al*., 2005). LeuT transmembrane segments 1 and 6 are involved in substrate interaction and also coordinate sodium ion binding (Merkle *et al*., 2018) (Figure 1.2A).

LeuT is proposed to function by an alternating access mechanism, the substrate binding site is alternately exposed to both sides of the membrane via induced conformational changes which control access to a central binding site (Zhang *et al*., 2018). Investigations analysing the structure of LeuT have revealed LeuT to have inward and outward conformations (Krishnamurthy and Gouaux, 2012). Furthermore, studies by Yamashita *et al*., 2005 and Singh *et al.,* 2008 revealed that LeuT in an outward-occluded conformation is bound by two sodium ions and a molecule of leucine. It's been proposed that conformational changes are only induced when both sodium ions and amino acid substrates are bound, or this mechanism prevents the uncoupled transport of amino acid or sodium ions (Zhang *et al*., 2018). Additional studies by Merkle *et al.* have proposed a LeuT transport mechanism model and illustrated the changes in LeuT structure conformations and their link with Gibbs free energy levels (Merkle *et al.*, 2018) (Figure 1.2B).
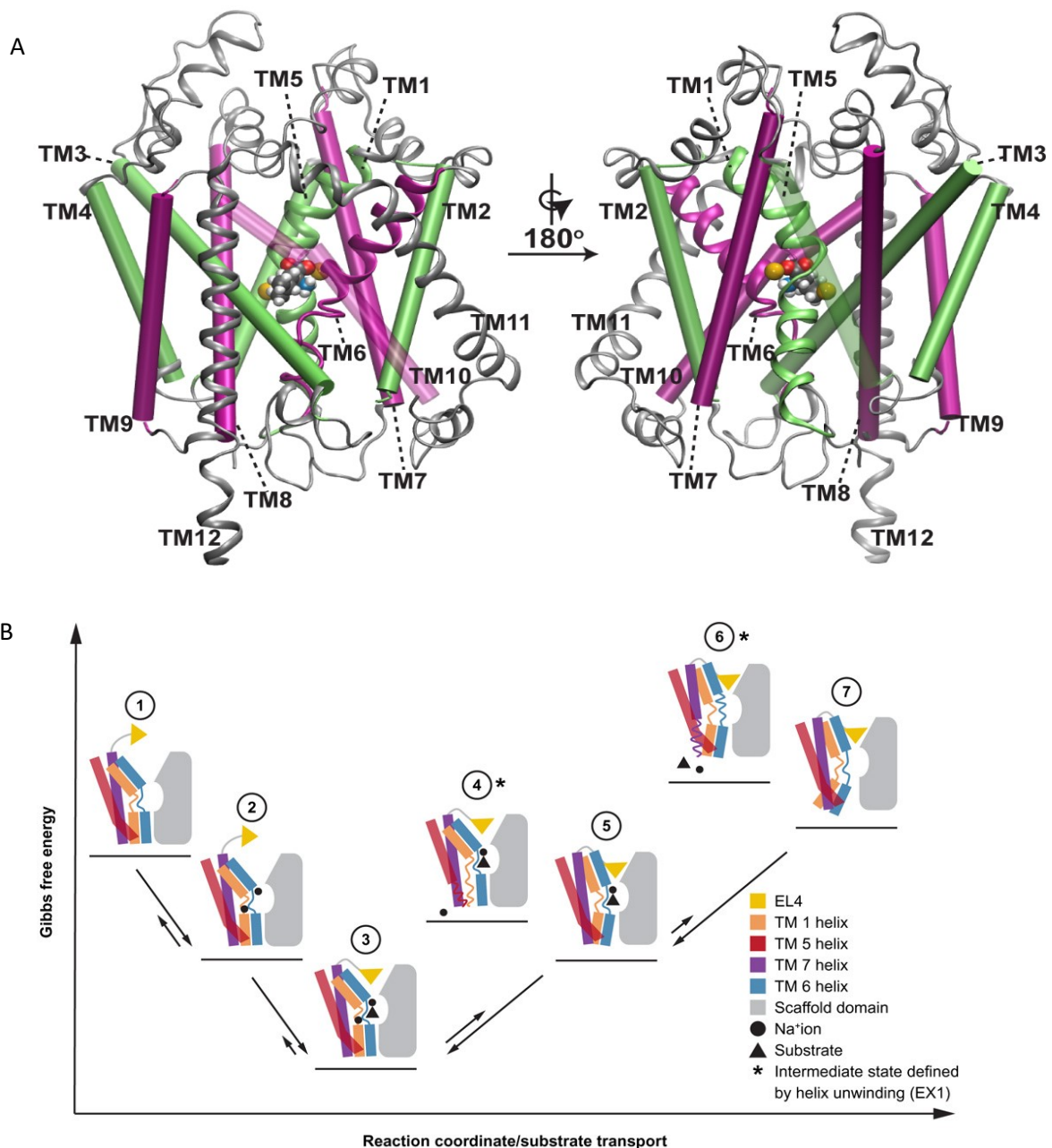
Figure 1.2 LeuT structure and conformational transitions during substrate transport*. A) LeuT structure. alignment and orientation is designed to illustrate LeuT positioning in the lipid bilayer plane. The upper side of the structure corresponds to the extracellular half of LeuT protein. Transmembrane helices 1 to 5 are shown in green and transmembrane helices 6 to 10 are shown in pink. The broken helices are shown in the core, transmembrane helices 1 and 6 are shown in ribbon pattern. Transmembrane helices 11 and 12 are shown in grey and ions bound in yellow. The leucine substrate is shown bound in the core and the colours present in substrate illustrate different elements (oxygen is red, carbon is grey, nitrogen is blue and hydrogen is white) (Shaikh, S.A. and Tajkhorshid, E. (2010) Modelling and dynamics of the inward-facing state of a Na$^+$/Cl$^-$ dependent neurotransmitter transporter homologue, PLOS Computational Biology 6(8). doi:10.1371/journal.pcbi.1000905) . B) LeuT conformational changes and associated changes in Gibbs free energy.(P. S. Merkle, K. Gotfryd, M. A. Cuendet, K. Z. Leth-Espensen, U. Gether, C. J. Loland,K. D. Rand (2018) Substrate-modulated unwinding of transmembrane helices in the NSS transporter LeuT. Sci. Adv. 4, eaar6179). Both figures reproduced under a Creative Commons licence agreement.*

Gibbs free energy analysis can be used to determine the amount of usable energy available in a system. Gibbs Free Energy levels can be calculated using the equation $\Delta G = \Delta H - T\Delta S$, where ΔH represents the change in enthalpy , ΔS represents the change in system entropy induced by reaction and T represents temperature (Cottis *et al.,* 2010). Gibbs free energy level changes can be determined by analysing the free energy levels at the start of a reaction such as the initial state/conformation of a protein during protein substrate interaction and at the final stage of a reaction such as molecule/substrate release. The changes in in Gibbs free energy can then subsequently be used to determine if the maximum usable energy was absorbed or released during the reaction/conformational changes in the protein from initial state to final state (Chemical thermodynamics , 2004). The changes in Gibbs free energy can also be used to determine the spontaneity and energetics of a reaction. If a reaction leads to a negative change in Gibbs free energy, then the reaction can occur spontaneously as this type of reaction releases energy and does not require an energy input. However, if a reaction led to a positive change in Gibbs free energy, then an energy input is required for the reaction to occur as this type of reaction absorbs energy (Khan Academy, 2015). Gibbs free energy levels change according to the type of reactions taking place.

Figure 1.2B displays LeuT structure at various stages of conformation and activity. Stage 1 displays LeuT adopting an outward-facing open conformation with reasonably high levels of Gibbs free energy in the absence of a substrate. Stage 2 illustrates LeuT maintaining an outward-facing open conformation upon Na^+ binding with a slight reduction in Gibbs free energy, implying stabilisation of the protein structure. Stage 3 illustrates LeuT in an outward-facing, substrate bound occluded state. Stage 3 shows that the binding of a substrate leads to a reduction in Gibbs free energy levels. Furthermore stage 3 also illustrates the closure of extracellular vestibule upon substrate binding and the obstruction of water from accessing substrate binding site by extracellular loop 4 (EL4). Stage 4 illustrates the unravelling of intracellular halves of transmembrane helices 1 and transmembrane helices 5, and how that leads to the creation of a solvent pathway from which a sodium ion can be released intracellularly. Stage 4 also illustrates an increase in Gibbs free energy. Stage 5 illustrates the release of sodium ion intracellularly and how that can induce LeuT to transition from an outward-facing, substrate bound occluded state to inward-facing, substrate bound occluded conformation. Stage 5 also illustrates a reduction in Gibbs free energy. Stage 6 illustrates that the unravelling of the intracellular part of transmembrane helices 7 facilitates the release of substrate and sodium ion. Stage 6 also illustrates an increase in Gibbs free energy. Stage 7 illustrates the isomerization of LeuT structure into an inward-facing open state following substrate release. Stage also illustrates a reduction in Gibbs free energy. Stages 1 to 3 show that binding of sodium ions and substrates leads to reduction of Gibbs free energy. Stages 4 and 6 show that unwinding of helices leads to an increase in Gibbs free energy. Stages 5 and 7 show that completion of transition leads to reductions in Gibbs free energy levels.

1.5 Atm1

The second protein of interest is NaAtm1, which is a bacterial homologue of Atm1 from *Novosphingobium aromaticivorans* (Lee *et al*., 2014*)*. *Novosphingobium aromaticivorans* is an aerobic and gram-negative bacterium*. Novosphingobium aromaticivorans* can be found in various places throughout the world including water, soil, and coastal plain sediments (Kaplan, 2004). Studies on *Novosphingobium aromaticivorans* have shown it to be genetically tractable and possess the ability to degrade aromatic compounds and metabolize xenobiotics (Kaplan, 2004; Linz *et al*., 2021).

Atm1 is an ATP binding cassette (ABC) transporter. ATP binding cassette transporters are a large family of integral membrane proteins and are found throughout the three kingdoms of life (Zutz, *et al*., 2009). ABC transporters are involved in various cellular processes, and facilitate the active transport of a wide range of solutes across cellular membranes including amino acids, peptides, lipids, polysaccharides, antibiotics, and toxins (Higgins, 1992; Dean, Rzhetsky and Allikmets, 2001). They are primary active transporters and use the energy from ATP hydrolysis to transport molecules against their concentration gradient. Although ABC transporters are present in various organisms, ABC transporter expression profiles and substrate specificities are highly diverse and differ with regards to individual cellular growth requirements (Zutz, *et al*., 2009). In *Saccharomyces cerevisia*e 22 ABC transporters are encoded for, the human genome encodes for 48 ABC transporters, whilst *E.coli* has 79 ABC transporters and the plant *Arabidopsis thaliana* has 130 ABC transporter genes (Gbelska, Krijger and Breunig, 2006; Jungwirth and Kuchler, 2006; Hwang et al., 2016). *Novosphingobium aromaticivorans* NaAtm1 is an orthologue of Atm1/ ABCB6/ ABCB7/HMT1 family of ATP Binding Cassette transporters, and it shares approximately 45% sequence identity with Heavy Metal Tolerance Factor-1 (HTM1), human ABCB7 and *S. cerevisiae* Atm1. Therefore, it is a valuable prokaryotic model for eukaryotic transporters and can be employed in ABC studies (Lee *et al*., 2014; Fan *et al.,* 2020).

ABC transporters can be separated into two distinct classes, ABC importers and ABC exporters. ABC importers are engaged in the uptake of nutrients and ABC exporters are implicated in export of toxic compounds. ABC importers typically function in conjunction with supplementary substrate-binding proteins which form complexes with solutes and help facilitate the transport of solutes over to ABC importers (Davidson and Chen, 2004). In *Saccharomyces cerevisiae* and other fungi and bacteria, ABC transporters have been shown to facilitate antimicrobial resistance and resistance against stress conditions (Zutz, *et al*., 2009; Jungwirth and Kuchler, 2006).

In eukaryotic organisms ABC transporters can be found located at the plasma membrane and in the intracellular membranes of Golgi apparatus, lysosomes, peroxisomes, endoplasmic reticulum, and mitochondria. The majority of eukaryotic ABC transporters function as exporters and are responsible for transporting a wide range of substances across cell membranes. ABC transporters in humans have been shown to be involved in various patho-physiological processes such as ion homeostasis of epithelial cells via cystic fibrosis transmembrane conductance regulator (CFTR/ABCC7), the release of

insulin from pancreatic beta cells via the sulfonylurea receptor (SUR1/2, ABCC8/9), cholesterol transport (ABCA1) and antigen processing and presentation via half transporters TAP1/TAP2 (ABCB2/ABCB3). ABC transporters have also been implicated in cancer cell multidrug resistance (Zutz, *et al*., 2009), predominantly through P-glycoprotein (ABCB1), multidrug resistance protein 1 (MRP1/ABCC1) or breast cancer resistance protein (BCRP/ABCG2).

In eukaryotes Atm1 is a mitochondrial exporter and exhibits an archetypal domain structure; two transmembrane domains which are responsible for offering selective solutes a passageway across the membrane and two nucleotide-binding domains which are responsible for generating energy via ATP hydrolysis and facilitating the directional transport of solutes (Zutz, *et al*., 2009).

ABC exporters in eukaryotes can be separated into two groups, full transporter, and half transporters. In half transporters one transmembrane domain is fused with one nucleotide binding domain and in order for the exporter to function two identical or different half-transporters have to assemble in order to form a functional homo or heterodimeric complex. Atm1 is a homodimeric transporter and furthermore surprisingly all mitochondrial ABC transporters studied thus far have all been homodimeric transporters (Chloupková *et al*., 2004; Hofacker *et al*., 2007).

In yeast Atm1 is localized on the inner mitochondrial membrane and it is involved in cellular iron homeostasis and is responsible for exporting unknown substrates into the cytosol for cellular iron regulation, iron-sulphur protein biogenesis and tRNA thio-modification (Kispal *et al*, 1997; Kispal, *et al*, 1999; Ellinghaus *et al*., 2021). Atm1 is approximately 70kDa in size and was the first mitochondrial transporter to be identified (Leighton and Schatz, 1995; Chloupková, *et al*., 2004).

In eukaryotes, the biogenesis of iron sulphur clusters is intricate, and it is comprised of three distinct and well-preserved separate systems; mitochondrial iron sulphur cluster assembly machinery, an exportation system facilitated by mitochondrial ABC transporters, and lastly a cytosolic iron sulphur cluster assembly system (Lill, Srinivasan and Mühlenhoff, 2014; Do *et al*., 2017).

Iron sulphur clusters are essential cofactors for iron sulphur cluster containing proteins which facilitate a variety of cellular processes. Iron-sulphur clusters are inorganic protein cofactors and are generally arranged via histidinyl and cysteinyl residues (Lill *et al*., 2015). Iron-sulphur clusters are known to function in electron transfer, regulation of gene expression and catalysis. Iron-sulphur clusters have also been proposed to act as sulphur donors for lipoate and biotin cofactor biosynthesis (Lill *et al*., 2015).

In eukaryotic organism's iron-sulphur proteins are involved in various essential processes and can be found in the nucleus, cytosol, and mitochondria (Lill *et al*., 2015). In the nucleus iron-sulphur proteins such as DNA polymerases and primases are involved in DNA replication and DNA repair. Furthermore iron-sulphur proteins such as ATP-dependent DNA helicases are involved in chromosome separation

or telomere length regulation (Lill and Mühlenhoff, 2008; Netz *et al*., 2012; Gari *et al*., 2012; Stehling *et al*., 2012; Stehling *et al*., 2013; Stehling, Wilbrecht and Lill, 2014; Paul and Lill, 2015; Lill *et al*., 2015).

Iron sulphur cluster dependent proteins such as DNA helicases have also been linked to hereditary disorders and conditions such as Xeroderma pigmentosum, Fanconi anaemia and Trichothiodystrophy (Lehmann, 2003). In the cytosol iron sulphur proteins are involved in tRNA (thio-) modifications, post-transcriptional regulation of the iron metabolism and amino acid biosynthesis. In mitochondria, iron sulphur proteins are involved in biosynthesis of lipoate, biotin and haem (Lill *et al*., 2015).

Atm1 is a homologue of human ABCB6 and ABCB7 and plant transporter atm3. ABCB6, ABCB7 and atm3 have previously been shown to be involved in iron homeostasis (Lill and Kispal, 2001; Pondarré *et al*., 2006; Cavadini *et al*., 2007; Zuo *et al*., 2017). Atm1 has been shown to bind glutathione (Kuhnke *et al*., 2006; Srinivasan, Pierik and Lill, 2014) and studies on *Novosphingobium aromaticivorans* orthologue NaAtm1 have shown it to bind glutathione derivatives and confer protection against mercury and silver toxicity when overexpressed in *E. coli* cells (Lee *et al*., 2014).

Glutathione is a tripeptide produced in the cytosol which is present in high levels in the body. It is involved in various processes including the detoxification of xenobiotic and endogenous compounds. Glutathione plays a vital role in protecting cellular macromolecules from endogenous and exogenous reactive species (Pizzorno, 2014). Glutathione is responsible for neutralising diverse oxidants such as hydroxyl radicals, carbon radicals, superoxide anions and nitric oxides. It is also involved in facilitating toxin excretion from cells and the body (Pizzorno, 2014) by the formation of glutathione S-conjugates, and it is essential for transporting mercury out of cells. Glutathione is also an important cofactor for various antioxidant enzymes glutathione peroxidase or glutathione-S-transferase and is involved in the regeneration of vitamins C and E (Pizzorno, 2014). Glutathione is required for cellular proliferation, apoptosis regulation and is indispensable for the protection and preservation of mitochondrial DNA and mitochondrial function as preceding studies have shown glutathione depletions to lead to progressive loss of mitochondrial function due to build up of mitochondrial DNA damage (Pizzorno, 2014).

Mitochondria are a major source of reactive oxygen species due to the mitochondrial respiratory chain and mitochondrial glutathione is the main form of defence against mitochondrial damage resulting from oxidative modifications. Mitochondrial glutathione can help maintain the mitochondrial redox environment and prevent damage by counteracting hydrogen peroxide and lipid hydroperoxides (Marí *et al*., 2009). Glutathione depletions have been implicated in various chronic degenerative diseases and disorders, including neurodegenerative disorders such as Alzheimer's, Huntington's, and Parkinson's diseases (Ballatori *et al.*, 2009). Glutathione depletion has also been implicated in pulmonary conditions such as asthma, and acute respiratory distress syndrome and cardiovascular conditions such as hypertension and myocardial infarction (Ballatori *et al*., 2009).

A direct link between dysfunction of mitochondrial ABC proteins and mitochondrial diseases has been proposed, for example dysfunction of mitochondrial ABC transporter ABCB7 has been shown to cause

X-linked sideroblastic anaemia with cerebella ataxia (Zutz, *et al*.,2009; Bekri *et al*., 2000). Furthermore, it has been proposed that ABCB7 may also be implicated in causing Refractory Anaemia with Ring Sideroblasts (Boultwood *et al.,* 2008).

Studies on yeast cells lacking Atm1 have shown the cells to have a severe growth phenotype as cells can only grow in the presence of fermentable carbon sources, indicating loss of oxidative respiration (Leighton and Schatz, 1995; Kispal, *et al*., 1997; Zutz, *et al*.,2009). Atm1 depletion has also been shown to result in a 30-fold increase in accumulation of mitochondrial iron levels (Kispal, *et al*., 1997). A depletion in Atm1 can also cause reactive oxygen species to be formed as non-ligated iron has redox properties. The consequent establishment of oxidative stress can subsequently lead to loss of the mitochondrial DNA and increased levels of glutathione and a substantial deficiency of apo forms of haem proteins (Zutz *et al*., 2009).

The bacterial homologue NaAtm1 used in this study has been identified as having a role in heavy-metal detoxification possibly due to exporting metalated glutathione species (Fan, Kaiser and Rees, 2020). It has been suggested NaAtm1 can bind and transport glutathione polysulfide, glutathione disulfide (GSSG), and glutathione trisulfide (GS-S-SG) (Schaedler et al., 2014). The findings from Schaedler et al., 2014 propose that the substrate of Atm1 must contain persulfide and glutathione, and that Atm1 can help facilitate the transport of glutathione polysulfide from the mitochondria to the cytosol. Furthermore ,glutathione is known to be involved in detoxification reactions (Daniel et al., 2020) and prokaryotic glutathione transferases (GSTs) enzymes are known to be involved in cellular detoxification (Allocati et al., 2008). It is therefore not surprising that *Novosphingobium aromaticivoran* bacteria can flourish in severely polluted environments as preceding studies have revealed *Novosphingobium aromaticivoran* to utilise Nu-class glutathione S-transferase enzymes to break down β-aryl ether bonds of lignin (Kontur et al., 2018). Lignin can be found in vascular plants, and it can potentially act as a renewable source of precious chemicals(Kontur et al., 2018).

The structure of NaAtm1 has been determined (Figure 1.3) at various stages of the transport cycle which has helped to build a model for the transport mechanism of Atm1 transporters (Lee *et al*., 2014).

The major binding site of glutathione disulfide is approximately 5 Å into the transmembrane region and dominated by transmembrane 5 and transmembrane 6 interactions. The binding site of glutathione disulfide is also accessible from the cytoplasmic side of protein (Lee *et al*., 2014). Substrate bindings lead to various interactions forming between carboxyl groups of glutathione disulfide and free amino groups of the NaAtm1 protein.

Transmembrane 3 and Transmembrane 6 residues which are responsible for interacting with GSSG are located close to helical irregularities. For example, a length of 310 helix is present between residues 314 and 317, a kink is present in transmembrane 6 conserved Pro 314 , a π helix is present in transmembrane 3 between residues 158 and 162 (Lee *et al*., 2014). It is proposed that these regions may experience conformational changes during the transport cycle. There are also non-polar

interactions between NaAtm1 and the GSSG substrate , these interactions are formed by the side chain residues of Leu 265 and Leu 268 and Gly part of GSSG. The side chains of Met 317 and Met 320 also interact with GSSG near the disulphide bond (Lee *et al*., 2014).

It is also proposed that there is a second GSSG binding site, which is located ≈5 Å away from the primary binding site and closer to the cytoplasmic surface (Lee *et al*., 2014). The physiological relevance of the second binding site in unknown however it proposed that Atm1 is capable of exporting glutathione-bound iron-sulfur clusters (Pearson and Cowan, 2021) and therefore, the second GSSG binding site may allow the binding of GSSG to iron-sulfur clusters (Lee *et al*., 2014).

The second binding site has conserved arginine residues 206 and 323 and it also has Arg 210. There are also two further pairs of Arg residues (conserved Arg 91 and variable Arg 313) which are located in the translocation pathway and closer to periplasmic side of protein (Lee *et al*., 2014). It is hypothesised that these additional pairs of Arg 91 and Arg 313 may be a binding site for substrates when orientated in an outward facing conformation (Lee *et al*., 2014).
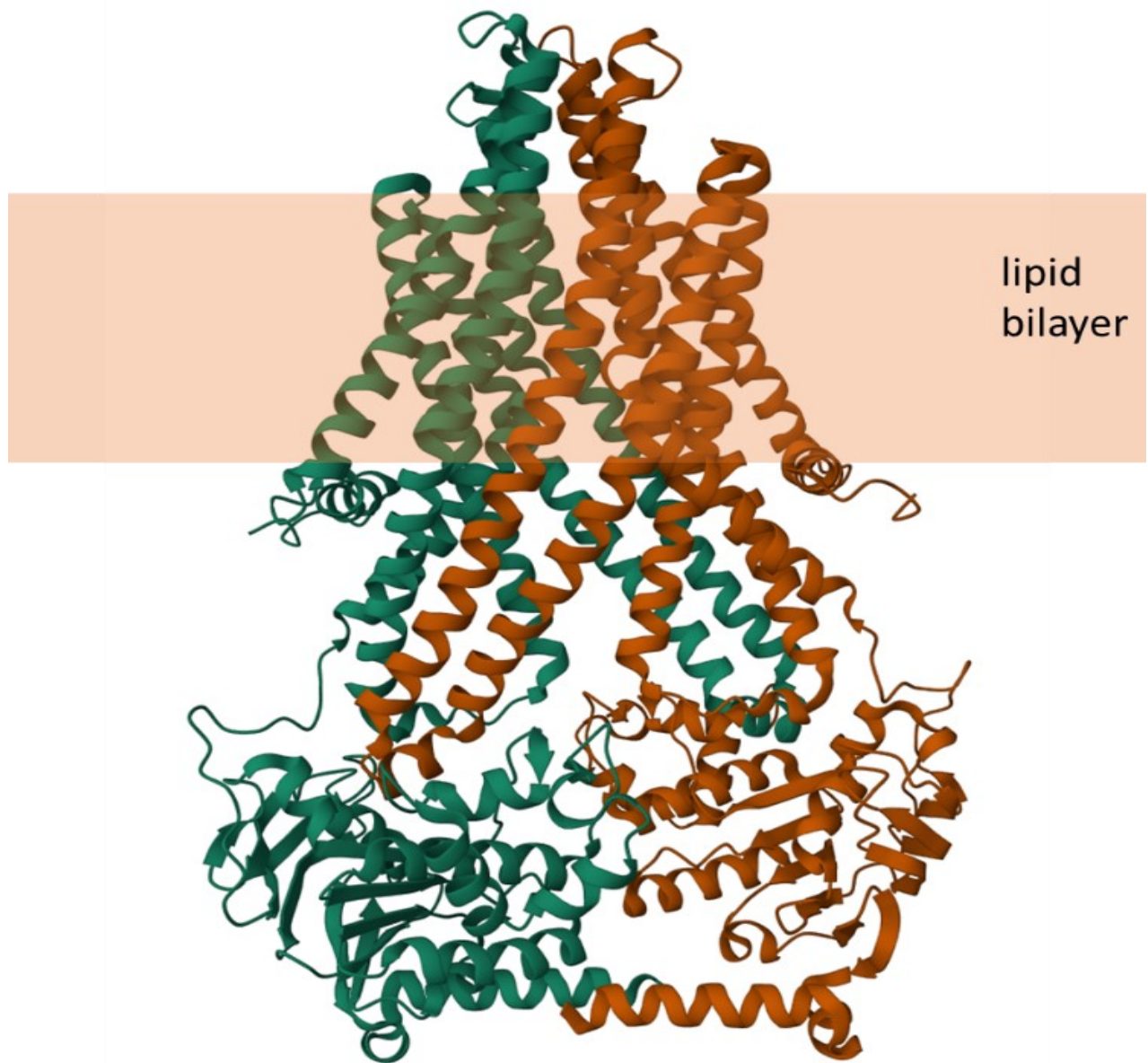
Figure 1.3 NaATM1 Structure. *NaAtm1 has a dimeric structure with membrane spanning domains towards the top and nucleotide binding domain towards the bottom. PDB ID: 4MRN. https://doi.org/10.2210/pdb4mrn/pdb .(Lee et al., 2014).*

1.6 Using SMALP isolated proteins for drug discovery

Although SMALP purified proteins have been shown to be applicable for many downstream applications, there have been limited reports to date of using SMALP purified membrane proteins for drug discovery using the techniques of surface plasmon resonance (SPR) or microscale thermophoresis (MST).

Surface plasmon resonance (SPR) is a commonly used technique that is typically employed to analyse protein ligand interactions (Bakheet and Doig, 2009). SPR has traditionally been used for drug screening, antibody engineering and analysis of mechanisms of molecular recognition (Cunningham and Wells, 1989; Wu *et al.*, 2007).

The SPR technique employs optical methods to analyse and quantify the changes observed in the refractive index of mediums in close vicinity to the surface of gold-coated biosensor chips (Patching, 2014). In a typical SPR experiment, one of the binding components referred to as ligand is immobilized on the biosensor surface and the other binding component known as analyte is injected across the biosensor surface at various concentrations and flow rates (Cooper, 2004; Besenicar *et al.*, 2006) (Figure 1.4).

The SPR technique examines the binding of analyte molecules to immobilized ligand by detecting the changes in the refractive index of the ultra-thin boundary layer that is in proportion to the amount of ligand + analytes present (Glück, Koenig and Willbold, 2011). The binding of analyte molecules to immobilised ligand leads to an increase in the amount of mass material bound to the surface of the chip and this increase in mass subsequently leads to a change in the angle of the polarised reflected light.

In SPR, in a specific angle of incidence, a portion of photons can interact with free electron groups in the metal surface (Nguyen *et al.*, 2015; Motsa and Stahelin, 2023). The interaction of photons with outer shell gold electrons leads to photons being absorbed and energy being transferred to the gold electrons. Subsequently gold electrons move due to excitation and transform into electron density waves referred to as surface plasmons (Nguyen *et al.*, 2015). Surface plasmon resonance arise as a result of incident light photons striking the surface the metal. Surface plasmons spread parallel to the gold surface. The plasmon oscillations subsequently create an electric field approximately 300 nm from the sample solution and gold metal boundary (Nguyen *et al.*, 2015; Motsa and Stahelin, 2023).

In an SPR machine, a high-reflective index glass prism is used to employ incident light. The specific angle at which resonance arises is dependent on the refractive index of the media near the gold metal surface (Nguyen *et al.,* 2015; Motsa and Stahelin, 2023). If there is a change in the refractive index of the sensing media due to molecule binding, plasmons will not be created. Therefore, in SPR, binding interactions are detected by measuring the changes in the reflected light and surface concentrations determined by observing the intensity of reflected light or tracing shifts in resonance angles. In SPR,

response/resonance units (RU) are utilised to portray changes in signal and 1 RU is equal to a 10−4-degree shit in critical angle (Nguyen *et al.*, 2015; Motsa & Stahelin, 2023).
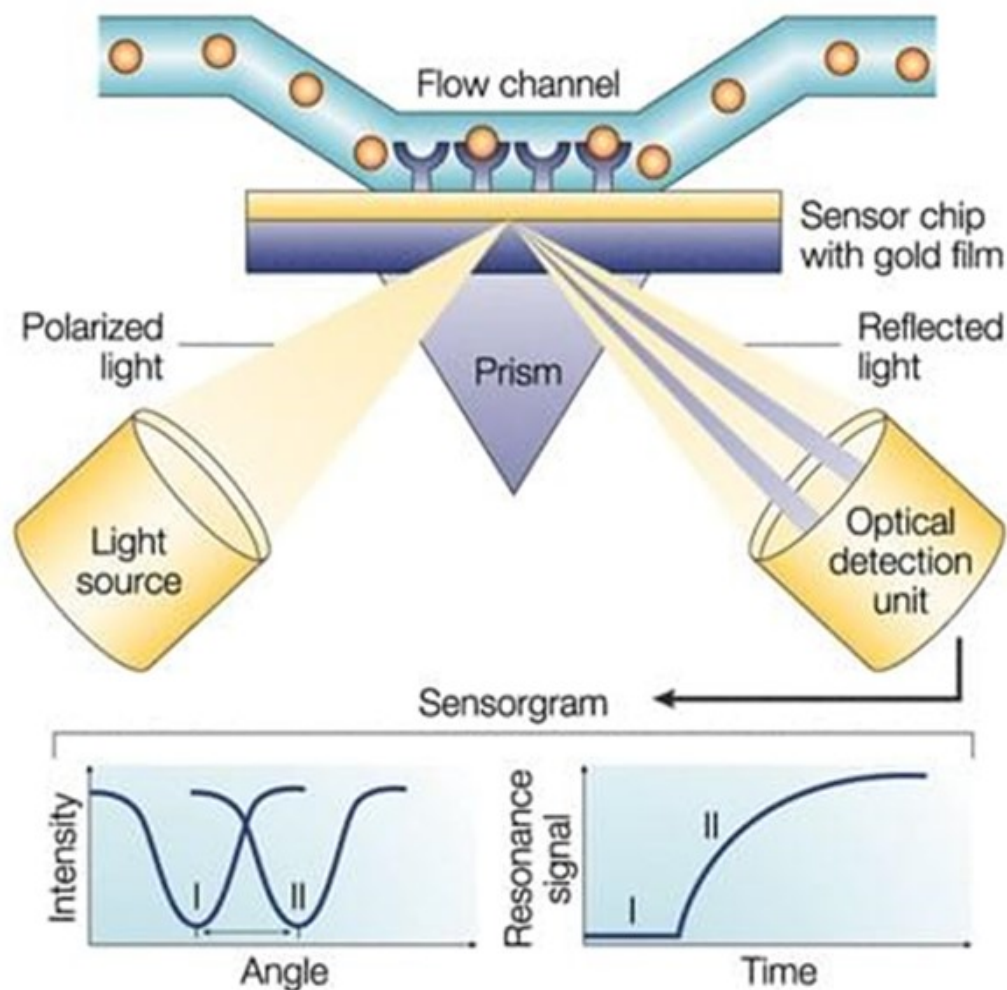
Figure 1.4 Surface Plasmon Resonance spectroscopy. Schematic diagram outlining the key features of SPR, and how they lead to the sensorgrams obtained. (Santos, A.O.; Vaz, A.; Rodrigues, P.; Veloso, A.C.A.; Venâncio, A.; Peres, A.M. (2019) Thin Films Sensor Devices for Mycotoxins Detection in Foods: Applications and Challenges. Chemosensors 7, 3. https://doi.org/10.3390/chemosensors7010003). Image reproduced under a Creative Commons licence.

The SPR technique has many advantages over alternative traditional methods of analysing protein ligand interactions. SPR analysis require small quantities of ligands and analytes, it also permits label free analysis of proteins in real time, and it can be used to measure binding kinetics and equilibrium constants (Glück, Koenig and Willbold, 2011). Furthermore, the SPR technique is very sensitive and can have a sensitivity of up to 1 nM for 20 kDa proteins (Englebienne *et al.*, 2003). The SPR technique can also be automated and therefore increase sample throughput (Grote *et al.*, 2005; Ahmed *et al.*, 2010). SPR permits analysis of real time reversible molecular interactions, and allows a wide variety of data types to be collected , for example the specificities of individual interactions, binding affinities, and binding levels. SPR analysis also allows the dissociation and association rate constants to be

determined and attain information on thermodynamic parameters such as entropy, enthalpy, and activation energy (Bakhtiar, 2012).

The SPR technique is also very versatile and applicable to various molecular systems. For example, it has been employed in vaccine design analysis (Hearty *et al*., 2010), DNA-drug binding analysis (Wolf *et al*., 2007), antibody–antigen interaction analysis (Ramakrishnan *et al*., 2009) and protein–carbohydrate interaction analysis (Smith *et al*., 2003).

However, the SPR technique also has limitations, for example one of the components of the molecular interaction have to be immobilised on the sensor chip surface and this can prove problematic as various conditions have to considered and optimised, in order to attain desired immobilisation levels. The molecular weight of the target component , the presence of any reactive groups , the stability and purity of component, pH levels and ion concentration of buffers, all have to be considered (Ezzati Nazhad Dolatabadi and de la Guardia, 2016).

Another disadvantage of the SPR technique is that sensor surface cannot easily distinguish between non-specific and specific interactions, and this can lead to false positive results (Ahmed *et al*., 2010). Furthermore, materials can non-specifically bind to the sensor chip surface and subsequently interfere with SPR analysis. Therefore, control samples are often required to correct for any nonspecific binding which may occur (Rich and Myszka, 2004). Also, SPR is mass sensitive and therefore the methodology is very sensitive to components with a larger molecular weight however the binding of smaller molecules or low molecular weight compounds, such as drugs, is harder to analyse (Ahmed *et al*., 2010). Finally, another challenge presented by the SPR technique is that the sensor chips employed in SPR studies have a limited surface area and therefore can limit the amount of sample being loaded onto the sensor chip, especially when working with larger molecules. This subsequently can lead to lower concentrations of components being immobilised and low immobilisations levels can prevent binding interactions from being detected.

It is important to analyse and quantify binding kinetics of novel drugs as minute differences in binding kinetics can have huge significance with regards to the applicability of novel drugs (Maynard *et al*., 2009). Binding kinetics can impact both the potency and dosing of drugs in *in vivo* environments. Therefore, binding kinetics analysis could be used to screen out ineffective drugs and select appropriate molecules for further development (Maynard *et al*., 2009). It's been shown that site directed kinetics analysis of variants could be used to analyse binding and shed light on the dynamics and mechanisms of binding (Rickert, 2004). It is therefore evident that binding kinetic analysis is vital for screening potential drugs and identifying potential therapeutic target.

Microscale Thermophoresis (MST) is an alternative , innovative technique for measuring protein-ligand interactions. MST is cost effective, and it can be used to study molecular interactions in solutions (Baaske *et al*., 2010; Jerabek-Willemsen *et al.,* 2011; Duhr, Arduini and Braun, 2004).

MST is an efficient method and consumes little time and sample volumes. MST also allows for free choice of buffers and doesn't require immobilisation of target proteins. MST functions by utilizing thermophoresis to study molecular interactions (Duhr, Arduini and Braun, 2004; Baaske *et al.*, 2010; Jerabek-Willemsen et al., 2011). Thermophoresis/Soret effect is a transport force which arises in mixtures of particles and fluids in the presence of a temperature gradient (Hemmat Esfe *et al.*, 2020). The thermophoresis phenomenon describes the movement of particles in a temperature gradient from hot regions to cold regions (Jerabek-Willemsen *et al.*, 2014). MST can be used to analyse and determine dissociation constants, stoichiometry, and thermodynamics.
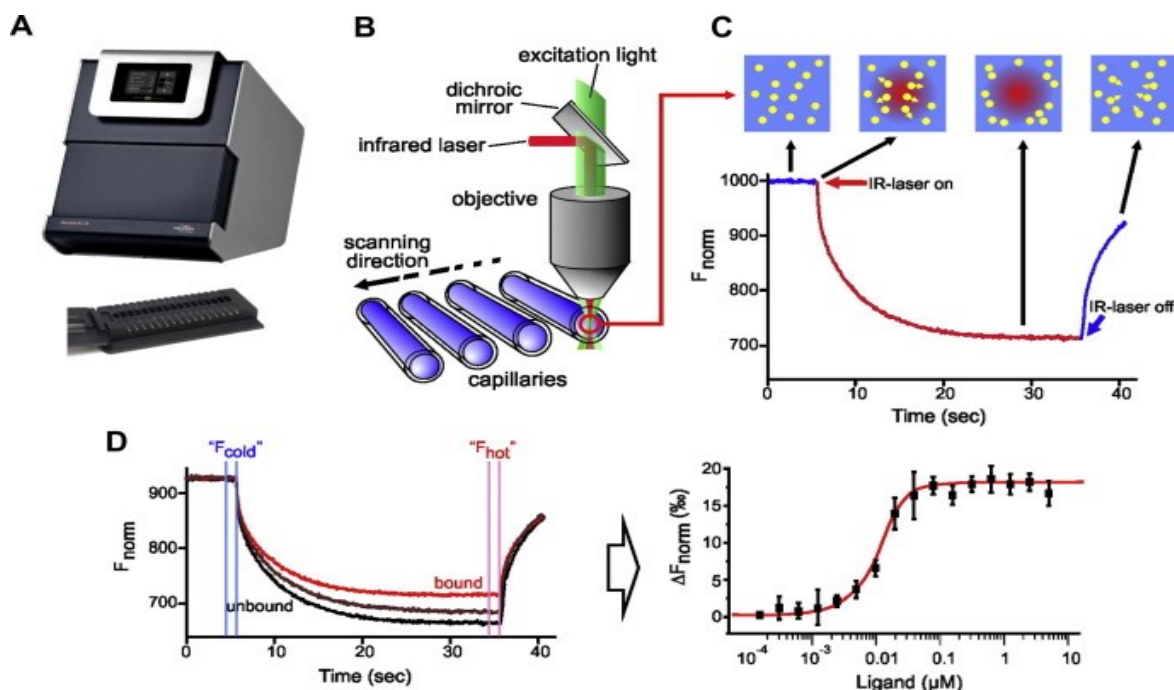
Figure 1.5 Microscale Thermophoresis. A) The Monolith NT.115. B) MST optics set up. C) A typical example of MST trace. D) Example of data from a typical binding experiment. Reprinted from Journal of Molecular Structure, 1077 , Moran Jerabek-Willemsen, Timon André, Randy Wanner, Heide Marie Roth, Stefan Duhr, Philipp Baaske, Dennis Breitsprecher, MicroScale Thermophoresis: Interaction analysis and beyond, 101-113,2014 , with permission from Elsevier.

In a typical MST experiment, samples are loaded into capillaries and inserted into an MST device. A temperature gradient is then created using an infrared laser. The generation of the temperature gradient leads to the thermophoretic migration of molecules. The movement of molecules is then tracked by fluorescence optics using the fluorescence of fluorophores which are attached to one of the binding components in the molecular interactions (Zillner *et al.*, 2011; Schubert *et al.*, 2012) (Figure 1.5). The movement of molecules is affected by charge, size and hydration shells (Braun and Libchaber, 2002; Duhr and Braun, 2006). Interactions between large proteins and small ligands, such as short peptides, which only entail slight changes in size and charge, can still noticeably affect the thermophoretic migration due to changes in the hydration shell (Plach, Grasser and Schubert, 2017).

1.7 Aim & objectives

In this project, the aim was to optimise lipid nanoparticle extracted and purified LeuT and/or Atm1 for drug screening and development using SPR and MST techniques.

Objectives included:

- Optimising conditions for immobilisation of LeuT/Atm1-SMALPs on to SPR chips, and measurement of binding interactions with substrates or inhibitors.
- Fluorescent labelling of LeuT/Atm1-SMALPs for analysis by MST, and measurement of binding interactions with substrates or inhibitors.
- Investigation of alternative polymers for LeuT and Atm1 solubilisation and purification, that may overcome some of the current limitations or facilitate easier immobilisation and/or labelling.

2. Methods & Materials

2.1 Preparation and expression of LeuT or NaAtm1 in *E. coli* cells

Plasmid pET16b-LeuT was a kind gift from Prof. Harald Sitte, Medical University of Vienna. pJL-H6-NaAtm1 was a gift from Douglas Rees (Addgene plasmid #78308; http://n2t/addgene:78308). BL21 *E. coli* (DE3) cells which had already been transformed with vector pET16b-LeuT or pJL-H6-NaAtm1 were used to grow a 5 ml culture overnight in LB (Luria broth) supplemented with 100 µg/ml ampicillin, at 37°C, 200 rpm. From this point forward NaAtm1 will simply be referred to as Atm1.The overnight culture was then used to inoculate two flasks containing 500ml LB supplemented with ampicillin (100 µg/ml). The cultures were incubated at 37°C, 200 rpm for several hours; a sample was extracted every hour and its OD (optical density) measured at 600nm until optical density of 0.6 was reached. The expression of LeuT protein was then induced by adding 0.5mM IPTG ,and then incubating LeuT culture at 37°C for 3 hours at 200rpm and then at 25°C, 200rpm overnight. The expression of Atm1 protein was also induced by adding 0.5mM IPTG however the Atm1 cultures were directly incubated at 37°C at 200rpm overnight. The cells were harvested by centrifugation at 5514g for 10 minutes at 4°C, following which they were stored at -20°C. *E. coli* pellets were resuspended in phosphate buffered saline (137 mM NaCl, 2.7 mM KCl, 8 mM Na_2HPO_4, and 2 mM KH_2PO_4, pH7.4) and centrifuged at 3220g for 10 minutes at 4°C, then resuspended in homogenisation buffer (50mM Tris pH 7.4, 250 mM sucrose, 0.25 mM $CaCl_2$) supplemented with a mixture of protease inhibitors (benzamidine (1.3 µM) , leupeptin (1.8 µM) and pepstatin (1 µM)). The cells were then disrupted using sonication (five 30 second cycles with 20 seconds intervals). Cell debris was removed from the solution by centrifugation at 726g for 15 minutes at 4°C. Finally, membranes were harvested by ultracentrifugation (100000g, 20 minutes, 4°C) and the pellets were suspended in Purification Buffer A for LeuT (20 mM Tris pH8, 150 mM KCl) or Purification Buffer B for Atm1 (20 mM Tris, pH8, 150mM NaCl) at a concentration of 60 mg/ml (wet weight of pellet). The membrane solution was then aliquoted in 2ml aliquots and stored at -80°C (Morrison *et al*., 2016).

2.2 Preparation of SMA2000

SMA2000 polymer was a kind gift from Cray Valley (Exton, PA, USA). SMA2000 polymer was provided as a styrene–maleic anhydride copolymer and therefore required conversion to styrene and maleic acid. To begin the conversion process 25g of Styrene–maleic anhydride copolymer was transferred into a 500 ml round bottom flask and 250 ml of 1M NaOH added to the flask. Next 0.5 g of anti-bumping granules were added to the round bottom flask and the flask transferred onto a heating mantle with the condenser coil attached. The condenser was then connected to a water supply and water flow ensured. The styrene–maleic anhydride copolymer and NaOH mixture was then gently heated until boiling point was achieved. Following which the heat levels were adjusted to allow the solution to maintain a steady boil rate for 2 hours. Subsequently the refluxed solution was cooled to room temperature whilst the condenser was still connected to flask and water flow maintained. The cooled solution was aliquoted

into two 500 ml centrifuge bottles and 1M HCl slowly added, at a ratio of approximately 1ml HCl per 6ml of polymer solution, to precipitate the polymer. Next distilled water was added to the centrifuge bottles until maximum bottle capacity had been reached. The precipitate-water mixtures were centrifuged at 11,000 g for 15 minutes and the resultant supernatants carefully removed without disturbing the precipitates. The precipitates were resuspended in distilled water and centrifuged again at 11,000 g for 15 minutes. This process was repeated 4 times. The precipitate pellets were dissolved in 125 ml of 0.6 M NaOH per bottle, and the pH adjusted to pH8. The solution was then transferred into round bottom flasks and frozen at - 20°C for 24 hours. The round bottom flasks containing the frozen solutions were then freeze dried into a dry powder using an Edwards Modulyo freeze dryer and stored at room temperature (Morrison *et al*., 2016; Lee *et al*., 2016).

2.2 Preparation of Esterified polymers

The partially esterified polymers (SMA 1440, SMA 17352 and SMA 2625) were a kind gift from Cray Valley (Exton, Pennsylvania, USA) and prepared according to the manufacturer guidelines. 10% (w/v) solutions of the appropriate esterified polymers were mixed with 1 M NaOH and heated at 50°C and stirred until all polymer crystals had dissolved fully. The solutions were then placed in SnakeSkin dialysis tubing with a molecular weight cut-off of 3 kDa. The solutions were then dialysed at 4°C against distilled water. The distilled water was replaced every 2 hours until the polymer had reached pH8. Lastly, the solutions were extracted from the dialysis tubing and freeze dried using an Edwards Modulyo freeze dryer (Hawkins *et al*., 2021).

2.3 Preparation of Benzylamine Polymer

The Benzylamine modified polymers were a kind gift from Professor Bert Klumperman (Stellenbosch University). The polymers were supplied ready for use and required no further preparation.

2.4 Solubilisation of *E. coli* membranes

SMA2000 (or alternative polymers) were resuspended in Purification Buffer A (150mM NaCl 20mM Tris pH8) for LeuT, or Purification Buffer B (150mM KCl 20mM Tris pH8) for Atm1, to give final concentrations of 5% (w/v). Samples from each solution were then mixed with an equal volume of *E. coli* membranes at 60 mg/ml (wet pellet weight), to give final concentrations of 2.5% (w/v) SMA and 30 mg/ml membrane (Gulati *et al* 2014; Morrison *et al* 2016). This mix was transferred to a shaking platform for an hour at room temperature. For detergent solubilisation, DDM was made up at 4% (w/v) in purification buffer A and then mixed with *E. coli* membranes in a 1:1 ratio, to give final concentrations of 2% (w/v) DDM and 30 mg/ml membranes. This was also transferred to a shaking platform for an hour at room temperature. Samples were then centrifuged at 100000g, for 20 minutes at 4°C. Following centrifugation, the supernatants containing solubilised proteins were harvested.

2.5 Nickel Affinity Purification

His Pur Ni-NTA resin (ThermoFisher) was initially washed with distilled water and then purification buffer A/B and subsequently mixed with solubilised proteins (100 µl resin bed volume/ 1ml solubilised protein), and then left on a rotating apparatus overnight at 4°C. The following day the mixture was added to a gravity flow column (Macherey-Nagel) and the flow through (unbound material) collected. The nickel resin was then successively washed with different volumes of purification buffer A/B with increasing concentrations of imidazole. For detergent purification, the purification buffers were supplemented with DDM to give final concentrations of 0.1% DDM, in order to maintain the concentration above the critical micelle concentration (Morrison *et al*., 2016). At first nickel resin was washed 5 times with 10 resin bed volumes of purification buffer A/B supplemented with 20mM imidazole , then it was washed twice with 10 resin bed volumes purification buffer A/B supplemented with 40mM imidazole and finally it was washed once with purification buffer A/B supplemented with 60mM imidazole (1 x resin bed volume). Proteins were then eluted by 6 washes of purification buffer A/B supplemented with 200mM imidazole (1/2 bed volume per elution). Samples from each fraction were then mixed with 5xLSB (0.25 M Tris-HCl, pH 6.8 ,0.5 M DTT ,10 % SDS ,50 % Glycerol, 0.5 % Bromophenol blue) and run on a 10% SDS-PAGE alongside marker (Pierce unstained markers) and solubilised protein samples. SDS page gels were stained using Instant Blue (Expedeon) and analysed using Image J. The eluted protein samples were then pooled together and stored at 4°C (Morrison *et al*., 2016).

2.6 Purified Protein Quantification

The concentration of purified LeuT/Atm1 was quantified using SDS-PAGE. Samples (10 µl and 20 µl) of purified LeuT/Atm1 were run on SDS-PAGE alongside BSA standards (0.25, 0.5, 0.75, 1, 1.25 µg) as described in (Rothnie *et al.,* 2004), because this method is not affected by imidazole, lipids or detergent/polymer. Gels were stained using Instant Blue (Expedeon). Following staining the intensity of bands on SDS-PAGE gels were analysed using densitometry (Image J) and a BSA standard curve developed, using Microsoft Excel. The BSA standard curve was used to calculate the concentration of purified LeuT/Atm1. To estimate the purity of LeuT/Atm1, an entire lane of SDS-PAGE gel was analysed using densitometry (Image J); purity was estimated by examining the intensity of LeuT/Atm1 as a percentage of total lane intensity present (Morrison *et al*., 2016). The different values obtained by detergent DDM and SMA2000/SMA-SH/SMASH-Biotin/DIBMA solubilisation were then compared.

2.7 Magnesium Sensitivity Assay

Purified LeuT/Atm1 protein samples were mixed with increasing concentrations of magnesium chloride (0-10 mM) and incubated at room temperature for 10 minutes. Following which the samples were centrifuged at 100000g, for 20 minutes at 4°C. The supernatants containing soluble proteins were extracted and the pellets resuspended in the same volume of purification buffer A/B. Samples were then prepared from the supernatants and the resuspended pellets and run on SDS-PAGE alongside

marker. SDS PAGE gels were stained with Instant Blue and analysed with densitometry. The percentage of LeuT/Atm1 proteins in supernatant or pellets were then assessed using densitometry values (Morrison *et al.,* 2016).

2.8 Preparation of DIBMA polymer

A 50ml sample of 25 % (w/v) Sokalan CP9 (a kind gift from BASF) was transferred to snakeskin dialysis tubing with a molecular weight cut-off of 3000 Da. Next the dialysis tubing was placed inside a large beaker containing a 1 litre solution of purification buffer A/B. The beaker was then transferred to a magnetic stirrer and dialysis allowed to take place overnight at 4°C. The following day the pH of dialysis buffer and volume of DIBMA solution inside dialysis skin was analysed. Finally, the DIBMA solution was extracted from dialysis tubing and freeze dried using an Edwards Modulyo freeze dryer and analysed by FTIR and NMR by Dr Aiman Gulamhussein to ensure it was the desired product (Gulamhussein *et al.*, 2020).

2.9 Modification of SMA2000 to SMA-SH

One gram of SMA2000 was dissolved in 10mls of 100mM, pH 7, MES buffer. Next 72 µM solutions of EDC (1-Ethyl-3-[3-dimethylaminopropyl]carbodiimide hydrochloride) and Sulfo-NHS (N-hydroxysulfosuccinimide) were prepared by dissolving 14mg of EDC and 16mg of Sulfo-NHS in 500µl solutions of 75mM MES, pH 5.8, 25% ethanol buffer. The SMA2000 solution was then transferred to a magnetic stirrer and the EDC and Sulfo-NHS solutions added to SMA2000 solution dropwise. Once all of the EDC and Sulfo-NHS solutions had been added, the SMA2000, EDC and Sulfo-NHS mixture was incubated at room temperature for 20 minutes whilst stirring. A 144 µM solution of cysteamine dihydrochloride was then prepared by dissolving 32mg of cysteamine dihydrochloride in 500µl solution of 25mM MES, pH 7, 25% ethanol buffer. Following the 20-minute incubation period, the cysteamine dihydrochloride solution was added to the SMA2000, EDC and Sulfor-NHS mixture dropwise with 60 seconds intervals. During cysteamine dihydrochloride addition, the SMA2000, EDC and Sulfor-NHS mixture was observed for aggregation and drops of 96% ethanol added when aggregation detected. Following cysteamine dihydrochloride addition, the mixture was covered with foil and incubated at room temperature whilst stirring for 16 hours. Following incubation, the SMA2000, EDC, Sulfor-NHS and cysteamine dihydrochloride mixture was dialysed at room temperature for an hour against a 100-fold excess volume of 20mM Tris, pH8 buffer using dialysis tubing with a molecular weight cut-off of 3000kDa. The dialysis process was subsequently repeated by exchanging used dialysis buffer with new batch after an hour and continuing dialysis for another 3 hours. Following successful dialysis, the SMA-SH solution was extracted from dialysis tubing and freeze dried using an Edwards Modulyo freeze dryer (Schmidt and Sturgis, 2018).

2.10 FTIR Analysis of SMA2000 and SMA-SH

SMA2000 and SMA-SH polymer samples were analysed separately using a bench top FTIR machine. A background scan was conducted in order to determine how much of the original IR intensity in percent transmittance was left after passing through the samples. The polymer samples in solid form were placed in small quantities onto the crystal and a force applied using the FTIR force arm to ensure good contact between the samples and the crystal surface. The samples were then scanned to acquire data with a scan range of $4000 - 650cm^{-1}$. The crystal was cleaned with methanol and a contamination check was conducted to ensure the crystal was properly cleaned.

2.11 SMA-SH Labelling

Dried SMA-SH polymer (0.2g) was dissolved in 2ml of 20mM Tris, pH8 buffer and 36μM TCEP was then added to dissolved SMA-SH. The SMA-SH and TCEP mixture was then incubated at room temperature for 15 minutes and then dialysed against a 10-fold excess volume of 20mM Tris, pH8, 200mM NaCl buffer for 2 hours at room temperature using dialysis tubing with a molecular weight cut-off of 3000 kDa. A 5mg/ml stock of biotin maleimide was then made in DMSO and immediately after dialysis a 1.3-fold excess added to the SMA-SH and TCEP mixture. Following maleimide addition the solution mixture was incubated at 22°C for 24 hours in 20mM Tris, pH8 200mM NaCl buffer. Next Micro Bio-spin columns from Biorad were used to remove unreacted biotin maleimide from the solution mixture. The column storage buffer was removed from columns by centrifugation at 1000g for 60 seconds, the columns were then loaded with 500μls of 20mM Tris, pH8 , 200mM NaCl buffer and centrifuged for 2 minutes at 1000g , and finally the solution mixture was loaded onto the columns and centrifuged at 1000g for 4 minutes . Following centrifugation, the labelled SMA-SH solution was collected and stored in at -4°C (Schmidt and Sturgis, 2018).

2.12 Tryptophan Fluorescence Quenching binding assays

The binding of substrates to purified LeuT was analysed using a PerkinElmer LS55 fluorescence spectrometer. Stock concentrations (100mM) of Leucine and Alanine were prepared by dissolving 13.1mgs of Leucine and 8.9mgs of Alanine in 1ml aliquots of distilled water. The stock concentrations of Leucine and Alanine were then used to make a series of concentrations ranging from 1mM to 0.5μM (1mM, 10μM, 5μM, 1μM, 0.5μM). The binding experiments were performed at room temperature with a scan speed of 100nm/min, and upon excitation at 280 ± 10 nm, emission spectra of samples were recorded between 310 -400 ± 20 nm. At first the fluorimeter cuvette was loaded with just a 100μl sample of SMA2000 purified LeuT and fluorescence analysed. The buffer was then supplemented with 190mM sodium chloride. and the fluorescence of sample was measured again, as LeuT is known to bind sodium ions in addition to amino acids. A series of Leucine/Alanine additions made at increasing concentrations to give a wide range of LeuT substrate concentrations (5nM – 500nM). The fluorescence of purified LeuT samples was measured after each addition of Leucine/Alanine. Control experiments

were performed utilising N-acetyltryptophanamide instead of purified LeuT but using identical methodology and concentrations of substrates to account for dilution factors, scattering and the inner filter effect. The fluorescence quenching percentage values obtained from control experiments were subtracted from values obtained from experiments utilising purified LeuT and the subsequent values were analysed via GraphPad Prism to generate binding affinity (Kd) and maximum specific binding (Bmax). The analysis of DDM and DIBMA extracted and purified LeuT was performed in identical method. Binding assays for purified Atm1 were carried out in a similar fashion, except GSH was used as substrate, at much higher concentrations (10-3180 µM), because the affinity for GSH is known to be low (Lee *et al.,* 2014).

2.13 Immobilisation of SMA2000, DIBMA and DDM purified LeuT for SPR

A 1 litre solution of Immobilisation buffer (150 mM NaCl, 20 mM Tris pH 8.0 and 0.005% Tween 20) was prepared and filtered for LeuT Immobilisation. A series S NTA sensor chip was inserted into the Biacore 8K machine and the system primed into the prepared buffer. A standard NTA capture method was used which consisted of several steps. The first step of the NTA capture method entailed conditioning of the NTA sensor chip via a one-minute wash with 350 mM EDTA, this was followed by cleansing of the flow system by immobilisation buffer washes. The NTA sensor chip surface was then loaded with $NiCl_2$ via a 1-minute loading of 0.5 mM $NiCl_2$. The loading of $NiCl_2$ onto NTA sensor chip was followed by a flow system wash with immobilisation buffer supplemented with 3mM EDTA. Next purified LeuT (20-40ug/ml) was diluted 1 in 2 using immobilisation buffer and Immobilisation onto NTA sensor chip attempted by a 10µl per min loading rate for7-minutes. Following LeuT Immobilisation another wash of the flow system was carried out using immobilisation buffer. The immobilisation methodologies of SMA2000, DIBMA and DDM purified LeuT for SPR were identical.

2.14 Leucine Binding analysis

New samples of purified LeuT were loaded onto NTA sensor chip surface following said protocol and the binding of leucine to immobilized LeuT was quantified via the single-cycle kinetics (SCK) method by setting up a five-point titration of leucine using 1 in 3 dilutions in assay buffer starting from 500 nM. Leucine binding analysis methodologies were identical for SMA2000, DIBMA and DDM purified LeuT. The data obtained from Immobilisation and ligand binding experiments was analysed by utilising the Biacore 8K software to view sensorgrams. The loading levels of LeuT were calculated manually as detailed examination via evaluation software of binding affinities or kinetics was not required.

2.15 Buffer optimisation for NTA capture of SMA and DIBMA solubilised LeuT

A 1 litre solution of immobilisation buffer comprised of 150 mM NaCl, 50 mM Sodium Phosphate, pH 8.0 and 0.005% Tween 20 was created and used as base buffer for buffer optimisation experiments. The effects of pH and NaCl concentrations on LeuT Immobilisation were investigated by creating 12

buffers of varying NaCl concentration (100mM, 200mM, 300mM, 400mM, 500mM) and pH (6.0, 6.5, 7.0, 7.5,8.0, 8.5,9.0) values by using concentrated stocks of NaCl (5 M), sodium phosphate (2 M pH 8.0), tris (2 M pH 8.0) and adjusting pH accordingly. Buffers exploring the effects of various pH were supplemented with 200mM NaCl concentrations and buffers exploring the effects of different NaCl concentrations had a pH of 8.0. All buffers created excluding buffers exploring the effects of pH at 8.0, 8.5 and 9.0 were additionally supplemented with 50mM Sodium Phosphate. Buffers exploring the effects of pH on Immobilisation at pH 8.0, 8.5 and 9.0 were supplemented with 50mM tris.

A series of S NTA sensor chip were inserted into the Biacore 8K machine and the system primed into prepared base buffer. A standard NTA capture protocol was then tweaked and employed to include a series of 'ABA' injections followed by regeneration injections to allow the testing of a series of buffer effects on LeuT Immobilisation without having to re-prime the system. The 'ABA' injection methodology was incorporated into protocol as it allowed the use of two different solutions with different pH or salt concentrations to be injected over the chip surface in the same cycle. The Immobilisation methodologies of SMA2000, and DIBMA purified LeuT for SPR were identical.

2.16 Immobilisation of SMA2000 and DIBMA solubilised and purified LeuT via anti-His capture kit

An anti-His capture kit was purchased from GE. Biacore 8K machine was primed into buffer (150 mM NaCl, 50 mM Sodium phosphate pH 7.5, 0.005 % Tween-20) and a CM5 chip inserted into machine .The anti-His antibody was then diluted in the sodium acetate buffer provided with the kit to 20 µg ml-1 and immobilized on the surface of CM5 chip as instructed in the kit provided. The LeuT ligand was then diluted 1 in 4 in running buffer and injected over the flow cell containing immobilised anti-his antibody at 10 µl min-1 for 600 seconds and response examined. The Immobilisation methodologies of SMA2000 and DIBMA purified LeuT for SPR were identical.

To investigate the effects of extended immobilisation time, and subsequent leucine binding an anti-His capture kit was employed in Biacore 8K machine as described above, however the immobilisation time of LeuT was doubled. The immobilisation of LeuT was followed by a blank injection of running buffer and then a 10 µM Leucine injection and binding observed. Antibody immobilisation was elucidated by Biacore 8K control software and therefore required no further analysis. The immobilisation of LeuT however required loading of data onto Biacore Insight Evaluation software and then manual analysis of captured levels. The data obtained from extended LeuT immobilisation experiment was also loaded onto Biacore Insight Evaluation software and then analysed manually. The blank and leucine injections were used to determine if binding response could be observed by subtracting blank response from leucine injection responses.

To try to improve immobilisation, the anti-His capture kit was also tested with a C1 chip inserted into machine . The anti-His antibody was then diluted in the sodium acetate buffer provided with the kit to 15 µg ml-1 and immobilized on the surface of C1 chip as instructed in the kit provided. The LeuT ligand was then diluted 1 in 2 in running buffer and injected over the flow cell containing immobilised anti-his antibody at 5 µl min-1 and response observed. The immobilisation of SMA-SH-LeuT and DDM-LeuT were also attempted on C1 chips utilising the aforementioned protocol. The immobilisation methodologies of SMA2000 and DIBMA purified LeuT for SPR were identical.

The Immobilisation levels of anti-His antibody were elucidated by Biacore 8K software and therefore required no further analysis and the immobilisation levels of LeuT were determined by loading data onto Biacore Insight evaluation software and then manually analysing captured levels.

2.17 NTA Capture-Couple Immobilisation of SMA2000, DIBMA and DDM solubilised and purified LeuT

A 1 litre solution of immobilisation buffer comprised of 500 mM NaCl, 50 mM Sodium Phosphate, pH 7.5 and 0.005% Tween 20 was prepared for LeuT Immobilisation. A series S NTA sensor chip was inserted into the Biacore 8K machine and the system primed into the prepared buffer. An NTA Capture-Couple method was used which consisted of several steps. The first step of the NTA capture method entailed conditioning of the NTA sensor chip via a one-minute wash of 350 mM EDTA, this was followed by cleansing of the flow system by Immobilisation buffer washes. The NTA sensor chip surface was then loaded with $NiCl_2$ via a 1-minute loading of 0.5 mM $NiCl_2$. The loading of $NiCl_2$ onto NTA sensor chip was followed by a flow system wash with immobilisation buffer supplemented with 3mM EDTA. Next the NTA sensor chip was treated with coupling solution (EDC+NHS) at 10 µl min-1 for 7 minutes. Following NTA chip treatment an ethanolamine wash was carried out. Next the immobilisation of LeuT onto NTA sensor chip was attempted by a 10µl per min flow rate for 7-minutes. Following LeuT immobilisation another ethanolamine wash was carried out and this was subsequently followed by treatment of the NTA sensor chip with 350 mM EDTA at 30 µl min-1 flow rate for 1 minute. Lastly a wash of the flow system was carried out using Immobilisation buffer. The Immobilisation methodologies of SMA2000, DIBMA and DDM purified LeuT for SPR were identical.

The quantification of leucine binding to capture-coupled immobilized LeuT was attempted by setting up a seven-point titration of leucine using 1 in 3 dilutions in assay buffer starting from 10µM. Leucine binding analysis methodologies were identical for SMA2000, DIBMA and DDM purified LeuT.

The Immobilisation of LeuT was determined by loading data onto Biacore Insight Evaluation software and the binding of leucine was also analysed via Biacore Insight Evaluation software

2.18 Maleimide Labelling of SMA-SH-LeuT

A 2nd Generation Monolith Protein Labelling RED-MALEIMIDE Kit was obtained from Nanotemper and used to label SMA-SH solubilised and purified LeuT according to the instruction provided in the kit. The labelled SMA-SH purified LeuT samples were loaded onto a small size exclusion column and elution factions collected. The labelling of the SMA-SH purified LeuT was assessed by MST instrument.

2.19 NTA-Labelling of SMA-LeuT

A 2nd Generation Monolith NT His-Tag Labelling RED-tris-NTA Kit was obtained from Nanotemper and used to label SMA2000 solubilised and purified LeuT according to the instruction provided in the kit. SMA2000 solubilised and purified LeuT at approximately 200nM concentration was mixed in a 1:1 ratio with NTA dye and incubated for 30 minutes, following which it was employed in initial capillary test experiments. Comparable labelling experiments were carried out with a sample of SMA2000 purified LeuT that was mixed with 0.5 % SDS and incubated at 95 ˚C for 15 minutes to allow denaturation, following this NTA labelling procedure was carried out as instructed in the kit and the mixed samples were incubated for 30 minutes and subsequently used in desipramine binding experiments.

2.20 MST Capillary tests

An assay buffer (150 mM NaCl, 20 mM Tris pH 8.0, 0.005 % Tween 20) was prepared and used to make ten 1 in 2 dilutions of labelled LeuT. The dilutions were then loaded into a standard capillary chip and the fluorescence signal of each dilution analysed. The excitation power was set at 40% and capillaries re-scanned after 30 minutes to examine occurrence of adsorption.

Following MST capillary tests, the affinity of the Red-NTA label for His tag on the SMA2000-LeuT was investigated according to the instructions provided by Nanotemper in the 2nd Generation Monolith NT His-Tag Labelling Kit.

2.21 Leucine Binding experiments

Single points test comprised of 0 μM and 1 μM leucine concentrations as well as titrations were used to analyse leucine binding to NTA-Labelled SMA2000 LeuT. Titrations series ranged from 1 μM concentration up to 1 mM, with 12 points Single point tests were used to analyse leucine binding to SMA-SH-LeuT as well.

2.22 Desipramine Binding Experiments

A twelve point 1 in 2 dilution series was prepared by dissolving desipramine in DMSO with the top starting concentration being at 40mM. The dilution series was then further diluted 1 in 100 in assay buffer and finally mixed in a 1 (10 μl) to 1 (10 μl) ratio with diluted NTA-labelled SMA-LeuT to give a final top concentration of 200 μM desipramine and 10 nM SMA-LeuT. Experiments were carried out at

medium MST power and high MST power. For both medium and high MST power experiments, an excitation power of 15 % was employed. Desipramine binding experiments utilising DDM purified LeuT utilized high MST power.

The data from fluorescence and labelling tests was examined using MO control and analysis software by analysing fluorescence levels. The data from NTA affinity test experiments was examined by loading data onto MO analysis software and selecting the titration data and fitting using a standard affinity model.

2.23 Statistical analysis

Graph Pad Prism was used to carry out Statistical analysis. One-way ANOVA tests were carried out on data obtained, with a Tukey post-hoc test. P values of less than 0.05 were considered significant. Non-linear regression/curve fit was used for tryptophan quenching analysis.

3. Target protein expression & purification

The initial aim of this study was to express, solubilise and purify two target proteins, LeuT and Atm1, using polymers (SMA2000 or DIBMA) or conventional detergent DDM.

3.1 LeuT purification

The secondary active transporter LeuT was expressed in BL21 *E. coli* (DE3) cells which had already been transformed with vector pET16b-LeuT. Membrane preparations were made and these were solubilised with either 2.5 %(w/v) SMA2000, 2.5% (w/v) DIBMA or 2% (w/v) DDM, and purified using Ni^{2+} affinity chromatography. Figure 3.1 shows that SMA2000, DDM and DIBMA solubilised LeuT were all successfully purified as there is visible dissimilarity between the total solubilised protein sample (sol) and elution lanes. The total solubilised protein shows many different proteins, but the overexpression of LeuT can be seen as an intense band at approximately 55-60kDa (molecular weight of LeuT is 57kDa). The flowthough (FT) sample, containing proteins that did not bind to the resin, contains many of the solubilised proteins but only minute amounts of LeuT, this indicates successful binding of LeuT to nickel resin. Wash one (W1) bands show some contaminants and wash five (W5) bands show even fewer indicating effective washing process. The elution bands on Figures 3.1 A,B and C predominantly show pure LeuT indicating successful purification process. However, Figure 3B, using DDM shows many more contaminants than SMA2000 and Figure3C, using DIBMA shows a higher molecular weight band, possibly a LeuT dimer. The purification with SMA2000 (Figure 3A) appears to give a greater degree of purity than the other two.

3.2 Analysis of purified LeuT

Following successful purification, the yields and purity of SMA2000, DDM and DIBMA purified LeuT were quantified using densitometric analysis of samples run on SDS-PAGE alongside BSA standards (Figure 3.2A). An average yield of 0.38 µg protein/mg membrane was obtained for SMA2000 purified LeuT, 0.28 µg/mg for DDM and 0.20 µg/mg for DIBMA. SMA2000 purified LeuT on average has the highest yield of purified LeuT and DIBMA lowest, however there are no statistically significant differences between the yields of SMA2000, DDM and DIBMA purified LeuT.

Figure 3.2B displays the purity of SMA2000, DDM and DIBMA, purified LeuT. SMA2000 purified LeuT on average is 61% pure, DDM purified LeuT 50%, and DIBMA purified LeuT 56%. There is a trend that the polymers give more pure protein than DDM, however this was not statistically significant.
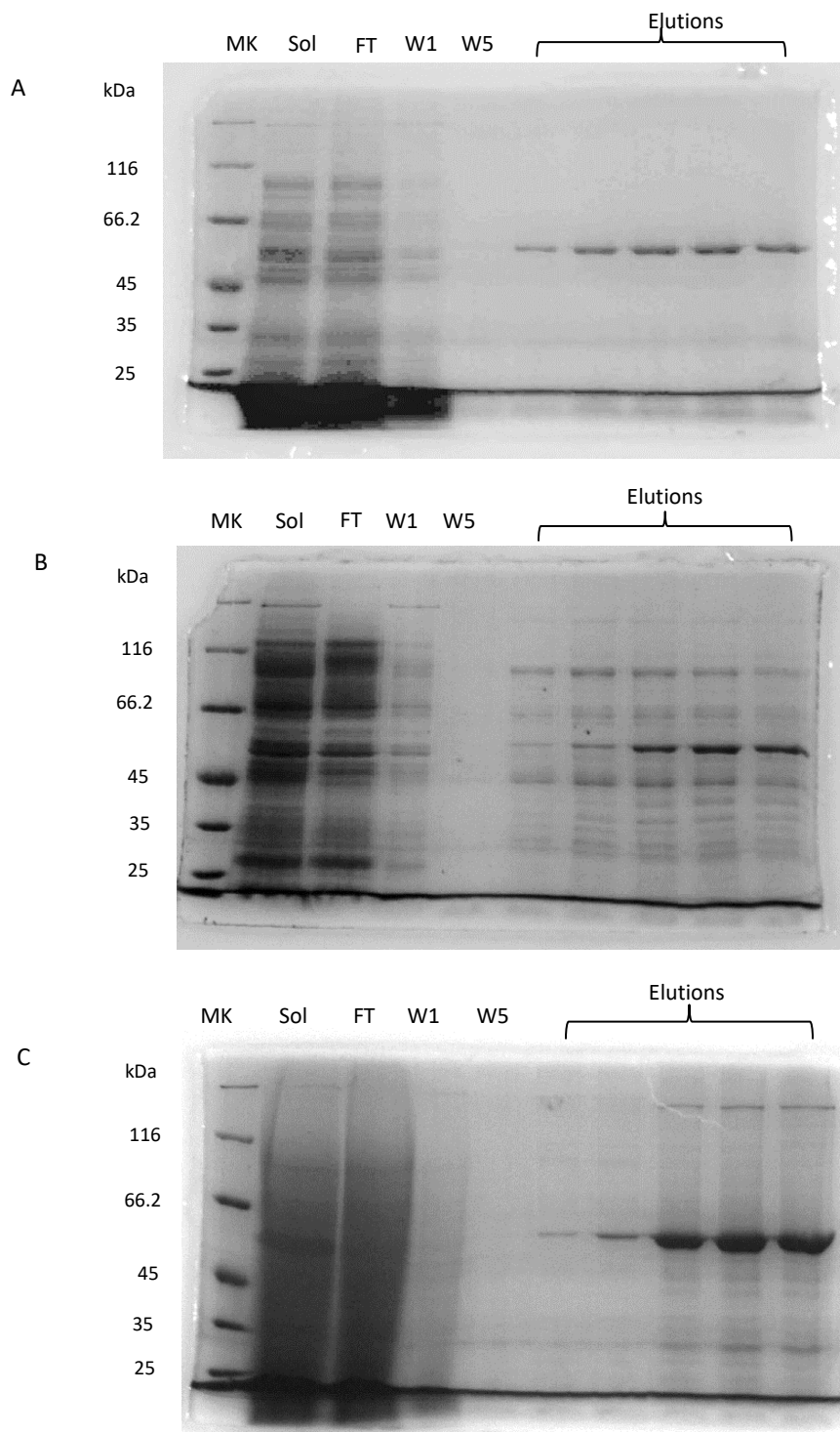
Figure 3.1 Affinity purification of SMA2000, DDM and DIBMA solubilised LeuT. *SMA2000 (A), DDM (B) and DIBMA (C) solubilised LeuT membranes (sol) were incubated overnight with Nickel-NTA Resin at 4°C, following which unbound material (FT) was removed and resin washed with purification buffers supplemented with increasing concentrations of Imidazole (20mM – 60 mM). For detergent purifications, the purification buffers were additionally supplemented with 0.1% (w/v) DDM. LeuT was eluted with buffers supplemented with 200mM imidazole. Samples were extracted from wash 1, wash 5, flow through and each elution collection, and run on SDS-PAGE along with a solubilisation sample. Gels were stained with Instant Blue.*
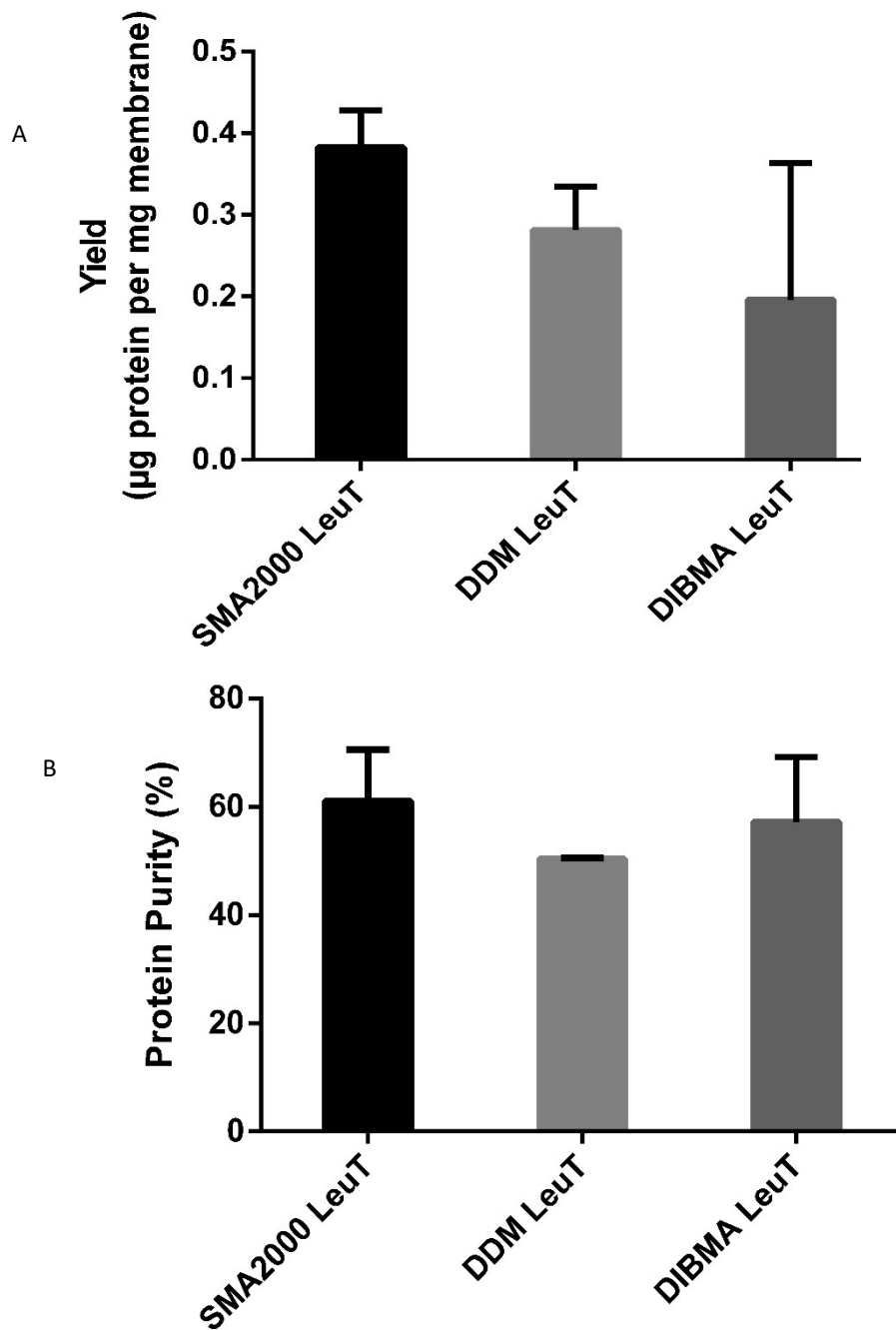
Figure 3.2 Quantification of SMA2000, DDM and DIBMA purified LeuT. *A) Samples (10 μl and 20 μl) of SMA2000, DDM and DIBMA purified LeuT were run on SDS-PAGE alongside BSA standards (0.25, 0.5, 0.75, 1, 1.25 μg) and gels stained with instant blue. The intensity of bands on gels were analysed using densitometry and yield calculated. B) Purity quantification. To estimate the purity of LeuT obtained, three SMA2000, DDM and DIBMA lanes were analysed using densitometry (Image J); purity was estimated by examining the intensity of LeuT band as a percentage of total lane intensity. Data are mean ± SEM, n=3. Data was analysed using One-way ANOVA tests, no significant differences were found.*

It has previously been shown that SMA2000 SMALPs are sensitive to divalent cations such as Mg^{2+} or Ca^{2+}, so the effect of magnesium chloride on the purified LeuT samples was tested. Figure 3.3 demonstrates that magnesium chloride concentrations of up to 4mM have no substantial impact on SMA2000 purified LeuT however concentrations over 4mM cause the majority of SMA2000 purified LeuT to precipitate out of solution. In contrast DDM and DIBMA purified LeuT are relatively unaffected and still present in solution even at 10mM concentrations of magnesium chloride.
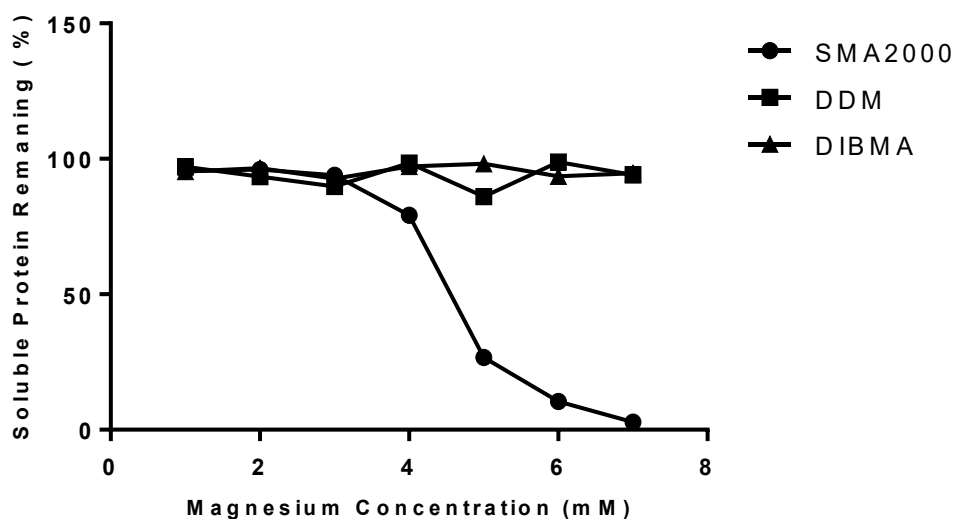
Figure 3.3 Magnesium Sensitivity Assay. SMA2000, DDM and DIBMA purified LeuT protein samples were mixed with increasing concentrations of magnesium chloride (0-10mM) and incubated at room temperature for 15 minutes. Following incubation, samples were centrifuged at 100000g, for 20 minutes at 4°C. Supernatants containing soluble proteins were extracted and pellets resuspended in buffer. Samples from supernatants and resuspended pellets were run on SDS-PAGE. Gels were stained with instant blue and analysed using densitometry (Image J) n=1.

3.3 Ligand binding to purified LeuT

Following the investigations into the effects of magnesium chloride on purified LeuT, the final step was to investigate whether the different solubilisation methodologies (SMA2000, DIBMA, DDM) had an impact on LeuT structure and function by analysing ligand binding via a tryptophan fluorescence quenching assay. Two LeuT substrates were tested; Leucine and Alanine (Figure 3.4). Tryptophan fluorescence quenching is a type of fluorescence spectroscopy which can be employed in binding studies. This assay methodology is dependent on the fluorescence emissions of tryptophan residues within proteins. This method functions by measuring tryptophan fluorescence of chosen proteins in the absence of binding partner and in the presence of various concentrations of binding partner. Tryptophan are amino acids which have intrinsic fluorescence (Yammine *et al*., 2019). The intrinsic fluorescence of

tryptophan can be used to analyse protein conformational changes and ligand binding. Tryptophan are relatively rare amino acids, and this is useful as it can translate well into sensitive fluorescence measurements in protein conformation studies (Yammine *et al*., 2019; Whyte, 2023).The fluorescence emission of tryptophan residues can change when a binding partner or ligand is introduced in the environment. The introduction of the binding partner can change the local environment polarity, lead to local changes near the interaction site of protein or induce conformational changes in the protein which alter the tryptophan's environment, all of which can lead to fluorescence emission decreasing. The reductions in fluorescence levels can therefore be interpreted as an indirect indicator of binding interactions (Yammine *et al*., 2019).

Figure 3.4A reveals leucine to have the greatest affinity for DIBMA purified LeuT and lowest for DDM purified LeuT. Similarly, Figure 3.4B reveals alanine to have the greatest affinity for DIBMA purified LeuT and lowest for DDM purified LeuT. Figure 3.4 A also demonstrates that leucine has the highest maximum specific binding with DDM purified LeuT and lowest for SMA2000 purified LeuT. Figure 3.4B reveals alanine to have the highest maximum specific binding with DIBMA purified LeuT and lowest for SMA2000 purified LeuT. Figures 3.4A and 3.4B both show relatively similar binding affinities and maximal degrees of quenching for both leucine and alanine.

Figure 3.4A shows there isn't a substantial difference between the binding affinity of leucine for SMA2000 purified LeuT and DIBMA purified LeuT, however Figure 3.4A also shows that there is a significant difference between the binding affinity of leucine for SMA2000 purified LeuT and DDM purified LeuT, as the P value was 0.0088. DDM purified LeuT binding affinity is significantly lower than SMA2000 purified LeuT.

 Figure 3.4A also shows that there is a significant difference between the binding affinity of leucine for DIBMA purified LeuT and DDM purified LeuT (P value 0.0088). Figure 3.4B shows no significant differences between the binding affinities of Alanine for SMA2000, DDM and DIBMA purified LeuT.

A
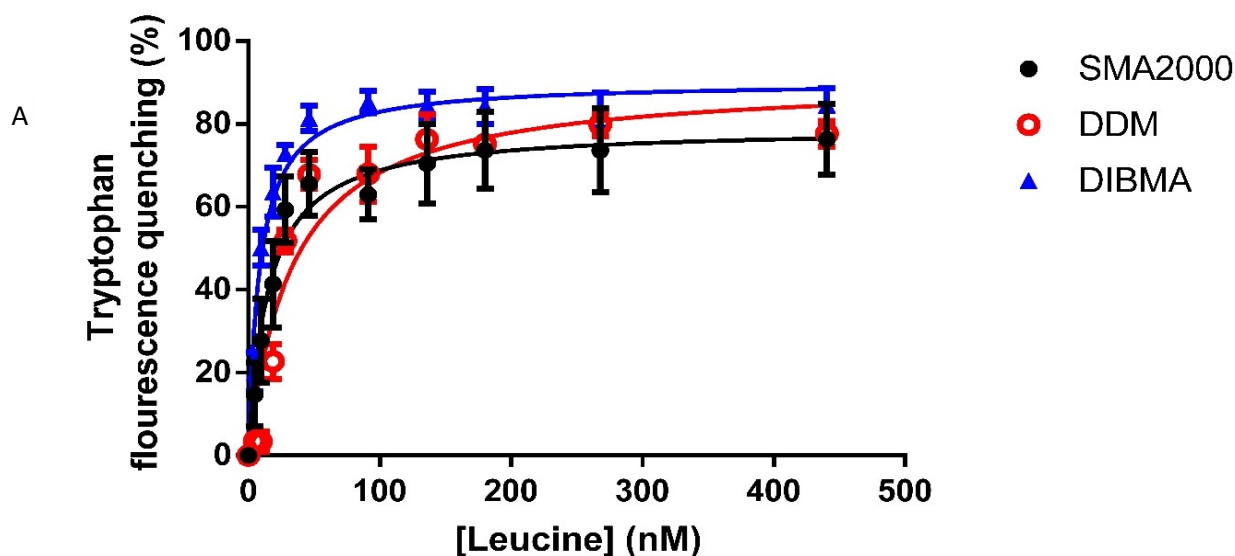
	SMA2000	DDM	DIBMA
Bmax	79.1	90.76	90.15
Kd	14.99	33.07 **	8.73

B
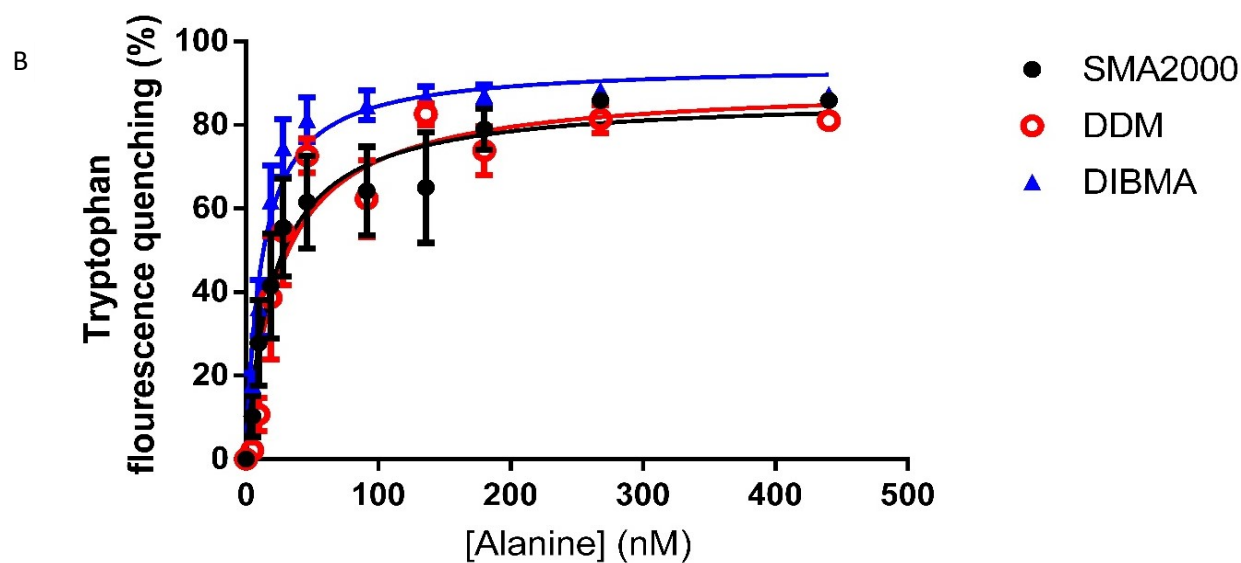
	SMA2000	DDM	DIBMA
Bmax	86.81	89.67	94.48
Kd	21.26	25.52	11.82

*Figure 3.4 Tryptophan fluorescence quenching analysis of ligand binding. SMA2000, DDM and DIBMA purified LeuT samples were loaded in a fluorometer and the quenching of intrinsic tryptophan fluorescence upon substrate (Leucine and Alanine) binding to LeuT measured. A) analysis of Leucine binding to SMA2000 (dark circle), DDM (red circle) and DIBMA (blue triangle) purified LeuT via tryptophan fluorescence quenching. B) analysis of Alanine binding to SMA2000 (dark circle), DDM (red circle) and DIBMA (blue triangle) purified LeuT via tryptophan fluorescence quenching. Data are mean ± SD. Kd from 3 replicates was analysed by one-way ANOVA. **P<0.01 significantly different to SMA2000.*

3.4 Purification of Atm1

Having successfully purified LeuT and confirmed ligand binding, the next step was to investigate if SMA2000 and DIBMA polymers and detergent DDM could also be used to solubilise and purify the ABC transporter Atm1. Atm1 was also expressed in BL21 *E. coli,* membranes were extracted, and protein solubilised using either SMA2000 and DIBMA polymers or the detergent DDM.

Figure 3.5 shows that SMA2000, DDM and DIBMA solubilised Atm1 was successfully purified. An intense band corresponding to the overexpression of Atm1 can be seen in the solubilised protein sample (Sol) as well as many other proteins. Very little Atm1 is seen in the flowthrough, indicating successful binding of Atm1 to the resin. Wash one (W1) bands show some contaminants and wash five (W5) bands show even fewer indicating effective washing process. The elution bands on Figures 3.5A, and 3.5C predominantly show a single band indicating successful purification process. The purified Atm1 runs at approximately 55-60kDa, which is a bit lower than its molecular weight of 66kDa, however it is common for membrane proteins to not run perfectly at their molecular weight, and is comparable with a previous study on Atm1 (Fan, Kaiser and Rees, 2020). Figure 3.5B, illustrating DDM purification reveals many more contaminants in the elution samples than is seen with SMA2000 or DIBMA.

3.5 Analysis of purified Atm1

Following successful purifications, the yields of SMA2000, DDM and DIBMA purified Atm1 were quantified using SDS-PAGE (Figure 3.6A). An average yield of 0.76 µg protein/mg membrane was obtained for SMA2000, 0.59 µg/mg for DDM and 0.51 µg/mg for DIBMA. Although SMA2000 appear to give a higher yield of purified Atm1 than DDM or DIBMA, these differences were not statistically significant (P value 0.1716).

Figure 3.6B displays the purity analysis of SMA2000, DDM and DIBMA purified Atm1. SMA2000 purified Atm1 on average was 77 % pure, DDM purified Atm1 63 %, and DIBMA purified Atm1 89 %. Although there is a trend that the polymers give a greater degree of purity than DDM, only DIBMA gave a statistically significant difference to DDM (P value 0.0139).
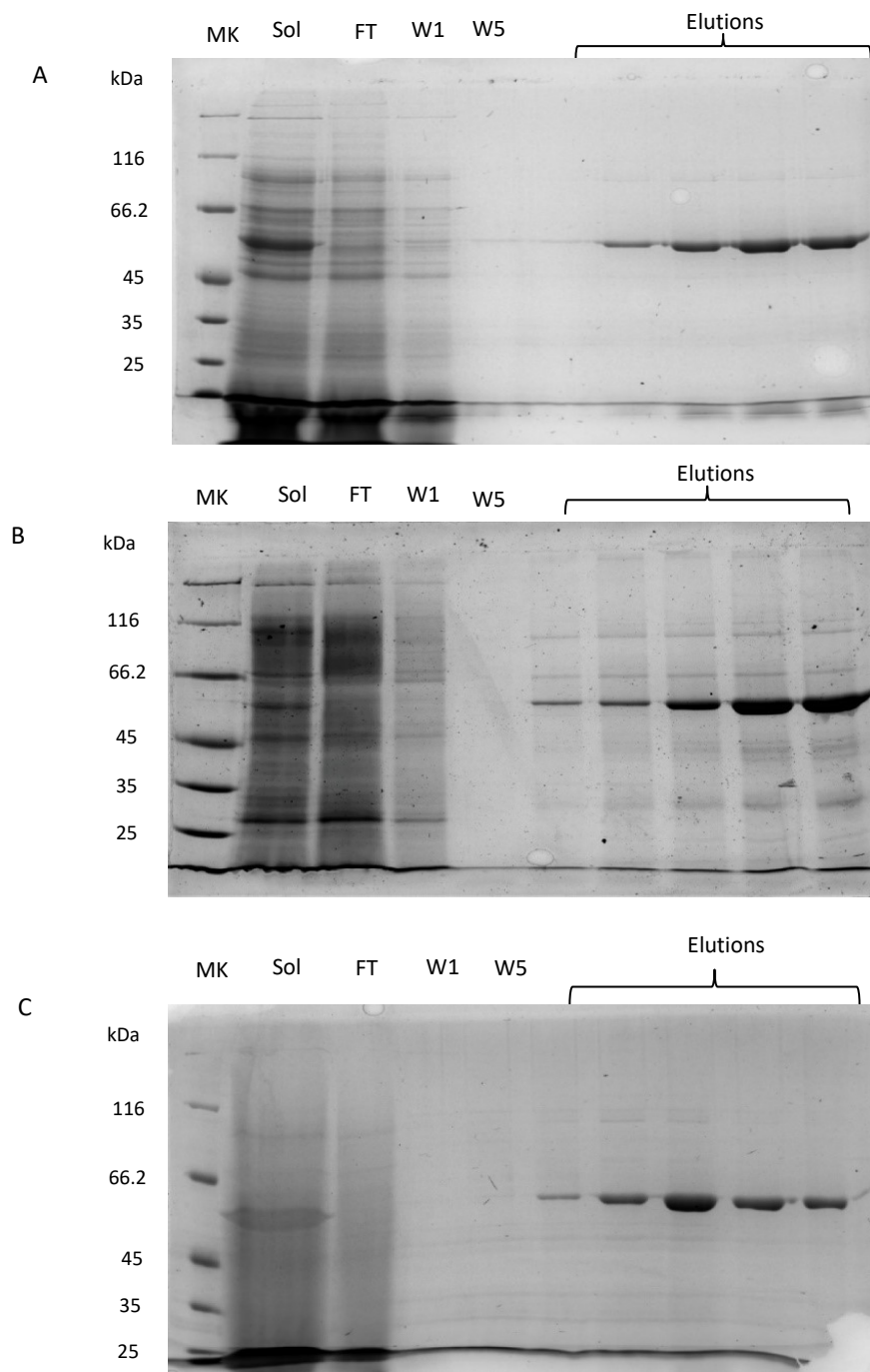
Figure 3.5 Affinity purification of SMA2000, DDM and DIBMA solubilised ATM1. *SMA2000 (A), DDM (B) and DIBMA (C) solubilised Atm1 membranes (sol) were incubated overnight with Nickel-NTA Resin at 4oC, following which unbound material (FT) was removed and resins washed with purification buffers supplemented with increasing concentrations of Imidazole (20mM – 60 mM). For detergent purifications, the purification buffers were additionally supplemented with 0.1% (w/v) DDM. ATM1 was eluted with buffers supplemented with 200mM imidazole. Samples were extracted from wash 1, wash 5, flow through and each elution collection, and run on SDS-PAGE along with a solubilisation sample. Gels were stained with Instant Blue.*
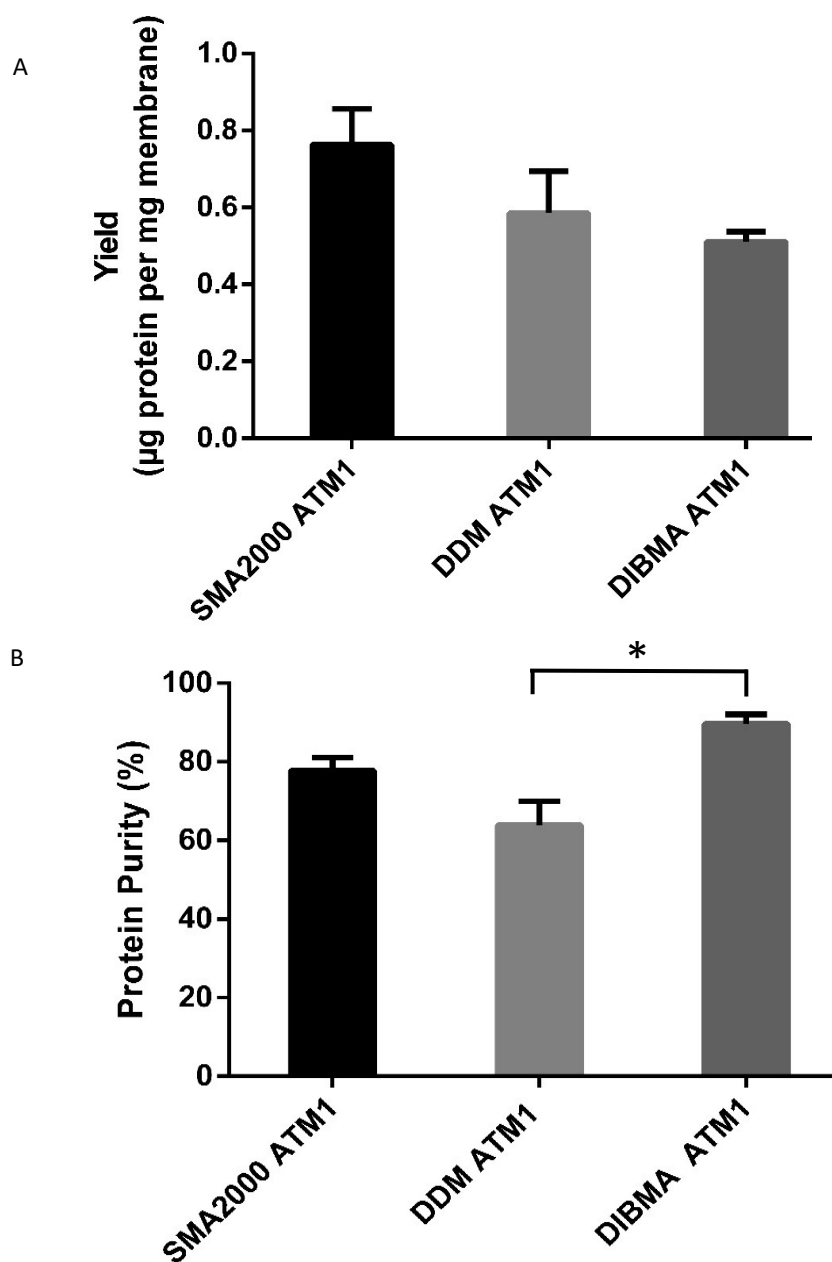
Figure 3.6 Quantification of SMA2000, DDM and DIBMA purified Atm1. *A) Samples (10 µl and 20 µl) of SMA2000, DDM and DIBMA purified Atm1 were run on SDS-PAGE alongside BSA standards (0.25, 0.5, 0.75, 1, 1.25 µg) and gels stained with instant blue. The intensity of bands on gels were analysed using densitometry and concentrations calculated. B) To estimate the purity of Atm1 obtained, three SMA2000, DDM and DIBMA lanes were analysed using densitometry (Image J); purity was estimated by examining the intensity of Atm1 band as a percentage of total lane intensity. Data are mean ± SEM, n=3. Data was analysed using One-way ANOVA tests.*P<0.05.*

Following Atm1 yield and purity analysis, the effect of magnesium chloride on precipitation of SMA2000, DDM and DIBMA purified Atm1 was investigated (Figure 3.7). Figure 3.7 demonstrates that magnesium chloride concentrations of up to 1mM have no impact on SMA2000 purified Atm1 however concentrations over 1mM cause the majority of SMA2000 purified Atm1 to precipitate out of solution. DIBMA purified Atm1 also displayed a high sensitivity to divalent cations as 1mM concentration of magnesium chloride causes approximately 40% of protein to precipitate out of solution. In contrast DDM purified Atm1 was relatively unaffected and still present in solution even at 10mM concentrations of magnesium chloride.
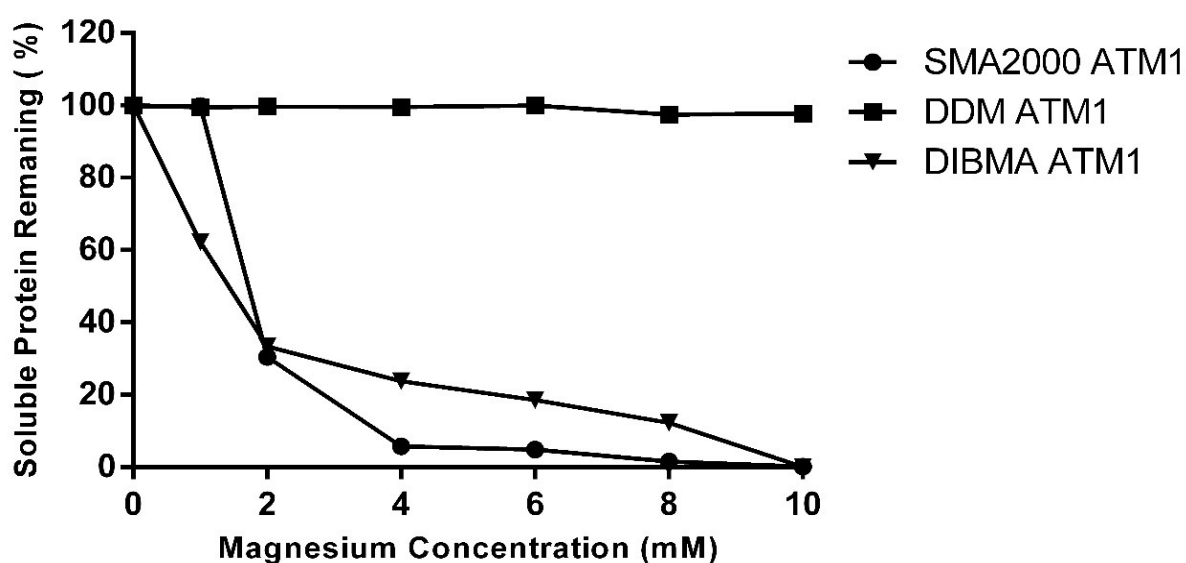
Figure 3.7 Magnesium Sensitivity Assay. SMA2000, DDM and DIBMA purified Atm1 protein samples were mixed with increasing concentrations of magnesium chloride (0-10mM) and incubated at room temperature for 15 minutes. Following incubation, samples were centrifuged at 100000g, for 20 minutes at 4°C. Supernatants containing soluble proteins were extracted and samples(20ul) run on SDS-PAGE. Gels were stained with instant blue and analysed using densitometry (Image J) n=2.

3.6 Ligand binding to purified Atm1

The next step was to explore whether the purified protein was functional, as measured by a ligand binding assay using tryptophan fluorescence quenching. Atm1 substrate glutathione (GSH) was testing for binding.

Figure 3.8 shows the binding of GSH to SMA2000 purified Atm1. Although the curve has not fully plateaued, the curve fitting gave a Kd for GSH binding to Atm1 within SMALPs of 1.82 mM, which is not too dissimilar to previous reports proposing a Km in the mM range (15±1mM) for GSH (Lee *et al*., 2014).
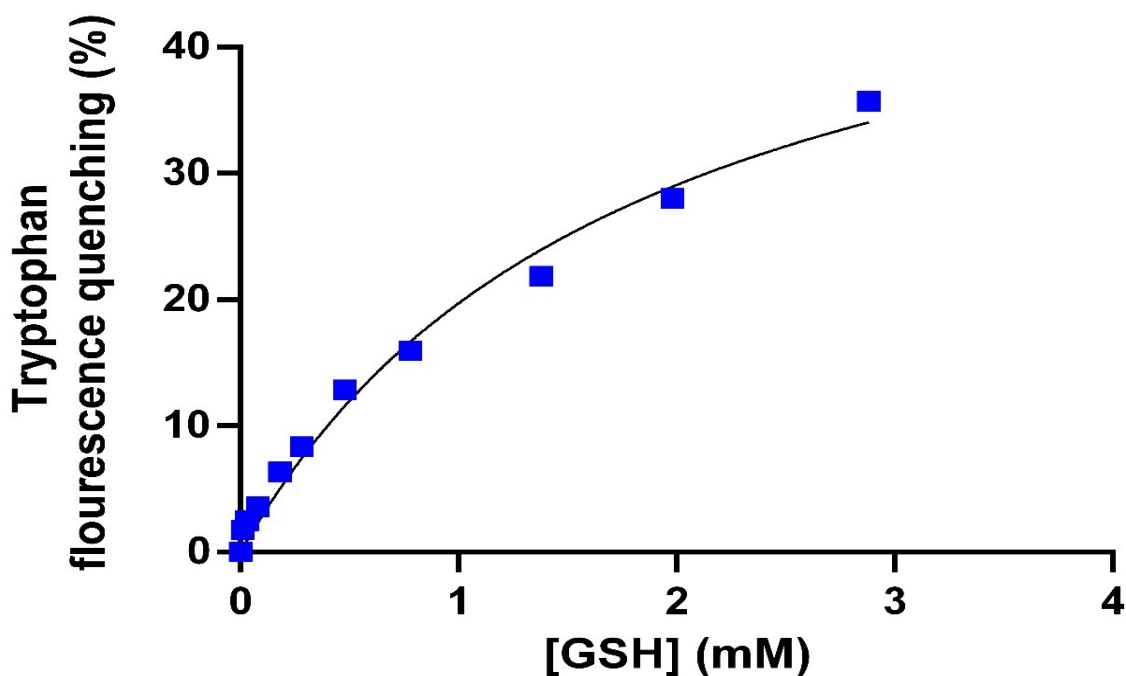
Bmax	55.49
Kd	1.82

Figure 3.8 Tryptophan fluorescence quenching analysis of ligand binding. SMA2000 purified Atm1 samples were loaded into fluorometer and the quenching of intrinsic tryptophan fluorescence upon addition of substrates (GSH) binding measured. Data is n = 1.

3.7 Summary

- Both LeuT and Atm1 could be successfully expressed in BL21 *E.coli*, extracted from the membrane using SMA2000, DIBMA or DDM and purified using Ni-NTA affinity chromatography.
- The yield of purified Atm1 was higher than LeuT, but there were no significant differences between the different polymers or DDM for each target protein.
- The degree of purity obtained showed a trend for both proteins that the polymers delivered a purer sample than DDM, however this was only statistically significant for Atm1 purified with DIBMA compared to DDM.
- Ligand binding to purified LeuT or Atm1 could be monitored by tryptophan fluorescence quenching.

4. Preliminary SPR studies

Surface Plasmon Resonance (SPR) is a commonly used approach to screen drug binding during the drug development process. In collaboration with the partner company Sygnature Discovery, it was investigated if SMA2000 or DIBMA encapsulated proteins could be used for SPR. LeuT was selected initially for these studies. SPR experiments require immobilisation of one of the binding components of a molecular interaction and therefore the first step was to investigate if and how SMA2000, DIBMA and DDM purified LeuT could be immobilized onto the surface of SPR sensor chips in a Biacore 8K machine.

4.1 Immobilisation using an NTA sensor chip

The initial approach was to utilise an NTA sensor chip which would allow the his-tag purified LeuT samples to immobilise (Figure 4.1).

In Figure 4.1C the immobilisation of DDM purified LeuT can be seen. This shows a fairly typical immobilisation, where upon addition of the protein sample an increase in signal is observed compared to the control channel, that reaches a plateau, and following washing gives an immobilisation signal at ~ 5560 RU. In contrast SMA2000 purified LeuT (Figure 4.1A) and DIBMA purified LeuT (Figure 4.1B) show much smaller increases in signal. SMA2000 gave an approximate immobilisation of ~ 23 RU and DIBMA purified LeuT had an approximate immobilisation of ~ 170 RU.

Although the immobilisation levels were not ideal, some protein was immobilised on the chip surface, so the next step was to examine the stability of immobilised LeuT samples by incorporating a wait step into the empty analysis method and monitoring the decay of immobilised LeuT samples. Figure 4.2A shows the signal decreases over time for SMA2000 purified LeuT, giving a disassociation rate of 0.5 RU per minute. Similarly, Figure 4.2B shows DIBMA purified LeuT disassociated at 0.7 RU per minute. However, Figure 4.2C shows that there was little to no decay of signal for DDM purified LeuT. Thus, DIBMA purified LeuT showed the highest disassociation rate and DDM purified LeuT the lowest.
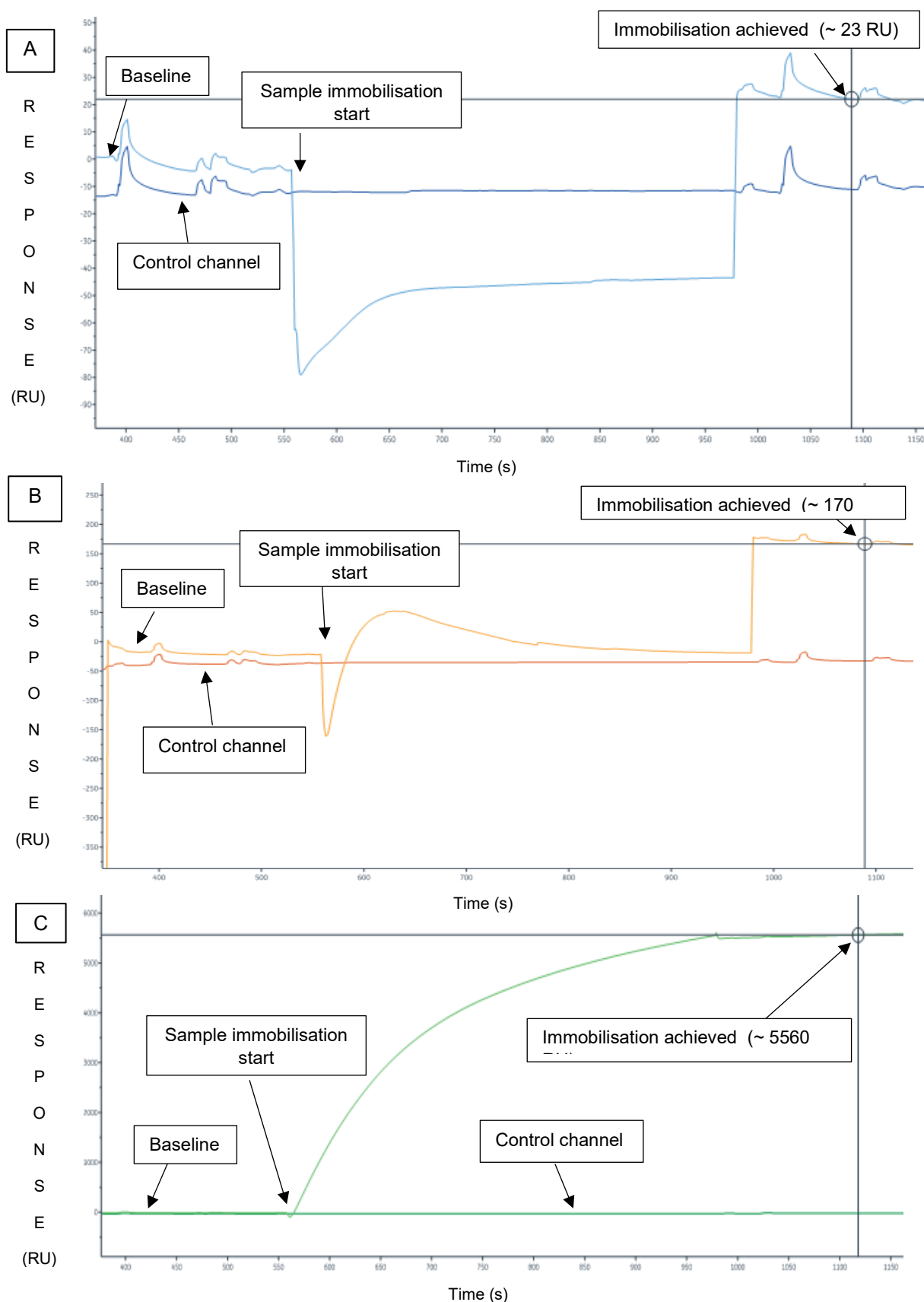
Figure 4.1 Immobilisation of SMA2000, DIBMA and DDM purified LeuT via His-tag interactions. *A standard NTA capture method was employed, Purified LeuT diluted into appropriate concentrations and flooded over NTA sensor chip surface at 10µl per min rate for 7-minutes. A) sensorgram of SMA2000 purified LeuT Immobilisation. B) sensorgram of DIBMA purified LeuT Immobilisation. C) sensorgram of DDM purified LeuT Immobilisation.*
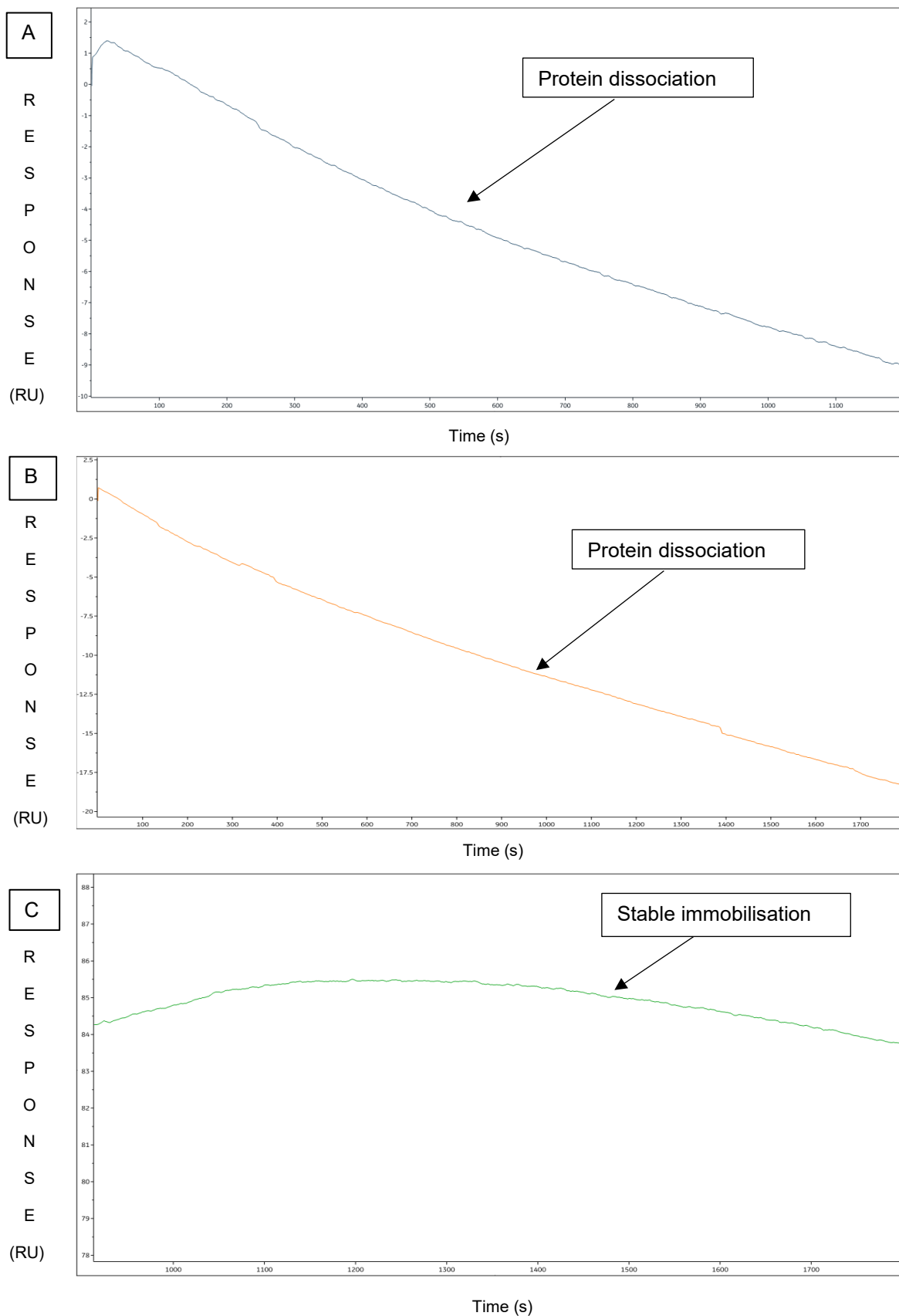
Figure 4.2 Immobilised LeuT Stability Analysis. *A standard NTA capture method was employed for immobilisation and a wait step incorporated into an empty analysis method. The resulting sensorgram was analysed for dissociation of ligand. A) analysis of SMA2000 purified LeuT Immobilisation. B) analysis of DIBMA purified LeuT Immobilisation. C) analysis of DDM purified LeuT Immobilisation.*

Following analysis of immobilized LeuT stability, the next step was to investigate if ligand binding to the immobilized LeuT could be measured (Figure 4.3).

Figure 4.3 shows no observable binding of Leucine to SMA2000, DIBMA or DDM purified LeuT. In fact, the majority of SMA2000 purified LeuT disassociated following the first injection. Therefore, it was decided to investigate different buffer conditions to try to improve the immobilisation, to disrupt hypothesised strong repulsive electrostatic interactions between the chip and the SMALP and DIBMALP particles and thereby increase LeuT immobilisation.
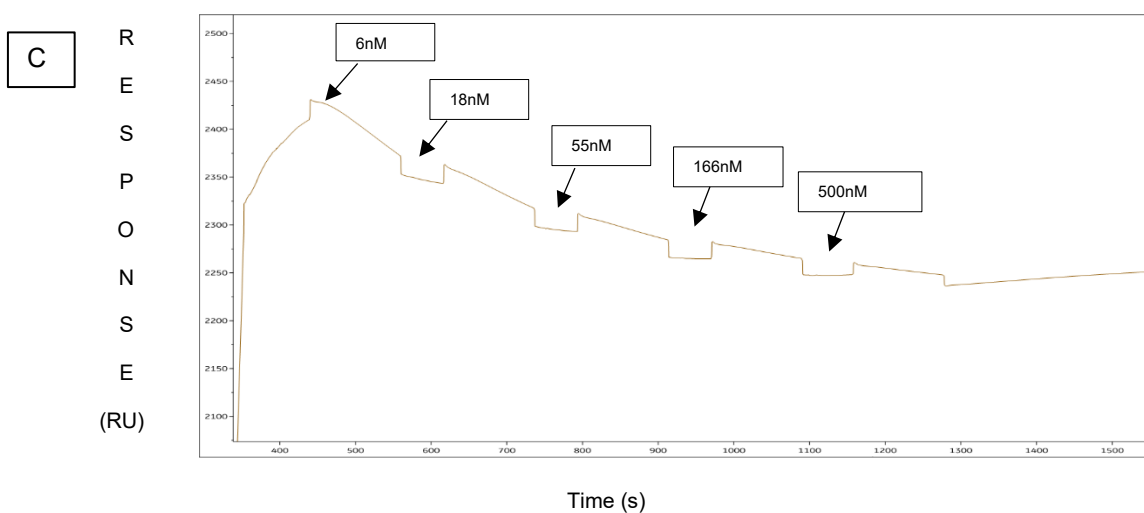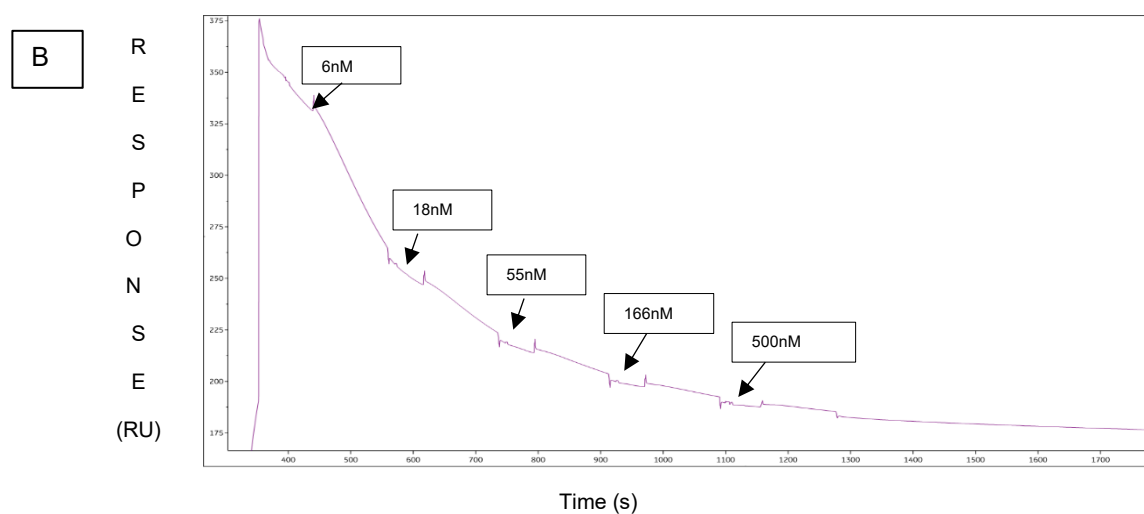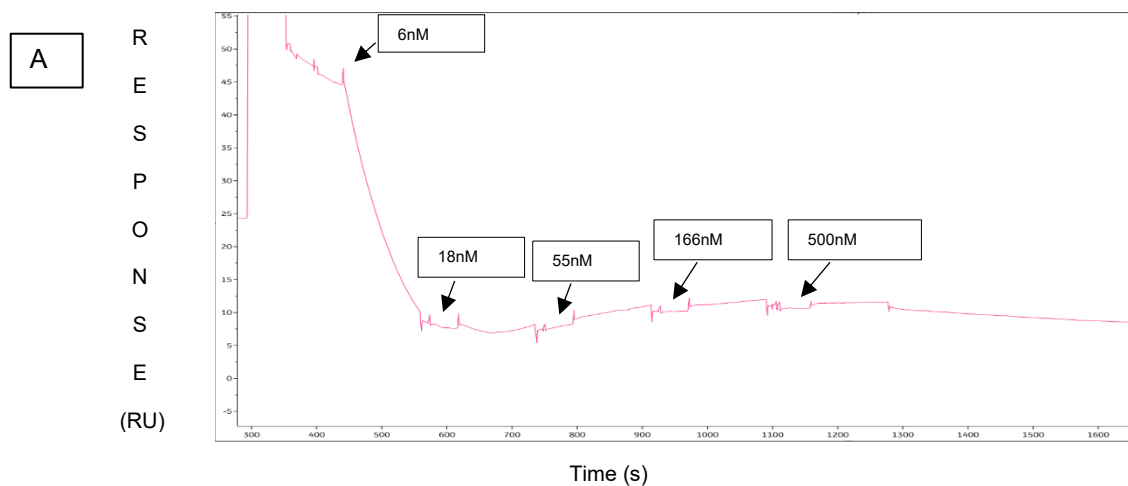
Figure 4.3 Leucine Binding Analysis. *SMA2000 (A), DIBMA (B) and DDM (C) purified LeuT samples were immobilised onto the surface of NTA sensor chips following a standard NTA protocol and the binding of leucine to immobilized LeuT investigated by creating a five-point titration series of Leucine concentrations using 1 in 3 dilutions starting at 500 nM.*

LeuT immobilisation at different NaCl concentrations was investigated first. In Figure 4.4A It can be seen that increasing the concentration of NaCl helped to increase the amount of SMALP encapsulated LeuT that was immobilised, reaching 144 RU at 500mM NaCl, compared to 23 RU at 200mM NaCl. Similarly, Figure 4.4B shows that DIBMA purified LeuT immobilised at the highest levels at 500mM NaCl, reaching up to 285 RU.
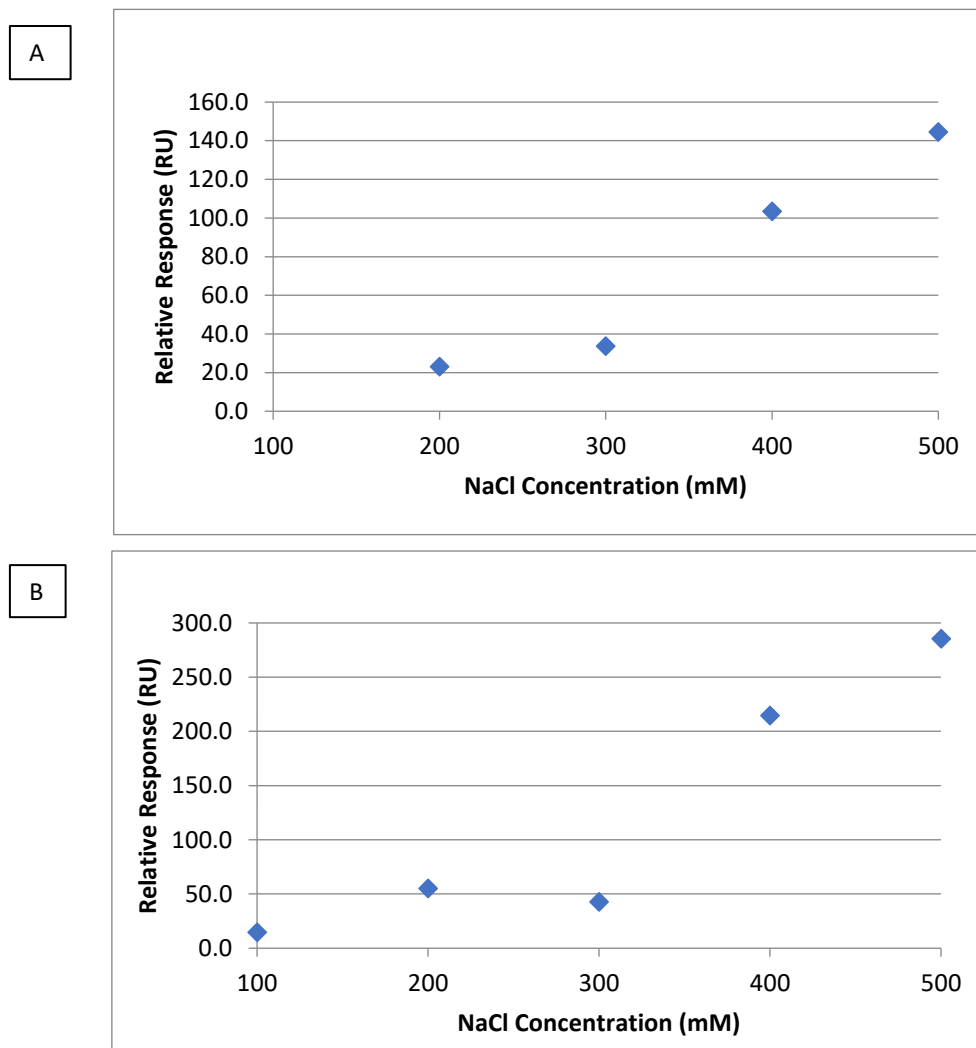
Figure 4.4 Buffer (NaCl) optimisation assay. *Five buffers of varying NaCl concentration (100mM,200mM,300mM,400mM,500mM) were created at pH 8. A standard NTA capture protocol was tweaked and employed to include a series of ABA injections followed by regeneration injections to allow the testing of a series of buffers effects on LeuT Immobilisation. A) representative analysis of the effects of NaCl concentrations on immobilisation of SMA2000 purified LeuT. B) representative analysis of the effects of NaCl concentrations on immobilisation of DIBMA purified LeuT. Data is n=1.*

Following NaCl optimisation experiments, the effects of various pH levels on immobilisation of SMA2000 and DIBMA purified LeuT was investigated (Figure 4.5).
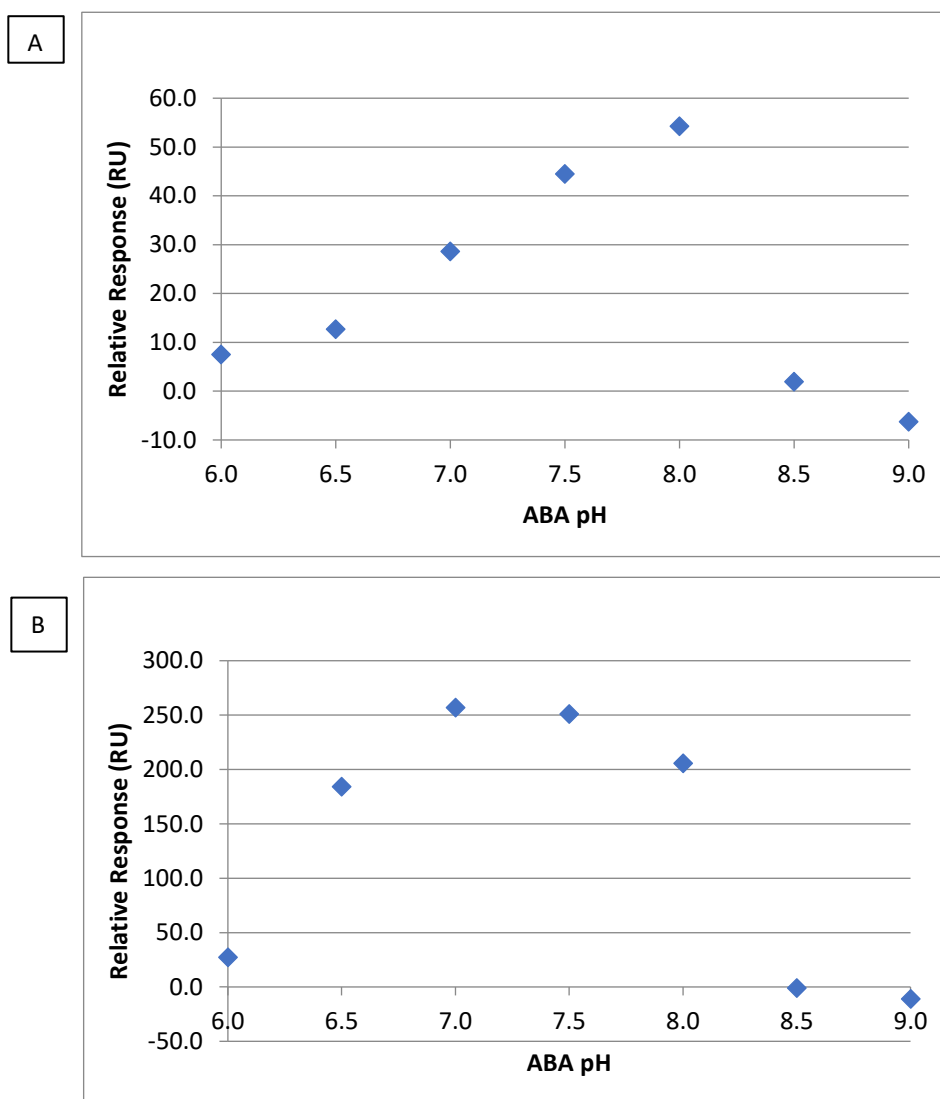
Figure 4.5 Buffer (pH) optimisation Assay. *Seven buffers of varying pH concentrations (6.0, 6.5, 7.0, 7.5 ,8.0, 8.5 ,9) were created at 200mM NaCl concentration. A standard NTA capture protocol was tweaked and employed to include a series of ABA injections followed by regeneration injections to allow the testing of a series of buffers effects on LeuT Immobilisation. A) representative analysis of the effects of pH on immobilisation of SMA2000 purified LeuT. B) representative analysis of the effects of pH on immobilisation of DIBMA purified LeuT. Data is n=1.*

Figure 4.5A shows that as the pH was increased from pH6 to pH8, the amount of SMA2000 purified LeuT immobilised increased, reaching a maximum at pH 8. However, increasing the pH further resulted in much lower levels of immobilisation. DIBMA purified LeuT (Figure 4.5B) however immobilised at the highest levels at pH 7, but again increasing the pH above pH8 led to a big loss in immobilisation.

4.2 Immobilisation using His-capture antibodies

Changing the buffer conditions did improve the immobilisation levels observed with both SMA2000 and DIBMA encapsulated LeuT, however, the level of immobilisation achieved was still much lower than seen with initial DDM experiments (~5560 RU), and much lower than is really needed for binding studies with small molecules to be carried out.

Therefore, it was decided to investigate alternative methods of LeuT immobilisation due to poor results from experiments utilising NTA chips. An alternative method of utilising CM5 chips and His-capture antibodies to immobilize his tagged proteins was investigated (Figure 4.6). The first step involves immobilising an anti-his antibody to the chip surface by traditional amine coupling, and then trying to bind the LeuT to the anti-his antibody.

Figure 4.6 shows that SMA2000 purified LeuT had a higher level of immobilisation than DIBMA purified LeuT. SMA2000 purified LeuT reached approximately 300 RU and DIBMA purified LeuT had an approximate immobilisation of 100 RU. For SMA2000 this was a substantial improvement over the NTA capture method, but to see if it could be further improved, the impact of increased immobilisation time was tested (Figure 4.7). Again, SMA2000 purified LeuT has a higher level of immobilisation than DIBMA purified LeuT. Figure 4.7A shows SMA2000 purified LeuT to have an approximate immobilisation of 500 RU and Figure 4.7B shows DIBMA purified LeuT to have an approximate immobilisation of 200 RU.
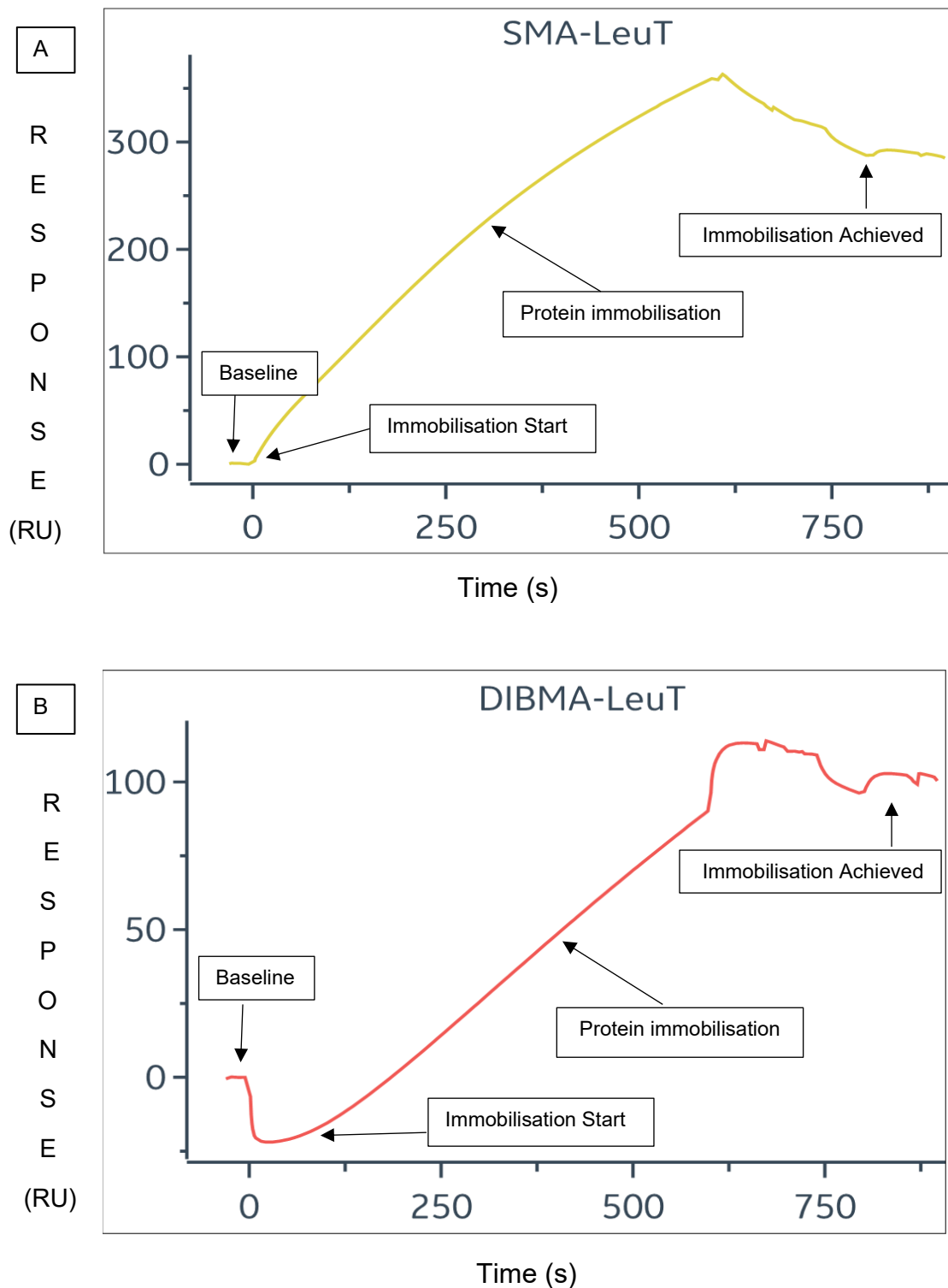
Figure 4.6 Immobilisation of SMA2000 and DIBMA purified LeuT via his capture antibody*. Biacore 8K machine was primed into buffer (150 mM NaCl, 50 mM Sodium phosphate pH 7.5, 0.005% Tween-20) and a CM5 chip inserted . An anti-His antibody was then immobilized on the surface of CM5 chip and SMA2000 and DIBMA purified LeuT samples injected over the immobilised anti-his antibody at 10 µl min-1 for 600 seconds and response examined. A) immobilisation of SMA2000 purified LeuT via anti-his antibody. B) immobilisation of DIBMA purified LeuT via anti-his antibody.*
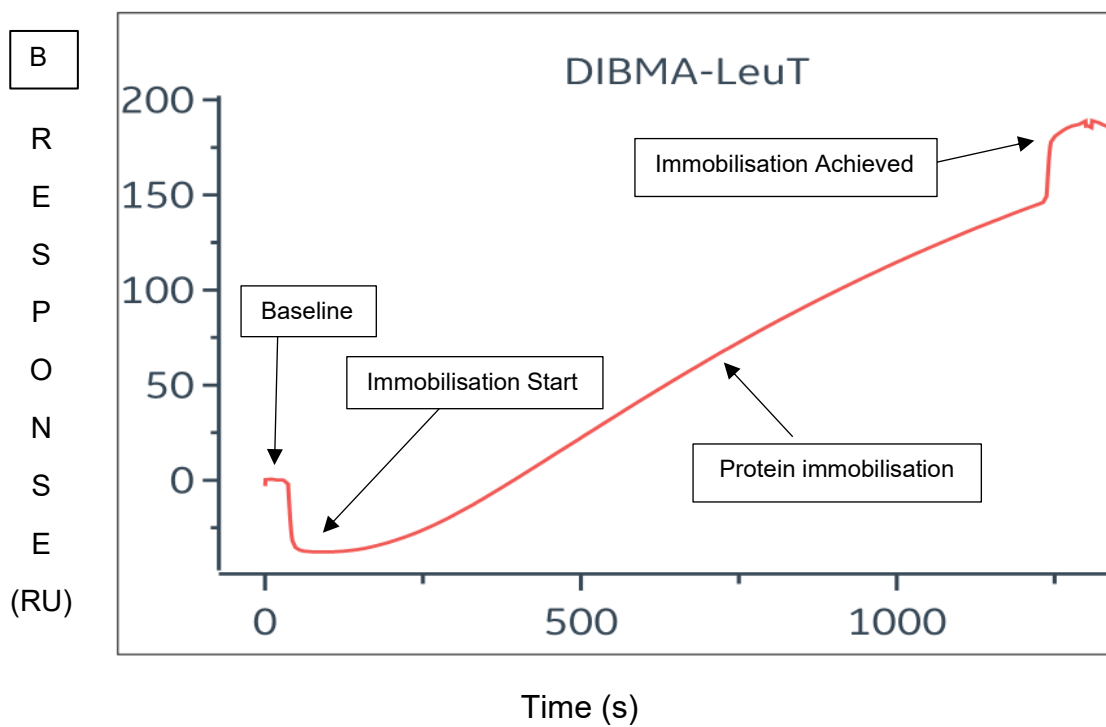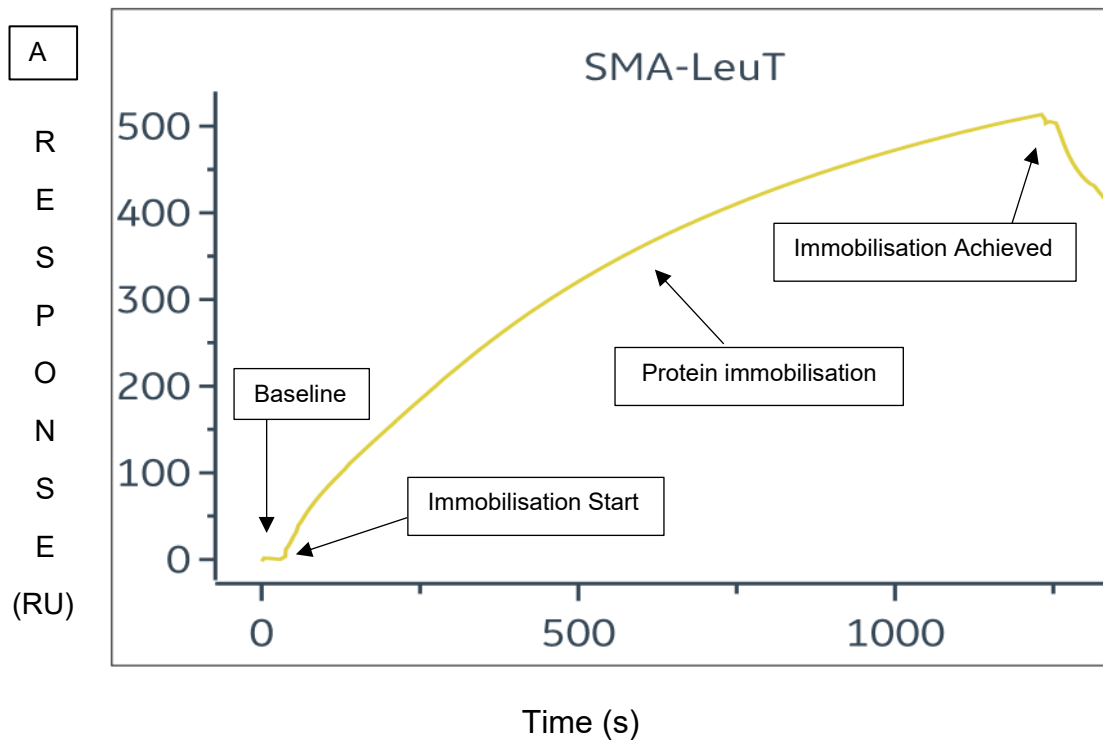
***Figure 4.7 Increased immobilisation time for SMA2000 and DIBMA purified LeuT via his capture antibody**. Biacore 8K machine was primed into buffer (150 mM NaCl, 50 mM Sodium phosphate pH 7.5, 0.005% Tween-20) and a CM5 chip inserted . An anti-His antibody was then immobilized on the surface of CM5 chip and SMA2000 and DIBMA purified LeuT samples injected over the immobilised anti-his antibody at 10 µl min-1 for 1200 seconds and response examined. A) immobilisation of SMA2000 purified LeuT via anti-his antibody. B) immobilisation of DIBMA purified LeuT via anti-his antibody.*

Whilst these levels of immobilisation were still lower than ideal, they were much higher than achieved with the previous approach, so it was next decided to investigate Leucine binding (Figure 4.8). However, Figure 4.8 does not exhibit any convincing signs of Leucine binding to SMA2000 or DIBMA purified LeuT.
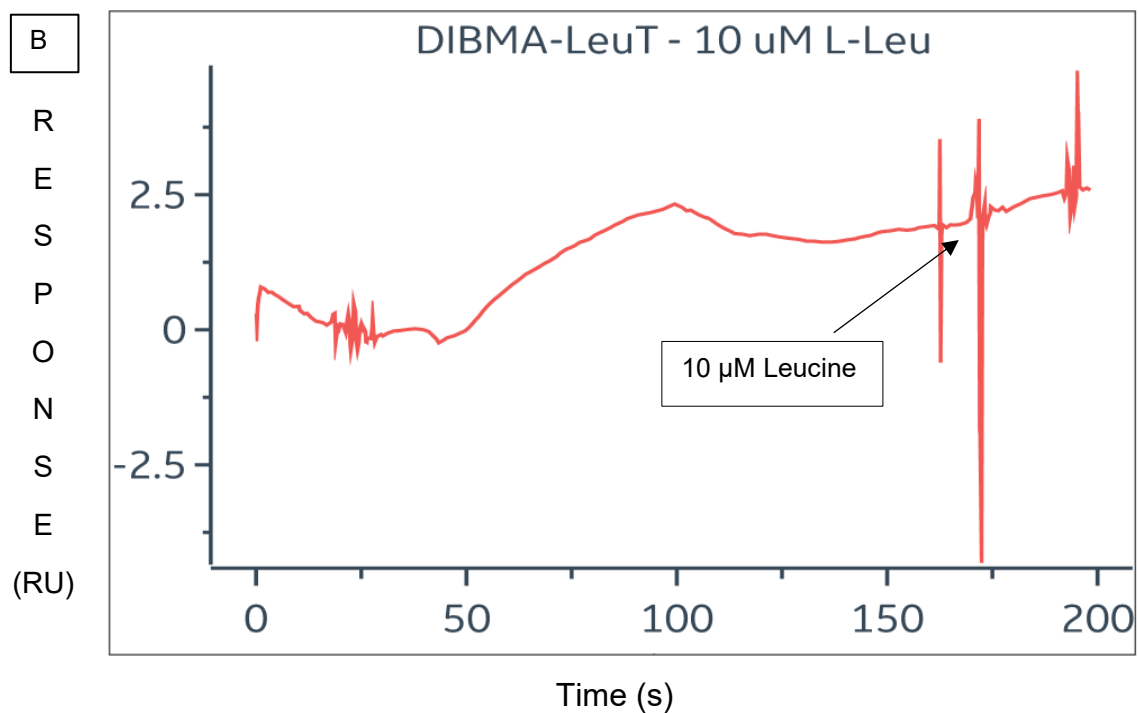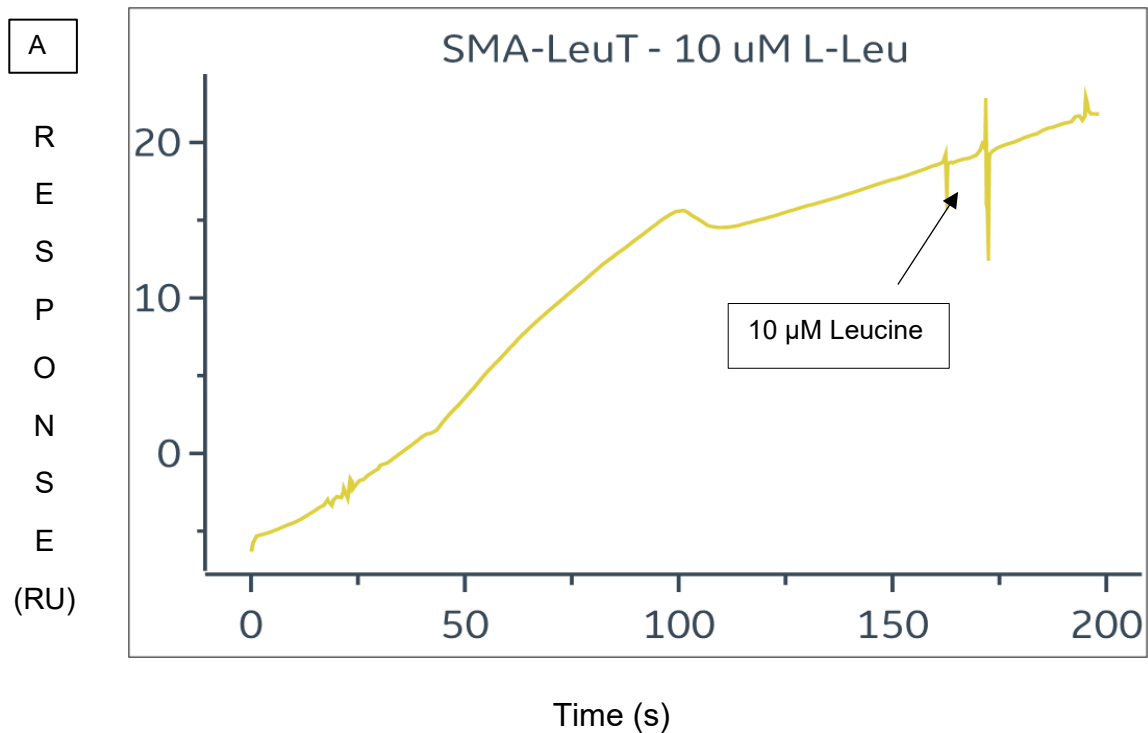
Figure 4.8 Leucine Binding Analysis. *Biacore 8K machine was primed into buffer (150 mM NaCl, 50 mM Sodium phosphate pH 7.5, 0.005 % Tween-20) and a CM5 chip inserted . An anti-His antibody was then immobilized on the surface of CM5 chip and SMA2000 and DIBMA purified LeuT samples were then immobilized on the surface of the CM5 chip via interactions with his capture antibody. A 10 µM Leucine sample was injected over immobilized LeuT samples and responses observed. A; Leucine binding to SMA2000 purified LeuT. B; Leucine binding to DIBMA purified LeuT*

Following on from the improved immobilisation observed with increased immobilisation time for the his-capture approach using CM5 chips, the next step was to investigate if using C1 chips with same his-capture approach would improve it further. C1 chips were proposed to be effective at immobilizing large molecules and proteins and have flat surfaces which allow interactions to take place closer to the surface.

Figure 4.9 shows that with these different chips, DIBMA purified LeuT has a higher level of immobilisation than SMA2000 purified LeuT. SMA2000 purified LeuT reached an approximate immobilisation of 20 RU and DIBMA purified LeuT reached 30 RU. Therefore, this approach clearly did not offer an improvement.
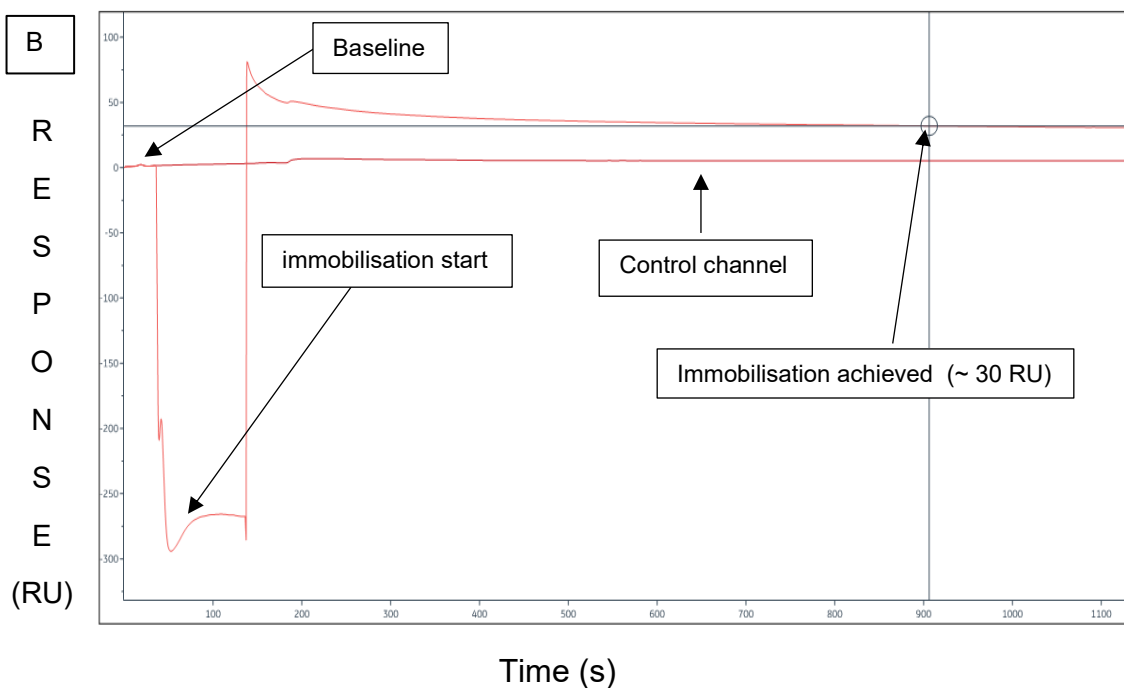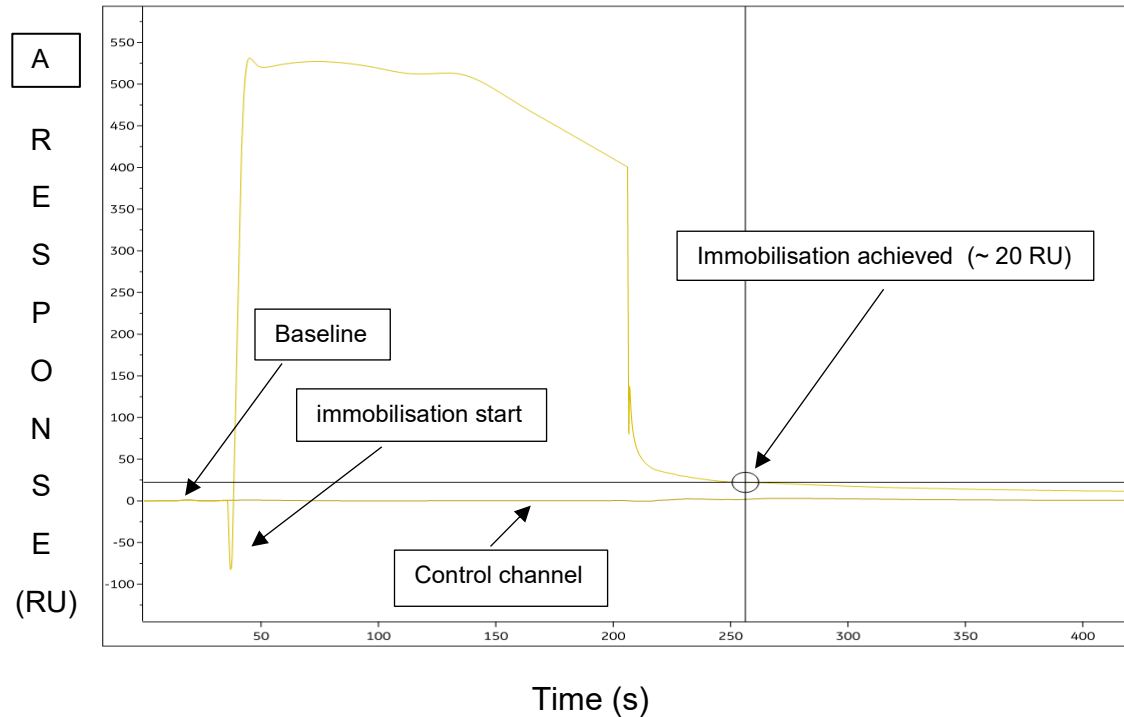
Figure 4.9 Immobilisation of SMA2000 and DIBMA purified LeuT on C1 chip via his capture antibody. *Biacore 8K machine was primed into buffer (150 mM NaCl, 50 mM Sodium phosphate pH 7.5, 0.005 % Tween-20) and a C1 chip inserted into 8K. The anti-His antibody was then diluted in the sodium acetate buffer provided with the kit to 15 µg ml-1 and immobilized on the surface of C1 chip as instructed in the kit. SMA2000 and DIBMA purified LeuT samples were then diluted 1 in 2 in assay buffer and injected over the immobilised anti-his antibody at 5µl min-1 for 600 seconds and response examined. A; representative immobilisation of SMA2000 purified LeuT via anti-his antibody. B; representative immobilisation of DIBMA purified LeuT via anti-his antibody.*

4.3 Immobilisation using NTA capture-couple

Another approach to improve immobilisation was NTA capture-couple. This consists of using the NTA chip to bind the his-tag on the LeuT protein, followed by traditional amine coupling to add stability.

Figure 4.10 shows that for this combined approach, as before when using the NTA chip, there is a substantial immobilisation difference between SMA2000, DIBMA and detergent DDM purified LeuT. SMA2000 purified LeuT reached an approximate immobilisation of ~ 62.5 RU. DIBMA purified LeuT was better than SMA2000, and reached an approximate immobilisation of ~ 409 RU, whereas DDM purified LeuT had an approximate immobilisation of ~ 1260 RU. Any differences in the rate of deposition were not due to differences in protein concentration.
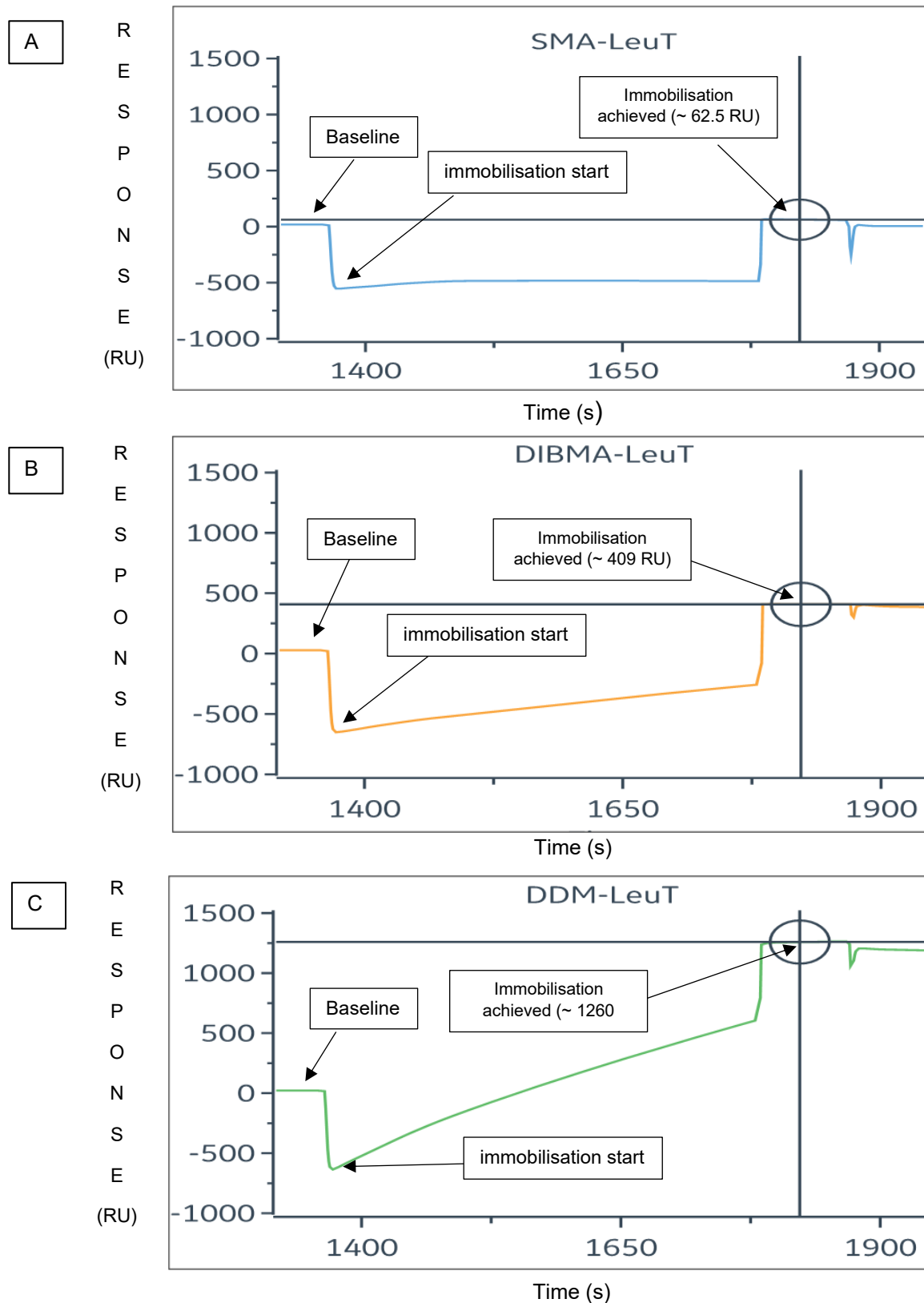
Figure 4.10 NTA Capture-Couple Immobilisation of SMA2000, DIBMA and DDM purified LeuT. *Biacore 8K machine was primed into buffer (500 mM NaCl, 50 mM Sodium Phosphate, pH 7.5 and 0.005% Tween 20) and NTA sensor chip docked. An NTA Capture-Couple method was used for Immobilisation. LeuT samples loaded at 10µl per min for 7-minutes and immobilisation observed. A; immobilisation of SMA2000 purified LeuT. B; immobilisation of DIBMA purified LeuT. C; immobilisation of DDM purified LeuT.*
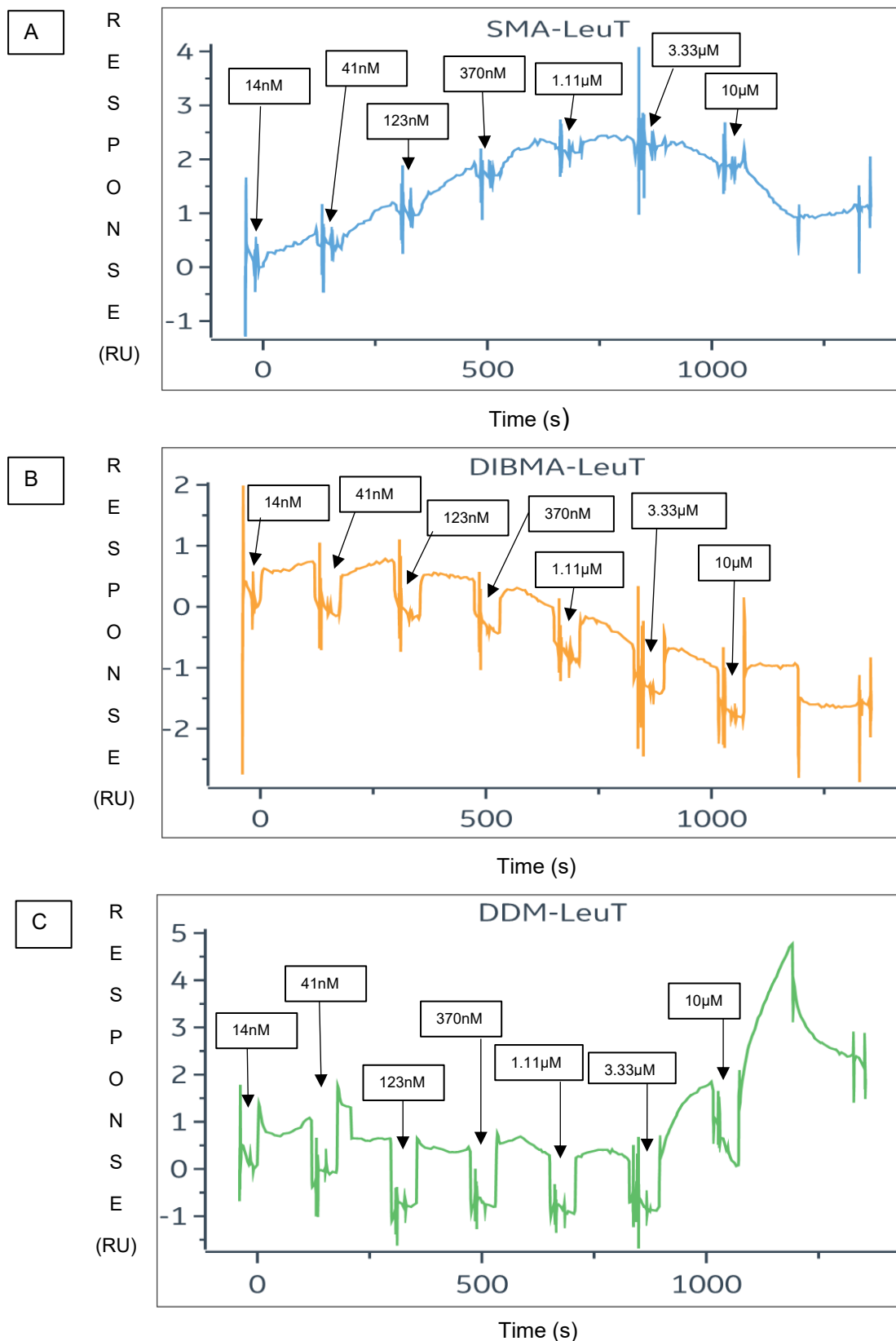
Figure 4.11 Leucine Binding Analysis. *SMA2000, DIBMA and DDM purified LeuT samples were immobilised onto the surface of NTA sensor chips following NTA Capture-Couple protocol and the binding of leucine to immobilized LeuT investigated by creating a seven-point titration series of Leucine using 1 in 3 dilutions starting at 10μM. A; analysis of Leucine binding to SMA2000 purified LeuT. B; analysis of leucine binding to DIBMA purified LeuT. C; analysis of leucine binding to DDM purified LeuT.*

The NTA Capture-Couple immobilized LeuT was then tested for leucine binding (Figure 4.11).Figure 4.11 does not show any leucine binding to SMA2000 or DIBMA purified LeuT. However, Figure 4.11C does show successful binding of leucine to DDM purified LeuT, particularly with the two highest concentrations of leucine used, where a clear curved increase in signal is observed after addition of ligand, that decreases again following washing.

4.4 Summary

- Immobilisation of purified LeuT using an NTA chip to bind the his-tag worked well for DDM purified protein, but poorly for SMA or DIBMA.
    - DIBMA-LeuT immobilisation was better than SMA-LeuT.
    - Both DIBMA and SMA immobilised proteins were unstable over time and resulted in substantial decay.
    - Increasing concentrations of NaCl was able to improve the level of immobilisation for SMA or DIBMA purified LeuT.
    - SMA immobilisation was optimal at pH8, whereas DIBMA was optimal at pH7.
    - Ligand binding could not be observed.
- An alternative approach of immobilising purified LeuT using a his-capture approach was tested.
    - SMA-LeuT was immobilised better than DIBMA-LeuT by this approach.
    - Increasing the immobilisation time improved the amount of protein bound.
    - CM5 chips were better than C1.
    - Ligand binding could not be observed.
- An NTA-capture approach combining NTA chips to bind the his-tag and amine coupling to add stabilisation, was also tested.
    - DIBMA-LeuT immobilisation was better than SMA-LeuT, but still much worse than DDM-LeuT.
    - Ligand binding could not be measured for SMA or DIBMA purified LeuT, but binding of leucine to immobilised DDM-LeuT was observed.
- Overall, the level of immobilisation able to be achieved for SMA or DIBMA purified samples was not high enough, especially for detection of small molecule binding.
    - Alternative approaches to immobilisation that don't involve the his-tag are needed.

5. Micro Scale Thermophoresis

Due to difficulties with the immobilisation step needed for SPR experiments, an alternative method, microscale thermophoresis (MST), was tested for investigating the binding of leucine to LeuT within SMALPs. This was also carried out in collaboration with Sygnature Discovery. MST experiments do not require immobilisation of a sample, but they do require one of the binding components of a molecular interaction to be labelled fluorescently.

5.1 Labelling LeuT with NTA-tagged fluorophore

One way to label LeuT is to target the his-tag. The first step was to investigate the ideal concentration of SMA2000 purified LeuT to label. A capillary test was carried out using SMA2000 purified LeuT at various concentrations (Figure 5.1).

Protein Concentration (nM)
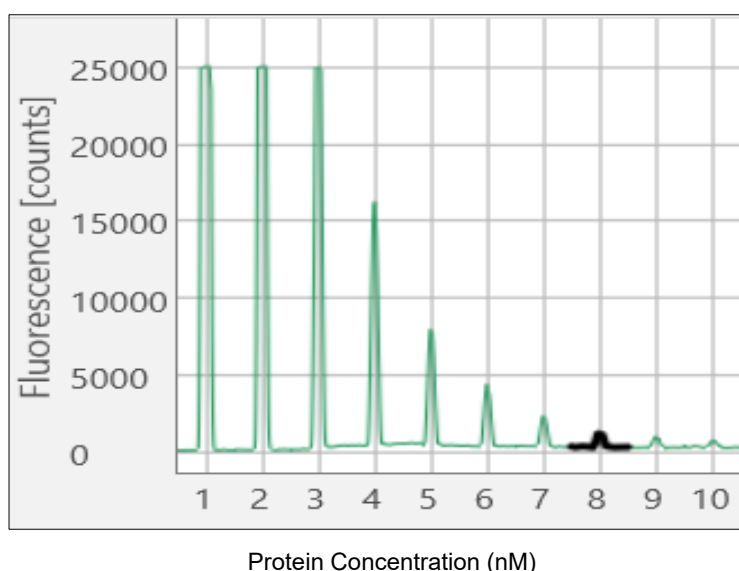
Figure 5.1 Capillary test. SMA 2000 purified LeuT (at ~200 nM) was fluorescently labelled and ten 1 in 2 dilutions of the labelled protein prepared using assay buffer with 1 representing highest concentration and 10 lowest. The dilutions samples were loaded onto a capillary chip and capillary chip loaded onto Monolith NT.115 and fluorescence observed at 50 % excitation power. Data is (n=1).

Figure 5.1 shows a good range of fluorescence levels, and no adsorption can be observed in any of the capillary peaks. Figure 5.1 also shows that fluorescence decreases with dilutions. Subsequently it was decided that 3.3 nM concentration of purified LeuT would be employed in the following experiments as 3.3 nM concentration of purified LeuT had adequate fluorescence levels and would be sufficient to measure L-Leucine binding as leucine had an affinity of 15-20 nM (Figure 3.5).

Following initial capillary tests, the next step was to investigate the affinity of the Red-NTA label for the His tag on the SMA2000 purified LeuT (Figure 5.2).

Figure 5.2A shows the MST traces obtained. When the laser is turned on (blue line), the fluorescent signal decreases over time as the fluorescent molecule moves away from the heat source . When the ligand binds, the rate of fluorescence decrease is slower. Ligand binding leads to formation of protein ligand complexes which increase the overall size of the protein and can also affect the hydration shells of the protein and reduce molecular motility of the protein in the buffer. The more ligand is added the slower it gets, until it reaches a plateau. In the plateau phase the thermodiffusion is counterbalanced by mass diffusion and because of this it represents the steady state. This can be plotted as a dose response curve by measuring the fluorescence signal at a given time point (red line) and plotting it against the ligand concentration (Figure 5.2B). A strong affinity (Kd 76 pM) was measured for the Red-NTA label binding to the His tag on SMA2000 purified LeuT. The plateau phase represents the steady state , the steady state is where the thermodiffusion is counterbalanced by mass diffusion.
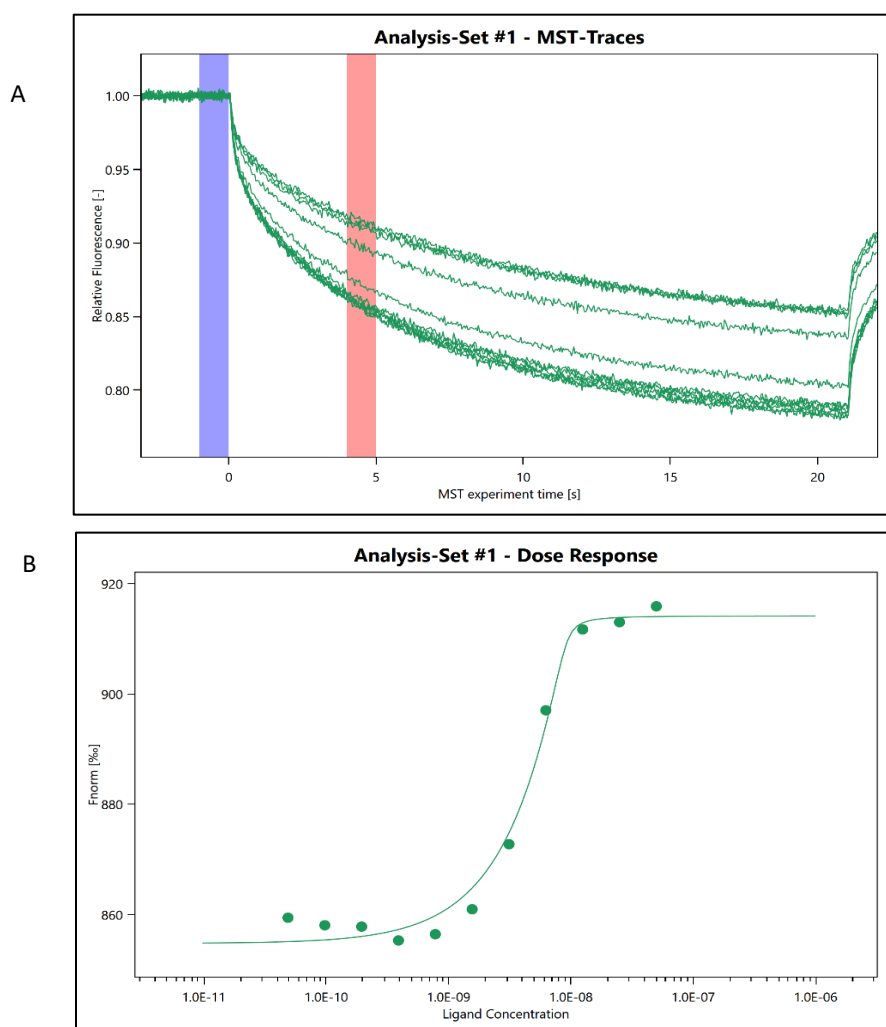
Figure 5.2 Labelling the his tag with a fluorescent label. *Affinity of Red-NTA label for His tag on the SMA2000 purified LeuT was examined by preparing LeuT and NTA samples according to the instructions provided by Nanotemper in the 2nd Generation Monolith NT His-Tag Labelling Kit. A) MST relative fluorescence trace of NTA affinity assay. B) a normalised fluorescence dose response graph of NTA label binding to His tag. Data is (n=1).*

5.2 Leucine binding to NTA labelled LeuT-SMALPs

Having labelled the his-tagged LeuT, next the binding of leucine to NTA-labelled SMA-LeuT was investigated by carrying out a single point test (Figure 5.3). Upon addition of leucine, a shift in the fluorescence trace can be seen (Figure 5.3A), which corresponds to a substantial difference in the response measured between SMA LeuT (Peak 3) and SMA LeuT in the presence of 1μM leucine (Peak 4) (Figure 5.3C).
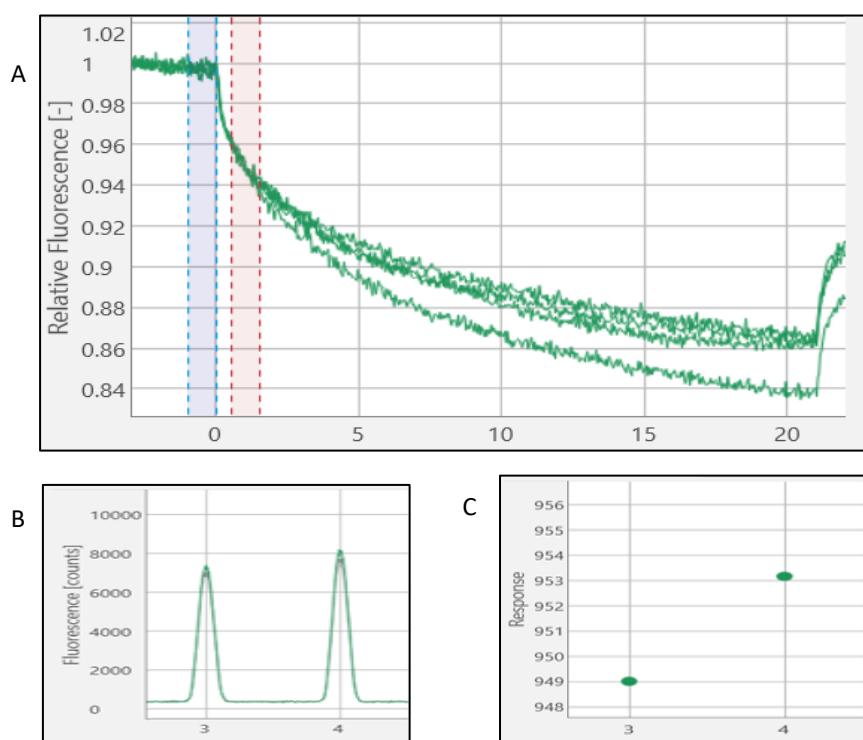
Figure 5.3 Initial leucine binding analysis. NTA-labelled SMA-LeuT samples were mixed with 0 μM and 1 μM L-Leucine concentrations and fluorescence observed. A) MST relative fluorescence trace of leucine binding assay. B) fluorescence count for ligand binding. Peak 3 (SMA LeuT), Peak 4 (SMA LeuT + 1 μM leucine). C) response graph for leucine binding. Data is (n=1).

Building upon this, the next step was to test leucine binding at various concentrations by preparing titrations with a range of leucine concentrations (Figure 5.4).
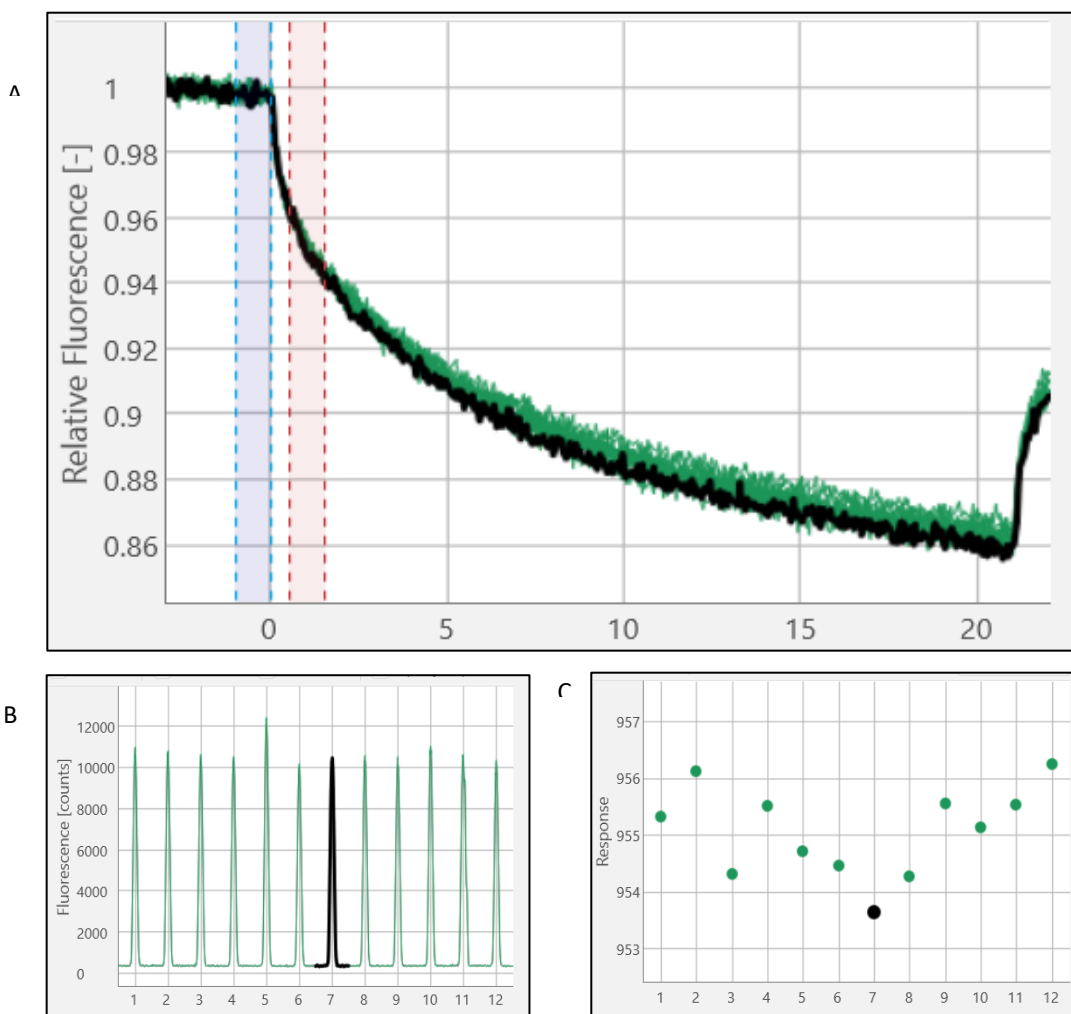
Figure 5.4 Leucine binding analysis for a range of leucine concentrations. *A twelve-point titration series of leucine were prepared by carrying out 1 in 2 dilutions of leucine starting at 1 µM concentration. NTA-labelled SMA-LeuT samples were mixed with leucine titration series and loaded into MST capillaries. Capillaries analysed via Monolith NT.115 and fluorescence observed. A) MST relative fluorescence trace of leucine binding assay. B) fluorescence count for ligand binding. C) response graph for leucine binding. Data is (n=1).*

Unfortunately, the traces shown in Figure 5.4 show no substantial difference in fluorescence following leucine titration series. Therefore, it was decided to carry out another single point spot test (Figure 5.5). In contrast to Figure 5.3, Figure 5.5C shows no substantial difference in the response of SMA LeuT (Peak 5) and SMA LeuT in the presence of 1µM leucine (Peak 6).
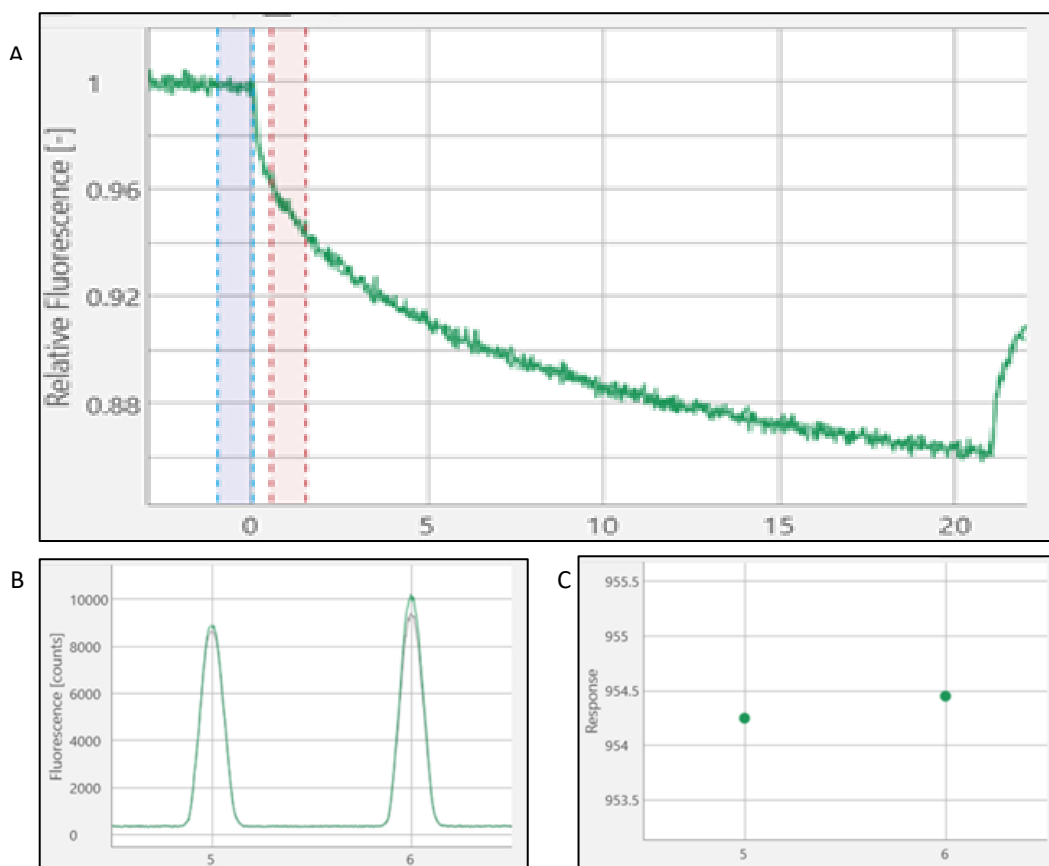
Figure 5.5 Leucine Binding Analysis – single point repeat. *NTA-labelled SMA-LeuT samples were mixed with 0 μM and 1 μM L-Leucine concentrations and fluorescence observed. Peak 5 (SMA LeuT), Peak 6 (SMA LeuT + 1 μM leucine). A) MST relative fluorescence trace of leucine binding assay. B) fluorescence count for ligand binding. C) response graph for leucine binding. Data is (n=1).*

Due to instability of the protein preparation, which was several days old. A freshly purified SMA LeuT sample was NTA labelled, and the effects of high sodium chloride concentrations on leucine binding via MST were explored.

The binding of leucine to NTA-labelled SMA-LeuT in the presence of 500mM NaCl was examined by carrying out a single point test in comparison with normal buffer conditions without supplementation of 500mM NaCl (Figure 5.6).
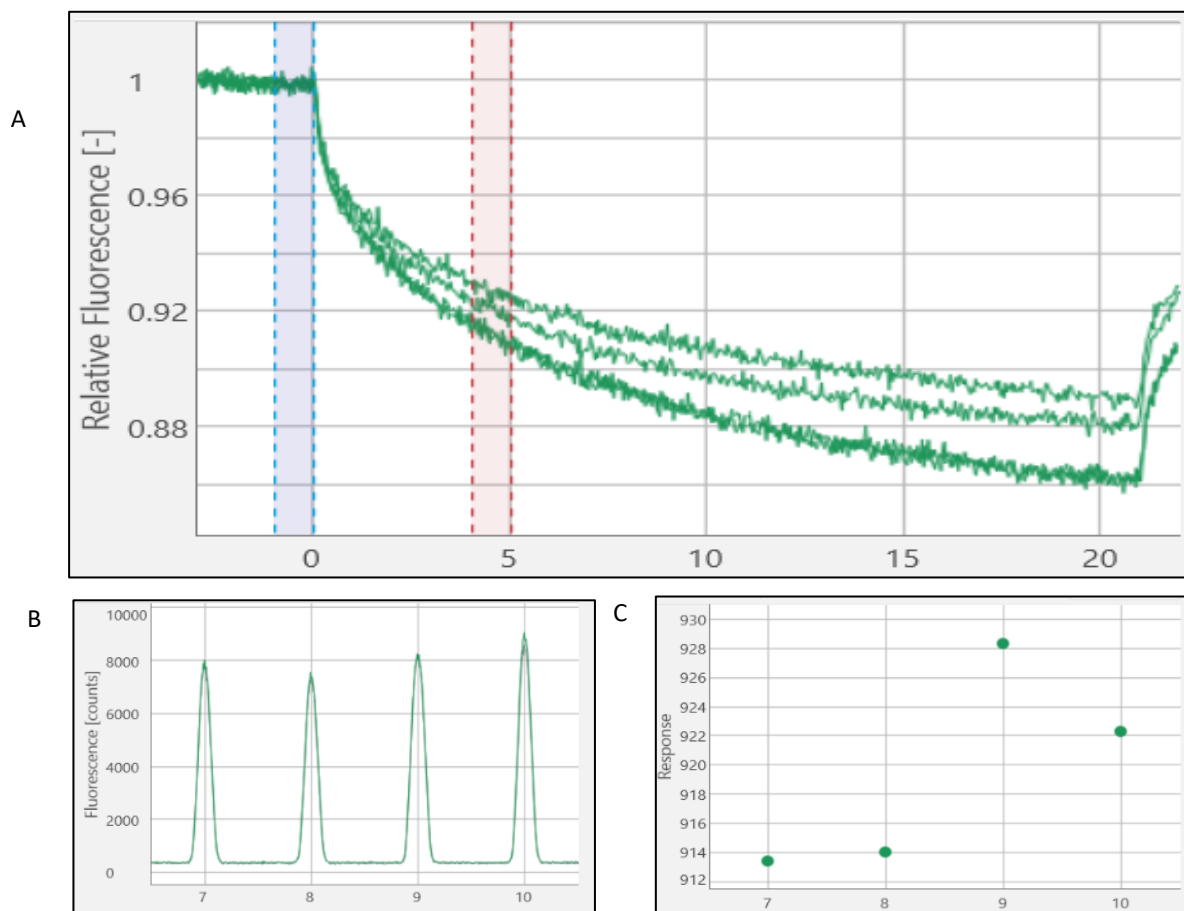
Figure 5.6 Leucine Binding Analysis testing the effect of high NaCl. *NTA-labelled SMA-LeuT samples were mixed with 0 µM (Peak 7) and 1 µM (Peak 8) concentrations of leucine. NTA-labelled SMA-LeuT samples were also supplemented with 500mM NaCl and mixed with 0 µM (Peak 9) and 1 µM (Peak 10) concentrations of leucine. The mixed samples were then loaded into MST capillaries and analysed via Monolith NT.115 and fluorescence observed. A) MST relative fluorescent trace of leucine binding assay. B) fluorescence count for leucine binding. C) response graph for leucine binding. Data is (n=1).*

Figure 5.6C shows a substantial difference in response between SMA LeuT + 1µM leucine (Peak 8) sample and SMA LeuT + 1µM leucine sample (Peak 10) supplemented with 500mM NaCl. This suggests that Na⁺ binding to LeuT can be measured. However, Figure 5.6C also shows that the response of SMA LeuT + 1µM leucine sample (Peak 10) is lower than SMA LeuT + 0µM leucine sample (Peak 9) despite both samples being supplemented with 500mM NaCl.

Therefore, it was decided to investigate the binding of leucine to NTA-labelled SMA-LeuT in the presence of 500mM NaCl by carrying out a titration series (Figure 5.7).
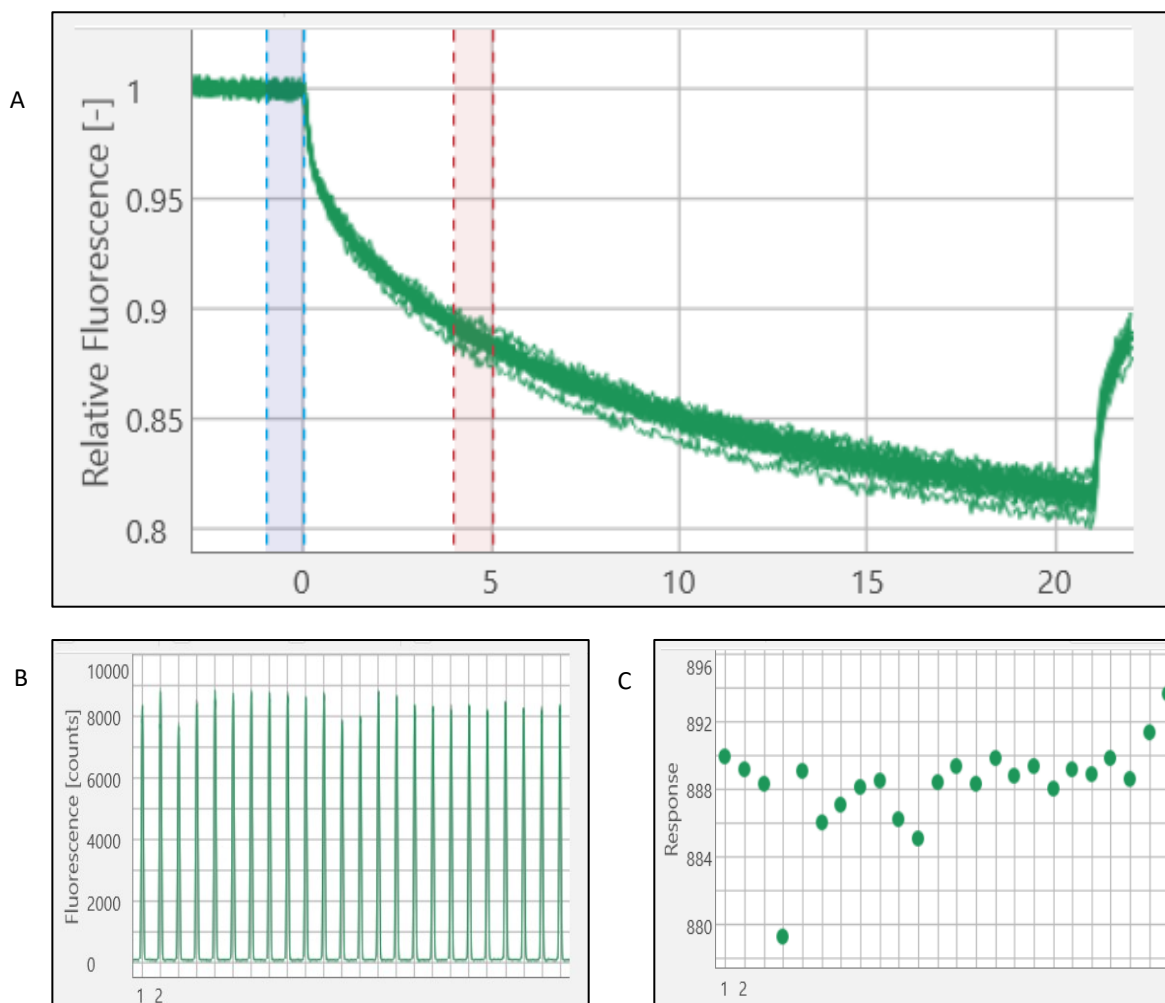
Figure 5.7 Leucine Binding Analysis across a range of leucine concentrations in the presence of high NaCl. *Two twelve-point titration series of leucine were prepared by carrying out 1 in 2 dilutions of leucine starting at 1 µM concentration. NTA-labelled SMA-LeuT samples were then mixed with leucine titration series and supplemented with 500mM NaCl. The supplemented samples were then loaded into MST capillaries and analysed via Monolith NT.115 and fluorescence observed. A) MST relative fluorescence trace of leucine binding assay. B) fluorescence count for ligand binding. C) normalised fluorescence response graph for leucine binding. Data is (n=1.*

Figure 5.7 shows no substantial differences in fluorescence across the leucine titration series, suggesting no specific binding of leucine to LeuT.

5.3 Desipramine binding to NTA labelled LeuT-SMALPs

Due to the variability and non-reproducibility of results, it was next decided to employ an alternative compound to analyse SMA-LeuT activity. Prior Studies by Zhou *et al.* had reported the binding of desipramine to LeuT. Therefore, the binding of desipramine to SMA2000 purified LeuT via MST was explored (Zhou *et al.*, 2007).

The initial dilution series test was carried out at medium MST power. Figure 5.8 shows a potential desipramine binding event. There is a poor signal: noise ratio, but the dose-response analysis is suggestive of binding at higher concentrations (Figure 5.8B).
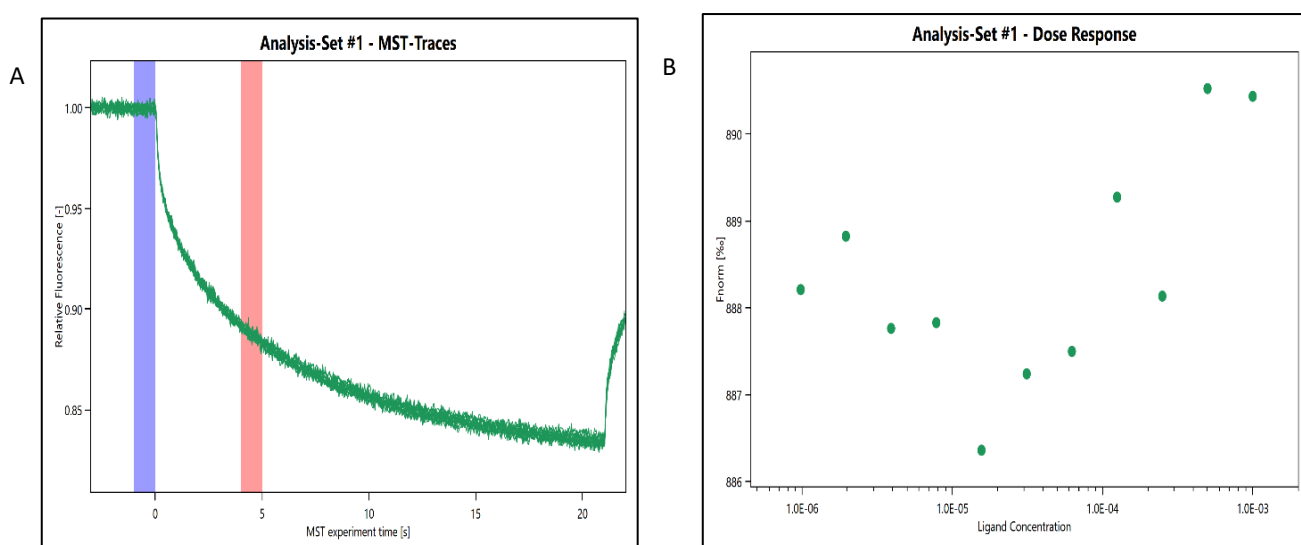
Figure 5.8 Initial Desipramine Binding Analysis. *A twelve-point dilution series of desipramine was prepared. Desipramine dilutions were then mixed with NTA-labelled SMA-LeuT and loaded into MST capillaries and analysed via Monolith NT.115 and fluorescence observed. A) MST relative fluorescence trace of desipramine binding assay. B) normalised fluorescence dose response graph for ligand binding. Data is (n=1).*

The initial desipramine dilution series test was carried out at medium MST power (40% Infrared laser power) and revealed a potential binding interaction, so next the effects when high MST power was used were examined. Figure 5.9 shows an improved shift indicative of a dose response. MST power corresponds to IR laser power and increasing the laser power can increase the temperature gradient induced from 2-6 °C. Low MST corresponds to 20% laser power, medium to 40% and high to 60% laser power. At high MST power, the thermophoretic movement of molecules and the decrease in fluorescence is generally larger and this can assist in examining molecular binding interactions.

A

B
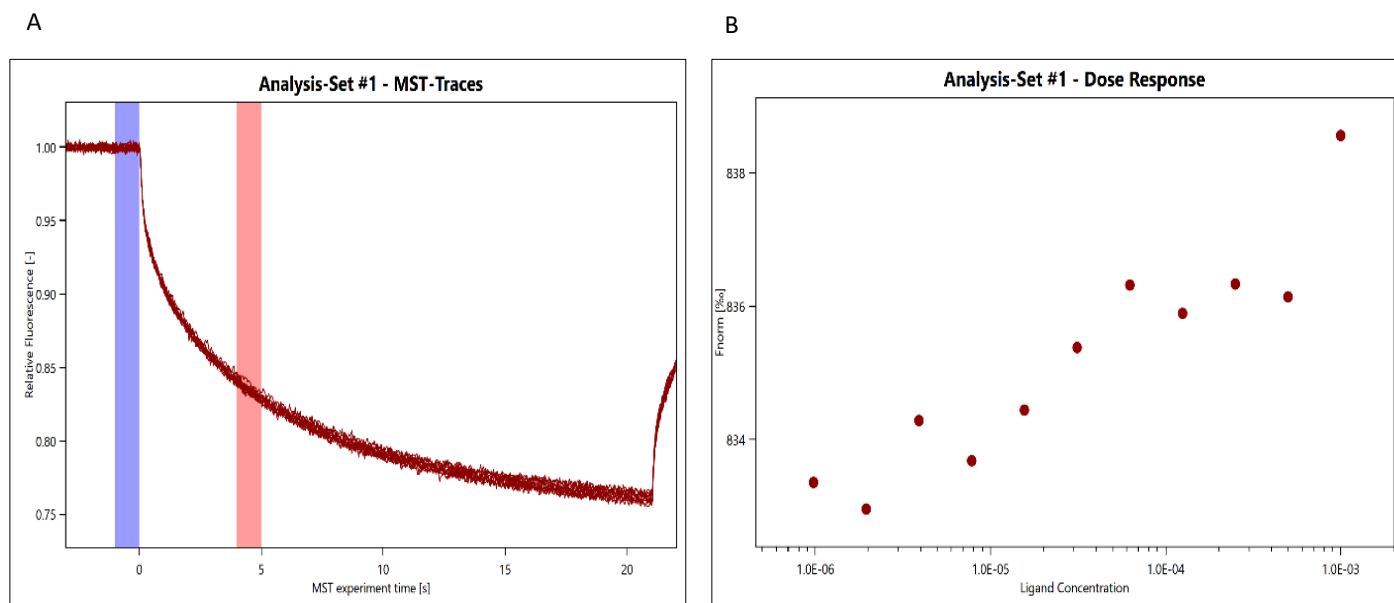
Figure 5.9 Desipramine Binding Analysis on high power. A twelve-point dilution series of desipramine was prepared. Desipramine dilutions were then mixed with NTA-labelled SMA-LeuT and loaded into MST capillaries and analysed via Monolith NT.115 and fluorescence observed. A) MST relative fluorescence trace of desipramine binding assay. B) normalised fluorescence (%) dose response graph for ligand binding. Data is (n=1).

Whilst moving through the MST on times (the point at which the signal is observed, shown by the red bar on the MST traces), it was noticed that a larger effect was occurring at 10 seconds and beyond. The 15 second time point appeared to be most optimal for this, as it produced the same signal as 20 seconds, but should be marginally less effected by experimental noise. Therefore, the experiment was replicated but the signal observation point moved close to 15 seconds (Figure 5.10).

Figure 5.10 displays data characteristics of a binding isotherm in spite of having comparatively small signal range.

A

B
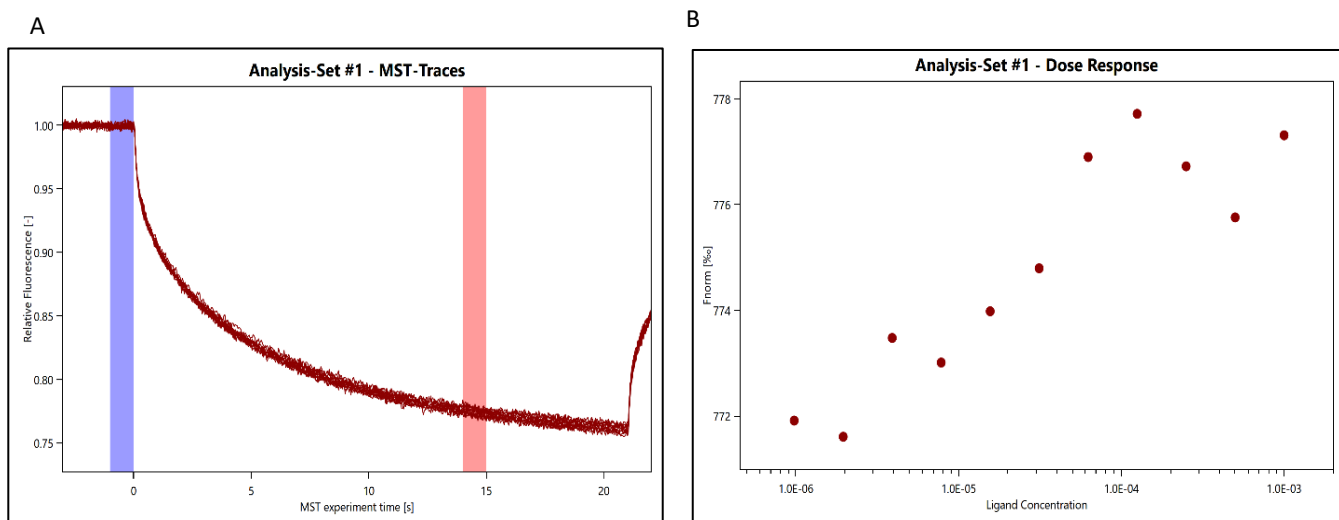
Figure 5.10 Desipramine Binding Analysis at a later time point. *A twelve-point dilution series was prepared by carrying out 1 in 2 dilutions of desipramine in DMSO and then further diluting samples in assay buffer and finally mixing with NTA-labelled SMA-LeuT samples to give a final top concentration of 200 µM. The samples were then loaded into MST capillaries and analysed via Monolith NT.115 and fluorescence observed. A) MST relative fluorescence trace of desipramine binding assay. B) normalised fluorescence dose response graph for ligand binding. Data is (n=1)*

Subsequently to confirm the results from desipramine dilution series experiment, an experiment was set up in duplicate and analysed using the same settings (Figure 5.11).

A

B
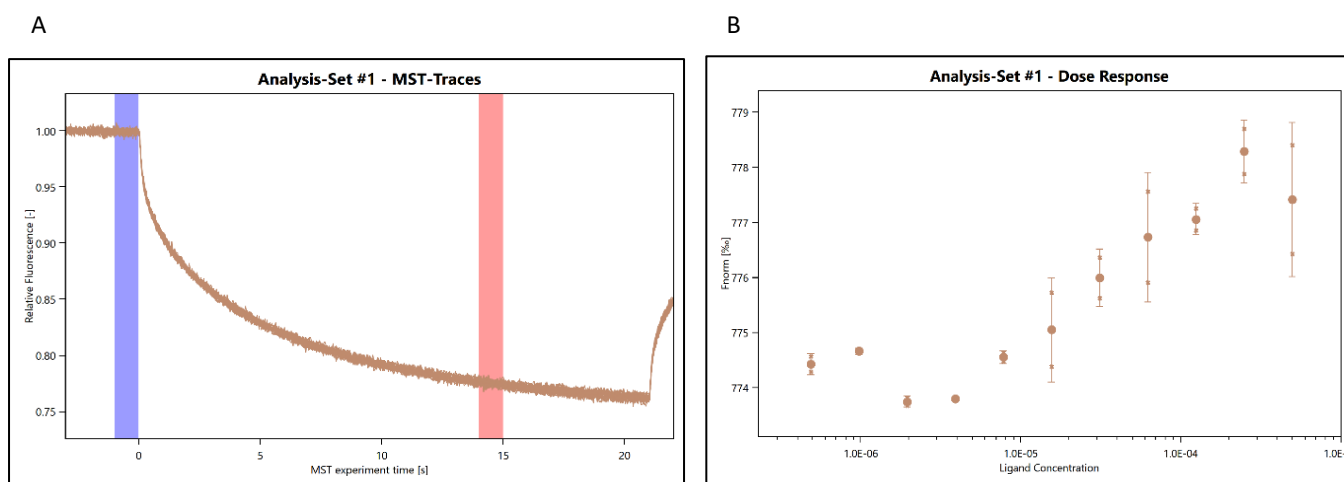
Figure 5.11 Desipramine Binding Analysis*. A twelve-point dilution series was prepared by carrying out 1 in 2 dilutions of desipramine in DMSO and then further diluting samples in assay buffer and finally mixing with NTA-labelled SMA-LeuT samples to give a final top concentration of 200 µM. The samples were then loaded into MST capillaries and analysed via Monolith NT.115 and fluorescence observed. A) MST relative fluorescence trace of desipramine binding assay. B) normalised fluorescence (%) dose response graph for ligand binding. Data is (n=2).*

Figure 5.11 displays a typical binding isotherm pattern and is comparable to that shown in Figure 5.10.

The MO analysis software was employed to further examine the data generated from desipramine binding experiments and potentially verify desipramine binding interactions (Figure 5.12). MO software analysis determined a Kd value of 40.6 µM for desipramine.
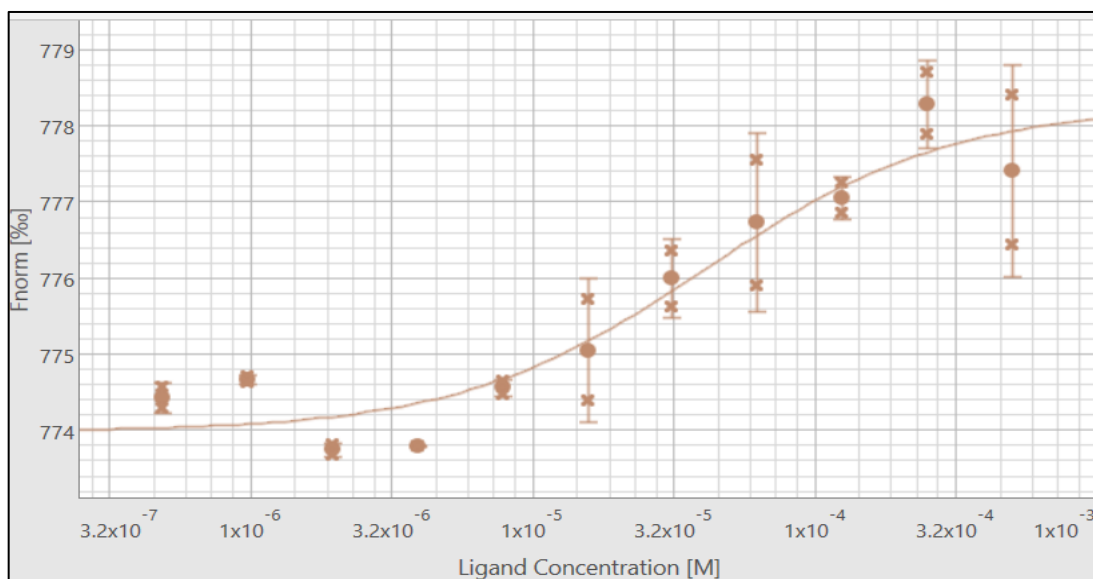
Figure 5.12 Desipramine Binding Analysis. *Data generated from desipramine dilution series experiments was analysed using the Kd fit option in Mo analysis software. Data is (n=1).*

For comparison, a duplicate experiment was set up using detergent DDM purified LeuT activity (Figure 5. 13).
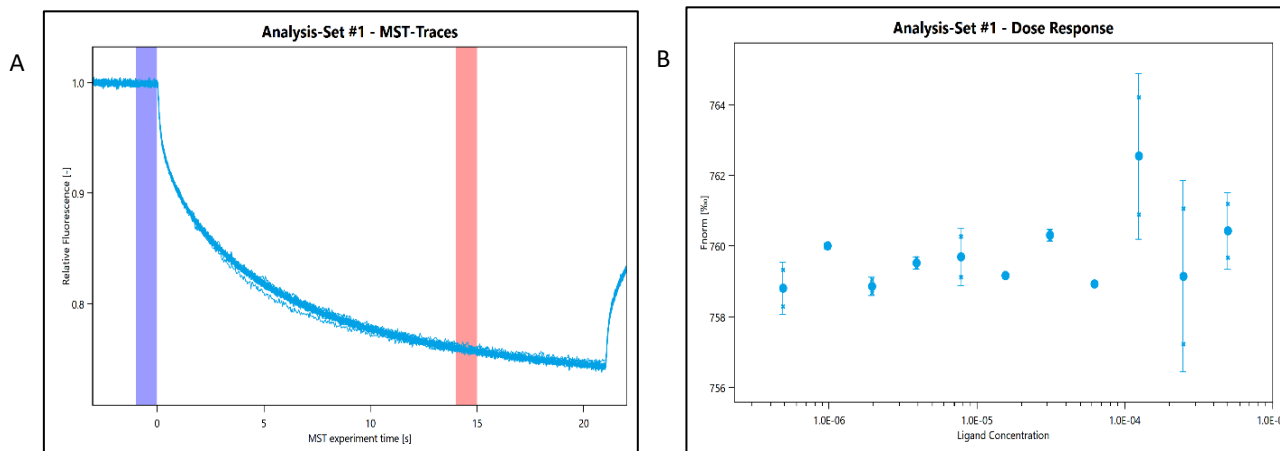
Figure 5.13 Desipramine Binding Analysis to DDM-LeuT*. A twelve-point dilution series was prepared by carrying out 1 in 2 dilutions of desipramine in DMSO and then further diluting samples in assay buffer and ultimately mixing with NTA-labelled DDM-LeuT samples to give a final top concentration of 200 μM. The samples were then loaded into MST capillaries and analysed via Monolith NT.115 and fluorescence observed. A) MST relative fluorescence trace of desipramine binding assay. B) normalised fluorescence dose response graph for ligand binding.*

Figure 5.13 does not show the same trend as previous SMA-LeuT experiments and does not display a typical binding isotherm pattern previously observed with SMA-LeuT experiments.

Therefore, to check the reproducibility of the findings with SMA-LeuT, the assay was repeated a further time to validate initial findings (Figure 5.14).
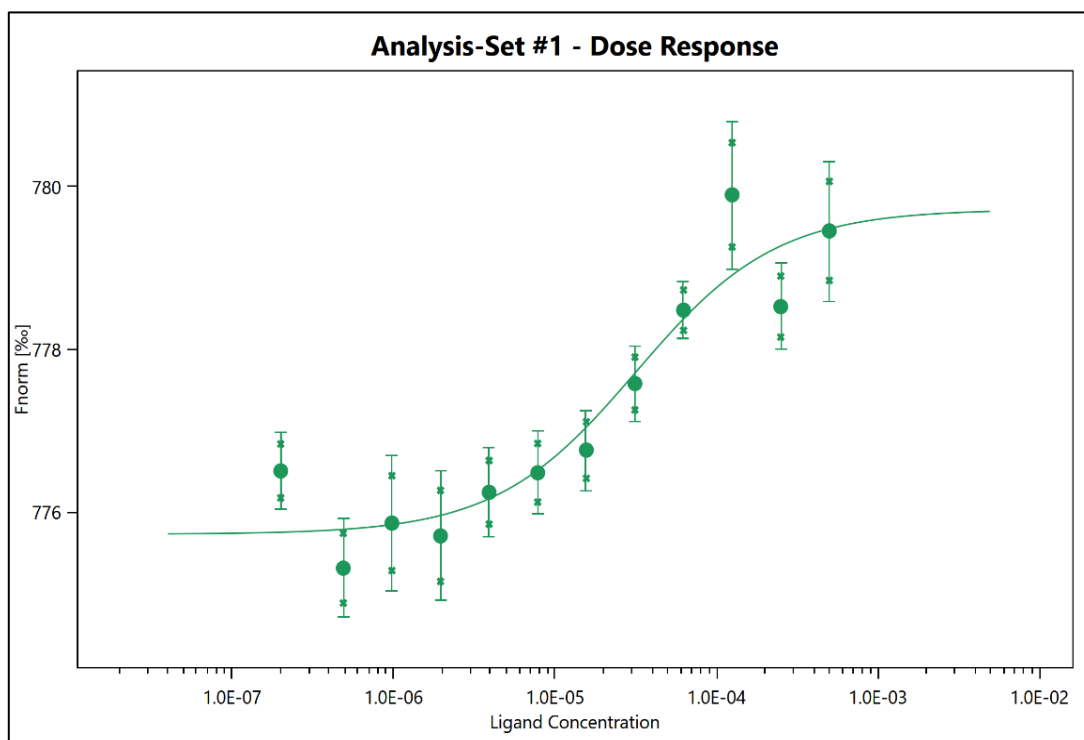
Figure 5.14 Desipramine Binding Analysis reproduction. *A twelve-point dilution series was prepared by carrying out 1 in 2 dilutions of desipramine in DMSO and further diluting samples in assay buffer and lastly mixing with NTA-labelled SMA-LeuT samples to give a final top concentration of 200 µM. The samples were then loaded into MST capillaries and analysed via Monolith NT.115 and fluorescence observed, and a normalised fluorescence dose response graph for ligand binding. Data is (n=1)*

Figure 5.14 displays a characteristic binding isotherm pattern and the same trend as obtained previously for SMA-LeuT experiments (Figure 5.12). A Kd value of 31.7µM was determined from Mo software analysis.

Finally, in order to dismiss the possibility of desipramine non-specifically binding to LeuT. A duplicate experiment was set up utilising partially denatured SMA2000 purified LeuT (Figure 5.15). SMA2000 purified LeuT sample was denatured by mixing with 0.5 % SDS in a 1 to 1 ratio , and incubation at 95 ˚C for 15 minutes.

Figure 5.15 does not display the same trend as previous SMA-LeuT experiments. The signal is different and has a greater amplitude, and the dose response curve is shifted to the right. A Kd value of 290µM was determined from Mo software analysis. This experiment does not seem to have fully reached saturation, but that it shows a quite different curve than that obtained prior to denaturation , furthermore, not having reached saturation will only shift the Kd even further.
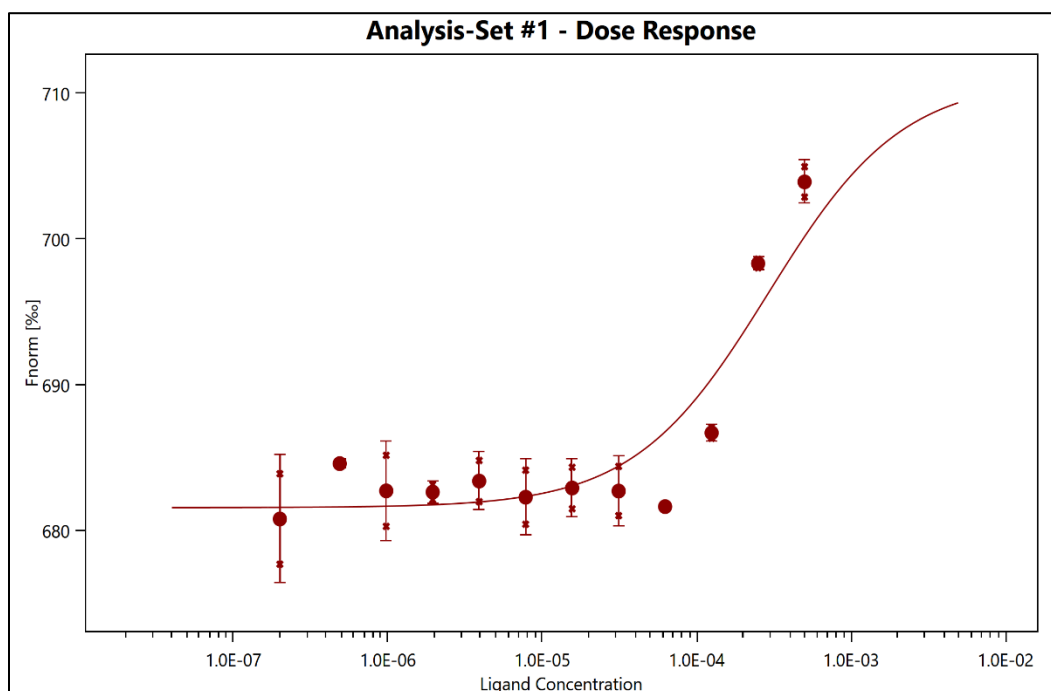
Figure 5.15 Desipramine Binding Analysis to partially denatured LeuT-SMALPs. *A twelve-point dilution series was prepared by carrying out 1 in 2 dilutions of desipramine in DMSO and then further diluting samples in assay buffer and lastly mixing with NTA-labelled denatured SMA-LeuT samples to give a final top concentration of 200 µM. The samples were then loaded into MST capillaries and analysed via Monolith NT.115 and fluorescence observed. Figure 4.15 normalised fluorescence dose response graph for ligand binding.*

5.4 Summary

- MST is an alternative method to study molecular interactions, which doesn't require immobilisation, but does require fluorescent labelling of one binding partner.
    - LeuT-SMALPs can be labelled with NTA-fluorescent dyes at the his tag.
- Whilst there were some suggestions that leucine binding to LeuT could be detected, it was inconsistent and not reproducible.
- Binding of the drug desipramine to SMA-LeuT could be measured by MST, but the signal change was low, requiring high power, and longer time points.
    - A Kd of 31-40 µM was measured.
    - Binding was disrupted by partial denaturation of LeuT.
    - Binding could not be detected when using DDM-LeuT.

6. Approaches to overcoming limitations of SMALPs for SPR and MST

Due to challenges encountered when trying to use SMA2000 or DIBMA for SPR (or MST) experiments, alternative approaches were investigated that might improve immobilisation.

The first idea was to modify the polymer so that immobilisation could involve the polymer rather than the protein. Preceding Studies by Lindhoud *et al*., had shown that it was possible to graft SMA polymers with cysteamine and produce SMA with solvent-exposed sulfhydryl's (SMA-SH). Sulphydryl chemistry offers the possibility of labelling with a range of different tags (Lindhoud et al., 2016). In 2018 an alternative protocol to create SMA-SH was published by (Schmidt and Sturgis, 2018) that was designed to be better suited to a Biosciences lab. Therefore, it was decided to follow this protocol to modify SMA2000 polymer to form SMA-SH.

The second idea was to add a SNAP tag to the target protein, which could be labelled with a wide range of different molecules to enable immobilisation or fluorescent labelling and might be more effective than the his-tag.

6.1 Generation and characterisation of SMA-SH

The protocol provided by Schmidt & Sturgis was followed to generate sulphydryl modified SMA2000 (Figure 6.1).
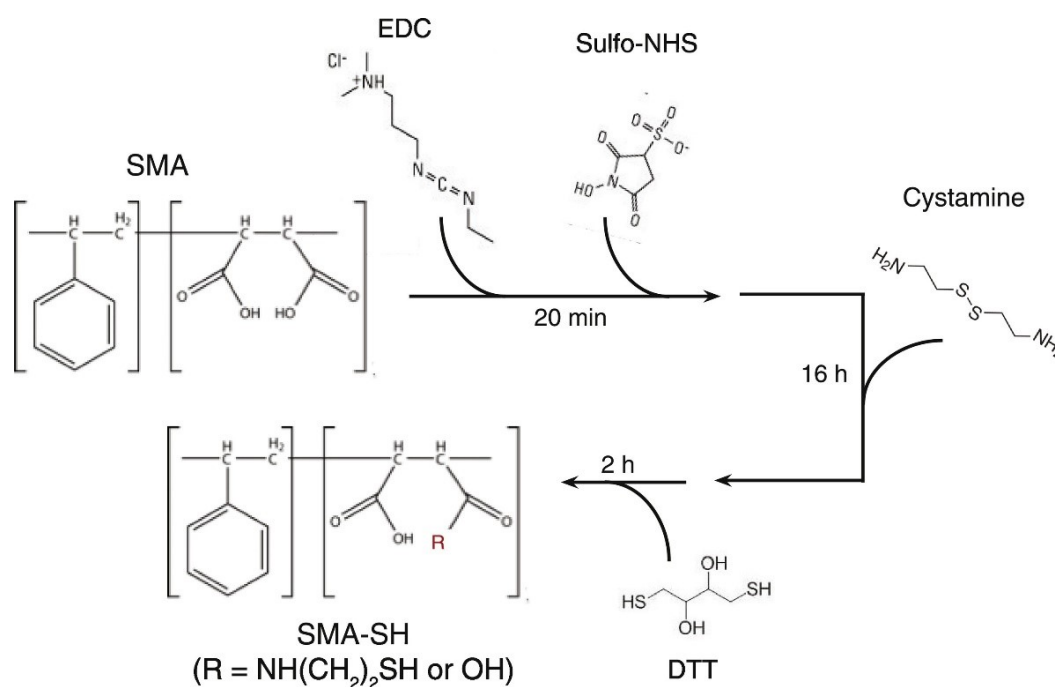
Figure 6.1 Schematic for generation of SMA-SH. *Schmidt & Sturgis, 2018, BBA Biomembranes 1860; 777-783. Full details of the protocol and guidance provided at Bio-protocols DOI: 10.21769/BioProtoc.2969. EDC (1-Ethyl-3-[3-dimethylaminopropyl]carbodiimide hydrochloride) , Sulfo-NHS (N-hydroxysulfosuccinimide).DTT(Dithiothreitol)*

In order to confirm the successful conversion of SMA2000 to SMA-SH, both SMA2000 and SMA-SH polymers were analysed by FTIR spectroscopy (Figure 6.2). Fourier transform infrared (FTIR) is a commonly used infrared spectroscopy. FTIR is a very useful technique as it does not require much time and it does not destroy the compound analysed. It is also sensitive and accurate. FTIR works on the principle that when infrared radiation passes through a compound, some of the radiation is absorbed by the covalent bonds present within the compound. Covalent bonds selectively absorb radiation of specific wavelengths, and this changes the vibrational energy in the bonds. Different types of vibrations can be induced by different types of atoms present within a bond. Different functional groups and bonds absorb infrared radiation at different frequencies and therefore the transmittance pattern produced is also different. Subsequently different compounds also produce different transmittance patterns. The spectrum generated can be visualised by plotting the transmittance on Y-axis and the wavenumber (cm^{-1}) on the X axis (Colthup, 2004; Fadlelmoula et al., 2022).
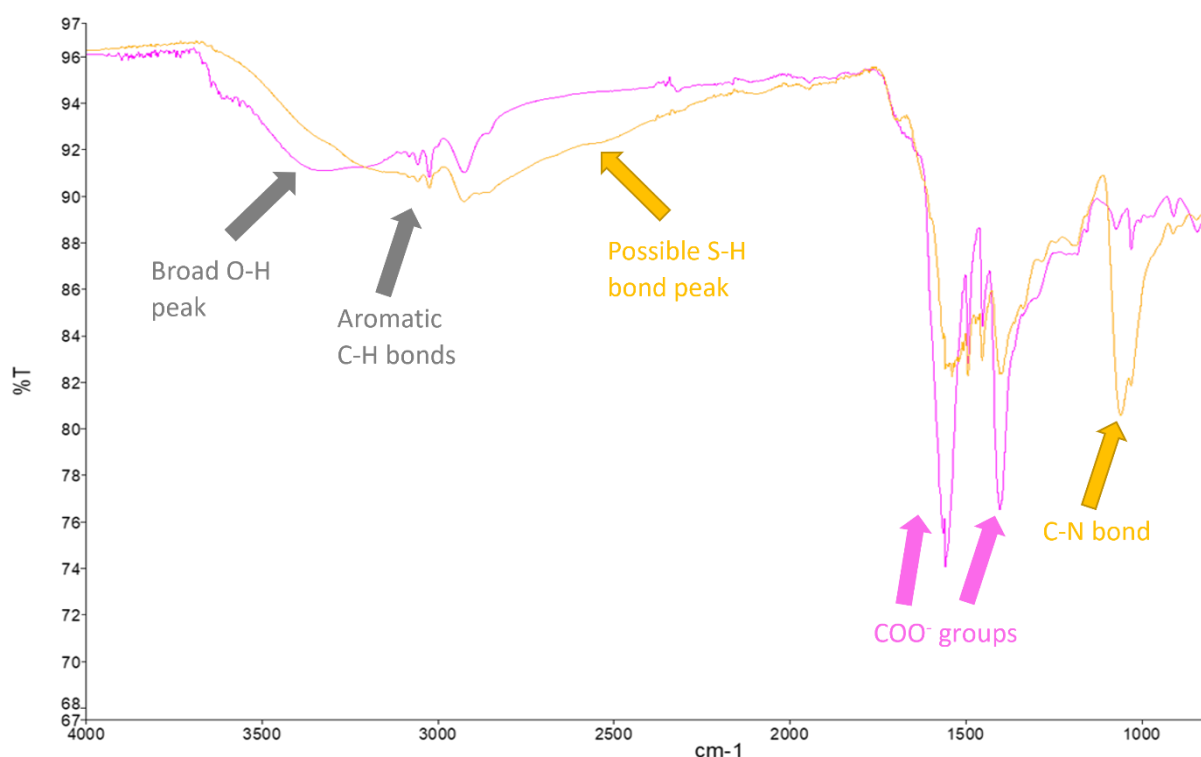
Figure 6.2 FTIR spectroscopy analysis of SMA2000 and SMA-SH. *SMA2000 and SMA-SH polymer samples in solid form were scanned with a scan range of 4000 – 650cm^{-1} and acquired data analysed. Purple spectra (SMA2000), Gold spectra (SMA-SH). The FTIR spectra were obtained by Dr Aiman Gulamhussein.*

Table 6.1 Common wavelengths associated with bond type in FTIR.

Wavelength (cm^{-1})	Bond type
3550-3200	O-H stretching
3100-3000	Aromatic C-H stretch
3000-2840	Aliphatic C-H stretch
2600-2550	S-H stretching
1550-1400	COO$^-$ stretching
1250-1020	C-N stretching

Figure 6.2 shows that for SMA2000 strong bands are observed between 1400 - 1550cm^{-1} indicating the stretching vibrations of carboxylate ions (COO$^-$), moreover broad OH bands are observed around 3300cm^{-1} indicating the presence of a carboxylic acid within the SMA polymer. For the SMA-SH sample generally similar peaks are observed, however there is the appearance of a weak peak around 2500 cm^{-1} which is characteristic of an S-H bond (these are always weak in signal) and a strong peak around 1000-1100 cm-1 which is characteristic of a C-N bond. The strong peak around 1000-1100 cm-1 demonstrates the modification of some of the maleic acid groups with the cysteamine group.

6.2 Using SMA-SH to solubilise and purify membrane proteins

Having established the polymer had been modified, the next step was to investigate if SMA-SH polymer could still be used to solubilise and purify membrane proteins (Figure 6.3).
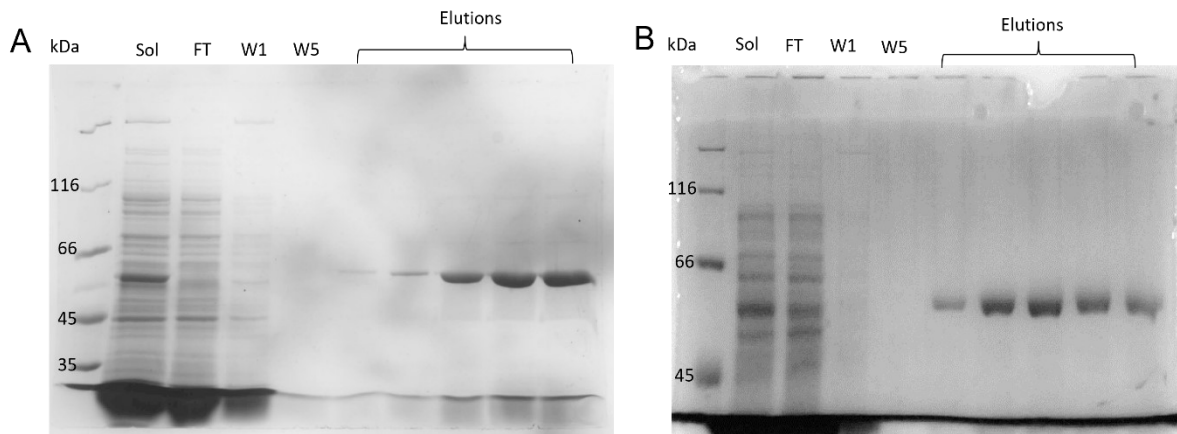
Figure 6.3 Affinity purification of SMA-SH solubilised membrane proteins. *SMA-SH solubilised membranes (sol) were incubated overnight with Nickel-NTA Resin at $4^{o}C$, following which unbound material (FT) was removed and resins washed with purification buffers supplemented with increasing concentrations of Imidazole (20mM – 60 mM). Proteins were eluted with buffers supplemented with 200mM imidazole. Samples were extracted from wash 1, wash 5, flow through and each elution collection, and run on SDS-PAGE along with a solubilisation sample. Gels were stained with Instant Blue. A) Atm1, B) LeuT.*

Figures 6.3 shows SMA-SH solubilised Atm1 or LeuT membranes were successfully purified. There are clear, quite pure bands within the elution fractions. Following successful purification of Atm1 and LeuT, the yield and purity of the SMA-SH purified proteins was analysed (Figure 6.4).

Figure 6.4 shows that an average yield of 0.44 µg protein/mg membrane and an average purity of 92 % was obtained for SMA-SH purified Atm1. Whereas a yield of 0.19 µg/mg and an average purity of 74% was obtained for SMA-SH purified LeuT.

There is a substantial difference between the average yield of SMA-SH purified Atm1 and SMA-SH purified LeuT, SMA-SH purified ATM1 has considerably higher average yield however LeuT experiments need to be repeated to establish validity of results.

There is also a significant difference in yield between SMA-SH purified Atm1 and SMA2000 purified Atm1 (P value 0.0142), where SMA2000 purified Atm1 gives a significantly higher yield. There is also a significant difference in yield between SMA2000 purified Atm1 and SMA2000 LeuT. SMA2000 purified Atm1 has higher yield in comparison to SMA2000 purified LeuT, but this may just reflect differences in expression levels.

There is no significant difference in purity between SMA2000 and SMA-SH purified Atm1 and LeuT. SMA-SH purification of Atm1 produced the highest purity and SMA-SH purification of LeuT the lowest however the difference in purity is not significant.
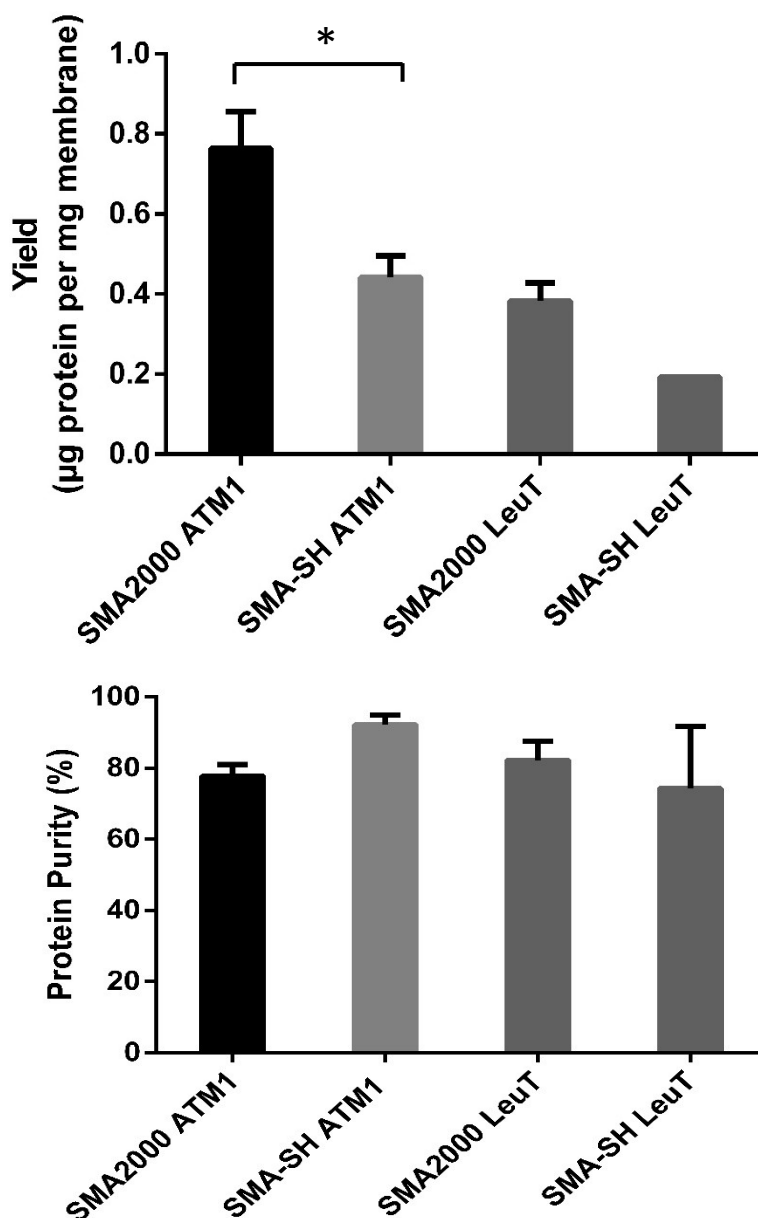
Figure 6.4 Analysis of SMA-SH & SMA2000 purified LeuT & Atm1 proteins. *A) protein yield quantification. Samples (20 µl) of SMA-SH or SMA2000 purified Atm1 and LeuT were run on SDS-PAGE alongside BSA standards (0.25, 0.5, 0.75, 1, 1.25 µg) and gels stained with instant blue. The intensity of bands on gels were analysed using densitometry and yield calculated. B) Purity quantification. To estimate the purity of Atm1 or LeuT proteins, elution fractions were analysed using densitometry (Image J); purity was estimated by examining the intensity of target protein band as a percentage of total lane intensity.* $P < 0.05$.

Next, the impact of magnesium chloride on SMA-SH purified Atm1 was investigated. It has been shown by others (Morrison *et al.* 2016), and in chapter 3 that SMA2000 SMALPs are extremely sensitive to divalent cations and therefore it was decided to examine if this was also the case for SMALPs formed from SMA-SH application. It has been proposed (Hawkins *et al.*, 2021) that the sensitivity is due to divalent cations binding to the two negatively charged groups of each maleic acid and causing some kind of conformational change which makes the polymer dissociate from the SMALP. With SMA-SH, some of the carboxyl groups are replaced with cysteamine, so it was investigated if this would make any difference to the divalent cation sensitivity.
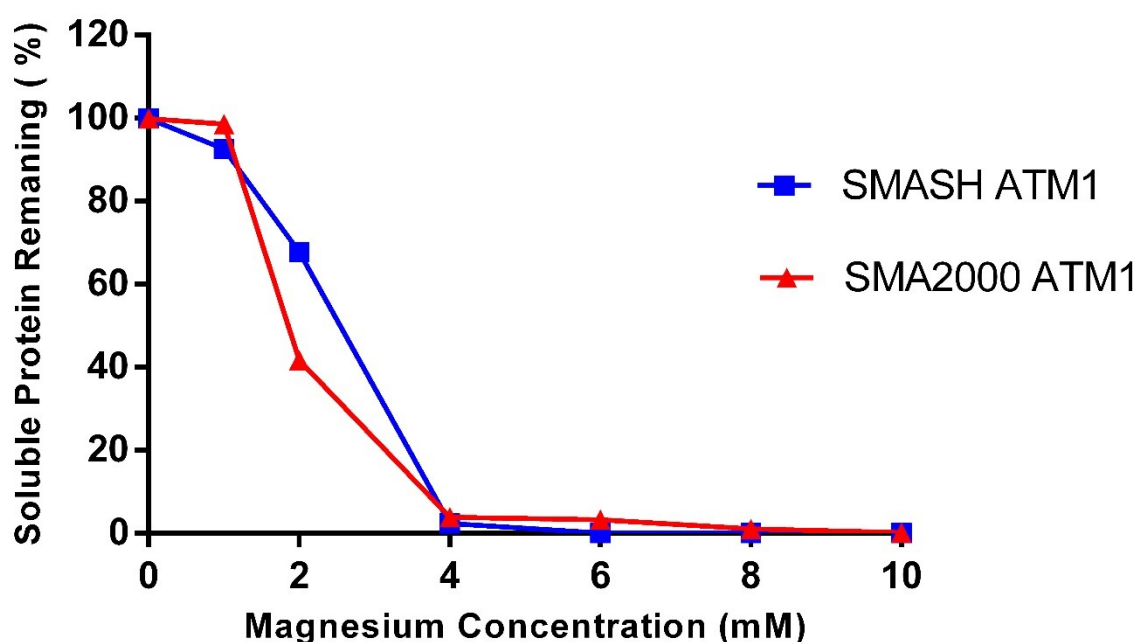
Figure 6.5 Magnesium sensitivity of SMA-SH purified Atm1. *SMA-SH purified Atm1 samples were mixed with increasing concentrations of magnesium chloride and centrifuged. Supernatants containing soluble proteins extracted and run on SDS-PAGE alongside marker. Gels stained with instant blue and analysed via densitometry (Image J) n=3.*

Figure 6.5 demonstrates that magnesium chloride concentrations of up to 1mM have no substantial impact on SMA-SH purified Atm1 however concentrations over 2mM cause the majority of SMA-SH purified Atm1 to precipitate out of solution. Therefore, the modification does not seem to improve the divalent cation sensitivity. Both SMA-SH purified and SMA2000 purified LeuT show similar magnesium chloride sensitivity profiles.

Finally, it was investigated if SMA-SH solubilisation had an impact on membrane protein LeuT structure and function by analysing ligand binding via a tryptophan fluorescence quenching assay. Two LeuT substrates were tested, Leucine and Alanine (Figure 6.6).

Figure 6.6 shows that both Leucine and Alanine bind to SMA-SH purified LeuT. Figures 6.6A and 6.6B both show relatively similar binding affinities and maximal degrees of quenching for both Leucine and Alanine. The binding affinities observed for SMA-SH purified LeuT are also very similar to SMA2000 purified LeuT. SMA-SH purified LeuT binding affinity to substrate leucine is nearly identical to SMA2000 purified LeuT and exhibits a higher degree of maximal quenching for substrate leucine. SMA-SH purified LeuT binding affinity for alanine is greater than SMA2000 purified LeuT however it exhibits a lower degree of maximal quenching for alanine in comparison to SMA2000 purified LeuT.
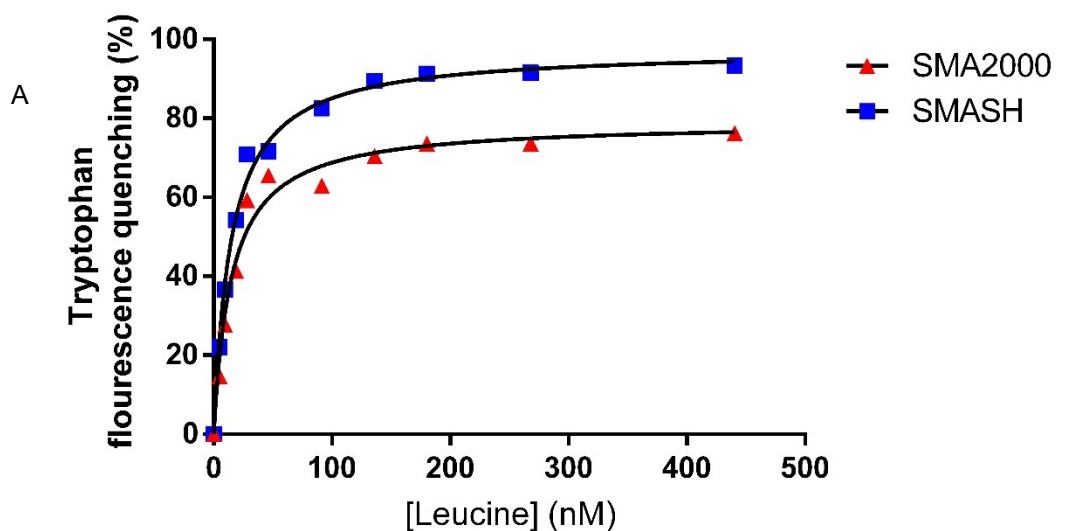
	SMASH	SMA2000
Bmax	97.49	79.1
Kd	14.57	14.99
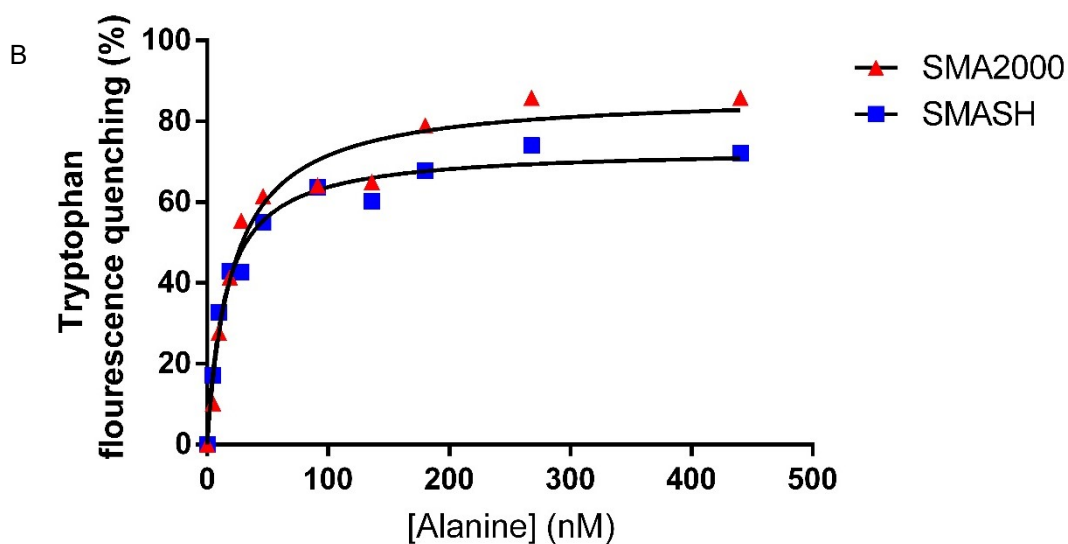
	SMASH	SMA2000
Bmax	73.28	86.81
Kd	14.92	21.26

Figure 6.6 Tryptophan fluorescence quenching ligand binding assay for SMA2000 and SMA-SH purified LeuT. *SMA2000 and SMA-SH purified LeuT samples were loaded into fluorometer and the quenching of intrinsic tryptophan fluorescence upon titration of substrates analysed (Leucine and Alanine). A) analysis of leucine binding to SMA2000 and SMA-SH purified LeuT. B) analysis of Alanine binding to SMA2000 and SMASH purified LeuT. n=1. Data are fitted with a one site binding curve by non-linear regression.*

6.3 Labelling SMA-SH with biotin maleimide

Biotin is frequently used as a tag for immobilisation of proteins due to its high affinity interaction with strepdavidin. Therefore, attempts to label the SMA-SH polymer with biotin maleimide were investigated, adapting the protocol of Sturgis & Schmidt to use biotin maleimide in place of a fluorophore maleimide (Figure 6.7). In order to verify successful incorporation of the biotin tag within SMA-SH, and the encapsulation of LeuT within biotin labelled SMALPs, it was planned to carry out a binding assay using streptavidin coated plates, but due to time constraints this wasn't possible.'
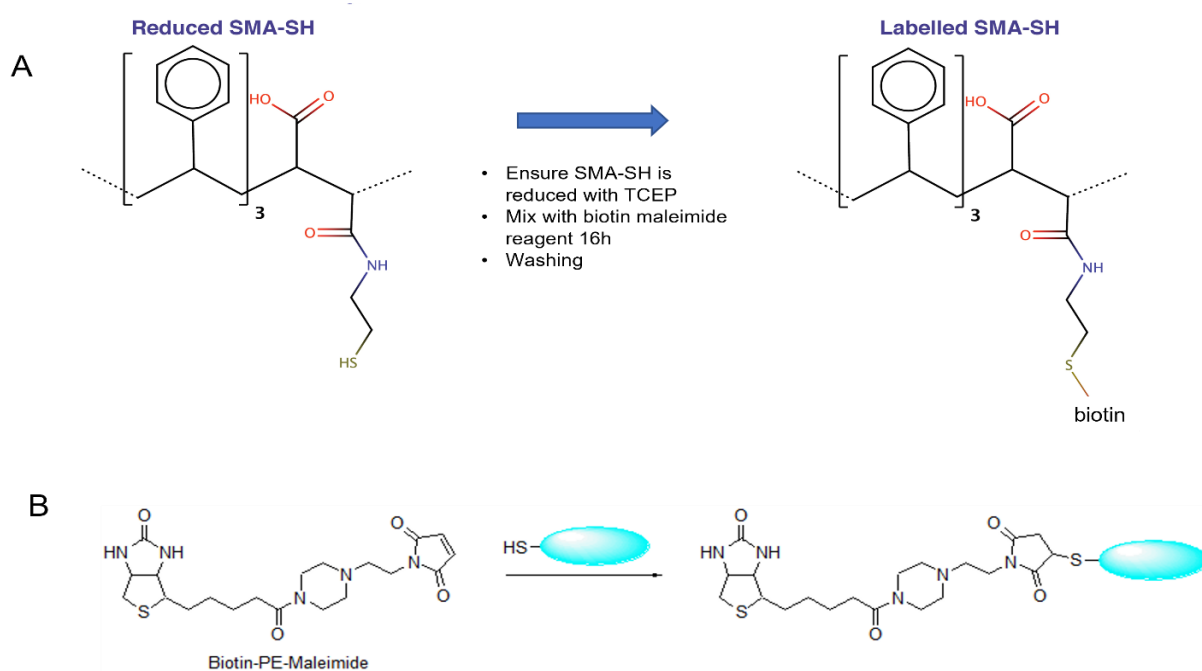
Figure 6.7 Mechanism for labelling SMA-SH with biotin maleimide. A; Schematic of labelling process, adapted from Bio-protocols DOI: 10.21769/BioProtoc.2969. B; Schematic of reaction between biotin maleimide and a sulphydryl group, adapted from Dojindo.eu.com.

Then biotinylated SMA-SH polymer was tested for solubilisation and purification of LeuT protein.

Figures 6.8 shows that SMA-SH Biotin solubilised LeuT membranes were successfully purified with clear bands visible in the elution fraction. Analysis of concentration and purity was undertaken and gave a purity of 94% using SMA-SH Biotin .
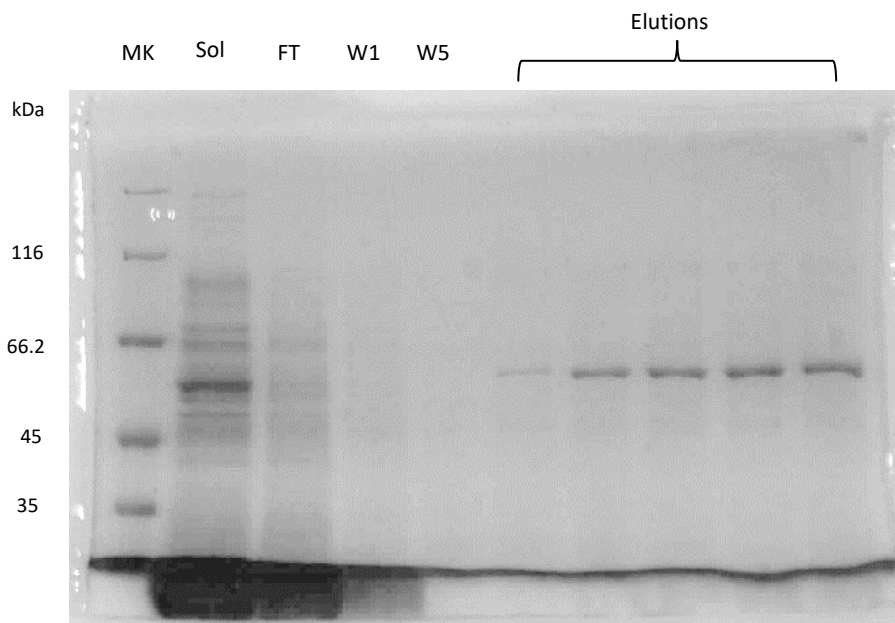
Figure 6.8 Affinity purification of SMA-SH Biotin solubilised LeuT. *SMA-SH Biotin solubilised LeuT membranes (sol) were incubated overnight with Nickel-NTA Resin at 4°C, following which unbound material (FT) was removed and resins washed with purification buffers supplemented with increasing concentrations of Imidazole (20mM – 60 mM). LeuT was eluted with buffers supplemented with 200mM imidazole. Samples were extracted from wash 1, wash 5, flow through and each elution collection, and run on SDS-PAGE along with a solubilisation sample. Gel was stained with Instant Blue.*

6.4 Use of SMA-SH purified protein in SPR or MST

Next, it was decided to investigate if SMA-SH purified LeuT could be employed in SPR studies. Initially it was tested if SMA-SH purified LeuT could be immobilized onto the surface of C1 sensor chip, which allows coupling between carboxyl groups on the chip surface and -SH, -NH$_2$ or -OH groups on the target. DDM purified LeuT was used as control.
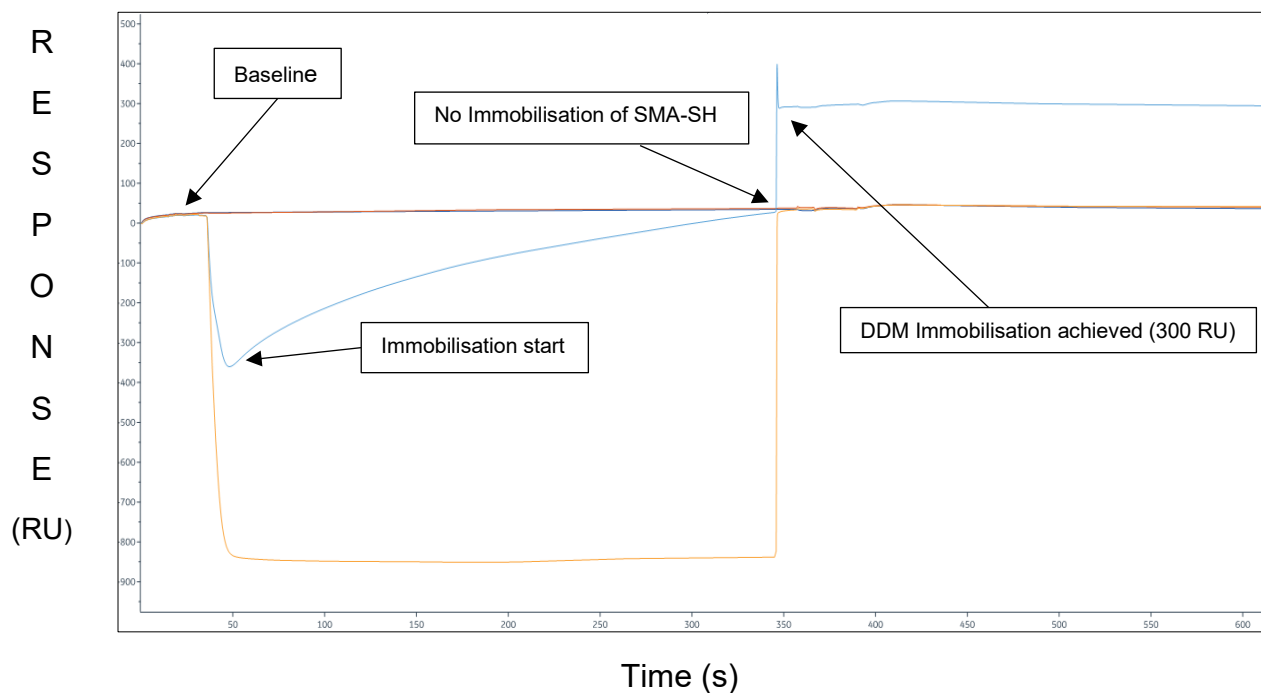
Figure 6.9 Immobilisation of SMA-SH and DDM purified LeuT on C1 chip. *Biacore 8K machine was primed into buffer (150 mM NaCl, 50 mM Sodium phosphate pH 7.5, 0.005 % Tween-20) and a C1 chip inserted . SMA-SH (yellow line) and DDM (blue line) purified LeuT samples were injected over the chip as instructed in the kit at 5µl min-1 for 600 seconds and response examined.*

Figure 6.9 shows no Immobilisation for SMA-SH purified LeuT and approximately 300 RU of Immobilisation for DDM purified LeuT. This clearly offered no improvement over previous immobilisation attempts. Due to time constraints, it wasn't possible to proceed to test the biotin-labelled SMA-SH sample.

Next the application of SMA-SH purified LeuT in MST experiments was trialled. MST experiments require one of the binding components of molecular interactions to be labelled, so SMA-SH purified LeuT samples were labelled with fluorescent maleimide. Since LeuT does not contain any cysteine residues there was no chance of the protein being labelled rather than the polymer.

Sample Number
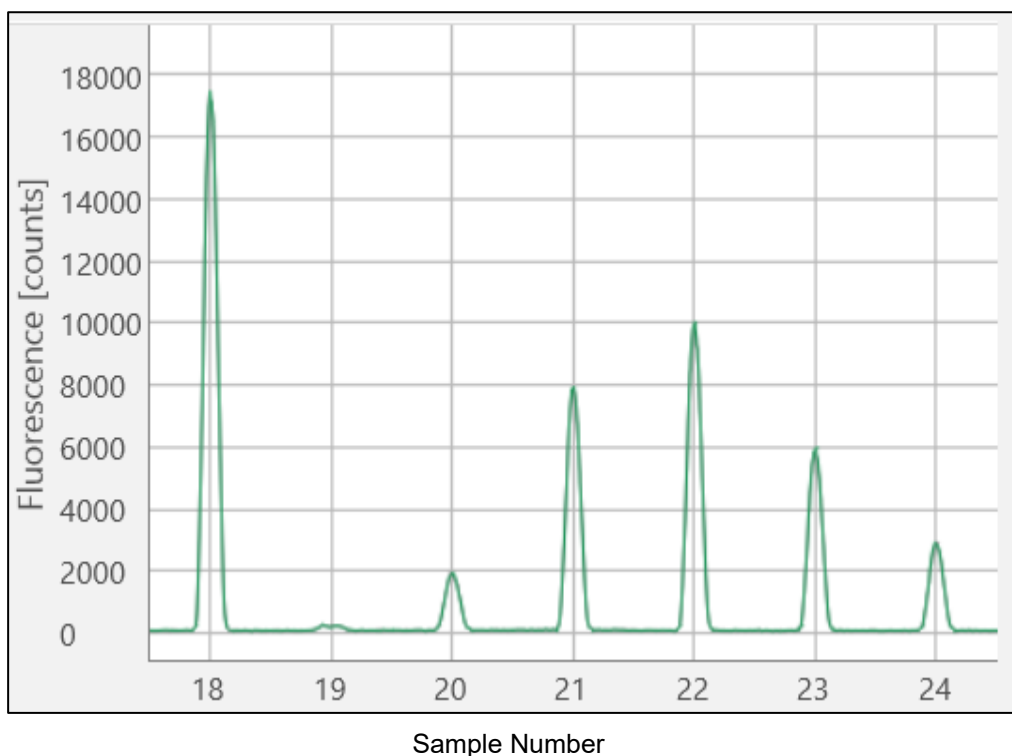
Figure 6.10 Fluorescent maleimide labelling analysis of SMA-SH LeuT. *A second-generation monolith protein labelling red-maleimide kit was obtained from Nanotemper and used to label SMA-SH purified LeuT . Next the labelled LeuT samples were loaded into a small size exclusion column and elution fractions collected and analysed by MST instrument. Sample numbers represent the order in which elution factions were collected from size exclusion column. Sample 18 representing elution 1 , samples 19,20,21,22,23 and 24 represent elution's 2,3,4,5,6 and 7.*

LeuT purified in SMA-SH was mixed with a red-maleimide dye and incubated at room temperature for 30 minutes, then SMALPs were separated from free dye using a small size exclusion column. Different elution factions from the column were analysed for fluorescence using the MST machine (Figure 6.10). Due to its larger molecular weight the SMA-SH LeuT would elute from the column first. The first elution corresponds to sample 18 on Figure 6.10, showing successful fluorescent labelling of the SMA-SH LeuT. In the second fraction (sample 19) very little fluorescence is detected. In fractions 3-7 (samples 20-24) peaks corresponding to free dye can be seen eluting. Therefore, the first elution (sample 18) was used in the following experiments.

Next it was decided to investigate the binding of leucine to fluorescent maleimide labelled SMA-SH LeuT by carrying out a single point spot test (Figure 6.11) Figure 6.11 shows that maleimide labelled SMA-SH LeuT samples have a similar response in the presence and absence of 1µM leucine , and no specific binding was detected.
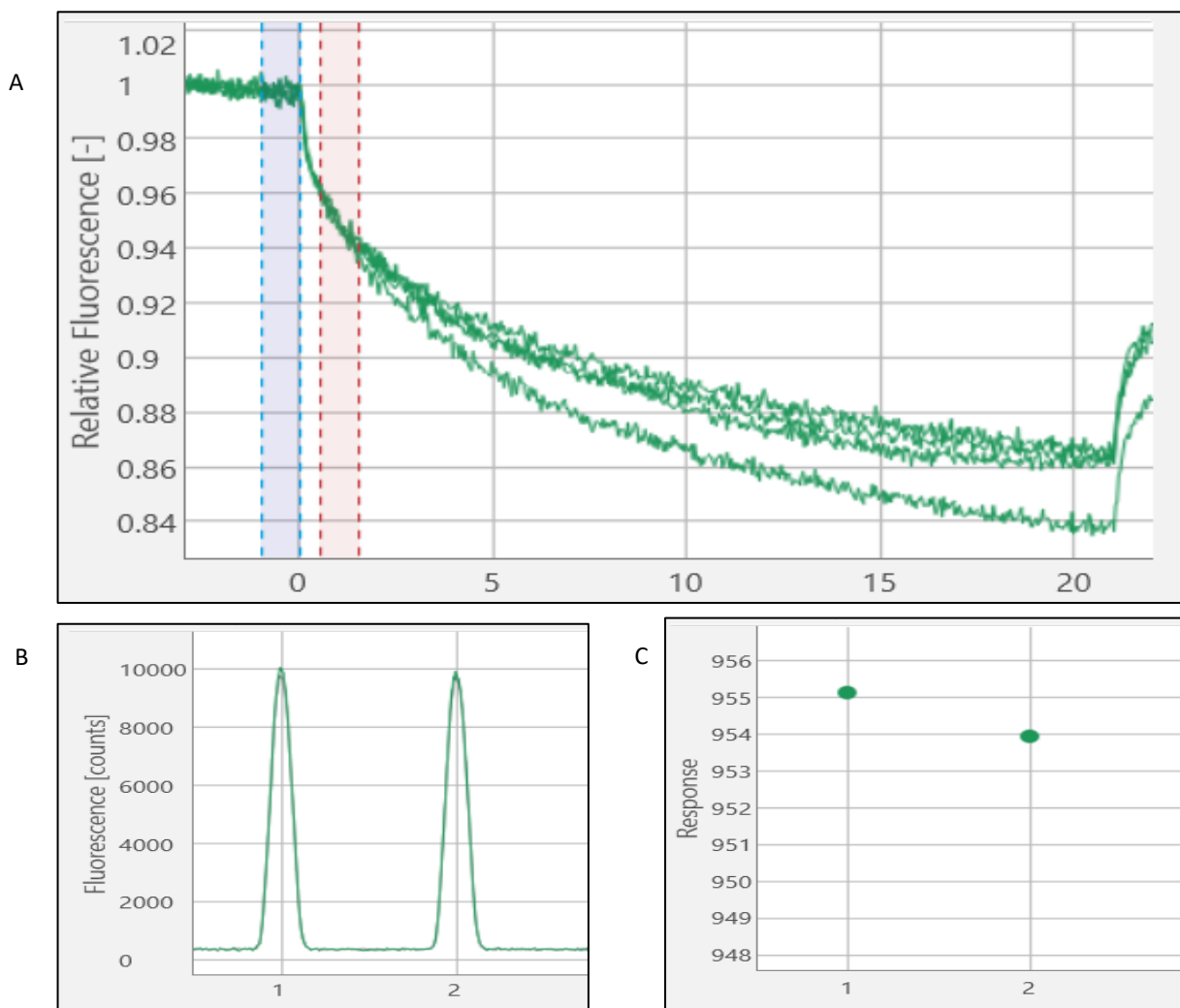
***Figure 6.11 Leucine Binding Analysis for Maleimide labelled SMA-SH LeuT**. Samples were mixed with 0 µM and 1 µM concentrations of Leucine and fluorescence observed via MST analysis. Peak 1 (SMA-SH LeuT), Peak 2 (SMA-SH LeuT + 1 µM leucine). A) representative MST trace of leucine binding assay. B) representative fluorescence count for ligand binding. C) representative response graph for leucine binding.*

6.5 Generation of a SNAP-tagged Atm1 construct

The SNAP tag is a genetically encoded 20kDa fusion protein tag that reacts specifically with benzylguanine derivatives to form an irreversible covalent labelling with a probe of your choosing (Cole, 2013) (Figure 6.12). A wide range of different benzylguanine probes are commercially available, including fluorescent probes or affinity molecules such as biotin. Also, the specificity of the SNAP tag reaction means there are no concerns with labelling the protein elsewhere within its sequence (as there can be with maleimide reactions and cysteines).
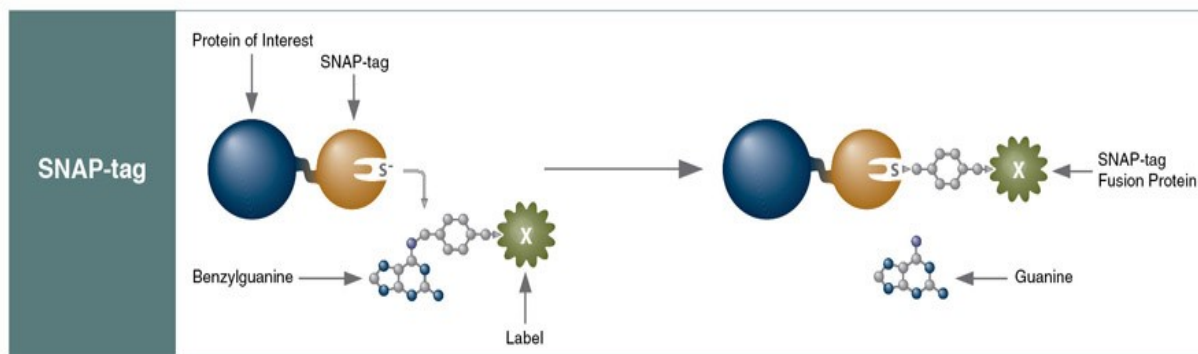
***Figure 6.12 Schematic for reaction of SNAP tagged proteins with benzylguanine probes**. From NEB.com.*

The plasmid pSNAP-tag(T7)-2 was selected for adding the SNAP tag to a protein, and Atm1 was chosen as the target protein to study. The pSNAP-tag(T7)-2 plasmid has two multiple cloning sites (Figure 6.13), to enable addition of the SNAP tag at either the N-terminal or C-terminal end of the protein. Two sets of primers were designed to amplify the Atm1 gene from the pJL-H6 vector. To add the SNAP-tag at the N-terminus primers included restriction sites for SbfI in the forward primer and XhoI in the reverse primer. To add the SNAP-tag at the C-terminus primers included NdeI sequences in the forward primer, and EcoRI in the reverse primer, as well as mutating the stop codon (Table 6.2).
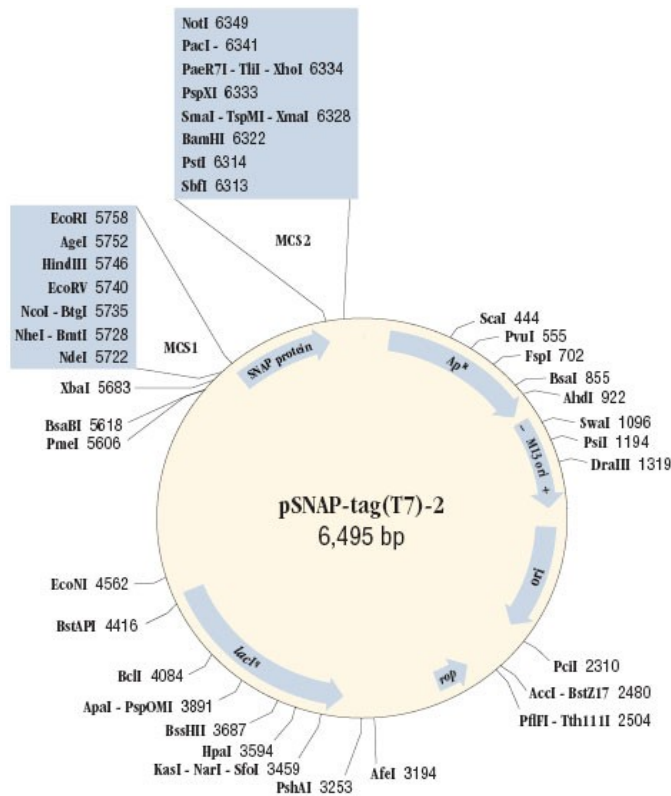
Figure 6.13 Plasmid map for pSNAP-tag(T7)-2. *Obtained from NEB.com.*

Table 6.2. PCR primers. Locations of restriction sites are underlined. The mutation of the stop codon is in bold. Atm1 sequences are in capitals.

Position of tag	PCR primer	Features	Primer sequence
N-terminal SNAP tag	Forward primer	SbfI	ggggcctgcaggcATGCCTCCCGAAACCGCAACG
	Reverse primer	XhoI	ccccctcgagTTAGTGATGATGGTGATGGTGCTCC
C-terminal SNAP tag	Forward primer	NdeI	ggggcatATGCCTCCCGAAACCGCAACG
	Reverse primer	EcoRI Remove stop codon	cccgaattcGTGATGATGGTGATG**GTG**GTGATGATGGTGATGGTGCTCC

As addition at the C-terminus would require a second step to add a stop codon after the SNAP tag, initial trials were undertaken to add the SNAP tag at the N-terminus of Atm1. The first step was to amplify the amount of starting material pJL-H6-Atm1 plasmid. DH5α *E. coli* cells were transformed with the plasmid, small overnight cultures grown and DNA harvested by mini-prep. A range of PCR

conditions were tested, varying the amount of primers and the annealing temperature (Table 6.3). Samples of the PCR products were then run-on agarose gel electrophoresis (Figure 6.14).

Table 6.3 PCR conditions and yield of DNA.

Sample number	DNA concentration (ng/ul)	Primer dilution	Temperature
1	97.3	1/10	62.3
2	18.5	1/20	62.3
3	12.0	1/30	62.3
4	109.7	1/10	59.5
5	67.2	1/20	59.5
6	11.1	1/30	59.5
7	71.4	1/10	55.7
8	86.0	1/20	55.7
9	19.7	1/30	55.7

All of the PCR conditions produced a band at the expected size of approximately 2kb, with condition 1 giving the most intense band. Three PCR samples (1-3) were selected and digested with the enzymes SbfI and XhoI. Following enzyme cleanup steps, they gave concentrations of 21-27 ng/µl.
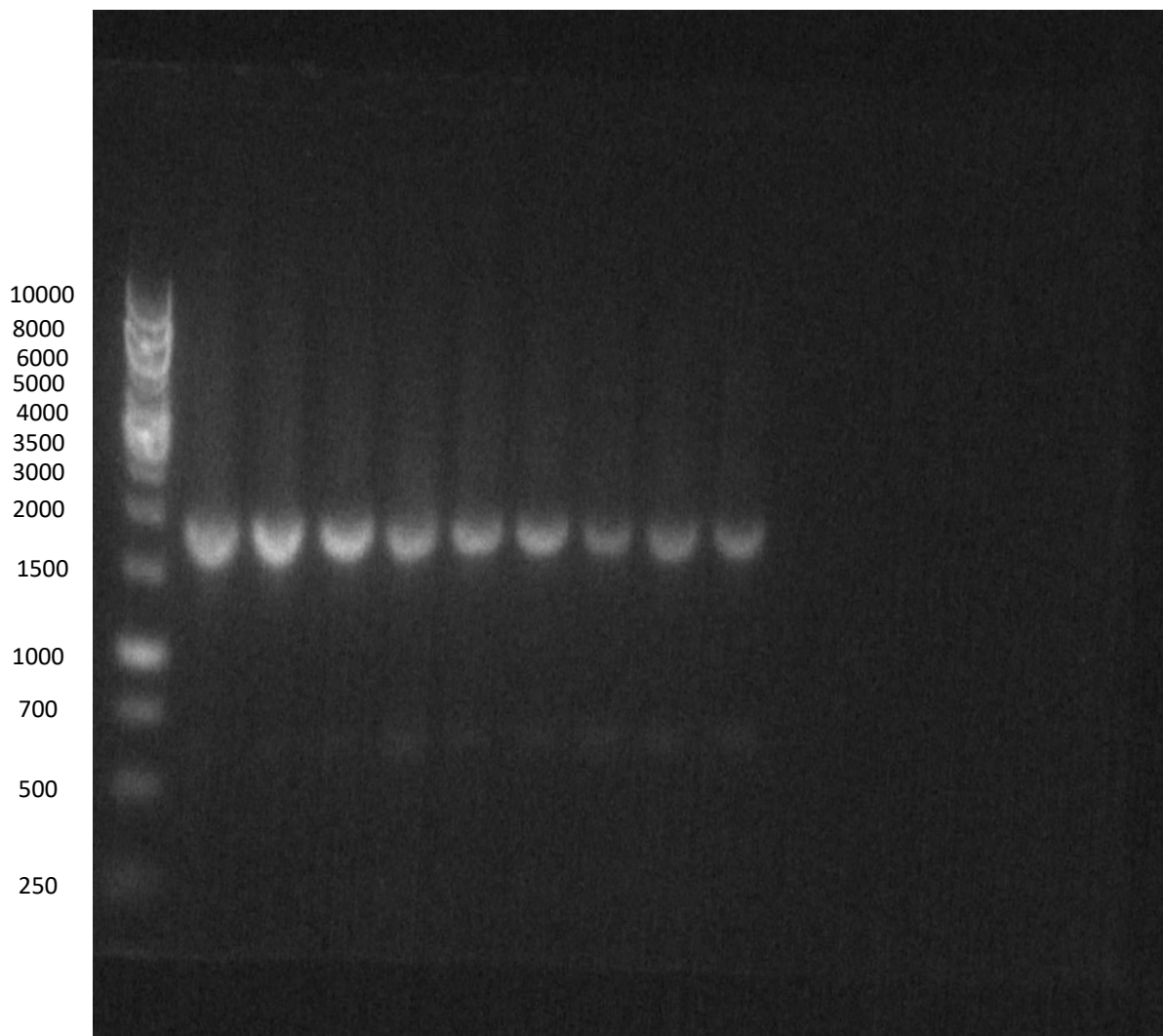
Figure 6.14 Agarose gel analysis of Atm1 PCR products. *Samples of PCR products were supplemented with 6X DNA loading dye and run a 1% agarose gel alongside 1KB DNA ladder.*

The plasmid pSNAP-tag(T7)-2 was also transformed into DH5α *E.coli* cells and amplified by miniprep before being digested with SbfI and XhoI. Ligation reactions were set up with the digested PCR products and digested pSNAP-tag(T7)-2 plasmid overnight, and this was then transformed into DH5α cells. However, no transformants were obtained. Due to time constraints further progress was not possible.

6.6 Summary

- Reaction of SMA2000 with cystamine was carried out to form SMA-SH.

- Proteins could be successfully solubilised and purified using SMA-SH.

- SMA-SH purified samples could be labelled with a fluorescent-maleimide tag.
  - This was carried out after protein purification. LeuT contains no cysteine residues so labelling of the protein couldn't occur, however this could be a problem for other proteins labelled in this manner.

- Reaction of SMA-SH with biotin-maleimide was carried out, and it had no apparent effect on the ability of the polymer to extract and purify LeuT.

- Initial tests for SPR and MST using SMA-SH were not successful.
  - Biotin-labelled SMA-SH was not tested and may offer a good approach for the future.
  - Further optimisation of fluorescent labelling is needed for MST.

- Addition of a SNAP-tag to Atm1 offers the possibility of specifically adding a range of probes/tags.
  - PCR amplification of Atm1 from pJL-H6-Atm1 was successful.
  - Ligation into the pSNAP-tag(T7)-2 plasmid was not successful.
  - Further work is needed to complete the molecular biology, test expression of the SNAP-tag protein, and investigate if the tag has any effect on protein function.

7. Testing novel polymers as an alternative to SMA2000

A range of SMA polymers and derivatives have been developed since the initial application of styrene maleic acid co-polymers for membrane solubilisation and extraction (Knowles *et al*., 2009). It is well established that SMA2000 does have several limitations, including problems with affinity resin binding, a sensitivity to low pH (Scheidelaar *et al*., 2016; Pollock *et al*., 2018) and a sensitivity to divalent cations (Oluwole *et al.,* 2017; Morrison *et al*., 2016) and it was shown in chapter 4 that it is challenging for immobilisation on SPR chips. For ABC transporters the sensitivity to divalent cations is particularly problematic as they require Mg^{2+} as a cofactor for ATP hydrolysis. Therefore, it was decided to investigate two different series of SMA polymer variants. Atm1 was used for these studies because it is an ABC transporter.

7.1 Partially esterified SMA polymers

An example of SMA polymer variants that have been presented in the literature is the partially esterified variants of SMA which have been shown to solubilise cyanobacterial thylakoid and plant membranes more effectively than SMA2000 (Korotych *et al.,* 2019; Brady *et al*., 2019; Cherepanov *et al.,* 2020; (Korotych *et al.,* 2021). Several partially esterified variants of SMA have been developed including SMA1440, SMA17352 and SMA2625 (Figure 7.1 & Table 7.1).
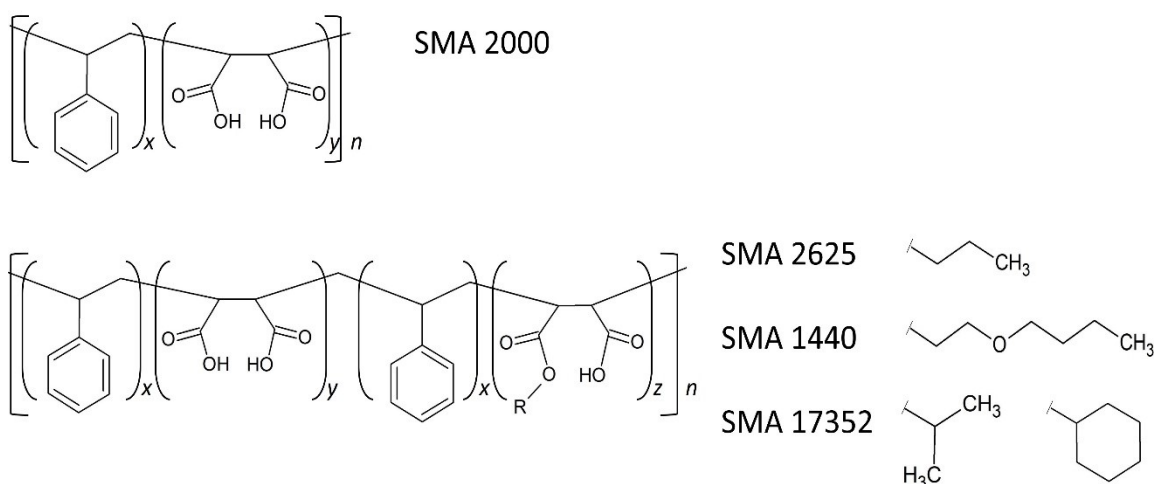
Figure 7.1 Structures of the partially esterified polymers. *SMA2000 is a co-polymer of styrene and maleic acid. SMA2625, SMA1440 and SMA17352 are partially esterified variants of SMA, with the ester moieties ® shown. Hawkins et al (2021) BBA Biomembranes 1863; 183758.*

Table 7.1 Properties of polymers according to the manufacturers. *The average ratio of styrene to maleic acid within the polymers. Mw, the average molecular weight of the polymers. The number average molecular weight (Mn), which is the total weight of the polymer molecules divided by the number of molecules. The polydispersity index (PDI), which is equal to Mw/Mn and is a measure of the distribution of the molecular weights. Hawkins et al (2021) BBA Biomembranes 1863; 183758*

Polymer	S:MA ratio (Cray Valley)	Modification	Mw (kDa)	Mn (kDa)	PDI	S:MA ratio (^{1}H-NMR)
SMA 2000	2:1		7.5	3.0	2.5	2.6:1
SMA 2625	2:1	1-propanol	9.0	3.6	2.5	2.7:1
SMA 1440	1.5:1	2-butoxyethanol	7.0	2.8	2.5	2.3:1
SMA 17352	1.7:1	Cyclohexanol & 2-propanol	7.0	2.8	2.5	1.8:1

Therefore, it was decided to investigate if SMA1440, SMA17352 and SMA2625 polymers could be used to solubilise and purify Atm1 protein. *E .coli* (BL21) cells expressing Atm1 protein were harvested, and membranes extracted. The Atm1 membranes were solubilised using either SMA1440, SMA17352 and SMA2625 and purified by nickel affinity chromatography (Figure 7.2).

Figure 7.2 shows that SMA1440, SMA17352 and SMA2625 solubilised Atm1 membranes were all successfully purified producing strong bands of Atm1 with very few contaminants. In all cases the strong Atm1 band seen in the solubilised protein sample (Sol) is not present in the flowthrough (FT) showing successful binding of Atm1 to Nickel resin. Figure 7.2B, with SMA17352 solubilisation and purification shows marginally more contaminants in the eluent bands than SMA2625 Figure 7.2C.
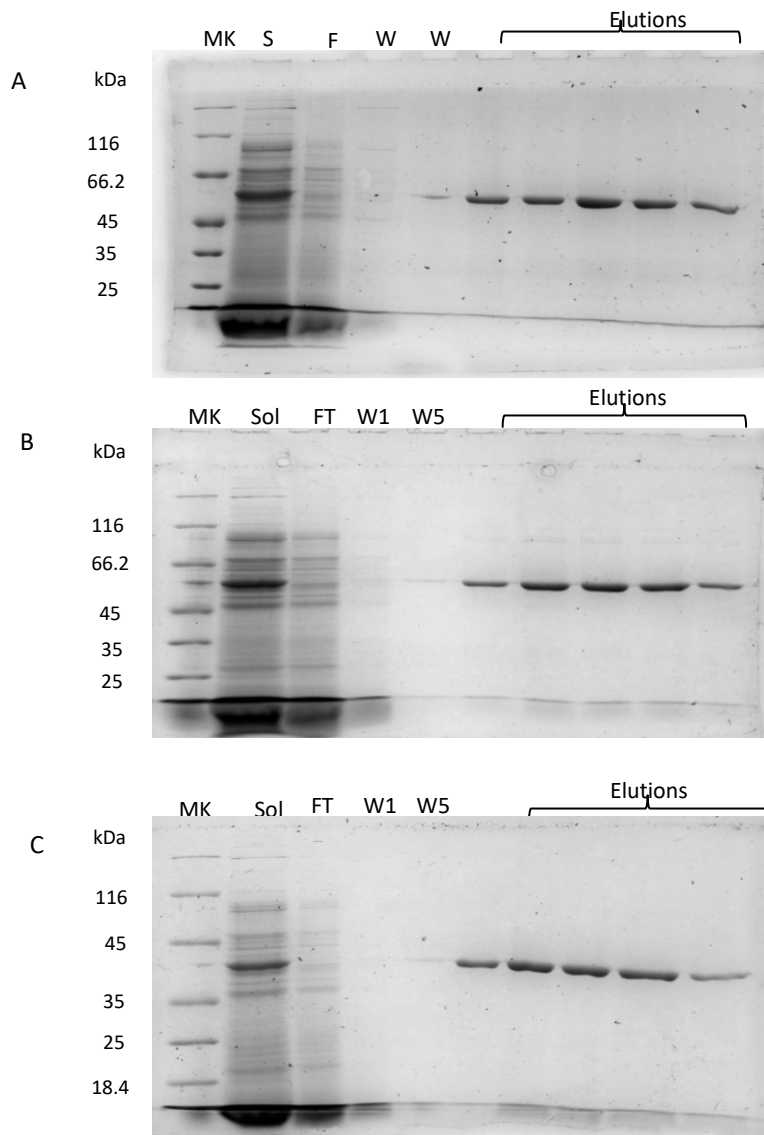
Figure 7.2 Affinity purification of SMA1440, SMA17352 and SMA2625 solubilised Atm1. *SMA1440 (A), SMA17352 (B) and SMA2625 (C) solubilised ATM1 membranes (sol) were incubated overnight with Nickel-NTA Resin at 4ºC, following which unbound material (FT) was removed and resins washed with purification buffers supplemented with increasing concentrations of Imidazole (20mM – 60 mM). Atm1 was eluted with buffers supplemented with 200mM imidazole. Samples were extracted from wash 1, wash 5, flow through and each elution collection, and run on SDS-PAGE along with a solubilisation sample. Gels were stained with Instant Blue.*

Following successful purifications, the yield of purified Atm1 obtained using SMA1440, SMA17352 or SMA2625 was quantified using SDS-PAGE (Figure 7.3A).

An average yield of 0.33 μg protein/mg membrane was obtained for SMA1440, 0.36μg/mg for SMA17352 and 0.47μg/mg for SMA2625. Although SMA2625 appeared to give a higher yield, statistical analysis showed there was no significant differences between the yield of SMA1440, SMA17352 and SMA2625 purified Atm1. However, there were significant differences between the yield of Atm1 obtained with each of the partially esterified polymers when compared to SMA2000, which had a significantly higher yield of 0.76 ug/mg.

Figure 7.3B displays the purity analysis of Atm1 purified with SMA2000, SMA1440, SMA17352 or SMA2625 polymer. SMA2000 purified ATM1 on average was 77% pure. SMA1440 purified Atm1 on average was 80 % pure, SMA17352 purified Atm1 78% and SMA2625 purified Atm1 75%. However no significant differences in purity were measured between SMA2000, SMA1440, SMA17352 and SMA2625 purified Atm1 (P value 0.9552).
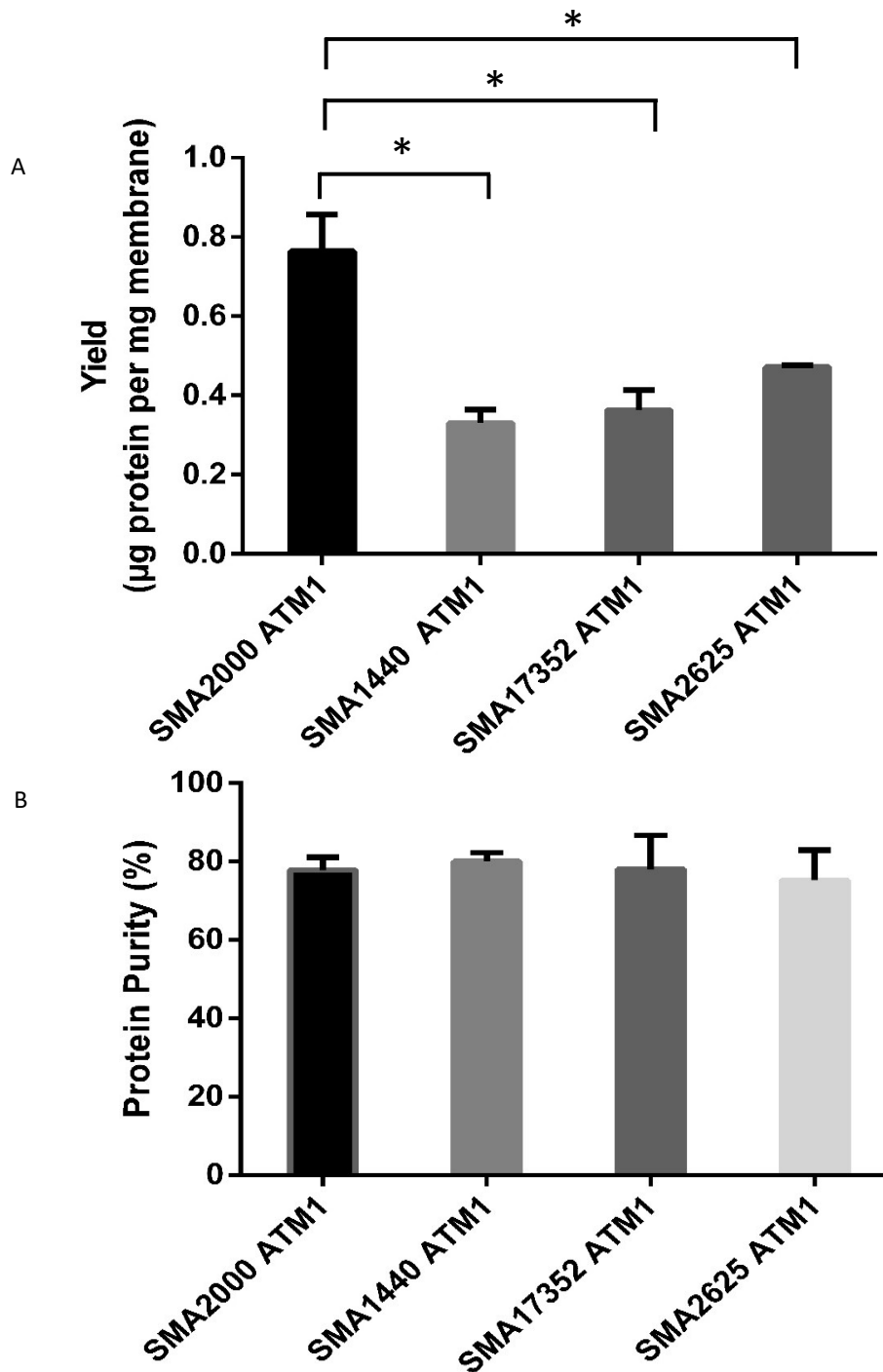
Figure 7.3 Quantification of SMA1440, SMA17352 and SMA2625 purified Atm1. *A) protein yield quantification. Samples (20 µl) of SMA1440, SMA17352 and SMA2625 purified Atm1 were run on SDS-PAGE alongside BSA standards (0.25, 0.5, 0.75, 1, 1.25 µg) and gels stained with instant blue. The intensity of bands on gels were analysed using densitometry and yield calculated. B) Purity quantification. To estimate the purity of Atm1 obtained, three SMA1440, SMA17352 and SMA2625 elution lanes were analysed using densitometry (Image J); purity was estimated by examining the intensity of ATM1 band as a percentage of total lane intensity. Data are mean ± SEM, n=3. Data was analysed using One-way ANOVA tests.*P<0.05.*

Having established all three partially esterified polymers could be used to solubilise and purify Atm1, the effect of magnesium chloride on precipitation of SMA1440, SMA17352 and SMA2625 purified Atm1 was investigated (Figure 7.4).
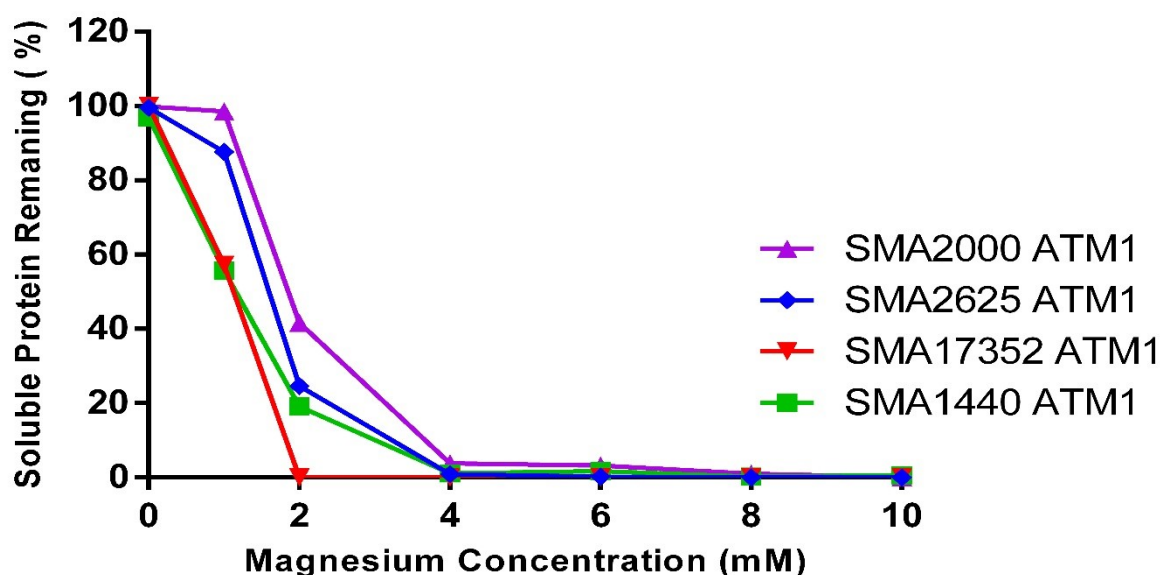
Figure 7.4 Magnesium Sensitivity Assay for partially esterified polymers. *SMA1440, SMA17352 and SMA2625 purified Atm1 protein samples were mixed with increasing concentrations of magnesium chloride (0-10mM) and incubated at room temperature for 15 minutes. Following incubation, samples were centrifuged at 100000g, for 20 minutes at 4°C. Supernatants (S) containing soluble proteins were extracted and samples(20µl) run on SDS-PAGE alongside marker (MK). Gels stained with instant blue and analysed using densitometry (Image J) Data are the average of 3 replicates.*

Figure 7.4 demonstrates that magnesium chloride concentrations of up to 1mM have no substantial impact on SMA2625 purified Atm1 however concentrations over 1mM cause the majority of SMA2625 purified Atm1 to precipitate out of solution. It also shows that over 40% of SMA1440 and SMA17352 purified ATM1 precipitated out of solution in the presence of 1mM concentration of magnesium chloride. All of SMA1440, SMA17352 and SMA2625 purified Atm1 precipitated out of solution at 4mM concentration of magnesium chloride. So rather than improving the tolerance to divalent cations, the partially esterified polymers were actually even more sensitive to Mg^{2+} than SMA2000.

7.2 Benzylamine modified SMA polymers

A second series of SMA polymer variants was provided by Professor Bert Klumperman (Stellenbosch University). These were a series of 1:1 styrene:maleic acid polymers which were modified by adding a benzylamine group to one of the carboxyl groups in each maleic acid (Figure 7.5). The rationale behind

the design of these polymers was that making a 1:1 polymer is much simpler than 2:1 (like SMA2000). It has been shown that 1:1 SMA polymers are not effective for membrane protein solubilisation (Morrison *et al*., 2016), however addition of the benzylamine group increases the hydrophobicity and mimics the 2:1 ratio of hydrophobic: hydrophilic seen with SMA2000. SMA1000-benzylamine was made from modification of the commercially available SMA1000 polymer. The others were made by RAFT polymerisation to generate 1:1 alternating SMA polymers of different sizes, that were then modified by benzylamine. The advantage of the RAFT polymerisation process is that the size distribution of polymers formed can be more tightly controlled, thus there are polymers with average molecular weights of 2kDa, 4kDa and 7kDa. The final difference is the end group, which is either -SH or N-phenyl maleimide (NPMI). Upon reaction with the benzylamine the RAFT end group will get reduced to -SH, which can dimerise. To prevent this, for some samples the end group was capped with NPMI.

Table 7.2 Properties of benzylamine modified polymers. A series of polymers with a 1:1 ratio of styrene:maleic anhydride with different molecular weights were generated by RAFT polymerisation at Stellenbosch University. These, or commercially produced SMA1000, were then modified by addition of benzylamine to the maleic anhydride groups. Upon amine addition to the polymer, the RAFT end group will be reduced to a thiol which can oxidize to form disulfide bridges. To block or minimize such oxidation, the formed thiol end groups were capped by reaction with N-phenylmaleimide (NPMI) in the presence of trimethylphosphite. The number average molecular weight (Mn), which is the total weight of the polymer molecules divided by the number of molecules. The polydispersity index (PDI), which is equal to Mw/Mn and is a measure of the distribution of the molecular weights.

Polymer name	Styrene:maleic anhydride in unmodified polymer	Modification	Mn (kDa)	PDI
SMA2000	2:1	-	3	2.5
SMA1000-benzylamine	1:1	benzylamine	2	2.75
SMA-benzylamine-NPMI 2kDa	1:1	benzylamine capped with NPMI	2.1	1.32
SMA-benzylamine-NPMI 4kDa	1:1	benzylamine capped with NPMI	4.5	1.36
SMA-benzylamine-SH 2kDa	1:1	benzylamine	2.1	1.32
SMA-benzylamine-SH 4kDa	1:1	benzylamine	4.5	1.36
SMA-benzylamine-SH 7kDa	1:1	benzylamine	7	1.34

SMA2000
x:y=2:1
Mn 3kDa Mw 7.5kDa
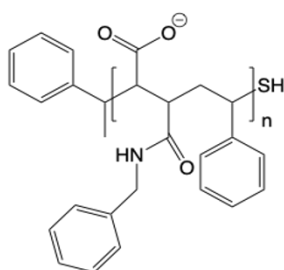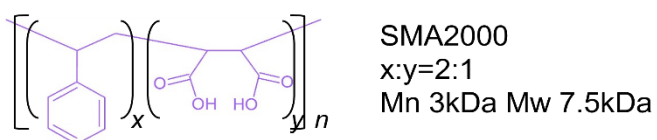
SMA-benzylamine-SH 2kDa   SMA-benzylamine-NPMI 2kDa   SMA1000-benzylamine
SMA-benzylamine-SH 4kDa   SMA-benzylamine-NPMI 4kDa
SMA-benzylamine-SH 7kDa
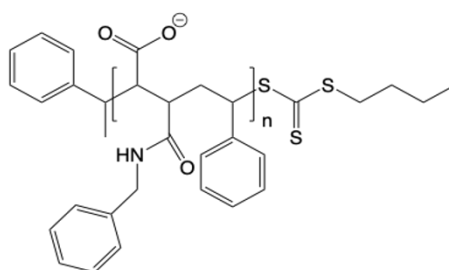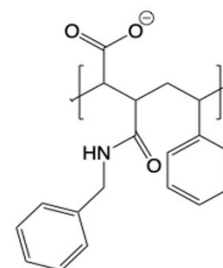
Figure 7.5 Structures of the benzylamine modified SMA polymers. *Provided by Prof. Bert Klumperman, Stellenbosch University.*

Trials of Atm1 solubilisation and purification were first carried out with SMA-Benzylamine-SH 2kDa, SMA-Benzylamine-SH 4kDa and SMA-Benzylamine-SH 7kDa (Figure 7.6).
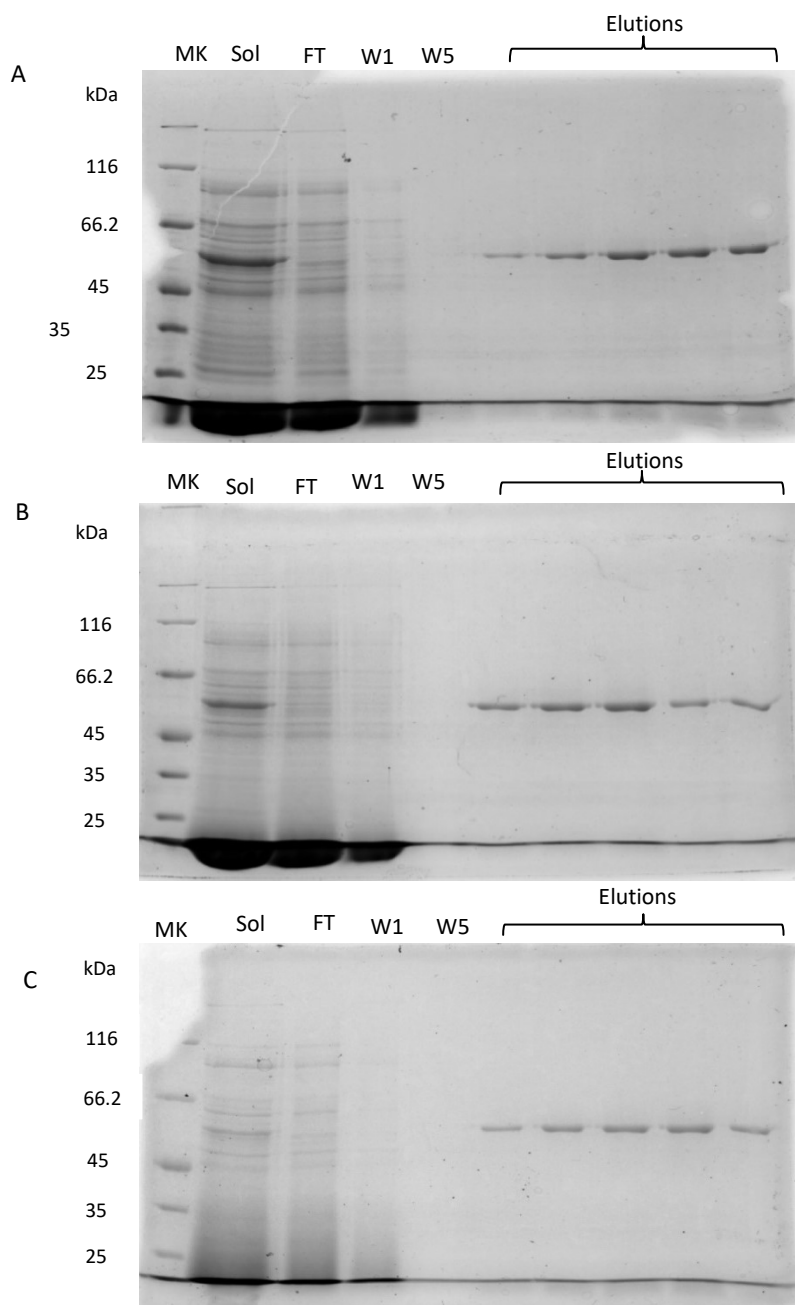
Figure 7.6 Affinity purification of Atm1 using benzylamine modified polymers. *SMA Benzylamine-SH 2kDa (A), SMA Benzylamine-SH 4kDa (B) and SMA Benzylamine-SH 7kDa (C) solubilised Atm1 membranes (sol) were incubated overnight with Nickel-NTA resin at 4°C, following which unbound material (FT) was removed and resins washed with purification buffers supplemented with increasing concentrations of Imidazole and Atm1 eluted. Samples of wash 1 (W1), wash 5 (W5), flow through (FT) and each elution were run on SDS-PAGE along with a solubilisation sample (sol). Gels were stained with Instant Blue*

All three polymers were able to solubilise and purify Atm1, producing very pure looking bands on SDS-PAGE. The yield of purified Atm1 obtained with each polymer was quantified using SDS-PAGE (Figure 7.7A). An average concentration of 0.51µg protein/mg membrane was obtained for SMA Benzylamine 2kDa, 0.46µg/mg for SMA Benzylamine 4kDa and 0.21µg/mg for SMA Benzylamine 7kDa.

There were no significant differences between the yields of Atm1 obtained with SMA Benzylamine-SH 2kDa and SMA Benzylamine-SH 4kDa, and similarly there were no significant differences between the yields of Atm1 obtained with SMA Benzylamine-SH 4kDa and SMA Benzylamine-SH 7kDa. However, there was a significant difference between the yields of SMA Benzylamine 2kDa purified Atm1 and SMA Benzylamine 7kDa purified Atm1 (P value 0.0419), showing that SMA benzylamine-SH 7kDa gave a significantly lower yield of purified protein. Likewise, there was also a significant difference between the yield of SMA2000 purified Atm1 and SMA Benzylamine 7kDa purified Atm1 (P value is 0.0056) . There are however no significant differences between SMA2000 purified and SMA Benzylamine 2kDa and SMA Benzylamine 4kDa purified Atm1 Yields.

Figure 7.7B displays the purity of SMA Benzylamine 2kDa, SMA Benzylamine 4kDa and SMA Benzylamine 7kDa purified Atm1. SMA Benzylamine 2kDa purified Atm1 on average is 88 % pure, SMA Benzylamine 4kDa purified ATM1 91 %, and SMA Benzylamine 7kDa purified Atm1 81 % pure. On average SMA Benzylamine 4kDa purified Atm1 has the highest purity and SMA Benzylamine 7kDa purified Atm1 the lowest. There are no significant differences in purity between SMA Benzylamine 2kDa, SMA Benzylamine 4kDa and SMA Benzylamine 7kDa purified Atm1. There are also no significant differences in purity between SMA2000 purified Atm1 and SMA Benzylamine 2kDa, SMA Benzylamine 4kDa and SMA Benzylamine 7kDa purified Atm1.
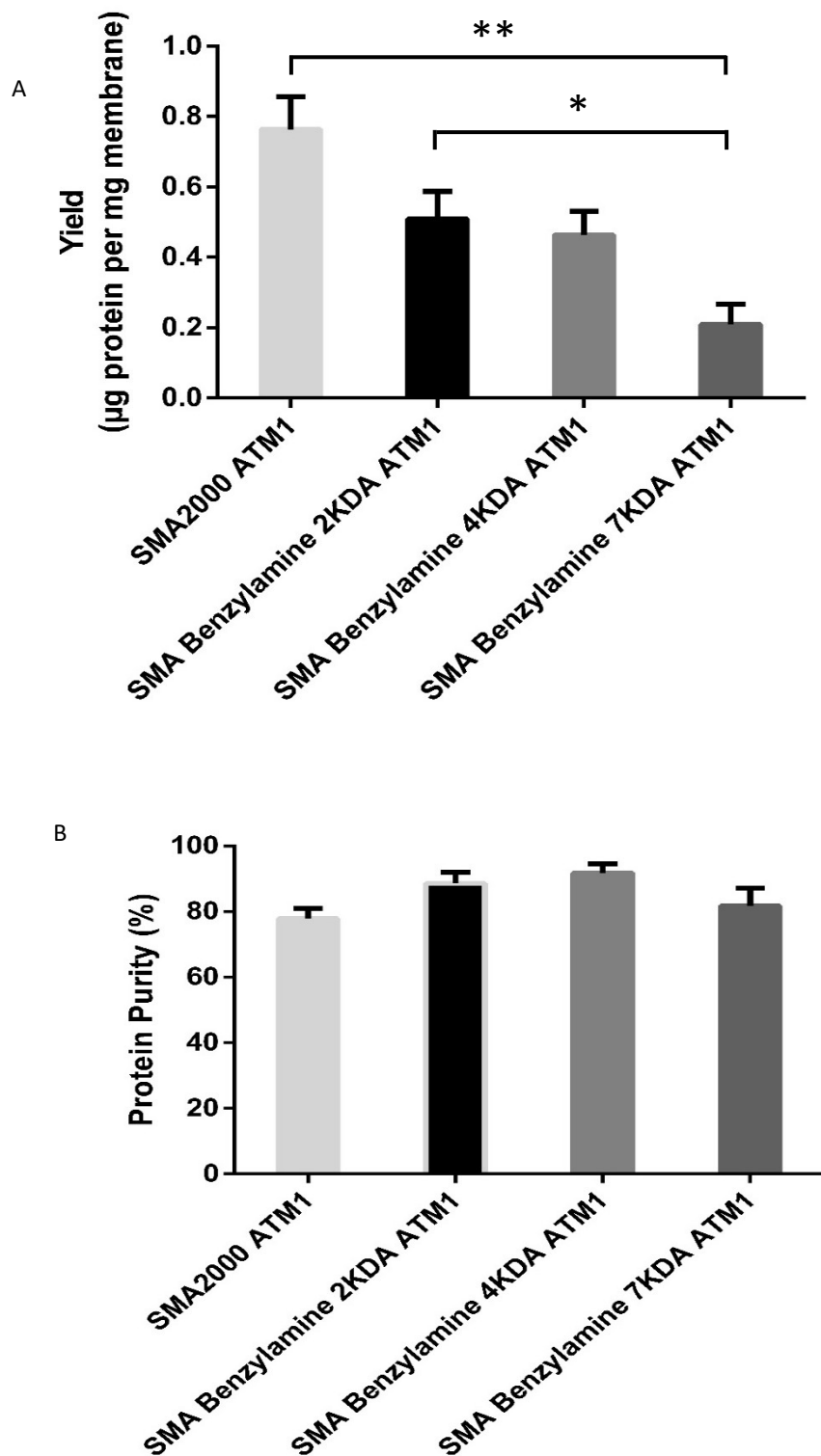
*Figure 7.7 Quantification of SMA Benzylamine-SH 2kDa, SMA Benzylamine-SH 4kDa and SMA Benzylamine-SH 7kDa purified Atm1.A) protein yield quantification. Samples (20 µl) of Atm1 purified with each benzylamine polymer were run on SDS-PAGE alongside BSA standards and gels stained with instant blue. The intensity of bands on gels were analysed using densitometry and yield calculated. B) Purity quantification. To estimate the purity of Atm1 obtained, Atm1 purified with each benzylamine polymer was analysed using densitometry (Image J); purity was estimated by examining the intensity of ATM1 band as a percentage of total lane intensity. Data are mean ± SEM, Data was analysed using One-way ANOVA tests. *P<0.05, **P<0.001.*

Following Atm1 yield and purity analysis, the effect of magnesium chloride on precipitation of SMA Benzylamine-SH 2kDa, SMA Benzylamine-SH 4kDa and SMA Benzylamine-SH 7kDa purified Atm1 was investigated (Figure 7.8).
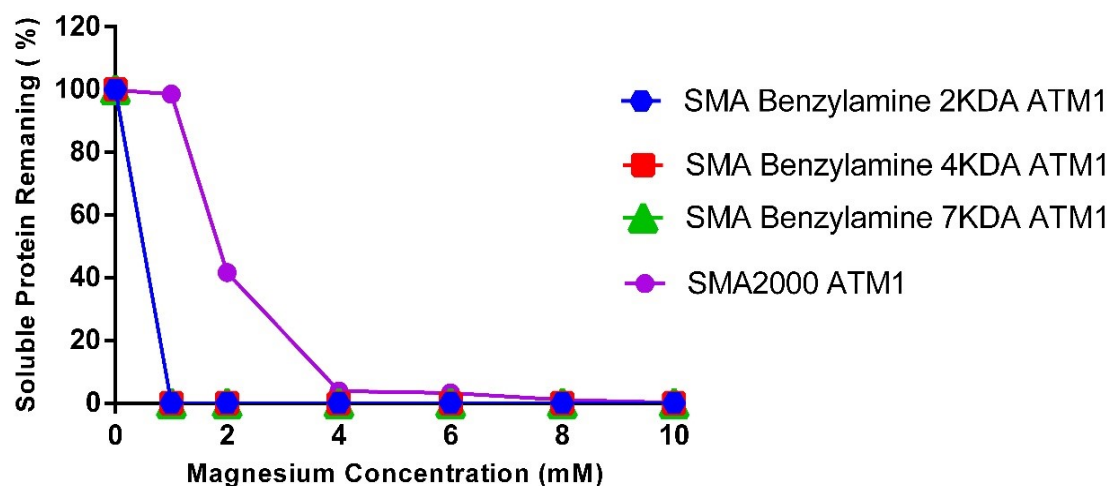
***Figure 7.8 Magnesium Sensitivity Assay for benzylamine-SH polymers**. Atm1 purified with SMA Benzylamine-SH 2kDa (blue diamond triangle), SMA Benzylamine-SH 4kDa (red square) or SMA Benzylamine-SH 7kDa (green triangle) were mixed with increasing concentrations of magnesium chloride (0-10mM) and incubated at room temperature for 15 minutes. Following incubation, samples were centrifuged at 100000g, for 20 minutes at 4°C. Supernatants (S) containing soluble proteins were extracted and samples (20µl) run on SDS-PAGE alongside marker (MK). Gels stained with instant blue and analysed using densitometry (Image J). Data are the average of 3 repeats.*

Figure 7.8 reveals that just a 1mM concentration of magnesium chloride caused all of SMA Benzylamine-SH 2kDa, SMA Benzylamine-SH 4kDa and SMA Benzylamine-SH 7kDa purified Atm1 to precipitate out of solution. So rather than improving the tolerance to divalent cations, the SMA Benzylamine polymers were actually even more sensitive to Mg^{2+} than SMA2000.

The second subset of benzylamine polymers which included SMA1000 Benzylamine, SMA Benzylamine-NPMI 2kDa and SMA Benzylamine-NPMI 4kDa were subsequently tested for Atm1 solubilisation (Figure 7.9). All three polymers gave successful purifications, with strong bands in the elution fractions and very few contaminants present. The yields of SMA1000 Benzylamine, SMA Benzylamine-NPMI 2kDa and SMA Benzylamine-NPMI 4kDa purified Atm1 were quantified using SDS-PAGE (Figure 7.10A).
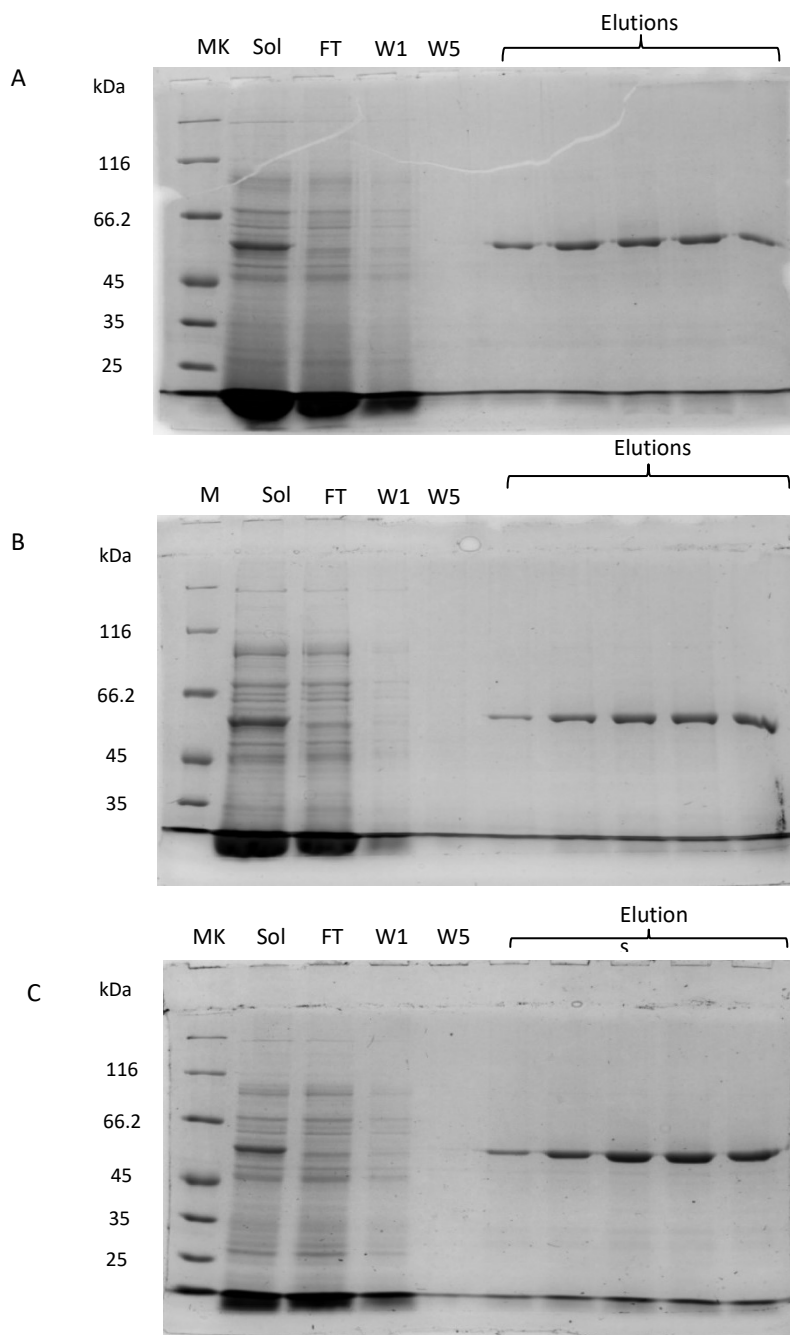
Figure 7.9 Affinity purification with benzylamine modified commercial polymer or with the RAFT end group capped. *SMA1000 Benzylamine (A), SMA Benzylamine-NPMI 2kDa (B) and SMA Benzylamine-NPMI 4kDa (C) solubilised Atm1 membranes (sol) were incubated overnight with Nickel-NTA Resin at 4ºC, following which unbound material (FT) was removed and resins washed with purification buffers supplemented with increasing concentrations of Imidazole and Atm1 eluted. Samples of wash 1 (W1), wash 5 (W5), flow through (FT) and elution factions were run on SDS-PAGE along with a solubilisation sample (sol). Gels were stained with Instant Blue.*
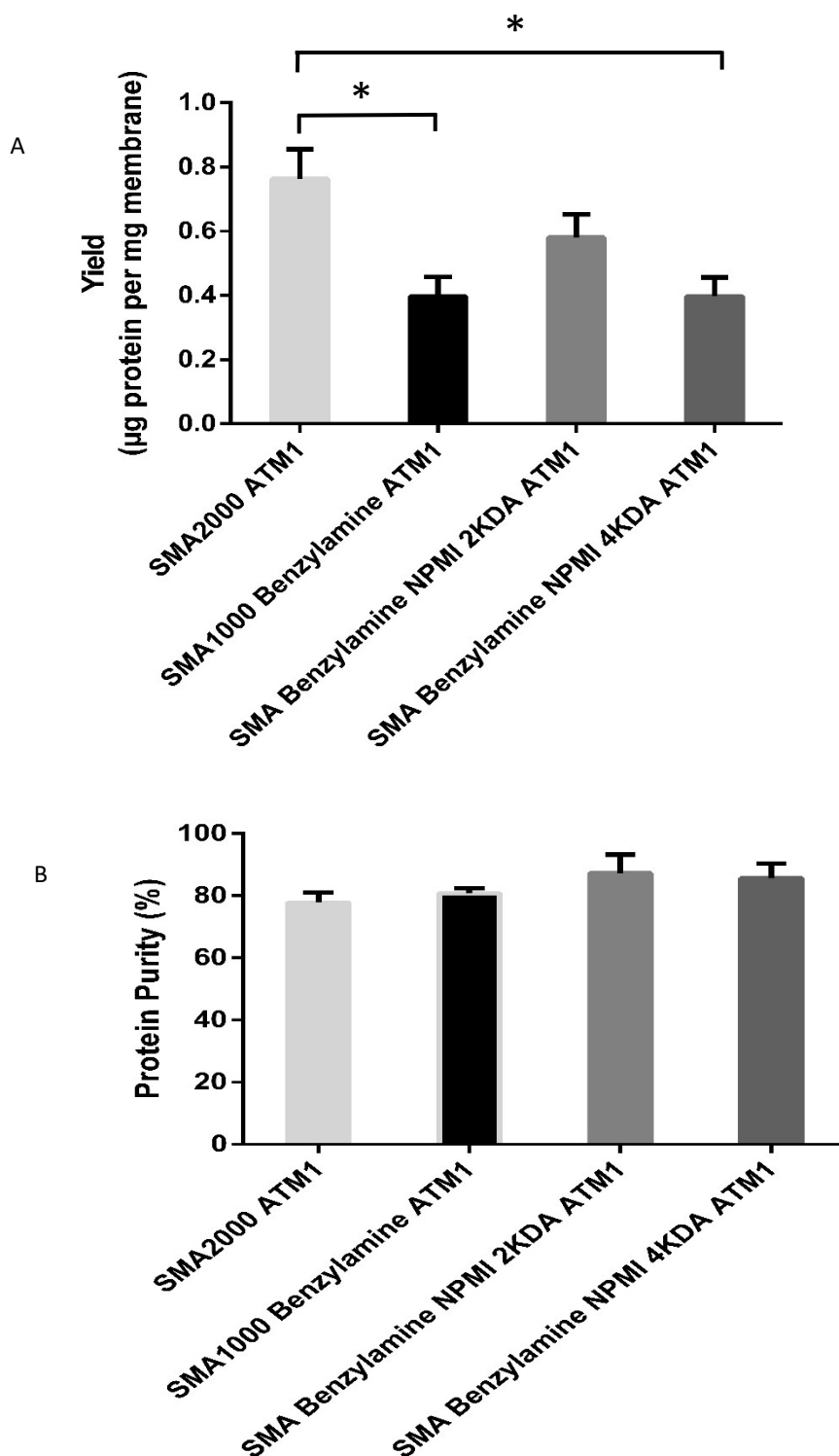
Figure 7.10 Quantification of SMA1000 Benzylamine, SMA Benzylamine-NPMI 2kDa and SMA Benzylamine-NPMI 4kDa purified Atm1. *A) protein yield quantification. Samples (20 µl) of SM Benzylamine purified were run on SDS-PAGE alongside BSA standards (0.25, 0.5, 0.75, 1, 1.25 µg) and gels stained with instant blue. The intensity of bands on gels were analysed using densitometry and yields calculated. B) Purity quantification. To estimate the purity of Atm1 obtained, elution fractions were analysed using densitometry (Image J); purity was estimated by examining the intensity of ATM1 band as a percentage of total lane intensity. Data are mean ± SEM, n=3. Data was analysed using One-way ANOVA tests.*P<0.05.*

An average yield of 0.40µg protein/mg membrane was obtained for SMA 1000 Benzylamine, 0.58 µg/mg for SMA Benzylamine-NPMI 2kDa and 0.39µg/mg for SMA Benzylamine-NPMI 4kDa. Although SMA benzylamine-NPMI 4kDa seemed to give a higher yield than the others, statistical analysis showed there were no statistically significant differences between the yields of purified Atm1 obtained with any of the polymers (P value 0.1446).

However, there is a significant difference in yield between SMA2000 and SMA1000 Benzylamine purified Atm1 (P value is 0.0198). There is also a significant difference in yield between SMA2000 and SMA Benzylamine NPMI 4kDA purified Atm1. Conversely there is no significant difference in yields between SMA2000 ATM1 and SMA Benzylamine NPMI 2 kDa purified Atm1.

Figure 7.10B displays the analysis of purity of Atm1 purified using SMA1000 Benzylamine, SMA Benzylamine-NPMI 2kDa and SMA Benzylamine-NPMI 4kDa. SMA1000 Benzylamine purified Atm1 was on average 80 % pure, SMA Benzylamine-NPMI 2kDa purified Atm1 87 %, and SMA Benzylamine-NPMI 4 kDa purified Atm1 85% pure. There were no significant differences in purity for Atm1 between these polymers (P value 0.5892). likewise, there were no significant differences in purity for Atm1 between these polymers and SMA2000.

Finally, the effect of magnesium chloride on SMA1000 Benzylamine, SMA Benzylamine-NPMI 2kDa and SMA Benzylamine-NPMI 4kDa purified Atm1 was investigated (Figure 7.11).
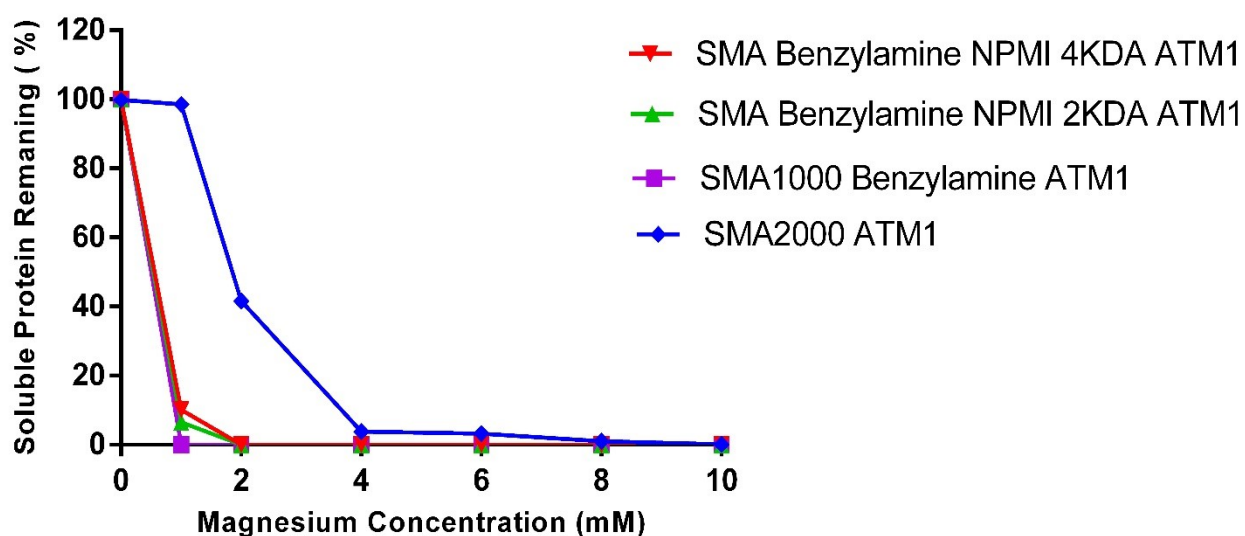
Figure 7.11 Magnesium Sensitivity Assay forSMA1000 Benzylamine, SMA Benzylamine-NPMI 2kDa and SMA Benzylamine-NPMI 4kDa purified ATM1. *Atm1 samples were mixed with increasing concentrations of magnesium chloride (0-10mM) and incubated at room temperature for 15 minutes. Following incubation, samples were centrifuged at 100000g, for 20 minutes at 4°C. Supernatants (S) containing soluble proteins were extracted and samples (20µl) run on SDS-PAGE alongside marker (MK). Gels stained with instant blue and analysed using densitometry (Image J). Data are an average of 3 replicates.*

Figure 7.11 reveals that just as with the other benzylamine modified polymers (Figure 7.8) 1mM concentration of magnesium chloride caused all the purified Atm1 to precipitate out of solution, with each of the polymers.

7.3 Summary

- Partially esterified polymers can be used to successfully solubilise and purify the ABC transporter Atm1.
  - No significant differences in yield or degree of purity between the different partially esterified polymers.
  - SMALPs formed from the partially esterified polymers are more sensitive to Mg^{2+} than SMA2000.
- Benzylamine modified SMA polymers can be used to successfully solubilise and purify the ABC transporter Atm1.
  - No significant difference observed between the different polymers for yield or degree of purity, suggesting the size differences and end group have little effect.
  - SMALPs formed from benzylamine modified polymers are even more sensitive to Mg^{2+} than SMA2000 or the partially esterified polymers.
- These novel polymers do not offer any improvement over SMA2000, giving somewhat similar yields of purified protein and degree of purity, and being even more sensitive to divalent cations. However, these results can hopefully help to further the wider understanding of how SMA polymer works and what features lead to what properties. Additionally, these novel polymers potential could further explored by employing them in protein function studies to examine effectiveness of the polymers in maintaining protein function.

8. Discussion

In the present project, the aim was to optimise lipid nanoparticle extracted and purified LeuT and Atm1 proteins for drug screening and development using SPR and MST techniques. The initial objective of the study was to investigate whether SMA2000, DIBMA or DDM purified LeuT and Atm1 could be utilised for SPR studies. To achieve this the first step was to solubilise and purify LeuT and Atm1 using each of the solubilisation agents.

8.1 Expression and purification of target proteins

LeuT and Atm1 were chosen because they are bacterial homologues of important eukaryotic proteins, meaning they could be expressed relatively easily and quickly in *E. coli*. Also, both of them have already had their structure determined. Prior studies had therefore shown that LeuT could be effectively solubilised and purified with detergents such as DDM (Khelashvili *et al*., 2013). LeuT was also used previously to test a series of SMA polymers with differing lengths and ratios of styrene:maleic acid (Morrison *et al*., 2016). The results from this current investigation regarding DDM and SMA2000 solubilisation and purification of LeuT agree well with those obtained previously. No significant difference between DDM and SMA2000 was found regarding yield of protein, which agrees with Morrison *et al*. However, although previous studies had proposed that a greater degree of protein purity could be obtained using SMA co polymers in comparison to detergents, and although this trend was also observed in this study, the difference in purity obtained was not significant (Gulati *et al*., 2014; Morrison *et al*., 2016). DIBMA is an alternative polymer to SMA, which has an aliphatic chain in place of styrene, and was first shown by Oluwole *et al*. to also be capable of solubilising membrane proteins (Oluwole *et al*., 2017). This study is the first to test DIBMA for solubilising and purifying LeuT and found that it worked comparably to both SMA2000 and DDM. This contrasts with some other studies which have found that DIBMA tends to give lower yields of proteins in comparison to SMA2000 (Grethen *et al*., 2017; Gulamhussein *et al*., 2020).

The second protein to be tested, Atm1, has previously been solubilised for structural studies using a mixture of 4 different detergents (LDAO, OG, CHAPSO, HEGA-11) (Lee *et al*., 2014), or a mix of 2 detergents (DDM and C12E8) (Fan, Kaiser and Rees, 2020). It was also previously solubilised with DDM only for investigations into liposome reconstitution (Rottet *et al.,* 2020) . The results in this current study support the fact that DDM alone is effective for solubilising and purifying Atm1. There are no previous reports of using SMA or DIBMA for Atm1, but there are several reports for other ABC transporters (Gulati *et al*., 2014; Morrison *et al*., 2016; Gulamhussein *et al*., 2020). The findings of this current study largely agree with those previous studies, showing both SMA2000 and DIBMA can be used to solubilise and purify Atm1. As with LeuT, a trend was seen that SMA2000 gave a higher yield than DIBMA, but this was not statistically significant. It was however found that DIBMA gave a greater degree of purity than DDM.

SMALP sensitivity to divalent cations such as Mg^{2+} has been highlighted in earlier studies (Dörr *et al.,* 2015; Morrison *et al*., 2016). Results in chapter 3 for LeuT and Atm1 agree with these previous studies, and it is evident that magnesium chloride concentrations have a definite impact on the amount of LeuT and Atm1 protein being lost. Concentrations of $MgCl_2$ up to 4mM for LeuT and up to 1mM for Atm1 were tolerated, however concentrations over this caused SMALP instability and lead to proteins loss. The LeuT findings agree very well with those shown previously in Morrison *et al*. Why the Atm1 SMALPs were more sensitive to Mg^{2+} than LeuT is not clear. It might be interesting in the future to test the sensitivity of SMALPs to other divalent cations such as Zinc and Calcium Chloride. On the other hand, the results from DDM magnesium assays along with preceding findings of (Matar-Merheb *et al*., 2011) imply that detergent solubilised proteins are not affected by the presence of divalent cations such as Mg^{2+}. Previous investigations have proposed that DIBMA solubilised proteins could tolerate up to 20mM concentrations of divalent cations (Oluwole *et al*., 2017; Gulamhussein *et al*, 2020), and initial findings from the LeuT magnesium assay experiments support these claims as DIBMA extracted LeuT was shown to have no sensitivity to magnesium ions, within the concentration range tested. However, the findings from DIBMA purified Atm1 magnesium assays contradict the previous findings, as Atm1 is shown to have high sensitivity to magnesium chloride ions and precipitate out of solution at low 1mM concentration of magnesium chloride. Therefore, perhaps the individual structure and composition of different membrane proteins in SMALPs may also contribute towards divalent cation sensitivity. Atm1has shown a much higher sensitivity in magnesium assays and it has substantially more negatively charged amino acids than LeuT . Atm1 has 35 Aspartic acids and 29 Glutamic acids whereas LeuT only has 12 Aspartic acids and 24 Glutamic acids . The difference in negatively charged amino acids could affect the overall charge of Atm1 and LeuT proteins .

Membrane protein instability is a major issue in membrane protein research as a failure to maintain membrane protein stability following extraction and purification can result in loss of protein function. This is especially true of integral membrane proteins which can have numerous polypeptide segments embedded in the membrane. It's been previously shown that membrane proteins extracted by SMA polymers can recognise ligands, transmit signals and activate other proteins and that proteins extracted using DIBMA polymer maintained their secondary structure and activity (Logez *et al.,* 2015; Oluwole *et al*., 2017). In this study the results from LeuT tryptophan quenching experiments support these findings as SMA2000 and DIBMA purified LeuT samples successfully bound leucine and alanine ligands. DDM solubilised LeuT was also shown to bind leucine and alanine. The binding affinity data obtained for leucine experiments agree well with previous studies which used a radioligand binding assay on DDM solubilised LeuT and reported a binding affinity of 20 ± 2 nM for LeuT (Singh *et al*., 2008).However, in the current study there was a significant difference between the binding affinity of leucine for DDM (33.07 nM) purified LeuT and SMA2000 (14.99 nM) purified LeuT, with the binding affinity of leucine for SMA2000 purified LeuT being stronger than the binding affinity of leucine for DDM purified LeuT. The same was also true for DIBMA (8.73 nM), leucine has a stronger binding affinity for DIBMA purified

LeuT in comparison to DDM purified LeuT. The difference in binding affinity could be due to the destabilizing effects of DDM; as it has been shown that DDM can cause small destabilizations in the binding domains of membrane protein (Yang *et al*., 2014). The findings from tryptophan quenching experiments for alanine however show no significant difference between the binding affinity of alanine for SMA2000, DDM or DIBMA purified LeuT. The findings for alanine binding affinity also differ from those previously published (Singh *et al.,* 2008), who reported a binding affinity of 512 ± 131 nM for LeuT whereas the findings from this investigation suggest a much stronger affinity at 21.26 nM for SMA2000, 25.52 nM for DDM and 11.82 for DIBMA purified LeuT.

Tryptophan fluorescence quenching was also used to study the binding of GSH to SMALP purified Atm1. An affinity of approximately 1.8mM was obtained. This is a bit lower than the 15mM Km value for GSH transport previously reported , but may reflect differences between initial binding and the whole transport process (Fan *et al*, 2020).

It would be interesting in the future to try different methods for binding assays to see if the Kd obtained was consistent across different methods, as fluorescence quenching is not a direct binding assay.

8.2 Immobilisation of LeuT for SPR

The key step in setting up an SPR experiment, which can often be challenging, is the immobilisation of one of the binding partners. It has been proposed that his-tags typically employed for protein purification were ideal for the immobilisation of ligands onto NTA Sensor Chips (Nieba *et al*., 1997). The findings from this study (chapter 4) utilising NTA sensor chips however showed extremely low levels of immobilisation for SMA2000 purified LeuT (~ 26 RU). DIBMA purified LeuT samples immobilized approximately 5-fold higher than SMA2000 purified sample at (190 RU) and therefore showed some promise. Detergent DDM purified LeuT samples performed the best and immobilized at 5560 RU. This ability to immobilise the DDM solubilised LeuT compares well to a previous study which had shown that DDM solubilised GPCRs could be immobilized on Ni NTA (Robertson *et al*., 2011). Similarly, his tagged A2aR has previously been immobilized via NTA capture and were very stable (Congreve *et al*., 2011). However, it has also been proposed that a common flaw with NTA chip application is slow and continuous dissociation of immobilized ligands (Willard and Siderovski, 2006; Kimple *et al.,* 2010). The results from the current study support these proposals as a slow level of decay at approximately 0.5 RU per minute was detected for SMA2000 purified LeuT. Although the decay rate was slow, it still represented a substantial loss in the amount of immobilised ligand as almost 50% of the immobilized ligand would be lost within 20 minutes. DIBMA purified LeuT had a slightly higher rate of decay at 0.7 RU per minute however it can be considered more stable as proportionally over 20 minutes it only lost 7.36% (~14 RU) of the initially immobilized LeuT. DDM immobilized LeuT showed no drift and was stable.

When attempting to bind leucine to the immobilised SMALP-LeuT, the majority of protein disassociated following first injection. DIBMA purified LeuT also showed a similar disassociation trend to SMA2000 purified LeuT. The levels of drift/protein dissociation observed in the leucine bindings experiment made it impossible to analyse leucine binding. Therefore, the results suggest that nitrilotriacetic acid (NTA) and histidine-tag (HT) interactions are suitable for transient applications like protein purification however binding studies can be compromised due to protein dissociation (Johnson and Martin, 2005). It should also be noted that even for protein purification SMALP-encapsulated proteins have been reported to show much poorer binding to Ni-NTA resin than detergent solubilised proteins (Broadbent *et al*., 2022). Exactly why isn't clear, possible reasons might include interactions between the polyhistidine-tag and the polymer or steric hindrance from the polymer or interference from excess free SMA.

Salts play a vital role in living organisms and the concentration of ionic species like sodium can vary greatly within organisms (1mM - 200 mM) (Wegner and Isenberg, 1983). Salt concentrations can affect the stability of biomolecules and prior investigations of Schlick, Li and Olson, 1994 have shown that the high negative charges on polyelectrolytes like nucleic acids can lead to destabilization. Other studies have proposed that increasing the ionic strengths of solvents can screen repulsive interactions and thereby stabilize the conformation of nucleic acids in solution (Beauchamp and Khajehpour, 2012). SMA is highly negatively charged, thus investigations into the effects of salt on immobilisation and stability were undertaken and increasing the concentrations of NaCl led to increased immobilisations of SMA2000 and DIBMA purified LeuT.

It has been shown previously that the pH of aqueous solutions could have an immense impact on the conformation of SMA, and at low pH even cause SMA polymers to precipitate (Dörr *et al.,* 2015). The results from the buffer optimisation experiments support these findings as low pH buffer conditions led to low immobilisation of both SMA2000 and DIBMA purified LeuT. Overall, although buffer optimisation offered some improvements, the degree of immobilisation obtained was still too low.

As an alternative approach to immobilisation, a his-capture process was used, where an anti-his antibody was amine coupled to the SPR chip, and then LeuT bound to the anti-his antibody via its his-tag. Previous studies have shown that α2-adrenergic receptors could be successfully immobilized onto CM5 sensor chips using this approach (Sen *et al*., 2005). The results for SMA2000 purified LeuT immobilisation using his-capture did show an improvement over the Ni-NTA approach, reaching immobilisation levels of 300 RU, which could be increased to 500 RU with optimisation of immobilisation time. DIBMA was not quite as good, with immobilisation of 100 RU, up to 200 RU with increased immobilisation time. These levels of immobilisation are comparable to those achieved in a recent study using SMALP-encapsulated proteins, who also used his-capture (Sharma, *et al*., 2021). Despite this improved level of binding, leucine binding could still not be detected. For efficient detection of small molecules binding to a larger molecule, a much higher level of immobilisation is needed. However, it

would be interesting to investigate if binding of a larger molecule, such as an antibody, could be detected, as was seen in (Sharma *et al,* 2021).

Capture-coupling is an alternative approach previously shown to aid immobilisation (Willard and Siderovski, 2006; Diskar *et al*., 2007; Kimple *et al*., 2010). The results from the NTA capture couple experiments in this study however were varied. SMA2000 purified LeuT immobilized poorly (62.5 RU) and DIBMA purified LeuT did substantially better at 409 RU. DDM purified LeuT had the highest levels of immobilisation at 1260 RU. None of the immobilisations attempts did as well as prior studies which had shown Immobilisation levels as high as 6000 RU for capture coupling method (Kimple *et al.,* 2010). The reason for the poor level achieved with SMA2000 may be related to the lower pH used for the second amine coupling step, which would likely disrupt the SMALP structure. Subsequent Leucine binding experiments show DDM purified LeuT to bind leucine in a dose dependent manner however the signal level and data quality was too low to generate affinity data.

In summary in this study a range of immobilisation methods were explored however they were all ineffective at achieving desired levels of immobilisation for SMA2000 and DIBMA purified LeuT. In the future alternative methods for immobilisation should be investigated. This could include using alternative tags. Notably, Sharma *et al,* 2022 found that using a FLAG tag on the SMALP-encapsulated protein and an anti-FLAG antibody gave improved results over the his-antibody and his-tag approach. Another tag that shows great potential is biotin, coupled with a streptavidin sensor chip, this has been used for immobilisation and SPR analysis of biotinylated peptides (Snow, Brothers and Siderovski, 2002) or neuropeptides (Zou *et al*., 2008). Furthermore, it's been shown that the biotinylated Gα subunits of RGS (Regulator of G-protein signalling) proteins can be immobilized onto streptavidin sensor chips (Kimple *et al*., 2007).

Alternatively, Cao *et al* have recently shown that they can successfully immobilise SMALP-encapsulated P-glycoprotein using an L1 chip, which has a surface of carboxymethylated dextran pre-immobilised with lipophilic groups, designed for capture of lipid vesicles (Cao *et al.,* 2022). Using this approach, they were able to immobilise SMALP-Pglycoprotein at levels of 6000 RU, and this enabled them to measure binding of small molecule inhibitors.

8.3 Microscale thermophoresis trials

An alternative approach for monitoring ligand binding to LeuT that was tried was. microscale thermophoresis (MST). MST doesn't require the immobilization of a protein or ligand however it does require the fluorescent labelling of one of the binding components of an interaction (Jerabek-Willemsen *et al.,* 2014). Previously it has been shown that Ni-NTA fluorescent labels can give high affinity and fluorescence signals, as well as an ideal signal to noise ratio in microscale thermophoresis experiments (Bartoschik *et al.,* 2018). The results from the current study, although using a different brand NTA label,

have also shown high affinity for an Ni-NTA fluorophore. The labelling experiment gave a binding affinity of 76 pM for the NTA label for SMA2000 purified LeuT. This result suggests that the NTA label can affectively bind to SMA2000 purified LeuT and that the His tags on LeuT protein are accessible in a SMALP structure. Although initial results from single point spot tests showed promise for detecting leucine binding, this was not reliably reproducible.

Therefore, it was next decided to employ an alternative compound to analyse SMA-LeuT activity. The drug desipramine has been reported to bind LeuT (Zhou *et al.*, 2007). Therefore, the binding of desipramine to SMA2000 purified LeuT via MST was explored. The objective of this experiment was to use desipramine as an alternative positive control to leucine. It was hoped that desipramine having a larger molecular weight, and drug like aromatic structure could produce a positive response in the MST assays.

Following several steps of optimisation, such as increasing the power and moving the observation point, a typical binding isotherm was achieved, however the signal range was still relatively small. This was reproducible and gave Kd values ranging from 32- 41µM, which is comparable to the IC_{50} of 80 µM previously observed (Zhou *et al.,* 2007). Thus, the findings from desipramine MST experiments suggest that the LeuT protein maintained its structure and function after being solubilised by SMA2000. As a final control, the SMALP-LeuT sample was partially denatured prior to MST analysis. The findings showed the signal and affinity for desipramine were changed dramatically, adding further weight to the specificity of the measurements taken for SMALP-LeuT and desipramine. This suggests that MST does have promise as a method for investigating drug binding to SMALP-encapsulated proteins.

Interestingly the DDM purified LeuT did not give any specific binding results for desipramine via MST, despite the fact DDM purified LeuT had showed some activity in SPR experiments. Clearly the optimisation required for the different types of samples is quite distinct and requires further work.

8.4 SMA-SH as an alternative polymer

Due to poor results obtained from SMA2000 purified LeuT samples in SPR and MST studies, it was decided to explore methods of modifying the SMA2000 polymer that would enable the polymer to be labelled or tagged rather than the protein. Lindhoud *et al.,* 2016 had shown that it was possible to graft SMA polymers with cysteamine and produce SMA with solvent-exposed sulfhydryls (SMA-SH). This was followed up by Schmidt and Sturgis, 2018, who offered an alternative method for producing SMA-SH. The method of Schmidt & Sturgis was chosen as the equipment and materials needed were less specialised (Lindhous et al., 2016; Schmidt and Sturgis 2016).   FTIR analysis showed that the modification was successful (Figure 6.2). In addition SMALPs formed with SMA-SH were successfully labelled with a sulphydryl reactive fluorophore, confirming the incorporation of the sulphydryl groups (Figure 6.10).

Prior Studies by Lindhoud *et al*., 2016 had also proposed that the SMA-SH polymer can successfully dissolve lipid bilayer membranes and solubilise proteoliposomes into protein-loaded nanodiscs. The results for LeuT solubilisations and purification supports this (Lindhoud *et al.,* 2016). However, the results from this study using SMA-SH polymer suggest that it gives a lower concentration of purified protein in comparison to SMA2000. However, the SMA-SH polymer gave comparable results to SMA2000 in terms of purity. In order to confirm protein activity, SMA-SH purified LeuT samples were employed in tryptophan quenching experiments. The results from this investigation reveal SMA-SH purified LeuT produced comparable binding affinity and maximal quenching data to SMA2000 purified LeuT for both leucine and alanine, thereby suggesting that the modification of SMA2000 to SMA-SH polymer does not interfere with or impact downstream ligand binding experiments.

After confirming the activity of SMA-SH purified LeuT, it was decided to label SMA-SH polymer with biotin maleimide. As previously discussed, biotin often offers a good way of immobilising proteins for SPR. Lindhoud *et al*., 2016 had shown that it was possible to covalently modify SMA-SH polymer nanodiscs with biotin derivatives and Schmidt and Sturgis, 2018 had shown that it was possible to label the SMA-SH polymer prior to use with Atto488 maleimide. In this study the same procedures were followed to incorporate biotin into the polymer, however due to time constraints it wasn't possible to fully confirm this. The potentially biotin-labelled SMA-SH could be used for solubilisation, and it appeared to give a greater degree of purity compared to SMA-SH, but this should be investigated further.

Initial trials of immobilization of SMA-SH purified LeuT in SPR experiments onto the surface of a C1 sensor chip was not successful. However, this was not thoroughly investigated due to time constraints. Also, use of the biotin-labelled SMA-SH to bind to a streptavidin chip would arguably be a better approach going forward. Initial experiments to test this could include binding of biotinylated-SMALPs to streptavidin coated 96 well plates. Also, in the future further experiments would need to be conducted to establish the amount of biotin labels per polymer and/or per SMALP. It would be interesting to try to produce different versions of SMA-SH with different proportions of sulphydryl modification. Some initial attempts to do this were carried out but increasing the cystamine led to precipitation part way through the process. The original method for generating SMA-SH given by Lindhoud *et al* might offer a better way to control the degree of modification.

8.5 SNAP-tag

SNAP- tags are small, genetically encoded, well expressed tags that can be fluorescently labelled as well as biotinylated (Cole, 2013; Hansen, Rodgers and Hoskins, 2016; Macias-Contreras, Little and Zhu, 2020). Therefore, it was hypothesised that if the Atm1 protein could be SNAP-tagged and subsequently biotinylated or fluorescently labelled then it could be employed in either SPR or MST studies. This could make use of high-affinity streptavidin (SA) sensor chips for SPR, and MST requires one of the binding components of an interaction to be fluorescently labelled.

Primers were designed for PCR amplification of the Atm1 gene to be introduced into the pSNAP-tag vector, with the tag at either the N-terminus or C-terminus of Atm1, and PCR was successfully carried out, but the ligation step into the pSNAP-tag vector was problematic. This did not progress further due to time constraints. Going forward this could be an important area to pursue. The specificity of binding to the SNAP tag is high, and a wide range of different probes are available commercially to react with it. This could overcome some of the issues associated with relying on the his-tag.

8.6 Novel polymers

In recent years a wide range of different polymer variants have been developed and tested for membrane protein solubilisation. One group of polymer variants is the partially esterified SMA polymers which were shown to be better than SMA2000 for solubilising membranes from plant thylakoids (Korotych *et al*., 2019; Brady *et al.,* 2019; Cherepanov *et al*., 2020; Korotych *et al*., 2021) . However, they hadn't been tested on proteins from other organisms/expression systems, therefore they were tested with Atm1. All three partially esterified polymers, SMA1440, SMA17352 and SMA2625, could be used to solubilise and purify Atm1 successfully. The concentration of purified Atm1 obtained utilizing SMA1440 SMA17352 and SMA2625 was considerably less than SMA2000, but there were no significant differences between the esterified polymers. There were no differences with the average purity of Atm1, with all the esterified polymers being comparable to SMA2000. So, the partially esterified polymers do work, but don't show any improvement over SMA2000 in terms of yield. This contrasts with the results for plant thylakoids, where SMA1440 in particular was shown to be more effective than SMA2000. One reason for this might be the differences in lipid composition for plant thylakoids compared to *E. coli*. Thylakoid membranes are densely packed and high in galactolipids (Korotych *et al*., 2021). It is known that membrane composition does have an impact on solubilisation kinetics (Kopf *et al.,* 2020).

The benzylamine modified polymers are novel polymers that have not previously been tested for membrane protein research. The results from this investigation show that membrane proteins can be solubilised and purified using all of the benzylamine modified polymers. SMA Benzylamine-SH 2kDa, SMA Benzylamine-SH 4kDa and SMA Benzylamine-SH 7kDa polymers produced similar concentrations of purified Atm1 to partially esterified polymers SMA1440 SMA17352 and SMA2625. However, on average the purity of Atm1 obtained from SMA Benzylamine-SH 2kDa, SMA Benzylamine-SH 4kDa and SMA Benzylamine-SH 7kDa application was higher. The polymers SMA1000 Benzylamine, SMA Benzylamine-NPMI 2kDa and SMA Benzylamine-NPMI 4kDa polymers gave purified Atm1 with similar levels of purity, however SMA benzylamine-NPMI 4kDa polymer seemed to produce Atm1 with a higher concentration than the other polymers, but statistical analysis revealed that this was not a statistically significant difference. Therefore, although the benzylamine modified polymers don't appear to offer an improvement over SMA2000, they do all work. This helps add to the

understanding of the requirements of a polymer in terms of ratio of hydrophobic and hydrophilic moieties. The size of polymer didn't make much difference. Previous studies investigating different size standard SMA polymers showed previously that the smaller molecular weight polymers gave a faster rate of solubilisation, but that the larger polymers gave a greater deal of stability (Cunningham *et al*., 2020). It would be interesting going forward to investigate in more detail the kinetics and stability of the benzylamine polymers, and importantly how they might affect protein function.

8.7 Divalent cation sensitivity

One of the biggest draw backs of SMA co polymer and derivative polymers application is the sensitivity to divalent cations (Dörr *et al.,* 2015; Morrison *et al.,* 2016) It has been proposed that the maleic acid carboxyl groups in SMALPs chelate divalent cations and this process causes increasing strain on SMALP stability. The occurrence of this strain subsequently results in conformational changes in SMA and if the changes in SMA conformation occur at large then it can cause the SMA in SMALPs to precipitate out and lead to SMALP structure devastation and protein loss (Morrison *et al.,* 2016). Based upon this hypothesis it was thought that removal/alteration of one of the carboxyl groups from each maleic acid might improve the tolerance to divalent cations.

SMA-SH has modifications to some of the carboxyl groups. Atm1 protein purified within SMA-SH was analysed for magnesium chloride sensitivity. The results suggest that the modification of SMA2000 to SMA-SH does not overcome this divalent cation sensitivity as a very similar magnesium sensitivity profile to SMA2000 was observed for SMA-SH purified Atm1. However, SMA-SH is likely only modified on a small number of maleic acid groups, and therefore maybe isn't sufficiently different to SMA2000 to see a difference.

SMA1440 SMA17352 and SMA2625 polymers are partially esterified, again modifying one of the carboxyl groups of maleic acid, for many of the maleic acid groups within the polymers. However, it is evident that Atm1 purified with partially esterified polymers SMA1440 SMA17352 and SMA2625 are highly sensitive to divalent cations as concentration over 2mM magnesium chloride cause the majority of Atm1 proteins to precipitate out of solution. The SMA17352 polymer is the most sensitive partially esterified polymer, as 2mM concentration of magnesium chloride caused the Atm1 protein to completely precipitate out of solution. SMA1440 and SMA2625 show similar magnesium sensitivity profiles to each other, which are not too dissimilar to SMA2000. Again, the partially esterified polymers are not modified on every maleic acid group, but SMA17352 is reported by the manufacturers to be more highly modified than SMA2625, and SMA17352 has got the greatest sensitivity to divalent cations.

Finally, the benzylamine polymers are modified on every maleic acid group. These polymers have all shown an extremely high sensitivity toward magnesium chloride ions as all purified Atm1 precipitated out of solution at 1mM concentration of magnesium chloride.

Therefore, it seems that the hypothesis about removing a carboxyl group would improve tolerance to divalent cations was incorrect.

The findings from this investigation agree with previous studies which have shown that increasing levels of SMA esterification via butoxyethanol also increased the sensitivity towards magnesium cations (Brady *et al.,* 2021). However, it contrasts with work that has shown it is possible to increase polymer tolerance towards divalent cations by modifying 1:1 Styrene: Maleic acid co polymers by reacting methylamine with the maleic anhydride to form an amide derivative (SMAma) instead of an ester (Esmaili *et al.,* 2020).

It appears that divalent cation sensitivity is a complicated issue. DIBMA polymer has increased tolerance towards divalent cations even though its structure contains identical maleic acid groups as SMA (Oluwole *et al.,* 2017; Cuevas Arenas et al., 2017; Simon, Pollock and Lee, 2018). () Other Studies have gone even further and suggested that supplementing DIBMA polymer with low millimolar concentrations of Mg^{2+} or Ca^{2+} can actually speed up the solubilisation process (Danielczak, Meister and Keller, 2019). Therefore, perhaps the divalent cation sensitivity is not dependent entirely on maleic acid groups and impacted more by the overall hydrophobicity of each polymer. For example, the 2:1 styrene: maleic acid polymer (SMA2000) is less hydrophobic than the 3:1 styrene: maleic acid polymer (SMA3000) and SMA2000 has been shown to be less sensitive to divalent cations than SMA3000 (Morrison *et al.*, 2016). The DIBMA polymer has a 1:1 ratio of diisobutylene:maleic acid and therefore is less hydrophobic than SMA2000, perhaps correlating with its greater tolerance towards divalent cations such as Mg^{2+} or Ca^{2+}.

Likewise, the amide derivative SMAma polymer should also be less hydrophobic and more hydrophilic as it has a 1:1 ratio of styrene:maleic acid and therefore it should be more tolerant towards divalent cations however it is important to note that there is a delicate balance of polymer hydrophilicity and polymer applicability. SMA 1000 polymer, which has a 1:1 ratio of styrene: maleic acid is ineffective in membrane solubilisation trials (Morrison *et al.,* 2016).

It is also possible that the divalent cations cause polymers to precipitate out of solution by neutralising the charges present on polymers despite polymers being able to tolerate high concentrations of Na^+ or K^+ ions, it may be due to differences in coordination chemistry between divalent cations such as Mg^{2+} and Ca^{2+} and Na^+ or K^+. Divalent cations may be able to form specific bonds with polymers or affect the alignment of polymer structure in a unique way which the single charged Na^+ or K^+ ion are unable to replicate.

A final explanation could be that the different polymers create discs of different sizes, and therefore the polymers already experience different strain depending on the circumference. SMA3000 is known to produce smaller discs than SMA2000 and it is more sensitive to divalent cations (Morrison *et al.*, 2016). DIBMA is known to create larger discs than SMA2000 and it is more tolerant (Oluwole *et al.*, 2017;

Gulamhussein *et al* 2020). It would be good going forward to examine the size of the discs formed using DLS and/or electron microscopy.

A range of other styrene maleic acid derivates have been reported in the literature to overcome the limitation of the standard SMA co polymers. Styrene maleimide (SMI) polymers have been used to solubilise membrane proteins with comparable efficiency to SMA co polymers for some proteins. Styrene maleimide polymers also remain functional at acidic pH and are compatible with high concentrations of divalent cations (Hall *et al*., 2018).. Therefore, in future studies, use of SMI polymers for LeuT or Atm1 could be tested. Although it was reported that to date SMI has proved unsuccessful for ABC transporters (*Hawkins et al.,* 2021). Studies have also shown that styrene maleic acid copolymers can be modified to form a pH-resistant form of SMA polymer (SMA-QA) which is capable of solubilising membrane proteins within a diverse pH range (2.5 to 10), the SMA-QA polymer discs are stable even in the presence of divalent cations (Ravula *et al.,* 2018a). Therefore SMA-QA polymers are another option which could be explored in the future.

SMA polymer can also be modified by amination reactions to form SMA-EA polymers and the resultant polymers are capable of solubilising lipid bilayers into varying sizing of nanodiscs. By varying the ratio of polymer to lipid, different size nanodiscs ranging from nanometer to sub-micrometer diameter could be formed (Ravula *et al.,* 2017b). The SMA-EA could be extremely useful for SPR future experiments as LeuT/Atm1 proteins could be purified into various size nanodiscs and immobilisation attempted to see if nanodisc size has an impact on immobilisation. Similarly, it has also been shown that ethylenediamine can be attached to SMA polymers to form SMA-ED polymer which are capable of solubilising multilamellar vesicles. Ravula et al., 2017a have also proposed that SMA-ED polymer could be dehydrated to form SMAd-A polymer which is effective at solubilising DMPC vesicles at acidic pH levels. SMA-ED and SMAd-A polymers can tolerate high concentrations of salt as well as high concentrations of divalent cation (200mM) (Ravula et al., 2017a). Testing these in the future would be interesting.

Finally, a zwitterionic styrene maleic acid copolymer (zSMA) has been created by replacing the carboxyl acid groups of SMA with zwitterionic phosphatidylcholine groups (Fiori *et al*., 2017). zSMA polymer could solubilise *E. coli* membranes, was compatible with low pH conditions and was tolerant to polyvalent cations. Therefore, the zSMA polymer is another option which could be explored for protein solubilisation in future experiments.

References

Ahmed, F.E., Wiley, J.E., Weidner, D.A., Bonnerup, C., Mota, H. (2010). 'Surface Plasmon Resonance (SPR) Spectrometry as a Tool to Analyze Nucleic Acid–Protein Interactions in Crude Cellular Extracts', in Cancer genomics & proteomics , 7(6), pp. 303–309. Available at: https://pubmed.ncbi.nlm.nih.gov/21156963/ (Accessed: 12 April 2023).

Allocati, N., Federici, L., Masulli, M. and Di Ilio, C. (2008). Glutathione transferases in bacteria. FEBS Journal, 276(1), pp.58–75. doi:10.1111/j.1742-4658.2008.06743.x.

Amara, S.G. and Sonders, M.S. (1998). Neurotransmitter transporters as molecular targets for addictive drugs. Drug and Alcohol Dependence, 51(1-2), pp.87–96. doi:10.1016/s0376-8716(98)00068-4.

Andersen, O.S. and Koeppe, R.E. (2007). Bilayer Thickness and Membrane Protein Function: An Energetic Perspective. Annual Review of Biophysics and Biomolecular Structure, 36(1), pp.107–130. doi:10.1146/annurev.biophys.36.040306.132643.

Arachea, B.T., Sun, Z., Potente, N., Malik, R., Isailovic, D. and Viola, R.E. (2012) 'Detergent selection for enhanced extraction of membrane proteins', Protein Expression and Purification, 86(1), pp. 12–20. doi: 10.1016/j.pep.2012.08.016.

Arey, B.J. (2012). The Role of Glycosylation in Receptor Signaling. Glycosylation. [online] doi:10.5772/50262.

Bagag, A., Jault, J.-M., Sidahmed-Adrar, N., Réfrégiers, M., Giuliani, A. and Le Naour, F. (2013). Characterization of Hydrophobic Peptides in the Presence of Detergent by Photoionization Mass Spectrometry. PLoS ONE, 8(11), p.e79033. doi:10.1371/journal.pone.0079033.

Bakheet, T.M. and Doig, A.J. (2009). Properties and identification of human protein drug targets. Bioinformatics, 25(4), pp.451–457. doi:10.1093/bioinformatics/btp002.

Bakhtiar, R. (2012) 'Surface plasmon resonance spectroscopy: A versatile technique in a biochemist's Toolbox', Journal of Chemical Education, 90(2), pp. 203–209. doi:10.1021/ed200549g.

Ballatori, N., Krance, S.M., Notenboom, S., Shi, S., Tieu, K. and Hammond, C.L. (2009). Glutathione dysregulation and the etiology and progression of human diseases. Biological Chemistry, [online] 390(3), pp.191–214. doi:10.1515/BC.2009.033.

Banerjee, P., Joo, J.B., Buse, J.T. and Dawson, G. (1995). Differential solubilization of lipids along with membrane proteins by different classes of detergents. Chemistry and Physics of Lipids, [online] 77(1), pp.65–78. doi:10.1016/0009-3084(95)02455-r.

Bartoschik, T., Galinec, S., Kleusch, C., Walkiewicz, K., Breitsprecher, D., Weigert, S., Muller, Y.A., You, C., Piehler, J., Vercruysse, T., Daelemans, D. and Tschammer, N. (2018). Near-native, site-

specific and purification-free protein labeling for quantitative protein interaction analysis by MicroScale Thermophoresis. Scientific Reports, 8(1). doi:10.1038/s41598-018-23154-3.

Bayly, G.R. (2014) 'Lipids and disorders of lipoprotein metabolism', Clinical Biochemistry: Metabolic and Clinical Aspects, Chapter 37 pp. 702–736. doi:10.1016/b978-0-7020-5140-1.00037-7.

Bazzacco, P., Emmanuelle Billon-Denis, K. Shivaji Sharma, Catoire, L., Mary, S., Christel Le Bon, Point, E., Jean-Louis Banères, Durand, G., Zito, F., Pucci, B. and Jean-Luc Popot (2012). Nonionic Homopolymeric Amphipols: Application to Membrane Protein Folding, Cell-Free Synthesis, and Solution Nuclear Magnetic Resonance. 51(7), pp.1416–1430. doi:10.1021/bi201862v.

Beauchamp, D.L. and Khajehpour, M. (2012). Studying salt effects on protein stability using ribonuclease t1 as a model system. Biophysical Chemistry, 161, pp.29–38. doi:10.1016/j.bpc.2011.11.004.

Bekri, S., Kispal, G., Lange, H., Fitzsimons, E., Tolmie, J., Lill, R. and Bishop, D.F. (2000). Human ABC7 transporter: gene structure and mutation causing X-linked sideroblastic anemia with ataxia with disruption of cytosolic iron-sulfur protein maturation. Blood, 96(9), pp.3256–3264. doi:10.1182/blood.v96.9.3256.

Beseničar, M., Maček, P., Lakey, J.H. and Anderluh, G. (2006). Surface plasmon resonance in protein–membrane interactions. Chemistry and Physics of Lipids, 141(1-2), pp.169–178. doi:10.1016/j.chemphyslip.2006.02.010.

Bichet, D.G. (2008). Vasopressin Receptor Mutations in Nephrogenic Diabetes Insipidus. Seminars in Nephrology, 28(3), pp.245–251. doi:10.1016/j.semnephrol.2008.03.005.

Billesbølle, C.B., Mie Barthold Krüger, Shi, L., Quick, M., Li, Z., Stolzenberg, S., Kniazeff, J., Kamil Gotfryd, Mortensen, J.S., Javitch, J.A., Weinstein, H., Loland, C.J. and Ulrik Gether (2015). Substrate-induced Unlocking of the Inner Gate Determines the Catalytic Efficiency of a Neurotransmitter:Sodium Symporter. 290(44), pp.26725–26738. doi:10.1074/jbc.m115.677658.

Bilsing, F.L., Anlauf , M.T., Hachani, E., Khosa, S., Schmitt, L. (2023). 'ABC transporters in bacterial Nanomachineries', International Journal of Molecular Sciences, 24(7), p. 6227. doi:10.3390/ijms24076227.

Bolanos-Garcia, V.M. and Miguel, R.N. (2003) 'On the structure and function of apolipoproteins: More than a family of lipid-binding proteins', Progress in Biophysics and Molecular Biology, 83(1), pp. 47–68. doi:10.1016/s0079-6107(03)00028-2.

Bordag, N. and Keller, S. (2010) 'A-helical transmembrane peptides: A "Divide and Conquer" approach to membrane proteins', Chemistry and Physics of Lipids, 163(1), pp. 1–26. doi: 10.1016/j.chemphyslip.2009.07.009.

Borroto-Escuela, D., Hinz, S., Navarro, G., Franco, R., Müller, C. and Fuxe, K. (2018). Understanding the Role of Adenosine A2AR Heteroreceptor Complexes in Neurodegeneration and Neuroinflammation. Frontiers in Neuroscience, 12, Article. 43. doi:10.3389/fnins.2018.00043.

Boultwood, J., Pellagatti, A., Nikpour, M., Pushkaran, B., Fidler, C., Cattan, H., Littlewood, T.J., Malcovati, L., Della Porta, M.G., Jädersten, M., Killick, S., Giagounidis, A., Bowen, D., Hellström-Lindberg, E., Cazzola, M. and Wainscoat, J.S. (2008). The Role of the Iron Transporter ABCB7 in Refractory Anemia with Ring Sideroblasts. PLoS ONE, 3(4), p.e1970. doi:10.1371/journal.pone.0001970.

Brady, N.G., Workman, C.E., Cawthon, B., Bruce, B.D. and Long, B.K. (2021). Protein Extraction Efficiency and Selectivity of Esterified Styrene–Maleic Acid Copolymers in Thylakoid Membranes. Biomacromolecules, 22(6), pp.2544–2553. doi:10.1021/acs.biomac.1c00274.

Brady, N.R., Liu, L., Ma, Y., Gumbart, J.C. and Bruce, B.D. (2019). Non-detergent isolation of a cyanobacterial photosystem I using styrene maleic acid alternating copolymers. 9(54), pp.31781–31796. doi:10.1039/c9ra04619d.

Braun, D. and Libchaber, A. (2002). Trapping of DNA by Thermophoretic Depletion and Convection. Physical Review Letters, 89(18). doi:10.1103/physrevlett.89.188103.

Broadbent, L., Depping, P., Lodé, A., Vaitsopoulou, A., Hardy, D., Ayub, H., Mitchell-White, J., Kerr, I.D., Goddard, A.D., Bill, R.M. and Rothnie, A.J. (2022). Detergent-Free Membrane Protein Purification Using SMA Polymer. Methods in Molecular Biology (Clifton, N.J.), [online] 2507, pp.389–404. doi:10.1007/978-1-0716-2368-8_21.

Broecker, J., Eger, B.T. and Ernst, O.P. (2017). Crystallogenesis of Membrane Proteins Mediated by Polymer-Bounded Lipid Nanodiscs. Structure, [online] 25(2), pp.384–392. doi:10.1016/j.str.2016.12.004.

Brunzell, J.D. (2009) 'Chapter 6 - Genetic dyslipidemia', Clinical Lipidology, Editor: Christie M. Ballantyne. W.B. Saunders. pp. 71–84. doi:10.1016/b978-141605469-6.50010-x.

Cantor, R.S. (1997) 'Lateral pressures in cell membranes:; a mechanism for modulation of protein function', The Journal of Physical Chemistry B, 101(10), pp. 1723–1725. doi:10.1021/jp963911x.

Cao, Y., Fang, J., Shi, Y.-W., Wang, H., Chen, X., Liu, Y., Zhu, Z., Cao, Y., Hong, Z. and Chai, Y. (2022). Screening potential P-glycoprotein inhibitors by combination of a detergent-free membrane protein extraction with surface plasmon resonance biosensor. 12(7), pp.3113–3123. doi:10.1016/j.apsb.2022.03.016.

Carpenter, B. and Lebon, G. (2017). Human Adenosine A2A Receptor: Molecular Mechanism of Ligand Binding and Activation. Frontiers in Pharmacology, 8, Article. 898. doi:10.3389/fphar.2017.00898.

Cavadini, P., Biasiotto, G., Poli, M., Levi, S., Verardi, R., Zanella, I., Derosas, M., Ingrassia, R., Corrado, M. and Arosio, P. (2006). RNA silencing of the mitochondrial ABCB7 transporter in HeLa cells causes an iron-deficient phenotype with mitochondrial iron overload. Blood, 109(8), pp.3552–3559. doi:10.1182/blood-2006-08-041632.

Cavigiolio, G. et al. (2010) 'Exchange of apolipoprotein A-I between lipid-associated and lipid-free states', Journal of Biological Chemistry, 285(24), pp. 18847–18857. doi:10.1074/jbc.m109.098434.

Charalambous, K., Miller, D., Curnow, P. and Booth, P.J. (2008). Lipid bilayer composition influences small multidrug transporters. BMC Biochemistry, 9(1). doi:https://doi.org/10.1186/1471-2091-9-31.

Charvolin, D., Perez, J.-B., Florent Rouvière, Giusti, F., Bazzacco, P., Alaa Abdine, Rappaport, F., Martinez, K.L. and Jean-Luc Popot (2009). The use of amphipols as universal molecular adapters to immobilize membrane proteins onto solid supports. Proceedings of the National Academy of Sciences of the United States of America, 106(2), pp.405–410. doi:10.1073/pnas.0807132106.

Chemical thermodynamics (2004) Gibbs Free Energy. Available at: https://chemed.chem.purdue.edu/genchem/topicreview/bp/ch21/gibbs.php (Accessed: 13 April 2023).

Cherepanov, D.A., Brady, N.G., Shelaev, I.V., Nguyen, J., Gostev, F.E., Mamedov, M.D., Nadtochenko, V.A. and Bruce, B.D. (2020). PSI-SMALP, a Detergent-free Cyanobacterial Photosystem I, Reveals Faster Femtosecond Photochemistry. Biophysical Journal, 118(2), pp.337–351. doi:10.1016/j.bpj.2019.11.3391.

Chloupková, M., Reaves, S.K., LeBard, L.M. and Koeller, D.M. (2004). The mitochondrial ABC transporter Atm1p functions as a homodimer. FEBS Letters, 569(1-3), pp.65–69. doi:10.1016/j.febslet.2004.05.051.

Clunes, M.T. and Boucher, R.C. (2007). Cystic fibrosis: the mechanisms of pathogenesis of an inherited lung disorder. Drug Discovery Today: Disease Mechanisms, 4(2), pp.63–72. doi:10.1016/j.ddmec.2007.09.001.

Cole, N.B. (2013). Site-Specific Protein Labeling with SNAP-Tags. Current Protocols in Protein Science, 73(1). doi:10.1002/0471140864.ps3001s73.

Colthup, N.B. and Meyers, R.A. (2002) 'Infrared Spectroscopy', in Encyclopedia of Physical Science and Technology. 3rd edn. San Diego: Academic Press, pp. 793–816. doi:10.1016/b0-12-227410-5/00340-9.

Congreve, M., Rich, R.L., Myszka, D.G., Figaroa, F., Siegal, G. and Marshall, F. (2011). Fragment Screening of Stabilized G-Protein-Coupled Receptors Using Biophysical Methods. pp.115–136. doi:10.1016/b978-0-12-381274-2.00005-4.

Cooper, M.A. (2004). Advances in membrane receptor screening and analysis. Journal of Molecular Recognition, 17(4), pp.286–315. doi:10.1002/jmr.675.

Cottis, R.A., Shreir, L.L. and Burstein, G.T. (2010) 'Chemical thermodynamics*', Shreir's Corrosion, 1, pp. 1–12. doi:10.1016/b978-044452787-5.00002-0.

Coyle, J.T. and Snyder, S.H. (1969). Antiparkinsonian Drugs: Inhibition of Dopamine Uptake in the Corpus Striatum as a Possible Mechanism of Action. Science, 166(3907), pp.899–901. doi:10.1126/science.166.3907.899.

Cuevas Arenas, R., Danielczak, B., Martel, A., Porcar, L., Breyton, C., Ebel, C. and Keller, S. (2017). Fast Collisional Lipid Transfer Among Polymer-Bounded Nanodiscs. Scientific Reports, 7(1). doi:10.1038/srep45875.

Cunningham, B. and Wells, J. (1989). High-resolution epitope mapping of hGH-receptor interactions by alanine-scanning mutagenesis. Science, 244(4908), pp.1081–1085. doi:10.1126/science.2471267.

Cunningham, R.D., Kopf, A.H., Elenbaas, W., Bram, B., Pfukwa, R., J. Antoinette Killian and Klumperman, B. (2020). Iterative RAFT-Mediated Copolymerization of Styrene and Maleic Anhydride toward Sequence- and Length-Controlled Copolymers and Their Applications for Solubilizing Lipid Membranes. 21(8), pp.3287–3300. doi:10.1021/acs.biomac.0c00736.

Daniel, T., Faruq, H.M., Laura Magdalena, J., Manuela, G. and Christopher Horst, L. (2020). Role of GSH and Iron-Sulfur Glutaredoxins in Iron Metabolism—Review. Molecules, 25(17), p.3860. doi:10.3390/molecules25173860.

Danielczak, B., Meister, A. and Keller, S. (2019). Influence of Mg2+ and Ca2+ on nanodisc formation by diisobutylene/maleic acid (DIBMA) copolymer. Chemistry and Physics of Lipids, [online] 221, pp.30–38. doi:10.1016/j.chemphyslip.2019.03.004.

Davey, J. (2004) 'G-protein-coupled receptors: New approaches to Maximise the impact of GPCRs in drug discovery', Expert Opinion on Therapeutic Targets, 8(2), pp. 165–170. doi: 10.1517/14728222.8.2.165.

Davidson, A.L. and Chen, J. (2004). ATP-Binding Cassette Transporters in Bacteria. Annual Review of Biochemistry, 73(1), pp.241–268. doi:10.1146/annurev.biochem.73.011303.073626.

Day, Y.S.N., Baird, C.L., Rich, R.L. and Myszka, D.G. (2002). Direct comparison of binding equilibrium, thermodynamic, and rate constants determined by surface- and solution-based biophysical methods. Protein Science, 11(5), pp.1017–1025. doi:10.1110/ps.4330102.

Dean, M. (2001). The Human ATP-Binding Cassette (ABC) Transporter Superfamily. Genome Research, 11(7), pp.1156–1166. doi:10.1101/gr.gr-1649r.

Debnath, D.K., Basaiawmoit, R.V., Nielsen, K.L. and Otzen, D.E. (2010) 'The role of membrane properties in Mistic folding and dimerisation', Protein Engineering Design and Selection, 24(1-2), pp. 89–97. doi: 10.1093/protein/gzq095.

Deller, M.C., Kong, L. and Rupp, B. (2016) 'Protein stability: A crystallographer's perspective', Acta Crystallographica Section F Structural Biology Communications, 72(2), pp. 72–95. doi:10.1107/s2053230x15024619.

Denisov, I.G. and Sligar, S.G. (2016). Nanodiscs for structural and functional studies of membrane proteins. Nature Structural & Molecular Biology, [online] 23(6), pp.481–486. doi:10.1038/nsmb.3195.

Denisov, I.G. and Sligar, S.G. (2017). Nanodiscs in Membrane Biochemistry and Biophysics. Chemical Reviews, 117(6), pp.4669–4713. doi:10.1021/acs.chemrev.6b00690.

Department of Health and Human Services (1995) NIH guide: STRUCTURAL BIOLOGY OF MEMBRANE PROTEINS. Available at: https://grants.nih.gov/grants/guide/pa-files/PA-95-035.html (Accessed: 5 March 2017).

Devaux, P.F. and Morris, R. (2004). Transmembrane Asymmetry and Lateral Domains in Biological Membranes. Traffic, 5(4), pp.241–246. doi:10.1111/j.1600-0854.2004.0170.x.

Diskar, M., Zenn, H.-M., Kaupisch, A., Prinz, A. and Herberg, F.W. (2007). Molecular basis for isoform-specific autoregulation of protein kinase A. Cellular Signalling, 19(10), pp.2024–2034. doi:10.1016/j.cellsig.2007.05.012.

Do, E., Park, S., Li, M., Wang, J., Ding, C., Kronstad, J.W. and Won Hee Jung (2017). The mitochondrial ABC transporter Atm1 plays a role in iron metabolism and virulence in the human fungal pathogen Cryptococcus neoformans. 56(4), pp.458–468. doi:10.1093/mmy/myx073.

Dörr, J.M., Koorengevel, M.C., Schäfer, M., Prokofyev, A.V., Scheidelaar, S., Cruijsen, E.A.W. van der, Dafforn, T.R., Baldus, M. and Killian, J.A. (2014). Detergent-free isolation, characterization, and functional reconstitution of a tetrameric K+ channel: The power of native nanodiscs. Proceedings of the National Academy of Sciences,111(52), pp.18607–18612. doi:10.1073/pnas.1416205112.

Dörr, J.M., Schäfer, M., Koorengevel, M.C. and Killian, J.A. (2016) 'Detergent-free isolation, characterization and functional Reconstitution of a K+ channel: The power of native Nanodiscs', Biophysical Journal, 110(3), p. 421a. doi: 10.1016/j.bpj.2015.11.2274.

Dörr, J.M., Scheidelaar, S., Koorengevel, M.C., Dominguez, J.J., Schäfer, M., van Walree, C.A. and Killian, J.A. (2015) 'The styrene–maleic acid copolymer: A versatile tool in membrane research', European Biophysics Journal, 45(1), pp. 3–21. doi: 10.1007/s00249-015-1093-y.

Duhr, S. and Braun, D. (2006). Why molecules move along a temperature gradient. Proceedings of the National Academy of Sciences, 103(52), pp.19678-19682.

Duhr, S., Arduini, S. and Braun, D. (2004). Thermophoresis of DNA determined by microfluidic fluorescence. The European Physical Journal E, 15(3), pp.277-286.

Dupré, D.J., Robitaille, M., Rebois, R.V. and Hébert, T.E. (2009). 'The role of gβγ subunits in the organization, assembly, and function of GPCR signaling complexes', Annual Review of Pharmacology and Toxicology, 49(1), pp. 31–56. doi:10.1146/annurev-pharmtox-061008-103038.

Duquesne, K., Prima, V. and Sturgis, J.N. (2016). Membrane Protein Solubilization and Composition of Protein Detergent Complexes. Methods in Molecular Biology, [online] pp.243–260. doi:https://doi.org/10.1007/978-1-4939-3637-3_15.

Ellinghaus, T.L., Marcellino, T., Srinivasan, V., Lill, R. and Kühlbrandt, W. (2021) .'Conformational changes in the yeast mitochondrial ABC transporter ATM1 during the transport cycle', Science Advances, 7(52). doi:10.1126/sciadv.abk2392.

Englebienne, P., Hoonacker, A.V. and Verhas, M. (2003) 'Surface plasmon resonance: Principles, methods and applications in biomedical sciences', Spectroscopy, 17(2–3), pp. 255–273. doi:10.1155/2003/372913.

Erlendsson, S., Gotfryd, K., Larsen, F., Mortensen, J., Geiger, M., van Rossum, B., Oschkinat, H., Gether, U., Teilum, K. and Loland, C. (2017). Direct assessment of substrate binding to the Neurotransmitter:Sodium Symporter LeuT by solid state NMR. eLife, 6.

Esmaili, M. and Overduin, M. (2018). Membrane biology visualized in nanometer-sized discs formed by styrene maleic acid polymers. Biochimica et Biophysica Acta (BBA) - Biomembranes, 1860(2), pp.257-263.

Esmaili, M., Tancowny, B., Wang, X., Moses, A., Cortez, L., Sim, V., Wille, H. and Overduin, M., (2020). Native nanodiscs formed by styrene maleic acid copolymer derivatives help recover infectious prion multimers bound to brain-derived lipids. Journal of Biological Chemistry, 295(25), pp.8460-8469.

Ezzati Nazhad Dolatabadi, J. and de la Guardia, M. (2016) 'Tips on ligand immobilization and kinetic study using surface plasmonresonance', Bioimpacts, 6(3), pp. 117–118. Doi:10.15171/bi.2016.17.

Fadlelmoula, A., Pinho, D., Carvalho, V.H., Catarino, S.O. and Minas, G. (2022). Fourier Transform Infrared (FTIR) Spectroscopy to Analyse Human Blood over the Last 20 Years: A Review towards Lab-on-a-Chip Devices. Micromachines, 13(2), p.187. doi:10.3390/mi13020187.

Fagerberg, L., Jonasson, K., von Heijne, G., Uhlén, M. and Berglund, L. (2010). Prediction of the human membrane proteome. PROTEOMICS, 10(6), pp.1141-1149.

Faham, S. and Bowie, J.U. (2002) 'Bicelle crystallization: A new method for crystallizing membrane proteins yields a monomeric bacteriorhodopsin structure', Journal of Molecular Biology, 316(1), pp. 1–6. Doi:10.1006/jmbi.2001.5295.

Fan, C., Kaiser, J.T. and Rees, D.C. (2020) 'A structural framework for unidirectional transport by a bacterial ABC Exporter', Proceedings of the National Academy of Sciences, 117(32), pp. 19228–19236. doi:10.1073/pnas.2006526117.

Feingold, K.R., Anawalt, B. and Blackman, M.R. (2000) Introduction to lipids and Lipoproteins, National Center for Biotechnology Information. Available at: https://pubmed.ncbi.nlm.nih.gov/26247089/ (Accessed: 22 April 2023).

Fiori, M.C., Jiang, Y., Altenberg, G.A. and Liang, H. (2017). Polymer-encased nanodiscs with improved buffer compatibility. Scientific Reports, [online] 7(1), p.7432. doi:https://doi.org/10.1038/s41598-017-07110-1.

Firth, A., Remillard, C. and Yuan, J. (2007). TRP channels in hypertension. Biochimica et Biophysica Acta (BBA) - Molecular Basis of Disease, 1772(8), pp.895-906.

Gao, X., Lu, F., Zhou, L., Dang, S., Sun, L., Li, X., Wang, J. and Shi, Y. (2009). Structure and Mechanism of an Amino Acid Antiporter. Science, 324(5934), pp.1565-1568.

Garavito, R.M. and Ferguson-Miller, S. (2001) 'Detergents as tools in membrane biochemistry', Journal of Biological Chemistry, 276(35), pp. 32403–32406. doi: 10.1074/jbc.r100031200.

Gari, K., León Ortiz, A., Borel, V., Flynn, H., Skehel, J. and Boulton, S. (2012) MMS19 Links Cytoplasmic Iron-Sulfur Cluster Assembly to DNA Metabolism. Science, 337(6091), pp.243-245.

Gbelska, Y., Krijger, J. and Breunig, K. (2006) Evolution of gene families: the multidrug resistance transporter genes in five related yeast species. FEMS Yeast Research, 6(3), pp.345-355.

Gether, U., Andersen, P., Larsson, O. and SCHOUSBOE, A. (2006). Neurotransmitter transporters: molecular function of important drug targets. Trends in Pharmacological Sciences, 27(7), pp.375-383.

Giros, B., Jaber, M., Jones, S., Wightman, R. and Caron, M. (1996). Hyperlocomotion and indifference to cocaine and amphetamine in mice lacking the dopamine transporter. Nature, 379(6566), pp.606-612.

Giusti, F., Kessler, P., Hansen, R., Della Pia, E., Le Bon, C., Mourier, G., Popot, J., Martinez, K. and Zoonens, M. (2015). Synthesis of a Polyhistidine-bearing Amphipol and its Use for Immobilizing Membrane Proteins. Biomacromolecules, 16(12), pp.3751-3761.

Glück, J., Koenig, B. and Willbold, D. (2011). Nanodiscs allow the use of integral membrane proteins as analytes in surface plasmon resonance studies. Analytical Biochemistry, 408(1), pp.46-52.

Green, R.J., Frazier, R.A., Shakesheff, K.M., Davies, M.C., Roberts, C.J. and Tendler, S.J.B. (2000). Surface plasmon resonance analysis of dynamic biological interactions with biomaterials. Biomaterials, [online] 21(18), pp.1823–1835. doi:10.1016/S0142-9612(00)00077-6.

Grethen, A., Oluwole, A.O., Danielczak, B., Vargas, C. and Keller, S. (2017). Thermodynamics of nanodisc formation mediated by styrene/maleic acid (2:1) copolymer. Scientific Reports, [online] 7(1). doi:https://doi.org/10.1038/s41598-017-11616-z.

Grote, J., Dankbar, N., Gedig, E. and Koenig, S. (2005). 'Surface plasmon resonance/mass spectrometry interface', Analytical Chemistry, 77(4), pp. 1157–1162. doi:10.1021/ac049033d.

Guiral, M. and Giudici-Orticoni, M.-T. (2020) 'Microbe profile: Aquifex Aeolicus: An extreme heat-loving bacterium that feeds on gases and inorganic chemicals', Microbiology, 167(1). doi:10.1099/mic.0.001010.

Gulamhussein, A., Uddin, R., Tighe, B., Poyner, D. and Rothnie, A. (2020) A comparison of SMA (styrene maleic acid) and DIBMA (di-isobutylene maleic acid) for membrane protein purification. Biochimica et Biophysica Acta (BBA) - Biomembranes, 1862(7), p.183281.

Gulati, S., Jamshad, M., Knowles, T., Morrison, K., Downing, R., Cant, N., Collins, R., Koenderink, J., Ford, R., Overduin, M., Kerr, I., Dafforn, T. and Rothnie, A. (2014) Detergent-free purification of ABC (ATP-binding-cassette) transporters. Biochemical Journal, 461(2), pp.269-278.

Günsel, U. and Hagn, F. (2021) 'Lipid nanodiscs for high-resolution NMR studies of membrane proteins', Chemical Reviews, 122(10), pp. 9395–9421. doi:10.1021/acs.chemrev.1c00702.

Hall, S., Tognoloni, C., Charlton, J., Bragginton, É., Rothnie, A., Sridhar, P., Wheatley, M., Knowles, T., Arnold, T., Edler, K. and Dafforn, T. (2018). An acid-compatible co-polymer for the solubilization of membranes and proteins into lipid bilayer-containing nanoparticles. Nanoscale, 10(22), pp.10609-10619.

Hang, H.C. (2010) 'Molecular probes for protein glycosylation', Comprehensive Natural Products II, 6, pp. 261–296. doi:10.1016/b978-008045382-8.00125-8.

Hansen, S., Rodgers, M. and Hoskins, A., 2016. Fluorescent Labeling of Proteins in Whole Cell Extracts for Single-Molecule Imaging. Single-Molecule Enzymology: Fluorescence-Based and High-Throughput Methods, pp.83-104.

Hawkins, O., Jahromi, C., Gulamhussein, A., Nestorow, S., Bahra, T., Shelton, C., Owusu-Mensah, Q., Mohiddin, N., O'Rourke, H., Ajmal, M., Byrnes, K., Khan, M., Nahar, N., Lim, A., Harris, C., Healy, H., Hasan, S., Ahmed, A., Evans, L., Vaitsopoulou, A., Akram, A., Williams, C., Binding, J., Thandi, R., Joby, A., Guest, A., Tariq, M., Rasool, F., Cavanagh, L., Kang, S., Asparuhov, B., Jestin, A., Dafforn, T., Simms, J., Bill, R., Goddard, A. and Rothnie, A. (2021) Membrane protein extraction and purification using partially-esterified SMA polymers. Biochimica et Biophysica Acta (BBA) - Biomembranes, 1863(12), p.183758.

He, J., Liu, Y., Wu, J. and Lubman, D.M. (2013)'Analysis of glycoproteins for Biomarker Discovery', Methods in Molecular Biology, pp. 115–122. doi:10.1007/978-1-62703-360-2_10.

Hearty, S., Conroy, P., B. Vijayalakshmi Ayyar, Byrne, B.J. and O'Kennedy, R. (2010). Surface plasmon resonance for vaccine design and efficacy studies: recent applications and future trends. 9(6), pp.645–664. doi:10.1586/erv.10.52.

Hediger, M., Romero, M., Peng, J., Rolfs, A., Takanaga, H. and Bruford, E. (2004). The ABCs of solute carriers: physiological, pathological and therapeutic implications of human membrane transport proteins. Pflügers Archiv European Journal of Physiology, 447(5), pp.465-468.

Hemmat Esfe, M., Esfandeh, S. and Kamyab, M.H. (2020) 'History and introduction', Hybrid Nanofluids for Convection Heat Transfer, pp. 1–48. doi:10.1016/b978-0-12-819280-1.00001-x.

Henry, S., El-Sayed, M., Pirie, C., Hoffman, A. and Stayton, P. (2006). pH-Responsive Poly(styrene-alt-maleic anhydride) Alkylamide Copolymers for Intracellular Drug Delivery. Biomacromolecules, 7(8), pp.2407-2414.

Hesketh, S.J., Klebl, D.P., Higgins, A.J., Thomsen, M., Pickles, I.B., Sobott, F., Sivaprasadarao, A., Postis, V.L.G. and Muench, S.P. (2020). 'Styrene maleic-acid lipid particles (smalps) into detergent or amphipols: An exchange protocol for membrane protein characterisation', Biochimica et Biophysica Acta (BBA) - Biomembranes, 1862(5), p. 183192. doi:10.1016/j.bbamem.2020.183192.

Higgins, C. (1992) ABC Transporters: From Microorganisms to Man. Annual Review of Cell Biology, 8(1), pp.67-113.

Hofacker, M., Gompf, S., Zutz, A., Presenti, C., Haase, W., van der Does, C., Model, K. and Tampé, R. (2007) Structural and Functional Fingerprint of the Mitochondrial ATP-binding Cassette Transporter Mdl1 from Saccharomyces cerevisiae. Journal of Biological Chemistry, 282(6), pp.3951-3961.

Hoffman, B.J., Hansson, S.R., Mezey, E. and Palkovits, M. (1998) 'Localization and dynamic regulation of biogenic amine transporters in the mammalian central nervous system', Frontiers in Neuroendocrinology, 19(3), pp. 187–231. doi:10.1006/frne.1998.0168.

Hoffman, T., Canziani, G., Jia, L., Rucker, J. and Doms, R. (2000). A biosensor assay for studying ligand-membrane receptor interactions: Binding of antibodies and HIV-1 Env to chemokine receptors. Proceedings of the National Academy of Sciences, 97(21), pp.11215-11220.

Hsu, Y., Hoenderop, J. and Bindels, R. (2007). TRP channels in kidney disease. Biochimica et Biophysica Acta (BBA) - Molecular Basis of Disease, 1772(8), pp.928-936.

Hwang, J., Song, W., Hong, D., Ko, D., Yamaoka, Y., Jang, S., Yim, S., Lee, E., Khare, D., Kim, K., Palmgren, M., Yoon, H., Martinoia, E. and Lee, Y. (2016) Plant ABC Transporters Enable Many Unique Aspects of a Terrestrial Plant's Lifestyle. Molecular Plant, 9(3), pp.338-355.

Iversen, L. (1971). Role of Transmitter Uptake Mechanisms in Synaptic Neurotransmission. British Journal of Pharmacology, 41(4), pp.571-591.

Iversen, L. (2009). Neurotransmitter transporters and their impact on the development of psychopharmacology. British Journal of Pharmacology, 147(S1), pp.S82-S88.

Jamshad, M., Charlton, J., Lin, Y., Routledge, S., Bawa, Z., Knowles, T., Overduin, M., Dekker, N., Dafforn, T., Bill, R., Poyner, D. and Wheatley, M. (2015a). G-protein coupled receptor solubilization and purification for biophysical analysis and functional studies, in the total absence of detergent. Bioscience Reports, 35(2), pp.1-10.

Jamshad, M., Grimard, V., Idini, I., Knowles, T.J., Dowle, M.R., Schofield, N., Sridhar, P., Lin, Y., Finka, R., Wheatley, M., Thomas, O.R.T., Palmer, R.E., Overduin, M., Govaerts, C., Ruysschaert, J.-M., Edler, K.J. and Dafforn, T.R. (2015b) 'Structural analysis of a nanoparticle containing a lipid bilayer used for detergent-free extraction of membrane proteins', Nano Research, 8(3), pp. 774–789. doi: 10.1007/s12274-014-0560-6.

Jamshad, M., Lin, Y., Knowles, T., Parslow, R., Harris, C., Wheatley, M., Poyner, D., Bill, R., Thomas, O., Overduin, M. and Dafforn, T. (2011). Surfactant-free purification of membrane proteins with intact native membrane environment. Biochemical Society Transactions, 39(3), pp.813-818.

Jerabek-Willemsen, M., André, T., Wanner, R., Roth, H., Duhr, S., Baaske, P. and Breitsprecher, D. (2014). MicroScale Thermophoresis: Interaction analysis and beyond. Journal of Molecular Structure, 1077, pp.101-113.

Jerabek-Willemsen, M., André, T., Wanner, R., Roth, H.M., Duhr, S., Baaske, P. and Breitsprecher, D. (2014). Microscale thermophoresis: Interaction analysis and beyond', Journal of Molecular Structure, 1077, pp. 101–113. doi:10.1016/j.molstruc.2014.03.009.

Jerabek-Willemsen, M., Wienken, C., Braun, D., Baaske, P. and Duhr, S. (2011). Molecular Interaction Studies Using Microscale Thermophoresis. ASSAY and Drug Development Technologies, 9(4), pp.342-353.

Johnson, D. and Martin, L. (2005). Controlling Protein Orientation at Interfaces Using Histidine Tags: An Alternative to Ni/NTA. Journal of the American Chemical Society, 127(7), pp.2018-2019.

Jones, S., Gainetdinov, R., Jaber, M., Giros, B., Wightman, R. and Caron, M. (1998). Profound neuronal plasticity in response to inactivation of the dopamine transporter. Proceedings of the National Academy of Sciences, 95(7), pp.4029-4034.

Jungwirth, H. and Kuchler, K. (2006) Yeast ABC transporters - A tale of sex, stress, drugs and aging. FEBS Letters, 580(4), pp.1131-1138.

Kantcheva, A.K., Quick, M., Shi, L., Winther, A.-M. . L., Stolzenberg, S., Weinstein, H., Javitch, J.A. and Nissen, P. (2013) .Chloride binding site of neurotransmitter sodium symporters, Proceedings of the National Academy of Sciences, 110(21), pp. 8489–8494. doi:10.1073/pnas.1221279110.

Kaplan, M.M. (2004) 'Novosphingobium aromaticivorans: A potential initiator of primary biliary cirrhosis', The American Journal of Gastroenterology, 99(11), pp. 2147–2149. doi:10.1111/j.1572-0241.2004.41121.x.

Khan Academy (2015). Gibbs free energy and spontaneity. [online] Khan Academy. Available at: https://www.khanacademy.org/science/chemistry/thermodynamics-chemistry/gibbs-free-energy/a/gibbs-free-energy-and-spontaneity.

Khelashvili, G., LeVine, M., Shi, L., Quick, M., Javitch, J. and Weinstein, H. (2013). The Membrane Protein LeuT in Micellar Systems: Aggregation Dynamics and Detergent Binding to the S2 Site. Journal of the American Chemical Society, 135(38), pp.14266-14275.

Kimple, A., Muller, R., Siderovski, D. and Willard, F. (2010). A Capture Coupling Method for the Covalent Immobilisation of Hexahistidine Tagged Proteins for Surface Plasmon Resonance. Methods in Molecular Biology, pp.91-100.

Kimple, A., Willard, F., Giguère, P., Johnston, C., Mocanu, V. and Siderovski, D. (2007). The RGS protein inhibitor CCG-4986 is a covalent modifier of the RGS4 Gα-interaction face. Biochimica et Biophysica Acta (BBA) - Proteins and Proteomics, 1774(9), pp.1213-1220.

Kispal, G., Csere, P., Guiard, B. and Lill, R. (1997). The ABC transporter Atm1p is required for mitochondrial iron homeostasis. FEBS Letters, 418(3), pp.346-350.

Kispal, G., Csere, P., Prohl, C. and Lill, R. (1999) The mitochondrial proteins Atm1p and Nfs1p are essential for biogenesis of cytosolic Fe/S proteins. The EMBO Journal, 18(14), pp.3981-3989.

Knowles, T.J., Finka, R., Smith, C., Lin, Y.-P., Dafforn, T. and Overduin, M. (2009) 'Membrane proteins Solubilized intact in lipid containing Nanoparticles bounded by styrene Maleic acid Copolymer', Journal of the American Chemical Society, 131(22), pp. 7484–7485. doi: 10.1021/ja810046q.

Kontur, W.S., Bingman, C.A., Olmsted, C.N., Wassarman, D.R., Ulbrich, A., Gall, D., Smith, R., Yusko, L.M., Fox, B.G., Noguera, D.R., Coon, J.J. and Donohue, T.J. (2018). Novosphingobium aromaticivorans uses a Nu-class glutathione S-transferase as a glutathione lyase in breaking the β-aryl ether bond of lignin. 293(14), pp.4955–4968. doi:10.1074/jbc.ra117.001268.

Kontur, W.S., Bingman, C.A., Olmsted, C.N., Wassarman, D.R., Ulbrich, A., Gall, D., Smith, R., Yusko, L.M., Fox, B.G., Noguera, D.R., Coon, J.J. and Donohue, T.J. (2018). Novosphingobium aromaticivorans uses a Nu-class glutathione S-transferase as a glutathione lyase in breaking the β-aryl ether bond of lignin. 293(14), pp.4955–4968. doi:https://doi.org/10.1074/jbc.ra117.001268.

Kopf, A., Dörr, J., Koorengevel, M., Antoniciello, F., Jahn, H. and Killian, J. (2020) Factors influencing the solubilization of membrane proteins from Escherichia coli membranes by styrene–maleic acid copolymers. Biochimica et Biophysica Acta (BBA) - Biomembranes, 1862(2), p.183125.

Kornberg, T. and Roy, S. (2014). Communicating by touch – neurons are not alone. Trends in Cell Biology, 24(6), pp.370-376.

Korotych, O., Mondal, J., Gattás-Asfura, K., Hendricks, J. and Bruce, B. (2019) Evaluation of commercially available styrene-co-maleic acid polymers for the extraction of membrane proteins from spinach chloroplast thylakoids. European Polymer Journal, 114, pp.485-500.

Korotych, O., Nguyen, T., Reagan, B., Burch-Smith, T. and Bruce, B. (2021) Poly(styrene-co-maleic acid)-mediated isolation of supramolecular membrane protein complexes from plant thylakoids. Biochimica et Biophysica Acta (BBA) - Bioenergetics, 1862(3), p.148347.

Krishnamurthy, H. and Gouaux, E. (2012). X-ray structures of LeuT in substrate-free outward-open and apo inward-open states. Nature, 481(7382), pp.469-474.

Kuhnke, G., Neumann, K., Mühlenhoff, U. and Lill, R. (2006) Stimulation of the ATPase activity of the yeast mitochondrial ABC transporter Atm1p by thiol compounds. Molecular Membrane Biology, 23(2), pp.173-184.

Laganowsky, A., Reading, E., Allison, T., Ulmschneider, M., Degiacomi, M., Baldwin, A. and Robinson, C. (2014). Membrane proteins bind lipids selectively to modulate their structure and function. Nature, 510(7503), pp.172-175.

Latorraca, N.R., Venkatakrishnan, A.J. and Dror, R.O. (2016) 'GPCR dynamics: Structures in motion', Chemical Reviews, 117(1), pp. 139–155. doi:10.1021/acs.chemrev.6b00177.

Le Bon, C., Della Pia, E., Giusti, F., Lloret, N., Zoonens, M., Martinez, K. and Popot, J. (2014). Synthesis of an oligonucleotide-derivatized amphipol and its use to trap and immobilize membrane proteins. Nucleic Acids Research, 42(10), pp.e83-e83.

Lee, J., Yang, J., Zhitnitsky, D., Lewinson, O. and Rees, D. (2014) Structural Basis for Heavy Metal Detoxification by an Atm1-Type ABC Exporter. Science, 343(6175), pp.1133-1136.

Lee, S., Knowles, T., Postis, V., Jamshad, M., Parslow, R., Lin, Y., Goldman, A., Sridhar, P., Overduin, M., Muench, S. and Dafforn, T. (2016). A method for detergent-free isolation of membrane proteins in their local lipid environment. Nature Protocols, 11(7), pp.1149-1162.

Lehmann, A. (2003) DNA repair-deficient diseases, xeroderma pigmentosum, Cockayne syndrome and trichothiodystrophy. Biochimie, 85(11), pp.1101-1111.

Leighton, J. and Schatz, G. (1995) An ABC transporter in the mitochondrial inner membrane is required for normal growth of yeast. The EMBO Journal, 14(1), pp.188-195.

Lill, R. and Kispal, G. (2001) Mitochondrial ABC transporters. Research in Microbiology, 152(3-4), pp.331-340.

Lill, R. and Mühlenhoff, U. (2008) Maturation of Iron-Sulfur Proteins in Eukaryotes: Mechanisms, Connected Processes, and Diseases. Annual Review of Biochemistry, 77(1), pp.669-700.

Lill, R., Dutkiewicz, R., Freibert, S., Heidenreich, T., Mascarenhas, J., Netz, D., Paul, V., Pierik, A., Richter, N., Stümpfig, M., Srinivasan, V., Stehling, O. and Mühlenhoff, U. (2015) The role of mitochondria and the CIA machinery in the maturation of cytosolic and nuclear iron–sulfur proteins. European Journal of Cell Biology, 94(7-9), pp.280-291.

Lill, R., Srinivasan, V. and Mühlenhoff, U. (2014) The role of mitochondria in cytosolic-nuclear iron–sulfur protein biogenesis and in cellular iron regulation. Current Opinion in Microbiology, 22, pp.111-119.

Lindhoud, S., Carvalho, V., Pronk, J. and Aubin-Tam, M. (2016). SMA-SH: Modified Styrene–Maleic Acid Copolymer for Functionalization of Lipid Nanodiscs. Biomacromolecules, 17(4), pp.1516-1522.

Linz, A.M., Ma, Y., Perez, J., Myers, K., Kontur, W.S., Noguera, D.R. and Donohue, T.J. (2021). Aromatic dimer dehydrogenases from novosphingobium aromaticivorans reduce monoaromatic diketones', Applied and Environmental Microbiology, 87(24). doi:10.1128/aem.01742-21.

Lodish, H., Berk, A., Zipursky, L.S., Matsudaira, P., Baltimore, D. and Darnell, J. (2000) Membrane proteins. Available at: https://www.ncbi.nlm.nih.gov/books/NBK21570/ (Accessed: 10 December 2016).

Logez, C., Damian, M., Legros, C., Dupré, C., Guéry, M., Mary, S., Wagner, R., M'Kadmi, C., Nosjean, O., Fould, B., Marie, J., Fehrentz, J., Martinez, J., Ferry, G., Boutin, J. and Banères, J. (2015). Detergent-free Isolation of Functional G Protein-Coupled Receptors into Nanometric Lipid Particles. Biochemistry, 55(1), pp.38-48.

Lundbaek, J., Koeppe, R. and Andersen, O. (2010). Amphiphile regulation of ion channel function by changes in the bilayer spring constant. Proceedings of the National Academy of Sciences, 107(35), pp.15427-15430.

Macias-Contreras, M., Little, K. and Zhu, L. (2020) Expanding the substrate selectivity of SNAP/CLIP-tagging of intracellular targets. Methods in Enzymology, pp.233-257.

Malinauskaite, L., Quick, M., Reinhard, L., Lyons, J., Yano, H., Javitch, J. and Nissen, P. (2014). A mechanism for intracellular release of Na+ by neurotransmitter/sodium symporters. Nature Structural & Molecular Biology, 21(11), pp.1006-1012.

Marí, M., Morales, A., Colell, A., García-Ruiz, C. and Fernández-Checa, J.C. (2009).Mitochondrial glutathione, a key survival antioxidant, Antioxidants; Redox Signaling, 11(11), pp. 2685–2700. doi:10.1089/ars.2009.2695.

Marsh, D. (2008). Protein modulation of lipids, and vice-versa, in membranes. Biochimica et Biophysica Acta (BBA) - Biomembranes, 1778(7-8), pp.1545-1575.

Marsh, D. (2013).Lipid bilayer lateral pressure profile, Encyclopedia of Biophysics, pp. 1253–1256. doi:10.1007/978-3-642-16712-6_544.

Masson, J., Sagné, C., Hamon, M., and Mestikawy, S. (1999). Neurotransmitter Transporters in the Central Nervous System , Pharmacological Reviews 51 (3); pp. 439-464.

Maynard, J., Lindquist, N., Sutherland, J., Lesuffleur, A., Warrington, A., Rodriguez, M. and Oh, S. (2009). Surface plasmon resonance for high-throughput ligand screening of membrane-bound proteins. Biotechnology Journal, 4(11), pp.1542-1558.

Merkle, P., Gotfryd, K., Cuendet, M., Leth-Espensen, K., Gether, U., Loland, C. and Rand, K. (2018) Substrate-modulated unwinding of transmembrane helices in the NSS transporter LeuT. Science Advances, 4(5).

Miller, D., Charalambous, K., Rotem, D., Schuldiner, S., Curnow, P. and Booth, P.J. (2009) 'In vitro unfolding and Refolding of the small Multidrug transporter EmrE', Journal of Molecular Biology, 393(4), pp. 815–832. doi: 10.1016/j.jmb.2009.08.039.

Morrison, K., Akram, A., Mathews, A., Khan, Z., Patel, J., Zhou, C., Hardy, D., Moore-Kelly, C., Patel, R., Odiba, V., Knowles, T., Javed, M., Chmel, N., Dafforn, T. and Rothnie, A. (2016). Membrane protein extraction and purification using styrene-maleic acid (SMA) copolymer: effect of variations in polymer structure. Biochemical Journal, 473(23), pp.4349-4360.

Morrissey, J., Pureza, V., Davis-Harrison, R., Sligar, S., Ohkubo, Y. and Tajkhorshid, E. (2008). Blood clotting reactions on nanoscale phospholipid bilayers. Thrombosis Research, 122, pp.S23-S26.

Motsa, B.B. and Stahelin, R.V. (2023) 'A beginner's Guide to Surface Plasmon Resonance', The Biochemist, 45(1), pp. 18–22. doi:10.1042/bio_2022_139.

Netz, D., Stith, C., Stümpfig, M., Köpf, G., Vogel, D., Genau, H., Stodola, J., Lill, R., Burgers, P. and Pierik, A. (2012) Eukaryotic DNA polymerases require an iron-sulfur cluster for the formation of active complexes. Nature Chemical Biology, 8(1), pp.125-132.

Nguyen, H., Park, J., Kang, S. and Kim, M. (2015). Surface Plasmon Resonance: A Versatile Technique for Biosensor Applications. Sensors, [online] 15(5), pp.10481–10510. doi:10.3390/s150510481.

Nieba, L., Nieba-Axmann, S., Persson, A., Hämäläinen, M., Edebratt, F., Hansson, A., Lidholm, J., Magnusson, K., Karlsson, Å. and Plückthun, A. (1997). BIACORE Analysis of Histidine-Tagged Proteins Using a Chelating NTA Sensor Chip. Analytical Biochemistry, 252(2), pp.217-228.

Nyola, A., Karpowich, N., Zhen, J., Marden, J., Reith, M. and Wang, D. (2010). Substrate and drug binding sites in LeuT. Current Opinion in Structural Biology, 20(4), pp.415-422.

Ohshima, H. and Ohki, S. (1984) 'Effects of divalent cations on the surface tension of a lipid monolayer-coated air/water interface', Journal of Colloid and Interface Science, 103(1), pp. 85–94. doi:10.1016/0021-9797(85)90079-7.

Oluwole, A., Danielczak, B., Meister, A., Babalola, J., Vargas, C. and Keller, S. (2017). Solubilization of Membrane Proteins into Functional Lipid-Bilayer Nanodiscs Using a Diisobutylene/Maleic Acid Copolymer. Angewandte Chemie International Edition, 56(7), pp.1919-1924.

Orwick, M., Judge, P., Procek, J., Lindholm, L., Graziadei, A., Engel, A., Gröbner, G. and Watts, A. (2012). Detergent-Free Formation and Physicochemical Characterization of Nanosized Lipid-Polymer Complexes: Lipodisq. Angewandte Chemie International Edition, 51(19), pp.4653-4657.

Orwick-Rydmark, M., Lovett, J., Graziadei, A., Lindholm, L., Hicks, M. and Watts, A. (2012). Detergent-Free Incorporation of a Seven-Transmembrane Receptor Protein into Nanosized Bilayer Lipodisq Particles for Functional and Biophysical Studies. Nano Letters, 12(9), pp.4687-4692.

Overduin, M. and Esmaili, M. (2019). Memtein: The fundamental unit of membrane-protein structure and function. Chemistry and Physics of Lipids, 218, pp.73-84.

Overington, J.P., Al-Lazikani, B. and Hopkins, A.L. (2006) 'How many drug targets are there?', Nature Reviews Drug Discovery, 5(12), pp. 993–996. doi: 10.1038/nrd2199.

Pan, L. and Segrest, J.P. (2016) 'Computational studies of plasma lipoprotein lipids', Biochimica et Biophysica Acta (BBA) - Biomembranes, 1858(10), pp. 2401–2420. doi:10.1016/j.bbamem.2016.03.010.

Patching, S. (2014). Surface plasmon resonance spectroscopy for characterisation of membrane protein–ligand interactions and its potential for drug discovery. Biochimica et Biophysica Acta (BBA) - Biomembranes, 1838(1), pp.43-55.

Pattnaik, P. (2005). Surface Plasmon Resonance: Applications in Understanding Receptor–Ligand Interaction. Applied Biochemistry and Biotechnology, 126(2), pp.079-092.

Paul, V. and Lill, R. (2015) Biogenesis of cytosolic and nuclear iron–sulfur proteins and their role in genome stability. Biochimica et Biophysica Acta (BBA) - Molecular Cell Research, 1853(6), pp.1528-1539.

Paulin, S., Jamshad, M., Dafforn, T., Garcia-Lara, J., Foster, S., Galley, N., Roper, D., Rosado, H. and Taylor, P. (2014). Surfactant-free purification of membrane protein complexes from bacteria: application to the staphylococcal penicillin-binding protein complex PBP2/PBP2a. Nanotechnology, 25(28), p.285101.

Pearson, S.A. and Cowan, J.A. (2021) 'Evolution of the human mitochondrial ABCB7 [2Fe–2s](GS)4 cluster exporter and the molecular mechanism of an E433K disease-causing mutation', Archives of Biochemistry and Biophysics, 697, p. 108661. doi:10.1016/j.abb.2020.108661.

Pebay-Peyroula, E., Rummel, G., Rosenbusch, J.P., and Landau, E.M. (1997). X-ray Structure of Bacteriorhodopsin at 2.5 Angstroms from Microcrystals Grown in Lipidic Cubic Phases. Science, 277(5332), pp.1676–1681. doi:10.1126/science.277.5332.1676.

Pereda, A. (2014). Electrical synapses and their functional interactions with chemical synapses. Nature Reviews Neuroscience, 15(4), pp.250-263.

Phillips, R., Ursell, T., Wiggins, P. and Sens, P. (2009). Emerging roles for lipids in shaping membrane-protein function. Nature, 459(7245), pp.379-385.

Pizzorno, J. (2014) Glutathione!, Integrative medicine (Encinitas, Calif.). Available at: https://www.ncbi.nlm.nih.gov/pmc/articles/PMC4684116/ (Accessed: 20 April 2023).

Plach, M., Grasser, K. and Schubert, T. (2017). MicroScale Thermophoresis as a Tool to Study Protein-peptide Interactions in the Context of Large Eukaryotic Protein Complexes. BIO-PROTOCOL, 7(23).

Pondarré, C., Antiochos, B., Campagna, D., Clarke, S., Greer, E., Deck, K., McDonald, A., Han, A., Medlock, A., Kutok, J., Anderson, S., Eisenstein, R. and Fleming, M. (2006) The mitochondrial ATP-binding cassette transporter Abcb7 is essential in mice and participates in cytosolic iron–sulfur cluster biogenesis. Human Molecular Genetics, 15(6), pp.953-964.

Popot, J. (2010). Amphipols, Nanodiscs, and Fluorinated Surfactants: Three Nonconventional Approaches to Studying Membrane Proteins in Aqueous Solutions. Annual Review of Biochemistry, 79(1), pp.737-775.

Postis, V., Rawson, S., Mitchell, J., Lee, S., Parslow, R., Dafforn, T., Baldwin, S. and Muench, S. (2015). The use of SMALPs as a novel membrane protein scaffold for structure study by negative stain electron microscopy. Biochimica et Biophysica Acta (BBA) - Biomembranes, 1848(2), pp.496-501.

Prabudiansyah, I., Kusters, I., Caforio, A. and Driessen, A. (2015). Characterization of the annular lipid shell of the Sec translocon. Biochimica et Biophysica Acta (BBA) - Biomembranes, 1848(10), pp.2050-2056.

Prevarskaya, N., Zhang, L. and Barritt, G. (2007). TRP channels in cancer. Biochimica et Biophysica Acta (BBA) - Molecular Basis of Disease, 1772(8), pp.937-946.

Privé, G.G. (2007) 'Detergents for the stabilization and crystallization of membrane proteins', Methods, 41(4), pp. 388–397. doi: 10.1016/j.ymeth.2007.01.007.

Quick, M., Shi, L., Zehnpfennig, B., Weinstein, H. and Javitch, J.A. (2012) 'Experimental conditions can obscure the second high-affinity site in LeuT', Nature Structural & Molecular Biology, 19(2), pp. 207–211. doi: 10.1038/nsmb.2197.

Ramakrishnan, M., Kandimalla, K.K., Wengenack, T.M., Howell, K.G. and Poduslo, J.F. (2009).Surface plasmon resonance binding kinetics of alzheimer's disease amyloid β peptide-capturing and plaque-binding monoclonal antibodies', Biochemistry, 48(43), pp. 10405–10415. doi:10.1021/bi900523q.

Rasmussen, S., Choi, H., Rosenbaum, D., Kobilka, T., Thian, F., Edwards, P., Burghammer, M., Ratnala, V., Sanishvili, R., Fischetti, R., Schertler, G., Weis, W. and Kobilka, B. (2007). Crystal structure of the human β2 adrenergic G-protein-coupled receptor. Nature, 450(7168), pp.383-387.

Ravula, T., Hardin, N., Bai, J., Im, S., Waskell, L. and Ramamoorthy, A. (2018a). Effect of polymer charge on functional reconstitution of membrane proteins in polymer nanodiscs. Chemical Communications, 54(69), pp.9615-9618.

Ravula, T., Hardin, N., Di Mauro, G. and Ramamoorthy, A. (2018b). Styrene maleic acid derivates to enhance the applications of bio-inspired polymer based lipid-nanodiscs. European Polymer Journal, 108, pp.597-602.

Ravula, T., Hardin, N., Ramadugu, S. and Ramamoorthy, A. (2017a). pH Tunable and Divalent Metal Ion Tolerant Polymer Lipid Nanodiscs. Langmuir, 33(40), pp.10655-10662.

Ravula, T., Hardin, N., Ramadugu, S., Cox, S. and Ramamoorthy, A. (2018). Formation of pH-Resistant Monodispersed Polymer-Lipid Nanodiscs. Angewandte Chemie International Edition, 57(5), pp.1342-1345.

Ravula, T., Ramadugu, S., Di Mauro, G. and Ramamoorthy, A. (2017b). Bioinspired, Size-Tunable Self-Assembly of Polymer-Lipid Bilayer Nanodiscs. Angewandte Chemie International Edition, 56(38), pp.11466-11470.

Reith, M. (2002). Neurotransmitter transporters. Totowa, NJ: Humana Press, pp.53-109.

Ressl, S., Terwisscha van Scheltinga, A., Vonrhein, C., Ott, V. and Ziegler, C. (2009). Molecular basis of transport and regulation in the Na+/betaine symporter BetP. Nature, 458(7234), pp.47-52.

Rich, R.L. and Myszka, D.G. (2004) 'Why you should be using more SPR Biosensor Technology', Drug Discovery Today: Technologies, 1(3), pp. 301–308. doi:10.1016/j.ddtec.2004.09.009.

Rickert, M. (2004). Compensatory Energetic Mechanisms Mediating the Assembly of Signaling Complexes Between Interleukin-2 and its alpha;, beta;, and gamma; Receptors. Journal of Molecular Biology.

Roberts, D., Keeling, R., Tracka, M., van der Walle, C., Uddin, S., Warwicker, J. and Curtis, R. (2014). Specific Ion and Buffer Effects on Protein–Protein Interactions of a Monoclonal Antibody. Molecular Pharmaceutics, 12(1), pp.179-193.

Robertson, N., Jazayeri, A., Errey, J., Baig, A., Hurrell, E., Zhukov, A., Langmead, C., Weir, M. and Marshall, F. (2011). The properties of thermostabilised G protein-coupled receptors (StaRs) and their use in drug discovery. Neuropharmacology, 60(1), pp.36-44.

Rottet, S., Iqbal, S., Beales, P., Lin, A., Lee, J., Rug, M., Scott, C. and Callaghan, R. (2020) Characterisation of Hybrid Polymersome Vesicles Containing the Efflux Pumps NaAtm1 or P-Glycoprotein. Polymers, 12(5), p.1049.

Rudnick, G. (1997).Mechanisms of Biogenic Amine Neurotransmitter Transporters, in M.E.A. Reith (ed.) Neurotransmitter Transporters . Totowa, New Jersey: Humana Press, pp. 73–100.

Ruediger, T. and Bolz, J. (2007). Neurotransmitters and the Development of Neuronal Circuits. Advances in Experimental Medicine and Biology, 621, pp.104-114.

Salgın, S., Salgın, U. and Bahadır, S. (2012). Zeta Potentials and Isoelectric Points of Biomolecules: The Effects of Ion Types and Ionic Strengths. Int. J. Electrochem. Sci., 7; 12404 - 12414

Santos, A., Vaz, A., Rodrigues, P., Veloso, A., Venâncio, A. and Peres, A. (2019). Thin Films Sensor Devices for Mycotoxins Detection in Foods: Applications and Challenges. Chemosensors, 7(1), p.3.

Schaedler, T., Thornton, J., Kruse, I., Schwarzländer, M., Meyer, A., van Veen, H. and Balk, J. (2014) A Conserved Mitochondrial ATP-binding Cassette Transporter Exports Glutathione Polysulfide for Cytosolic Metal Cofactor Assembly. Journal of Biological Chemistry, 289(34), pp.23264-23274.

Scheidelaar, S., Koorengevel, M., Pardo, J., Meeldijk, J., Breukink, E. and Killian, J. (2015). Molecular Model for the Solubilization of Membranes into Nanodisks by Styrene Maleic Acid Copolymers. Biophysical Journal, 108(2), pp.279-290.

Scheidelaar, S., Koorengevel, M., van Walree, C., Dominguez, J., Dörr, J. and Killian, J. (2016) Effect of Polymer Composition and pH on Membrane Solubilization by Styrene-Maleic Acid Copolymers. Biophysical Journal, 111(9), pp.1974-1986.

Schlick, T., Li, B. and Olson, W. (1994). The influence of salt on the structure and energetics of supercoiled DNA. Biophysical Journal, 67(6), pp.2146-2166.

Schmidt, V. and Sturgis, J.N. (2018) Modifying styrene-maleic acid co-polymer for studying lipid nanodiscs. Biochimica et Biophysica Acta (BBA) - Biomembranes, 1860(3), pp.777–783.

Schubert, T., Pusch, M., Diermeier, S., Benes, V., Kremmer, E., Imhof, A. and Längst, G. (2012). Df31 Protein and snoRNAs Maintain Accessible Higher-Order Structures of Chromatin. Molecular Cell, 48(3), pp.434-444.

Schuler, M.A., Denisov, I.G. and Sligar, S.G. (2014) 'Nanodiscs as a new tool to examine lipid–protein interactions', Methods in Molecular Biology, pp. 415–433. doi:10.1007/978-1-62703-275-9_18.

Schulman, H. (2013) 'Chapter 9 - Intracellular Signaling', in Fundamental neuroscience. Fourth edition. Oxford: Elsevier/Academic Press. Editor(s): Larry R. Squire, Darwin Berg, Floyd E. Bloom, Sascha du Lac, Anirvan Ghosh, Nicholas C. Spitzer, Academic Press.

Seddon, A., Curnow, P. and Booth, P. (2004). Membrane proteins, lipids and detergents: not just a soap opera. Biochimica et Biophysica Acta (BBA) - Biomembranes, 1666(1-2), pp.105-117.

Sen, S., Jaakola, V., Pirilä, P., Finel, M. and Goldman, A. (2005). Functional studies with membrane-bound and detergent-solubilized α2-adrenergic receptors expressed in Sf9 cells. Biochimica et Biophysica Acta (BBA) - Biomembranes, 1712(1), pp.62-70.

Shaffer, P., Goehring, A., Shankaranarayanan, A. and Gouaux, E. (2009). Structure and Mechanism of a Na+-Independent Amino Acid Transporter. Science, 325(5943), pp.1010-1014.

Shaikh, S. and Tajkhorshid, E. (2010). Modeling and Dynamics of the Inward-Facing State of a Na+/Cl⁻ Dependent Neurotransmitter Transporter HomologHomologueue. PLoS Computational Biology, 6(8), p.e1000905.

Sharma, P., Plant, M., Lam, S. and Chen, Q. (2021) Kinetic analysis of antibody binding to integral membrane proteins stabilized in SMALPs. BBA Advances, 1, p.100022.

Shi, L., Quick, M., Zhao, Y., Weinstein, H. and Javitch, J. (2008). The Mechanism of a Neurotransmitter:Sodium Symporter—Inward Release of Na+ and Substrate Is Triggered by Substrate in a Second Binding Site. Molecular Cell, 30(6), pp.667-677.

Simon, K., Pollock, N. and Lee, S. (2018). Membrane protein nanoparticles: the shape of things to come. Biochemical Society Transactions, 46(6), pp.1495-1504.

Singh, S., Piscitelli, C., Yamashita, A. and Gouaux, E. (2008). A Competitive Inhibitor Traps LeuT in an Open-to-Out Conformation. Science, 322(5908), pp.1655-1661. doi:10.1126/science.1166777.

Singh, S.K. (2008). LeuT: A prokaryotic stepping stone on the way to a eukaryotic neurotransmitter transporter structure. Channels, 2(5), pp.380–389. doi:10.4161/chan.2.5.6904.

Skaar, K., Korza, H., Tarry, M., Sekyrova, P. and Högbom, M. (2015). Expression and Subcellular Distribution of GFP-Tagged Human Tetraspanin Proteins in Saccharomyces cerevisiae. PLOS ONE, 10(7), p.e0134041.

Smith, E.A., Thomas, W., Kiessling, L.L. and Corn, R.M. (2003). Surface Plasmon Resonance Imaging Studies of Protein-Carbohydrate Interactions. Journal of the American Chemical Society, 125(20), pp.6140–6148. doi:https://doi.org/10.1021/ja034165u.

Snow, B., Brothers, G. and Siderovski, D. (2002). Molecular Cloning of Regulators of G-Protein Signaling Family Members and Characterization of Binding Specificity of RGS 12 PDZ Domain. Methods in Enzymology, 344, pp.740–761. doi: 10.1016/s0076-6879(02)44752-0.

Sonders, M., Quick, M. and Javitch, J. (2005). How did the neurotransmitter cross the bilayer? A closer view. Current Opinion in Neurobiology, 15(3), pp.296-304.

Srinivasan, V., Pierik, A. and Lill, R. (2014) Crystal Structures of Nucleotide-Free and Glutathione-Bound Mitochondrial ABC Transporter Atm1. Science, 343(6175), pp.1137-1140.

Stangl, M., Veerappan, A., Kroeger, A., Vogel, P. and Schneider, D. (2012).Detergent properties influence the stability of the glycophorin a transmembrane helix dimer in lysophosphatidylcholine micelles', Biophysical Journal, 103(12), pp. 2455–2464. doi:10.1016/j.bpj.2012.11.004.

Stehling, O., Mascarenhas, J., Vashisht, A., Sheftel, A., Niggemeyer, B., Rösser, R., Pierik, A., Wohlschlegel, J. and Lill, R. (2013) Human CIA2A-FAM96A and CIA2B-FAM96B Integrate Iron Homeostasis and Maturation of Different Subsets of Cytosolic-Nuclear Iron-Sulfur Proteins. Cell Metabolism, 18(2), pp.187-198.

Stehling, O., Vashisht, A., Mascarenhas, J., Jonsson, Z., Sharma, T., Netz, D., Pierik, A., Wohlschlegel, J. and Lill, R. (2012) MMS19 Assembles Iron-Sulfur Proteins Required for DNA Metabolism and Genomic Integrity. Science, 337(6091), pp.195-199.

Stehling, O., Wilbrecht, C. and Lill, R. (2014) Mitochondrial iron–sulfur protein biogenesis and human disease. Biochimie, 100, pp.61-77.

Swainsbury, D., Scheidelaar, S., Foster, N., van Grondelle, R., Killian, J. and Jones, M. (2017). The effectiveness of styrene-maleic acid (SMA) copolymers for solubilisation of integral membrane proteins from SMA-accessible and SMA-resistant membranes. Biochimica et Biophysica Acta (BBA) - Biomembranes, 1859(10), pp.2133-2143.

Swainsbury, D., Scheidelaar, S., van Grondelle, R., Killian, J. and Jones, M. (2014). Bacterial Reaction Centers Purified with Styrene Maleic Acid Copolymer Retain Native Membrane Functional Properties and Display Enhanced Stability. Angewandte Chemie International Edition, 53(44), pp.11803-11807.

Szundi, I., Pitch, S.G., Chen, E., Farrens, D.L. and Kliger, D.S. (2021).Styrene-maleic acid copolymer effects on the function of the GPCR rhodopsin in lipid nanoparticles, Biophysical Journal, 120(20), pp. 4337–4348. doi:10.1016/j.bpj.2021.09.012.

Tedesco, D., Maj, M., Malarczyk, P., Cingolani, A., Zaffagnini, M., Wnorowski, A., Czapiński, J., Benelli, T., Mazzoni, R., Bartolini, M. and Jóźwiak, K. (2021). Application of the SMALP technology to the isolation of gpcrs from low-yielding cell lines, Biochimica et Biophysica Acta (BBA) - Biomembranes, 1863(9), p. 183641. doi:10.1016/j.bbamem.2021.183641.

Terstappen, G. and Reggiani, A. (2001) 'In silico research in drug discovery', Trends in pharmacological sciences., 22(1), pp. 23–6.

Thibault Tubiana, Sillitoe, I., Orengo, C. and Reuter, N. (2022).Dissecting peripheral protein-membrane interfaces', PLOS Computational Biology, 18(12). doi:10.1371/journal.pcbi.1010346.

Torres, G., Gainetdinov, R. and Caron, M. (2003). Plasma membrane monoamine transporters: structure, regulation and function. Nature Reviews Neuroscience, 4(1), pp.13-25.

Tribet, C., Audebert, R. and Popot, J.-L. (1996) 'Amphipols: Polymers that keep membrane proteins soluble in aqueous solutions', Proceedings of the National Academy of Sciences, 93(26), pp. 15047–15050. doi:10.1073/pnas.93.26.15047.

Välimaa, L. and Laurikainen, K. (2006). Comparison study of streptavidin-coated microtitration plates. Journal of Immunological Methods, 308(1-2), pp.203-215.

van den Brink-van der Laan, E., Chupin, V., Killian, J.A. and de Kruijff, B. (2004).Stability of KcsA tetramer depends on membrane lateral pressure, Biochemistry, 43(14), pp. 4240–4250. doi:10.1021/bi036129d.

Verkman, A., Ruiz-Ederra, J. and Levin, M. (2008). Functions of aquaporins in the eye. Progress in Retinal and Eye Research, 27(4), pp.420-433. doi:10.1016/j.preteyeres.2008.04.001.

von Heijne, G. (2007) 'The membrane protein universe: What's out there and why bother?', Journal of Internal Medicine, 261(6), pp. 543–557. doi: 10.1111/j.1365-2796.2007.01792.x.

Wallin, E. and Heijne, G.V. (2008) 'Genome-wide analysis of integral membrane proteins from eubacterial, archaean, and eukaryotic organisms', Protein Science, 7(4), pp. 1029–1038. doi: 10.1002/pro.5560070420.

Warschawski, D., Arnold, A., Beaugrand, M., Gravel, A., Chartrand, É. and Marcotte, I. (2011). Choosing membrane mimetics for NMR structural studies ofStudies by transmembrane proteins. Biochimica et Biophysica Acta (BBA) - Biomembranes, 1808(8), pp.1957-1974.

Wegner, A. and Isenberg, G. (1983). 12-fold difference between the critical monomer concentrations of the two ends of actin filaments in physiological salt conditions. 80(16), pp.4922–4925. doi:10.1073/pnas.80.16.4922.

Weis, W.I. and Kobilka, B.K. (2018) 'The molecular basis of G protein–coupled receptor activation', Annual Review of Biochemistry, 87(1), pp. 897–919. doi:10.1146/annurev-biochem-060614-033910.

Welty, F.K., Lichtenstein, A.H., Barrett, P.H.R., Dolnikowski, G.G. and Schaefer, E.J. (1999). Human Apolipoprotein (Apo) B-48 and ApoB-100 Kinetics with Stable Isotopes. Arteriosclerosis, Thrombosis, and Vascular Biology, 19(12), pp.2966–2974. doi:10.1161/01.atv.19.12.2966.

Weyand, S., Shimamura, T., Yajima, S., Suzuki, S., Mirza, O., Krusong, K., Carpenter, E.P., Rutherford, N.G., Hadden, J.M., O'Reilly, J., Ma, P., Saidijam, M., Patching, S.G., Hope, R.J., Norbertczak, H.T., Roach, P.C.J., Iwata, S., Henderson, P.J.F. and Cameron, A.D. (2008). Structure and molecular mechanism of a nucleobase-cation-symport-1 family transporter. Science (New York, N.Y.), 322(5902), pp.709–713. doi:10.1126/science.1164440.

White, S. (2016) Membrane proteins of known structure. Available at: http://blanco.biomol.uci.edu/mpstruc/ (Accessed: 7 December 2016).

Whyte, D.B. (2023) Tryptophan fluorescence: Nature's probe: BMG LABTECH, Tryptophan Fluorescence: nature's probe | BMG LABTECH. Available at: https://www.bmglabtech.com/en/blog/tryptophan-fluorescence/ (Accessed: 08 May 2023).

Willard, F.S. and Siderovski, D.P. (2006). Covalent immobilization of histidine-tagged proteins for surface plasmon resonance. Analytical Biochemistry, 353(1), pp.147–149. doi:10.1016/j.ab.2006.02.004.

Wilson, J. and Hunt, T. (2002) 'Membrane structure', in Molecular biology of the cell. 4th edn. New York: Garland Science, pp. 1508–1519.

Wolf, L.K., Gao, Y. and Georgiadis, R.M. (2007) 'Kinetic discrimination of sequence-specific dna−drug binding measured by surface plasmon resonance imaging and comparison to solution-phase measurements', Journal of the American Chemical Society, 129(34), pp. 10503–10511. doi:10.1021/ja072401l.

Wu, H., Pfarr, D., Johnson, S., Brewah, Y.A., Woods, R.J., Patel, N., White, W.M., Young, J.B. and Kiener, P.A. (2007). Development of Motavizumab, an Ultra-potent Antibody for the Prevention of Respiratory Syncytial Virus Infection in the Upper and Lower Respiratory Tract. Journal of Molecular Biology, 368(3), pp.652–665. doi:10.1016/j.jmb.2007.02.024.

Yamashita, A., Singh, S.K., Kawate, T., Jin, Y. and Gouaux, E. (2005). Crystal structure of a bacterial homologue of Na+/Cl--dependent neurotransmitter transporters. Nature, [online] 437(7056), pp.215–223. doi:10.1038/nature03978.

Yammine, A., Gao, J. and Kwan, A. (2019) 'Tryptophan fluorescence quenching assays for measuring protein-ligand binding affinities: Principles and a practical guide', BIO-PROTOCOL, 9(11), pp. 4097–4097. doi:10.21769/bioprotoc.3253.

Yang, D., Zhou, Q., Labroska, V., Qin, S., Darbalaei, S., Wu, Y., Yuliantie, E., Xie, L., Tao, H., Cheng, J., Liu, Q., Zhao, S., Shui, W., Jiang, Y. and Wang, M.-W. (2021). G protein-coupled receptors: structure- and function-based drug discovery. Signal Transduction and Targeted Therapy, 6(1), pp.1–27. doi:10.1038/s41392-020-00435-w.

Yang, Z., Wang, C., Zhou, Q., An, J., Hildebrandt, E., Aleksandrov, L.A., Kappes, J.C., DeLucas, L.J., Riordan, J.R., Urbatsch, I.L., Hunt, J.F. and Brouillette, C.G. (2014). Membrane protein stability can be compromised by detergent interactions with the extramembranous soluble domains. Protein Science, 23(6), pp.769–789. doi:10.1002/pro.2460.

Yeagle, P.L. (2014). Non-covalent binding of membrane lipids to membrane proteins. Biochimica et Biophysica Acta (BBA) - Biomembranes, 1838(6), pp.1548–1559. doi:10.1016/j.bbamem.2013.11.009.

Yeow, J., Tan, K.W., Holdbrook, D.A., Chong, Z.-S., Marzinek, J.K., Bond, P.J. and Chng, S.-S. (2018). The architecture of the OmpC–MlaA complex sheds light on the maintenance of outer membrane lipid asymmetry in Escherichia coli. Journal of Biological Chemistry, 293(29), pp.11325–11340. doi:10.1074/jbc.ra118.002441.

Yin, H. and Flynn, A.D. (2016a) 'Drugging membrane protein interactions', Annual Review of Biomedical Engineering, 18(1), pp. 51–76. doi:10.1146/annurev-bioeng-092115-025322.

Zhang, Y.W., Tavoulari, S., Sinning, S., Aleksandrova, A.A., Forrest, L.R., and Rudnick, G. (2018). Structural elements required for coupling ion and substrate transport in the neurotransmitter transporter homolog LeuT. Proceedings of the National Academy of Sciences, 115(38), pp.8854–8862. doi:10.1073/pnas.1716870115.

Zhou, H.-X. and Cross, T.A. (2013) 'Influences of membrane mimetic environments on membrane protein structures', Annual Review of Biophysics, 42(1), pp. 361–392. doi: 10.1146/annurev-biophys-083012-130326.

Zhou, Z., Zhen, J., Karpowich, N.K., Goetz, R.M., Law, C.J., Reith, M.E.A. and Wang, D.-N. . (2007). LeuT-Desipramine Structure Reveals How Antidepressants Block Neurotransmitter Reuptake. Science, [online] 317(5843), pp.1390–1393. doi: 10.1126/science.1147614.

Zillner, K., Moran Jerabek-Willemsen, Duhr, S., Braun, D., Gernot Längst and Baaske, P. (2012). Microscale Thermophoresis as a Sensitive Method to Quantify Protein: Nucleic Acid Interactions in Solution. pp.241–252. doi:10.1007/978-1-61779-424-7_18.

Zoonens, M. and Popot, J.-L. (2014) 'Amphipols for each season', The Journal of Membrane Biology, 247(9–10), pp. 759–796. doi:10.1007/s00232-014-9666-8.

Zou, C., Kumaran, S., Markovic, S., Walser, R. and Zerbe, O. (2008). Studies of the Structure of the N-Terminal Domain from the Y4 Receptor-a G Protein-Coupled Receptor-and its Interaction with Hormones from the NPY Family. 9(14), pp.2276–2284. doi:10.1002/cbic.200800221.

Zuo, J., Wu, Z., Li, Y., Shen, Z., Feng, X., Zhang, M. and Ye, H. (2017). Mitochondrial ABC Transporter ATM3 Is Essential for Cytosolic Iron-Sulfur Cluster Assembly. 173(4), pp.2096–2109. doi:10.1104/pp.16.01760.

Zutz, A., Gompf, S., Schägger, H., and Tampé, R. (2009). Mitochondrial ABC proteins in health and disease. Biochimica et Biophysica Acta (BBA) - Bioenergetics, 1787(6), pp.681–690. doi:10.1016/j.bbabio.2009.02.009.